INFORMATION TO USERS

This manuscript has been reproduced from the microfilm master. UMI films the text directly from the original or copy submitted. Thus, some thesis and dissertation copies are in typewriter face, while others may be from any type of computer printer.

The quality of this reproduction is dependent upon the quality of the copy submitted. Broken or indistinct print, colored or poor quality illustrations and photographs, print bleedthrough, substandard margins, and improper alignment can adversely affect reproduction.

In the unlikely event that the author did not send UMI a complete manuscript and there are missing pages, these will be noted. Also, if unauthorized copyright material had to be removed, a note will indicate the deletion.

Oversize materials (e.g., maps, drawings, charts) are reproduced by sectioning the original, beginning at the upper left-hand corner and continuing from left to right in equal sections with small overlaps.

Photographs included in the original manuscript have been reproduced xerographically in this copy. Higher quality 6" x 9" black and white photographic prints are available for any photographs or illustrations appearing in this copy for an additional charge. Contact UMI directly to order.

ProQuest Information and Learning
300 North Zeeb Road, Ann Arbor, MI 48106-1346 USA
800-521-0600

An Experimental Study of the Early Stages of the Pyrolysis of Acetylene

by

Xuejun Xu

Submitted in partial fulfillment of the requirements for the degree of Doctor of Philosophy

at

Dalhousie University

Halifax, Nova Scotia

September, 2001

DALHOUSIE UNIVERSITY

FACULTY OF GRADUATE STUDIES

The undersigned hereby certify that they have read and recommend to the Faculty of Graduate Studies for acceptance a thesis entitled "An Experimental Study of the Early Stages of the Pyrolysis of Acetylene" by Xuejun Xu in partial fulfillment of the requirements for the degree of Doctor of Philosophy.

Dated: November 2, 2001

External Examiner:

Research Supervisor:

Examining Committee:

DALHOUSIE UNIVERSITY

DATE: November 02, 2001

AUTHOR: Xuejun Xu

TITLE: An Experimental Study of the Early Stages of the Pyrolysis of Acetylene

DEPARTMENT: Chemistry

DEGREE: Ph.D. CONVOCATION: spring YEAR: 2001

Permission is herewith granted to Dalhousie University to circulate and to have copied for non-commercial purposes, at its discretion, the above title upon the request of individuals or institutions.

Signature of Author

To Tiantian, Le, and my parents

Table of Contents

page

List of Figures xi

List of Tables xvii

Abstract xxi

List of Abbreviations xxii

Acknowledgments xxiv

CHAPTER 1. INTRODUCTION 1

1-1. Observed products 2

1-1-1. Static and flow reactor studies 2

1-1-2. Shock tube studies 6

1-2. Evidence for radicals 7

1-2-1. Static and flow reactor studies 7

1-2-2. Shock tube studies 9

1-3. Dependence on the reaction time, pressure and temperature 10

1-3-1. Static and flow reactor studies 10

1-3-2. Shock tube studies 13

1-4. Surface reactions 14

1-5. Proposed mechanisms 15

1-5-1. The molecular polymerization mechanism involving diradicals 15

1-5-2. The free radical chain mechanism initiated by a bimolecular disproportionation reaction between two acetylene molecules 17
1-5-3. A free radical mechanism dominated by C_4H_3 and H 20
1-5-4. The molecular mechanism initiated by the isomerization of acetylene to form vinylidene 22
1-5-5. The free radical chain mechanism initiated by acetone impurity in acetylene. 23
1-5-6. The combined molecular/radical mechanism 26
1-5-7. The free radical mechanism involving 1,4-diradicals 29
1-6. Summary 32
References for Chapter 1 37
CHAPTER 2. EXPERIMENTAL TECHNIQUE AND APPARATUS 40
2-1. Linear flow technique 40
2-1-1. Incomplete radial heat transfer 41
2-1-2. Mass transfer 43
2-1-3. Volume contraction 44
2-1-4. Pressure drop 44
2-2. Materials and apparatus 46
2-2-1. Reagent 46
2-2-2. The design of the micro-reactor 47
2-2-3. The design of the flow system 48
2-2-4. Experimental procedure 53
2-2-4-1. General experimental procedure 53

2-2-4-2. Experimental procedure used in chapters 3 and 4 55

2-2-4-3. Experimental procedure used in chapter 5 57

2-2-4-4. Experimental procedure used in chapter 6 57

References for Chapter 2 59

CHAPTER 3. INTERACTIONS BETWEEN ACETYLENE AND CARBON NANOTUBES AT 893 AND 1019 K 60

3-1. Introduction 60

3-2. Results 63

3-2-1. Deposition of carbon on the surfaces of reactors 63

3-2-2. The structure of the carbon deposit 68

3-2-3. Effect of surface on the gaseous products 71

3-2-4. Treating the surfaces of the reactors 75

3-3. Discussion 80

3-3-1. The formation of carbon nanotubes 80

3-3-2. The rate of deposition of carbon 81

3-3-3. The precursor to the formation of carbon nanotubes 82

3-3-4. Diffusion of species to the surface of the reactor 85

3-3-5. The effect of the carbon deposit on the pyrolysis of acetylene 88

3-3-6. The behavior of coatings of LiOH/KOH/H_3BO_3 and Li_3PO_4/K_3PO_4 91

3-3-7. Estimation of rate constants for surface reactions 92

3-3-8. A new mechanism for the formation of carbon nanotubes 98

3-4. Conclusion 99

References for Chapter 3 100

CHAPTER 4. AN INDUCTION PERIOD IN THE PYROLYSIS OF ACETYLENE .. 103

4-1. Introduction 103

4-2. Results 105

4-2-1. Observation of induction periods for the formation of vinylacetylene and benzene 105

4-2-2. Results of fitting the induction periods for vinylacetylene and benzene 107

4-3. Discussion 115

4-3-1. Effect of incomplete radial heat transfer 117

4-3-2. Pressure drop, axial diffusion and volume contraction 117

4-3-3. Surface reaction and the effect of impurities 118

4-3-4. Mechanism of the reaction 119

4-3-5. Properties of the initiation and termination reactions 123

4-3-6. Properties of the steady state rates 129

4-3-7. The parameters, *b* 133

4-3-8. The parameters, *c* 135

4-4. Conclusion 136

References for Chapter 4 138

CHAPTER 5. THE ACCELERATION OF THE PYROLYSIS OF ACETYLENE BY NEOPENTANE 141

5-1. Introduction 141

5-2. Results 146

5-2-1 Acceleration by neopentane 146
5-3. Discussion 160
5-3-1. Possible sources of errors 160
5-3-2. Effect of neopentane on the induction periods and steady-state rates 160
5-3-3. The rate constant for the initiation reaction in the pyrolysis of pure acetylene 162
5-3-4. The mechanism of the reaction and the initiation reaction 162
5-3-5. The rate constants of termination and propagation steps 167
5-4. Conclusion 173
References for Chapter 5 174
CHAPTER 6. MINOR PRODUCTS FORMED IN THE PYROLYSIS OF ACETYLENE 177
6-1. Introduction 177
6-2. Results 178
6-2-1. Observation and identification of minor products 178
6-2-2. Pressure and temperature dependences of the rates of formation of primary products 189
6-3. Discussion 195
6-3-1. Possible sources of errors 195
6-3-2. Initiation reaction 198
6-3-3. Termination reactions 198
6-3-4. Propagation reactions 206

6-3-5. Reactions involving impurities 215

6-4. Conclusion 219

References for Chapter 6 221

CHAPTER 7. SUMMARY AND FUTURE WORK 224

7-1. Observed products 225

7-2. Evidence for radicals 225

7-3. Dependence on the reaction time, pressure and temperature 226

7-4. Surface reactions 226

7-5. Mechanisms proposed by previous workers 227

7-6. Mechanism proposed in the present work 229

7-6-1. Mechanism of the pyrolysis of pure acetylene 229

7-6-2. Reactions with impurities in acetylene 231

7-6-3. Reactions with neopentane 232

7-6-4. Rate constants determined in the present work 232

7-7. Significance of findings in the present work 235

7-8. Future work 235

References for Chapter 7 238

Appendix 239

List of Figures

Figure 2-1. The schematic diagram of a micro-reactor. 49

Figure 2-2. The schematic diagram of the system. 50

Figure 3-1. Dependence of the extinction (E) of the laser beam by carbon on the deposition time (t_d) at 1016 K and 56 Torr at a residence time of 55 ms in 4-mm id reactor. A, quartz surface treated with HNO_3, $X_{acetone}$ = 35 ppm; B, surface treated with HNO_3, $X_{acetone}$ = 28000 ppm; C, surface treated with HF, $X_{acetone}$ = 103 ppm. The arrows indicate the beginnings and ends of the acceleration period and of the constant growth period. 64

Figure 3-2. Dependence of the rates of deposition of carbon, measured as the slopes of graphs like Figure 3-1, on the residence time at 1016 K and 56 Torr in a 4-mm id reactor treated with HNO_3. ●, the rates in the acceleration periods; ▼, the rates in the constant growth periods. 66

Figure 3-3.a, SEM image of carbon deposited on an HNO_3-treated surface; b, SEM image of carbon deposited on an HF-treated surface; c, TEM image of carbon deposited on an HNO_3-treated surface, magnification = 14760. Experimental conditions, 1019 K and 56.5 Torr at a residence time of 22 ms in 1-mm id reactors, $X_{acetone}$ = 90 ppm, t_d = 10 min, t_b = 5 min. 70

Figure 3-4. Dependence of the rates of formation of vinylacetylene and benzene (left axis), and of the laser extinction (E) due to carbon deposition (right axis) on the deposition time at 1016 K and 57.5 Torr at a residence time of 55 ms in a 4-mm id

reactor treated with HNO_3, x = vinylacetylene or benzene; ■, extinction; ▲, vinylacetylene; ▼, benzene. 74

Figure 3-5. Dependence of the rates of formation of vinylacetylene and benzene on the deposition time at 1017 K and 58.6 Torr at a residence time of 22 ms in a 1-mm id reactor coated with $LiOH/KOH/H_3BO_3$; ■, vinylacetylene; ●, benzene..... 78

Figure 3-6. Dependence of the rate constant for the surface termination of free radicals (at 1016-1018 K and 58 Torr at residence times of 24-55 ms) on the surface-to-volume ratio. The reactors were coated with carbon at these conditions for 110 minutes..... 94

Figure 3-7. Dependence of the extinction (■) of a laser beam by carbon (left axis) and of the rate constant (●) for surface termination (right axis) on the deposition time at 1016 K and 57.5 Torr at a residence time of 55 ms in a 4-mm id reactor washed with HNO_3. 97

Figure 4-1. Dependence of the rates of formation of vinylacetylene and benzene on the residence time at 27 Torr and 935 K in a 4-mm-id reactor; ■, vinylacetylene; ▲, benzene; solid curve, non-linear least-squares fit of equation (E4-1) to the data for vinylacetylene; dotted curve, non-linear least-squares fit for benzene..... 106

Figure 4-2. Dependence of the rates of formation of vinylacetylene and benzene on the residence time at 68 Torr and 936 K in a 2-mm-id reactor; ■, vinylacetylene; ▲, benzene; solid lines, non-linear least-square fits of equation (E4-1) to the data..... 108

Figure 4-3. Dependence of the induction period, τ, on the acetylene concentration at 934-936 K; solid squares, results for vinylacetylene; hollow triangles, results for benzene; solid line, weighted least-squares fit to the data for both vinylacetylene and benzene.

..... 111

Figure 4-4. Dependence of the steady-state rates, R^{ss}, on the acetylene concentration at 934-936 K; squares, results for vinylacetylene; triangles, results for benzene..... 112

Figure 4-5. Arrhenius plot of $k_i k_t$; solid squares, results for vinylacetylene; hollow triangles, results for benzene; solid line, weighted least-squares fit to the data for both vinylacetylene and benzene. 113

Figure 4-6. Arrhenius plots for k/L^n mol^{-n} s^{-1} (n = 1 for vinylacetylene, and 1.4 for benzene), the effective rate constants in the steady-state regime; squares, results for vinylacetylene; triangles, results for benzene. 114

Figure 4-7. Arrhenius plots for the absolute values of the parameters, c, for secondary reactions; squares, results for vinylacetylene; triangles, results for benzene..... 116

Figure 4-8. Arrhenius plot for k_{VA}/L mol^{-1} s^{-1}; ●, Bradley and Kistiakowsky[44]; ■, Ogura[42]; ▲, Kiefer et al.[45]; ▼, Duran et al.[46]; ◆, Dimitrijevic et al.[19]; □, this work. 131

Figure 5-1. Dependence of the rates of formation of vinylacetylene on the residence times at 120 Torr and 856 K in a 3.96-mm-id reactor; ■, acetylene doped with 0.596% neopentane; □, purified acetylene; lines, non-linear least-square fits of equation (E4-1) to the data. 148

Figure 5-2. Dependence of the rates of formation of benzene on the residence times at 120 Torr and 856 K in a 3.96-mm-id reactor; ▲, acetylene doped with 0.596% neopentane; △, purified acetylene; lines, non-linear least-square fits of equation (E4-1) to the data. 149

Figure 5-3. Dependence of Q^2-1 on $X_{C5H12}/[C_2H_2]$ (mol^{-1} L) at 930-934 K; ■, vinylacetylene at 34.1 Torr of acetylene; □, vinylacetylene at 51.6 Torr of acetylene; ▲, benzene at 34.1 Torr of acetylene; △, benzene at 51.6 Torr of acetylene; solid line, least-squares fit of equation (E5-2), assuming z = 2 and forcing the line to pass the origin , to the data for both vinylacetylene and benzene. 153

Figure 5-4. Dependence of Q-1 on $X_{C5H12}/[C_2H_2]$ (mol^{-1} L) at 930-934 K; ■, vinylacetylene at 34.1 Torr of acetylene; □, vinylacetylene at 51.6 Torr of acetylene; ▲, benzene at 34.1 Torr of acetylene; △, benzene at 51.6 Torr of acetylene; solid line, least-squares fit of equation (E5-2), assuming z = 1 and forcing the line to pass the origin, to the data for both vinylacetylene and benzene. 154

Figure 5-5. Dependence of $(Q^2-1)/X_{C5H12}$ on $1/[C_2H_2]$ at 930-934 K; ■, data for vinylacetylene; △, data for benzene; solid line, least-squares fit of equation (E5-3), assuming z = 2, to the data for both vinylacetylene and benzene..... 156

Figure 5-6. Dependence of $(Q^2-1)/X_{C5H12}$ on $1/[C_2H_2]$ at 969-972 K; ■, data for vinylacetylene; △, data for benzene; solid line, least-squares fit of equation (E5-3), assuming z = 2, to the data for both vinylacetylene and benzene..... 157

Figure 5-7. Arrhenius plot for $k_{i,C5H12}/k_{i,C2H2}$; ■, data from vinylacetylene and △, data from benzene. 159

Figure 5-8.Arrhenius plot for the initiation reaction; ◆, Frank and Just;[38] ○, Gay et al.;[37] △, Dimitrijevic et al.;[21] ■, the present work. 166

Figure 6-1. GC chromatogram of a gaseous sample collected at 298 K from a furnace external to the GC oven after pyrolysis at 970 K, 200 Torr, and 700 ms; column,

alumina, 50 m × 0.32 mm × 8 μm; detector, FID. Identities of some of the numbered peaks are listed in Table 1. 180

Figure 6-2. An expanded area from Figure 6-1. 181

Figure 6-3. GC chromatogram of a gaseous sample collected at 483 K with the reactor furnace inside the GC oven, after pyrolysis at 970 K, 200 Torr, and 1420 ms; column, Porapak Q, 2 m; detector, FID. Identities of the numbered peaks are listed in Table 1. The signal was attenuated by a factor of two after twelve minutes. 183

Figure 6-4. Dependence of concentrations of five light products, X, on the residence times at 970 K and 203 Torr; ○, ethylene; ●, 1,3-butadiene; ▼, cyclopentadiene; ∇, C_6H_6(34'); ■, C_6H_6(36'); lines are least-square fits of equation (E6-1) to the data. 187

Figure 6-5. Dependence of concentrations of six light products, X, on the residence times at 937 K and 202 Torr; ●, C_5H_6(27.52'), ○, 1,3-cyclohexadiene; ▼, C_5H_6(28.37'); ∇, 1,4-cyclohexadiene; ■, C_4H_2; and □, C_6H_6(48.22'); lines are least-square fits of equation (E6-1) to the data. 188

Figure 6-6. Dependence of concentrations of four heavy products, X, on the residence times at 970 K and 200 Torr; □, styrene; ●, C_{10}(34'); ○, C_{10}(63'); ▼, naphthalene; lines are least-square fits of equation (E6-1). 190

Figure 6-7. Order plots for the primary rates of formation of five light products at 970-971 K; ○, ethylene; ●, 1,3-butadiene; ▼, cyclopentadiene; ∇, C_6H_6 (34'); ■, C_6H_6 (36'). 192

Figure 6-8. Order plots for the primary rates of formation of six light products at 970-971 K. ●, C_5H_6(27.52'); ○, 1,3-cyclohexadiene; ▼, C_5H_6(28.37'); ∇, 1,4-cyclohexadiene; ■, C_4H_2; and □, C_6H_6(48.22'). 193

Figure 6-9. Arrhenius plots for the primary formation of five minor products; ○, ethylene, m = 1.35; ●, 1,3-butadiene, m = 1.66; ▼, cyclopentadiene, m = 1.46; ∇, C_6H_6 (34'), m = 0.94; ■, C_6H_6 (36'), m = 0.94. 196

Figure 6-10. Arrhenius plots for the primary formation of six minor products; ●, C_5H_6(27.52'), m = 2.87; ○, 1,3-cyclohexadiene, m = 2.57; ▼, C_5H_6(28.37'), m = 2.64; ∇, 1,4-cyclohexadiene, m = 1.40; ■, C_4H_2, m = 3.48; and □, C_6H_6(48.22'), m = 4.11. 197

Figure 6-11. Dependence of $ln(\Sigma b)$ on the number, n, of carbon atoms in the products at 970 K and 203 Torr; ■, C_nH_n, vinylacetylene, benzene, and styrene, (Σb values for vinylacetylene and benzene were calculated using the Arrhenius parameters measured in Chapter 4); ●, C_nH_{n+2}, ethylene, 1,3-butadiene and C_6H_8; ▲, C_nH_{n+1}, C_5H_6..... 202

List of Tables

Table 3-1. Rates of carbon deposition in 4-mm (id) reactors 67

Table 3-2. Rates of formation of vinylacetylene and benzene at 895 K 72

Table 3-3. Rates of formation of vinylacetylene and benzene at 1018±1 K, and at two pressures, after burning off the carbonaceous deposits for times, t_b, in reactors with different surface treatments 76

Table 3-4. Rates of vinylacetylene and benzene formation in three reactors washed with HF solution. Carbon was burned off for 5 minutes between injections. 79

Table 3-5. The rates of diffusion of species to the surface of the reactor at 1016 K and 57.5 Torr at a residence time of 55 ms in a 4-mm id reactor 87

Table 3-6. The estimated rate constants of surface termination on different surfaces at 1018 and 894 K 95

Table 4-1. Parameters of the progress curves for vinylacetylene and benzene obtained by nonlinear least-squares fits of equation (E4-1) to experimental data. 109

Table 4-2. Estimated fractional rates of formation of vinylacetylene and benzene from a possible, parallel, molecular pathway obtained by nonlinear least-squares fits of equation (E4-10) to the experimental data. * 121

Table 4-3. Orders and Arrhenius parameters measured for the formation of vinylacetylene. 130

Table 5-1. Acceleration by neopentane of the rates of formation of vinylacetylene and benzene. 150

Table 5-2. Acceleration factors measured using steady-state rates and using induction periods. 152

Table 5-3. Ratios of $k_{i,C5H12}/k_{i,C2H2}$ determined at various temperatures. 158

Table 5-4. Rate constants reported for the unimolecular initiation reaction of neopentane 163

Table 5-5. Arrhenius parameters estimated and measured for the initiation reaction $C_2H_2 + C_2H_2 \rightarrow C_4H_3 + H$ 165

Table 5-6. Rate constants of the termination reaction 168

Table 5-7. Rate constants estimated and measured for the reaction $C_2H_3 + C_2H_3 \rightarrow C_4H_6$. 169

Table 5-8. Rate constants for the formation of vinylacetylene and benzene from propagation steps. 172

Table 6-1. Identification of GC peaks illustrated in Figures 1 and 3 using an alumina column and a Porapak Q column 182

Table 6-2. The rates, $b \times 10^8$ mol L^{-1} s^{-1}, of formation of twelve products from primary reactions obtained by fitting yields of various products to equation (E6-1). 191

Table 6-3. Orders, Arrhenius parameters and acceleration factors, Q, (by 0.38% neopentane at 970 K and 104 Torr) for the formation of some products. 194

Table 6-4. Rates of the initiation reaction, and of the formation of ethylene, 1,3-butadiene, 1,4-cyclohexadiene, and diacetylene from primary reactions. 200

Table 6-5. The rate constants of reaction [B4a], k_{B4a}. 214

Table 7-1. The estimated rate constants of surface termination on different surfaces at 1018 and 894 K 234

Table 7-2. Orders, Arrhenius parameters and acceleration factors, Q, (by 0.38% neopentane at 970 K and 104 Torr) for the formation of some products. 236

Table 8-1. Yields of vinylacetylene (VA) and benzene (B) measured at 895 K and 60 Torr in a 3.96 mm (i.d.) reactor by pyrolysing purified and unpurified acetylene..... 239

Table 8-2. Yields of vinylacetylene (VA) and benzene (B) measured at 935 K and 27 Torr in a 3.96 mm (i.d.) reactor by pyrolysing purified and unpurified acetylene..... 240

Table 8-3. Yields of vinylacetylene (VA) and benzene (B) measured at 935 K and 34 Torr in a 3.96 mm (i.d.) reactor by pyrolysing purified and unpurified acetylene..... 241

Table 8-4. Yields of vinylacetylene (VA) and benzene (B) measured at 934 K and 52 Torr in a 3.96 mm (i.d.) reactor by pyrolysing purified and unpurified acetylene..... 242

Table 8-5. Yields of vinylacetylene (VA) and benzene (B) measured at 935 K and in a 3.96 mm (i.d.) reactor by pyrolysing purified and unpurified acetylene. 243

Table 8-6. Yields of vinylacetylene (VA) and benzene (B) measured at 935 K and in a 3.96 mm (i.d.) reactor by pyrolysing purified and unpurified acetylene. 244

Table 8-7. Yields of vinylacetylene (VA) and benzene (B) measured at 935 K and in a 3.96 mm (i.d.) reactor by pyrolysing purified and unpurified acetylene. 245

Table 8-8. Yields of vinylacetylene (VA) and benzene (B) measured at 937 K and 52 Torr, at a residence time of 0.377 s in a 3.96 mm (i.d.) reactor by pyrolysing purified acetylene and acetylene doped with CCl_4..... 246

Table 8-9. Yields of vinylacetylene (VA) and benzene (B) measured at 936 K and 52 Torr, at a residence time of 0.389 s in a 3.96 mm (i.d.) reactor by pyrolysing purified acetylene and acetylene doped with propylene. 246

Table 8-10. Yields of vinylacetylene (VA) and benzene (B) measured at 935 K in a 3.96 mm (i.d.) reactor by pyrolysing purified acetylene and acetylene doped with butene-1. 246

Table 8-11. The rates, $c \times 10^8$ mol L^{-1} s^{-2}, of formation of twelve products from secondary reactions obtained by fitting yields of various products to equation (E6-1). 247

Table 8-12. The rates, $d \times 10^8$ mol L^{-1} s^{-3}, of formation of twelve products from tertiary reactions obtained by fitting yields of various products to equation (E6-1). 248

Abstract

Acetylene is believed to be a precursor of polycyclic aromatic hydrocarbons (PAHs) and soot in the industrial pyrolysis and combustion of various hydrocarbons. The first experiment on the pyrolysis of acetylene was performed by Berthelot in 1866. However, the mechanism below 1500 K is still the subject of sharp controversy. Free radical mechanisms and molecular mechanisms were proposed by previous workers. Published experimental results are limited and are subject to interference by secondary and even tertiary reactions, so neither proposed mechanism could be eliminated. Study of the pyrolysis of acetylene at low conversions should provide crucial information regarding the mechanism.

A series of micro-reactors were developed to pyrolyse acetylene at temperatures between 854 and 971 K, pressures between 20.4 and 403 Torr, and residence times between 8 and 3320 milliseconds. Gaseous products were separated and characterized by gas chromatography, mass spectrometry, and gas chromatography-mass spectrometry (GC-MS). Solid products such as carbon nanotubes were examined by optical microscopy, scanning electron microscopy (SEM) and transmission electron microscopy (TEM), and were quantified by laser extinction.

The effect of surface reactions is the most serious disadvantage of the micro-reactors and thus was thoroughly studied first. Carbon nanotubes were observed in the pyrolysis of acetylene without adding metal catalyst. The carbon deposit was found to inhibit the formation of gaseous products by a heterogeneous termination process. Washing the reactor with HF solution almost eliminated both the formation of carbon on the surface and the resulting inhibition of the formation of gaseous products. For the first time, acetylene and intermediates formed directly from acetylene were shown to be the main precursors of the formation of carbon nanotubes.

Induction periods for the formation of vinylacetylene and benzene have been observed between 854 and 970 K for the first time in acetylene pyrolysis below 1600 K. This is crucial evidence for a free radical mechanism. The product of the rate constants for the initiation and termination steps was determined from the induction periods. For the first time, the orders and Arrhenius parameters for the formation of vinylacetylene and benzene were measured without significant effects from surface reactions.

Trace amounts of neopentane were observed to accelerate the rates of formation of vinylacetylene and benzene by similar factors. This confirms that a free radical mechanism dominates the pyrolysis of acetylene. The rate constant for initiation in the pyrolysis of acetylene was experimentally determined for the first time in the present temperature range without effects by a surface termination. The rate constants for the termination reaction and for the formation of vinylacetylene and benzene from chain propagation steps were also determined.

More than twenty-four minor products were observed. Of these products, fifteen species were found to be primary or partially primary products for the first time. The orders and the rate constants for the formation of eleven partially primary products were measured for the first time. A complete mechanism has been proposed to interpret the formation of all the primary and partially primary products.

List of Abbreviations

A	pre-exponential factor
[A]	concentration of species A
C_p	heat capacity at constant pressure
C_i	molar concentration of species i
D	diffusion coefficient
E_A	activation energy
E	extinction of a laser beam by carbon
F	flow rate
η	coefficient of viscosity
id	internal diameter
k_i	rate constant of reaction i or of an initiation reaction
k_t	rate constant of a termination reaction
κ	coefficient of thermal diffusivity
L	length of reactor
λ	coefficient of thermal conductivity
M_i	molar mass (kg mol^{-1}) of carbon in species i
n	number of moles of a gas or an order of a reaction
P	pressure
P_i	partial pressure of species i
Q	acceleration factor

r	radius of reactor
γ	probability of a reaction on each collision
γ_x	stoichiometric coefficient of species x
R	gas constant
R_x	rate of reaction x or rate of formation of species x
σ	collision diameter
ss	steady state
τ	induction period
t, t_{res}	residence time
t_b	burning time of carbon in a reactor
t_d	deposition time of carbon in a reactor
T	absolute temperature
X_i	mole fraction of species i
z	order of a reaction

Acknowledgments

I wish to express my deepest gratitude to Dr. Philip D. Pacey for his constant encouragement, valuable advice and patience throughout this work. Dr. Pacey did everything he could do to help me with not only my research, but also my study and life. I sincerely appreciate what he did for me.

I would like to give my special thanks to Dr. Hiroshi Furue for his kind help in setting up, and modifying the equipment and for many valuable discussions.

I would like to thank Jason Lorette for assistance with experiments during his summer work.

I would also like to thank Greg Glasier for his assistance in my work.

I would like to thank Dr. John Roscoe for assistance with modeling.

I would like to thank Dr. Donald R. Arnold, Dino Mangion, Dr. Louis Ramaley, Dr. Robert D. Guy, and Dr. Stuart J. Grossert for assistance with GC-MS analysis.

I would like to thank Dr. Walter A. Aue for lending a gas chromatograph.

I would like to thank Dr. Nelly M. Rodriguez, Dr. R. Terry K. Baker, and Dr. Paul Anderson in Catalytic Materials Ltd., and Ping Li in the Department of Biology, for assistance with the microscopy.

I would like to thank Merck Frosst Canada Inc. for lending a GC-MS system.

Many thanks are extended to Mr. Jurgen Mueller, Mr. Brian Millier, Mr. Rick Conrad and Mr. Ross Shortt for building the equipment.

I am grateful to the Faculty of Graduate Studies for the award of a Dalhousie Graduate Fellowship.

I would also like to thank the Natural Sciences and Engineering Research Council of Canada for a grant in support of this work.

CHAPTER 1. INTRODUCTION

Acetylene has been proposed to be a precursor of polycyclic aromatic hydrocarbons (PAHs) and of soot in the combustion and industrial pyrolysis of hydrocarbons.[1-5] It is also a source of carbon nanotubes.[6-9] Many PAHs are carcinogens and soot is a pollutant, so they have attracted considerable concern. To control the emission of PAHs and soot, it is necessary to understand the mechanism of the pyrolysis of acetylene. The earliest kinetic experiment on acetylene pyrolysis was performed in 1929 by Pease.[10] Unfortunately, reliable experimental data are still not available due to the complexity of the process. The mechanism of acetylene pyrolysis is also an unsolved problem; quite divergent mechanisms have been proposed. Both free radical mechanisms[11-14] and molecular mechanisms[15-17] have been proposed. Therefore, a deep and comprehensive study of the pyrolysis of acetylene is necessary.

Experiments on the pyrolysis of acetylene have been performed in static reaction vessels, flow reactors and in shock tubes. Static and flow reactor studies started near the beginning of this century. Shock tube studies were popular from the 1960s. The upper limit of studies in static vessels was *ca.* 800 K,[18] and the lower limit of the shock tube studies was *ca.* 1000 K. Flow reactors have been used below 1500 K.

Previous work carried out in static reactors, flow reactors and shock tubes will be introduced in this chapter. Various aspects will be discussed first, including observed products, evidence for radicals, dependence of the decomposition of acetylene on the

reaction time, pressure and temperature, surface reactions, and mechanisms proposed. Then, previous work will be summarized and the present project will be outlined.

1-1. Observed products

1-1-1. Static and flow reactor studies

Various products can be formed in the pyrolysis of a hydrocarbon. A primary product refers to a product formed directly from a reaction (called a primary reaction), involving only the reactant and/or initial radicals. The concentration of a primary product is directly proportional to the reaction time at low conversions. A secondary product is a product formed from a reaction (called a secondary reaction), involving a primary product. The concentration of a secondary product is directly proportional to the square of the reaction time at low conversions. It is much easier to measure kinetic data for a primary product than for a secondary product, because the formation of a secondary product is more complicated than the formation of a primary product.

Since the early work of Pease,[10] the pyrolysis of acetylene has been studied with static and flow reactors at moderate temperatures (below 1200 K).[10,18-32] The major gaseous products were observed to be C_4H_4 (vinylacetylene), C_6H_6 (benzene), C_2H_4, C_4H_2, CH_4, and H_2.[23,26,28;30,19,31] The condensable products were PAHs and other unidentified large polymers.[22,23,31] Vinylacetylene was proposed by some to be the sole primary

product,[22,30,31] but others argued that both vinylacetylene and benzene were primary products.[19,27,28]

Minkoff[25] gave a very good review of studies of acetylene pyrolysis before 1958. At low temperatures (below 773 K) the main products were polycyclic and substituted aromatic compounds. Above 973 K the main products were said to be carbon and hydrogen. Products in the intervening temperature range varied from hydrogen and methane to lower aromatics including benzene, mainly depending on the temperature, but also on other factors.

Among the studies before 1950, Frank-Kamenetzky[22] published the most thorough experimental results. Using static techniques combined with pressure measurement and gas analysis, over the temperature range of 673-973 K, and the pressure range from 50 Torr up to atmospheric pressure, at residence times up to 50 minutes, and at conversions from 10% to 50%, he found three stages of pyrolysis.

In the first stage the pressure remained unchanged and the rate of the reaction began to increase rapidly. The pressure-time dependence fit the second-order kinetics of a dimerization reaction in the second stage. The dimer of acetylene was said to be formed in the first two stages. No carbon or tars (polymers) were observed during those stages, but condensation of tars occurred after the gaseous products had cooled down.

The third stage appeared after the conversion was greater than 50%. The formation of tars on the colder parts of the reaction vessel and of carbon in the hot part of the reaction vessel was observed during this stage. In addition, it was only during the third stage that hydrogen appeared, followed by olefins and finally, by saturated hydrocarbons. The pressure decrease was much greater than predicted according to second order kinetics.

Frank-Kamenetzky suggested that the dimer, C_4H_4, should be the only primary product, and benzene and other aromatic hydrocarbons were secondary products.

Silcocks' work[23] was an excellent study in the 1950s. His experiments were performed using a static reaction vessel combined with pressure measurement and gas analysis, at temperatures of 625-725 K, pressures of 65-1044 Torr, residence times from 3 to 120 minutes, and conversions from 12% to 80% or more. Both homogeneous and heterogeneous reactions were investigated. The products were almost entirely (99%) polymers, starting from C_4H_4. Small amounts of methane, ethylene, propylene, and hydrogen were formed at a later stage of the reaction as secondary products.

Cullis and Franklin[31] investigated the pyrolysis of acetylene in the temperature range of 773-1273 K, at pressures from 96 to 400 Torr, and residence times from 0.3 to 60 seconds. They used static and flow reactors, respectively, for high and low conversions (from 0.6% to 50%). The products were analyzed by gas chromatography or ultraviolet (UV) spectroscopy. The analyzed gaseous products were vinylacetylene, diacetylene, methylacetylene, methane, hydrogen, ethylene, ethane, and benzene. The yields of allene and an unknown compound, probably an unsaturated C_5 compound, were too low to be quantitatively determined. Vinylacetylene was said to be the sole primary product. Methane was the predominant final gaseous product at their experimental conditions. The non-volatile products were analyzed using an ultra-violet absorption spectrophotometer and were found to include many PAHs, in particular chrysene, pyrene, phenanthrene, 1,2-benzpyrene, and 3,4-benzpyrene.

Palmer and Dormish[18] pyrolyzed acetylene employing a flow reactor and gas chromatograph with residence times from 46 to 200 milliseconds, conversions from 3.9%

to 39.7%, and temperatures from 1300 to 1500 K, the lower limit of shock tube work. They found that the main product was vinylacetylene at 1333 K, and diacetylene at 1528K.

In some experiments benzene was reported as the main primary product.[27,33] Munson and Anderson[28] performed experiments on acetylene pyrolysis using a flow reactor and gas chromatograph at temperatures from 773 K to 1073 K, and conversions from 25% to 95%. Both benzene and vinylacetylene were said to be primary products. Ethylene, methane, and hydrogen were observed as secondary products.

Stehling, Frazee, and Napier[27] reported that styrene was the third product after vinylacetylene and benzene below 1000 K.

Duran, Amorebieta and Colussi (DAC)[32] pyrolyzed mixtures of acetylene with benzene and acetylene with toluene using a flow reactor coupled to a mass spectrometer at temperatures from 820 to 970 K and conversions up to 50%. When the mixture of acetylene with benzene was pyrolyzed, the species at m/z equal to 78+26n (n=1, 2, 3, and 4) were suspected to be polyvinyl benzenes. When the mixture of acetylene with toluene was pyrolyzed, the peaks at m/z 104 and 118 were proposed to be styrene and methyl styrene. They interpreted these results as evidence for the addition of vinylidene to the benzene ring.

Becker and Huttinger[33] studied the pyrolysis of acetylene at 1273 K and at high conversions (13-75% at 30 Torr) in a flow system. They reported the formation of hydrogen, methane, ethylene, benzene, toluene, styrene, ethylbenzene, indene, diethylbenzene, naphthalene, biphenyl and anthracene. Benzene was said to be a primary product.

Dimitrijevic et al.[19] recently observed the formation of vinylacetylene and benzene, two primary products, in a flow system at 914-1039 K and 45-353 Torr. However, their result were likely affected by a surface termination reaction.

1-1-2. Shock tube studies

Almost all of the other recent work (starting in the 1960s) employed shock tube techniques. A wide range of high temperatures (>1000 K) were achieved homogeneously without significant wall effects. Therefore, a shock tube is a good reactor for fast, high temperature reactions, and has been extensively used for the pyrolysis of acetylene.[34-48] The disadvantages of shock tube techniques include the difficulty of varying the reaction time over a wide range, and the inaccuracies in the calculations of reaction temperature and time, which cannot be measured directly.

The shock tube data for high temperatures confirm and extend many conclusions obtained using static and flow reactors at low temperatures. Also, some new information was reported with this technique.

The primary product was still vinylacetylene at temperatures below 1500 K,[34,36-48] and diacetylene at higher temperatures.[37,38,41,43,46-48] Small amounts of C_6H_6 (benzene), C_6H_8 (phenylacetylene) and ethylene, and trace amounts of C_3H_4 (allene and propyne), C_4H_6 (1,3-butadiene), and methane were found in the most sensitive experiments.[41,47]

The only shock tube study at low conversions was performed by Ogura[41] in the temperature range from 1000 to 1670 K with a residence time of about 1 millisecond. The

main primary product was vinylacetylene below 1500 K or diacetylene (and also hydrogen) above 1500 K. A number of minor products were detected, including CH_4, C_2H_4, allene, propyne, and benzene. (There was no quantitative analysis for benzene). In addition, trace amounts of C_2H_6 and 1,3-butadiene were found. The results were in good accord with those obtained by Cullis and Franklin[31] using static and flow reactors.

Colket[47] investigated the pyrolysis of acetylene in a shock tube in the temperature range between 1100 and 2400 K, and at residence times of about 0.700 milliseconds. The observed products were C_4H_2, H_2, C_6H_2, vinylacetylene, benzene, and phenylacetylene.

1-2. Evidence for radicals

1-2-1. Static and flow reactor studies

Previous work investigating the possible involvement of free radicals in static and flow systems will be reviewed here.

Nitric oxide (NO) is believed to be a scavenger of free radicals. To investigate the reaction mechanism, NO was added to acetylene by many researchers to test if radicals were involved in the pyrolysis. Some workers found nitric oxide, even in only trace amounts, could almost completely inhibit the polymerization of acetylene.[10,21-24]

Frank-Kamenetzky[22] observed that addition of about 1% nitric oxide could lengthen the auto-acceleration period to several hours at low temperatures. After the nitric oxide was used up, the reaction proceeded at the normal rate. The reaction rate was found to be

proportional to the square of the acetylene concentration, but did not depend on that of NO. The expressions for the lengthened induction period will be given in section 1-3.

Burnham and Pease,[21] and Minkoff, Newitt, and Rutledge[24] also observed the inhibition of the reaction by nitric oxide.

Silcocks[23] investigated the influences of nitric oxide on the homogenous and heterogeneous reactions. A trace amount of nitric oxide (0.3%) could completely inhibit the homogenous reaction, which was proposed to be a free radical process with a chain length of about 100. The heterogeneous reaction could be inhibited by addition of 25% nitric oxide. The heterogeneous process was said to have a chain length of about 5. The products volatile at 193 K were found to be N_2, CO, CH_4, and C_2H_4.

However, Hou and Anderson[30] could not find any evidence of radicals in the pyrolysis of acetylene using a flow system coupled to a mass spectrometer over the temperature range 773-973 K. Colket, Seery and Palmer[13] argued the concentrations of radicals were too low for the mass spectrometer to detect in Hou and Anderson's experiments.

Duran, Amorebieta and Colussi (DAC)[32] observed a series of products with mass-to-charge ratios of 78 + 26n (n=1, 2, 3, and 4) by pyrolyzing mixtures of acetylene with benzene and acetylene with toluene. They interpreted this as the evidence for the addition of vinylidene to the benzene ring, a molecular process instead of a free radical process.

Therefore, there is a controversy about the involvement of free radicals in the pyrolysis of acetylene at the temperature below 1500 K. More experiments are needed.

1-2-2. Shock tube studies

Previous work on the involvement of free radicals in shock tubes will be reviewed here.

There is strong evidence for the presence of radicals at high temperatures. The free radical, C_4H_3, was observed by Gay, Kistiakowski, Michael, and Niki[38] with time-of-flight (TOF) mass spectrometry in the temperature range 1600-2400 K. They also observed rapid isotopic mixing in a C_2H_2-C_2D_2 mixture. Bopp and Kern,[40] and Wu, Singh, and Kern[48] also detected C_4H_3 radicals by use of TOF mass spectrometry at high temperatures. Ogura[41] found nearly complete isotopic scrambling in the vinylacetylene product in C_2H_2-C_2D_2 pyrolysis below 1350 K.

In addition, the radical, H, was observed by Frank and Just[45] with the technique of atomic resonance absorption spectrophotometry (ARAS) in a shock tube in the temperature range from 1850 to 3000 K.

Kruse and Roth[35] pyrolyzed acetylene in a shock tube at between 2580 and 4650 K. They observed the formation of C atoms by atomic resonance absorption spectroscopy, C_2 radicals by ring dye laser absorption spectroscopy, and C_3 radicals by a combination of a spectrograph and an intensified CCD (charge coupled device) camera system.

Therefore, it is widely believed that radical processes occur at high temperatures, although the radical chain length is believed to be short. However, the involvement of free radicals at low temperatures is still the subject of sharp controversy.

1-3. Dependence on the reaction time, pressure and temperature

1-3-1. Static and flow reactor studies

When a free radical reaction begins, it usually takes a short time, called an induction period, for free radicals to be formed and to build up to their steady-state concentrations. During this period, the rates of formation of primary products would gradually increase until a steady state is established. With the gradual, subsequent buildup of products, one or more of the products may be involved in secondary reactions. An example is decomposition of the product, providing new sources of free radicals and accelerating the overall reaction. The period of time needed for the product concentration to increase and for acceleration to begin is usually called an auto-acceleration period. Typical durations are a few milliseconds for an induction period and a few seconds for an auto-acceleration period. They describe different stages of a free radical reaction. An induction period is crucial evidence for the presence of a free radical mechanism. It is much easier to extract kinetic information during an induction period than during an auto-acceleration period, because an auto-acceleration reaction is more complicated.

An auto-acceleration period was observed by some researchers at low temperatures in static or flow reactors.[22,24,26,31] It was usually assumed that this period was caused by the formation of a comparatively stable dimeric intermediate, and its increase to a steady state concentration, at which point its rate of formation equaled its rate of decomposition. The radicals formed by the decomposition of the dimer were supposed to catalyze the further

polymerization. Minkoff[25] discussed this and noted that it was a rather weak effect; the initial rate was finite and the rate at the end of the auto-acceleration period increased only by a factor of 1.5-3. Cullis, Minkoff, and Nettleton[26] reported a factor of 3-5. The rate during the auto-acceleration period was proposed to be second order in acetylene.[24,26]

The homogeneous reaction was reported to be second order in acetylene by many workers.[10,18,22-24,26,31] However, an order of 1.5 was proposed by Colket, Seery and Palmer after reviewing and modeling previous experimental data.[13]

As mentioned in section 1-1, Frank-Kamenetzky[22] observed an auto-acceleration period of about 12 seconds at 877 K and 192 Torr. The general expression for the auto-acceleration period, τ, at temperatures, T, higher than 773 K was given as,

$$\tau = \frac{7.5\times10^{-5}}{p^2} Torr^2 e^{\frac{124 kJ/mol}{RT}} \; min. \qquad \text{(E1-1)}$$

Here, R is the gas constant, and p is the pressure in Torr. However, the auto-acceleration period was found to be very long and independent of pressure at temperatures lower than 773 K.

In the second stage, the rate of polymerization was found to be second order in acetylene, and the rate constant was determined to be,

$$k = 4.8\times10^{4} e^{-\frac{125 kJ/mol}{RT}} \; Torr^{-1} \, min^{-1}. \qquad \text{(E1-2)}$$

The auto-acceleration period lengthened by nitric oxide was described as,

$$\tau_{NO} = \frac{p_{NO}\times8.9\times10^{-14}}{p^2} Torr \; e^{\frac{284 kJ/mol}{RT}} \; min. \qquad \text{(E1-3)}$$

The reaction rate between acetylene and nitric oxide was shown to be second order in acetylene, and zero order in nitric oxide. The rate constant was expressed as,

$$k_{NO} = 10^{14.81} e^{-\frac{287 kJ/mol}{RT}} Torr^{-1} min^{-1}. \quad \text{(E1-4)}$$

Silcocks[3] found the homogenous reaction was a second order radical chain reaction with a rate constant,

$$k = 3.72 \times 10^{13} e^{-\frac{210 kJ/mol}{RT}} L\, mol^{-1} s^{-1}. \quad \text{(E1-5)}$$

Cullis and Franklin[31] observed an auto-acceleration period, during which the initial, slow decomposition of acetylene increased rapidly to a maximum rate, and then declined again when the consumption of acetylene was appreciable. The second-order kinetic law was supposed to be obeyed until about 30% of the acetylene was consumed. In addition, they measured effects of many additives, including nitrogen, and some gaseous products, such as hydrogen, methane, ethane, ethylene, methylacetylene, and several PAHs. No additives had any appreciable effect, except that methylacetylene and 2-methylnaphthalene had slight accelerating influences on the formation of hydrogen and methane.

After reviewing the previously determined rate constants at low and high temperatures, Palmer and Dormish[18] suggested a transition near 1000 K between two different mechanisms, a long chain mechanism at low temperatures and non-chain behavior at high temperatures.

Recently, an induction period of 20 milliseconds was observed in this laboratory[49] at 914 K, but the observation was not reproduced due to high pressure drops across the reactor, and significant effects by incomplete radial heat transfer and by a surface termination reaction.

1-3-2. Shock tube studies

The difficulty of varying residence times and the high conversions in shock tubes would make the observation of any possible induction periods very difficult. Furthermore, no observations of auto-acceleration periods in shock tubes have been reported.

The high temperature decomposition of acetylene was shown to be close to second order in acetylene, and the rate constants derived on this basis were fairly consistent with the earlier low temperature work.[18,23,24,29,31,36-38,41] However, a number of the studies at high temperatures did suggest a lower order.[34,37,43,44,48]

Ogura[41] reported the reaction order for vinylacetylene formation was 2.35±0.15. Rounding the order to two, the second-order rate constant for vinylacetylene formation was calculated to be,

$$k = 10^{11.39\pm0.26} e^{-\frac{(194\pm5.9)kJ/mol}{RT}} L\,mol^{-1}s^{-1}. \qquad \text{(E1-6)}$$

Wu, Singh, and Kern[48] pyrolyzed acetylene in the temperature range 1900-2500 K and at pressures from 228 to 418 Torr using a shock tube coupled to a time-of-flight mass spectrometer. The decomposition of acetylene was supposed to involve competition between two channels. The decay was predominantly first order in acetylene when the concentration of acetylene in the C_2H_2/Ne-Ar mixture was less than 200 ppm. However, when the concentration of acetylene in the mixture was greater than 200 ppm, the dominant reaction was second order. The rate constant for the second-order reaction was described as,

$$k = 2\times10^{11} e^{-\frac{186kJ/mol}{RT}} L\,mol^{-1}s^{-1}. \qquad \text{(E1-7)}$$

1-4. Surface reactions

Before 1958, some workers found effects if glass or other materials were packed into static or flow reactors. Frank-Kamenetzky[22] found an increase in the surface-to-volume ratio did not affect the reaction rate. Pease,[10] however, found the rate to be decreased by about 30%. Minkoff, Newitt, and Rutledge[24] reported a weak inhibitory influence of Pyrex glass surface, while Silcocks[23] stated that the rate of reaction was considerably increased by packing the vessel, and that the heterogeneous reaction on glass was a first-order radical chain reaction with an activation energy of 184 kJ/mol at the unusually low temperatures, 625-745 K.

Some workers suggested C_2H_4, CH_4, H_2 and C_4H_2 were formed by heterogeneous processes.[22,23,30,31] Most of the hydrogen and methane were said by Silcocks[23] to be formed in heterogeneous reactions. Cullis and Franklin[31] reported that diacetylene was formed by heterogeneous decomposition of vinylacetylene at ambient temperatures in the presence of carbonaceous deposits.

Palmer and Dormish[18] reported the decomposition of acetylene was a mixed first-order heterogeneous and second-order homogeneous reaction. The rate constant of the heterogeneous reaction was measured to be,

$$k_{het} = 5.25 \times 10^2 e^{-\frac{109 kJ/mol}{RT}} cm.\sec^{-1}. \qquad \text{(E1-8)}$$

Some workers found that the treatment of the surface of a reaction vessel could also influence the reaction rate. Taylor and Van Hook[20] found that reproducible results were available in the presence of a carbonaceous deposit in a reaction vessel at temperatures of

768-808 K, pressures of 24-748 Torr, and reaction times from 0.5 to 120 minutes. Minkoff, Newitt, and Rutledge[24] observed that treatment with 30% HF could accelerate the reaction by 30% at 773 K, but that there was no effect from treatment with KCl.

The effects of surface reactions are negligible in shock tubes because of the very large ratios of volume-to-surface. So, pyrolysis in shock tubes can be safely considered as homogeneous.

1-5. Proposed mechanisms

1-5-1. The molecular polymerization mechanism involving diradicals

This mechanism was proposed by Minkoff in 1958.[25] Frank-Kamenetzky had observed an auto-acceleration period,[22] during which he assumed that a stable dimeric intermediate was formed, and built up to a steady state concentration. The radicals formed by the decomposition of the dimer were supposed to catalyze further polymerization. Minkoff argued that the rate should increase considerably from an initial, small value according to the above assumptions. This did not agree with Minkoff's observation[24] that the initial rate was usually 30-50% of the maximum value. Another difficulty found by Minkoff was that the length of the auto-acceleration period was independent of the initial pressure below 773K.[22,24] Therefore, Minkoff said that a new mechanism should be proposed, including a slow, bimolecular initiation, followed by a series of comparatively rapid, bimolecular, addition steps,

$$A + A \xrightarrow{surface} \begin{cases} A^x + A^x \\ A^x + A \\ A_2^x \end{cases} \qquad \begin{cases} A = C_2H_2 \\ A^x = \cdot C_2H_2 \cdot \\ A_2^x = \cdot C_4H_4 \cdot \end{cases}$$ Initiation [M1]

$$A^x + A \longrightarrow A_2^x$$ Polymerization [M2]

$$A_n^x + A \longrightarrow A_{n+1}^x$$ [M(n+1)]

$$A_n^x + A \longrightarrow A^x + M_n \quad (M = stable\ product)$$ Chain Transfer [M3]

$$A_m^x + A_n^x \longrightarrow Products$$ Termination [M4]

$$A_n^x \xrightarrow{surface} M_n$$ [M5]

Minkoff proposed this mechanism by referring to Flory's scheme for vinyl polymerization in a liquid,[50] because he found the graphs of inverse concentration against time in his paper and in Flory's paper were identical in form. Minkoff suggested that the chain carrier was ·CH=CH· (an acetylene diradical) instead of CH≡C·, because it was said that opening the third C-C bond in acetylene to form ·CH=CH· needed only 125-250 kJ/mol, but breaking a C—H bond in acetylene needed about 506 kJ/mol. The acetylene diradical was assumed to be in the triplet state. The conversions between those two states could be accomplished on the surface of the reactor during the initiation and termination reactions. Thus, the influences of the surface on the reaction could be explained to some extent.

Also, Minkoff mentioned that the shapes of triplet acetylene could be the "trans" configuration in a lower state, and the "cis" configuration in a higher state. At low

temperatures, the "trans" configuration would be important, and polymers with long carbon skeletons would be the main products. At higher temperatures, the "cis" configuration would become significant in the reaction, and benzene would be formed.

1-5-2. The free radical chain mechanism initiated by a bimolecular disproportionation reaction between two acetylene molecules

In 1960, a bimolecular disproportionation between two acetylene molecules was first proposed by Stehling, Frazee, and Anderson.[27] M. Back proposed a complete mechanism in 1971.[11]

Back pointed out that the likely activation energy for the initiation reaction in the pyrolysis of acetylene, between 167 and 188 kJ/mol, was too low to allow initiation by unimolecular fission of bonds in the acetylene molecule. On the other hand, the thermal formation of an excited acetylene molecule in the triplet state or a biradical species, $\cdot C_4H_4\cdot$, seemed uncertain. Back noted that the pyrolysis of acetylene strongly resembled the pyrolysis of ethylene;[51] both activation energies were low, between 167 and 188 kJ/mol, and auto-acceleration periods were observed. Also, both initial rates and both maximum rates after the auto-acceleration periods were second order. In the ethylene system, the initiation reaction was suggested to occur by the bimolecular disproportionation reaction of two ethylene molecules to form an ethyl and a vinyl radical. Such a reaction was suggested to be reasonable in the pyrolysis of acetylene.

Thus, referring to the mechanism of the pyrolysis of ethylene, a similar mechanism for the pyrolysis of acetylene was proposed by Back as the following 17 reactions,

$C_2H_2 + C_2H_2 \rightarrow C_2H + C_2H_3$		[MB1]
$C_2H_3 \rightarrow C_2H_2 + H$		[MB2]
$C_2H + C_2H_2 \rightarrow C_4H_3$		[MB3]
$C_4H_3 \rightarrow C_4H_2 + H$		[MB4]
$H + C_2H_2 \rightarrow H_2 + C_2H$	High temperature	[MB5]
$2C_2H \rightarrow C_4H_2$		[MB6]
$C_2H_3 + C_2H_2 \rightarrow C_4H_5$		[MB7]
$C_4H_5 \rightarrow C_4H_4 + H$		[MB8]
$C_2H_3 + C_2H_2 \rightarrow C_2H_4 + C_2H$		[MB9]
$C_4H_3 + C_2H_2 \rightarrow C_4H_4 + C_2H$		[MB10]
$C_4H_3 + C_2H_2 \rightarrow C_6H_5$	Intermediate temperature	[MB11]
$2C_4H_3 \rightarrow C_8H_6$		[MB12]
$2C_2H_3 \rightarrow C_4H_6$		[MB13]
$C_4H_5 + C_2H_2 \rightarrow C_6H_7$		[MB14]
$C_6H_7 \rightarrow C_4H_4 + C_2H_3$		[MB15]
$C_6H_7 + C_2H_2 \rightarrow C_8H_9$	Low temperature	[MB16]
$C_nH_{n+1} + C_2H_2 \rightarrow C_{n+2}H_{n+3}$		[MB17]

It was suggested that the products depended on the reaction temperatures. At high temperatures, vinyl radicals would largely decompose and the chain would be carried by hydrogen atoms and C_2H. Decomposition of C_4H_3 would be more important than addition

to acetylene molecules. Thus, diacetylene would be the primary product. This agreed with the observation of Gay et al.[38] In the intermediate temperature region, vinyl radicals would be more important than C_2H, and the products should be vinylacetylene, ethylene, butadiene, etc. At low temperatures, further addition reactions would dominate the reaction, and form higher molecular weight products, such as C_6 and C_8 products. However, the product molecules were predicted not to be too large, because of the ease of C-C bond fission in larger radicals. The formation of methane and other products containing an odd number of carbon atoms was accounted for by isomerization, such as a 1,5 hydrogen shift, followed by the dissociation of radicals.

By assuming a steady state and a long chain reaction, expressions for the rates of formation of various products formed in different temperature regions were derived by Back. The order was predicted to be two, in agreement with many observations. In addition, the overall rate constant was estimated and was found to be in reasonable agreement with various workers' experimental results. Back believed that this mechanism should work in a wide temperature range, from 600 K to 2,400 K. She did not believe the transition region[18] around 1,000 K in the Arrhenius plot was caused by an entire change of reaction mechanism, but believed the explanation was the large errors in rate constants from acetylene pyrolysis.

Also, Back explained an alternative initiation step suggested by Gay et al.[38] and by Cullis and Read,[39] $2C_2H_2 \rightarrow C_4H_3 + H$, which is kinetically indistinguishable from reaction [MB1], as the occurrence of reactions [MB1], [MB2], and [MB3] in series.

1-5-3. A free radical mechanism dominated by C_4H_3 and H

In 1980, Tanzawa and Gardiner (TG) extended the proposals of Gay et al.[38] and Cullis et al.,[39] and proposed a complete radical mechanism dominated by C_4H_3 and H.[12]

From the distributions of the products of acetylene pyrolysis, they believed that different types of chain reactions occurred at low and high temperatures. At low temperatures, the primary product was vinylacetylene; while at high temperatures diacetylene and hydrogen were primary products. They recognized that it was necessary to propose a set of elementary reactions to account quantitatively for the rates over the wide temperature ranges which had been studied experimentally.

The complete chain mechanism was compiled as follows.

$C_2H_2 + M \rightarrow C_2H + H + M$ [TG1]

$C_2H_2 + C_2H_2 \rightarrow C_4H_3 + H$ [TG2]

$H + C_2H_2 \rightarrow C_2H_3$ [TG3]

$C_2H_3 + C_2H_2 \rightarrow C_4H_4 + H$ [TG4]

$C_4H_3 + H + M \rightarrow C_4H_4 + M$ [TG5]

$C_2H + H_2 \rightarrow C_2H_2 + H$ [TG6]

$C_2H + C_2H_2 \rightarrow C_4H_2 + H$ [TG7]

$C_2H + C_4H_4 \rightarrow C_2H_2 + C_4H_3$ [TG8]

$C_4H_3 + M \rightarrow C_4H_2 + H + M$ [TG9]

$C_4H_2 + M \rightarrow C_4H + H + M$ [TG10]

$C_2H + C_4H_2 \rightarrow C_6H_2 + H$ [TG11]

$C_4H + C_2H_2 \rightarrow C_6H_2 + H$ [TG12]

$C_6H + C_2H_2 \rightarrow C_8H_2 + H$ [TG13]

$C_2H + C_6H_2 \rightarrow C_8H_2 + H$ [TG14]

$C_4H_2 + C_4H \rightarrow C_8H_2 + H$ [TG15]

$C_6H_2 + M \rightarrow C_6H + H + M$ [TG16]

$C_8H_2 + M \rightarrow C_8H + H + M$ [TG17]

$H_2 + M \rightarrow H + H + M$ [TG18]

Reactions [TG1] and [TG2] were initiation reactions. [TG1] was important at high temperatures, and [TG2] was important at low temperatures.

At low temperatures and early stages of the pyrolysis, the chain propagation reactions were reactions [TG3], [TG4], and [TG5], which formed vinylacetylene as the primary product. Reactions [TG6], [TG7], [TG9], and [TG10] were the main chain propagation reactions at high temperatures and low conversions, and produced diacetylene and hydrogen as primary products. At high temperatures and high conversions, reactions [TG11]-[TG18] would occur to form polyacetylenes.

A modeling study was performed by these authors. The experimental data came from their high-temperature shock-tube study of acetylene pyrolysis at 1500-3400 K,[43] Palmer and Dormish's flow reactor study at 1330-1530 K,[18] Munson and Anderson's flow reactor study at 770-1120 K,[29] and Silcocks' bulb pyrolysis results at 625-745 K.[23] A good match was achieved between modeling and experiment from 625 to 3400 K.

TG found the initiation reaction in Back's mechanism[11] could not be considered as an alternative to reaction [TG2], because the modeling results otherwise would not agree

with the reported mass-spectrometric results. They likewise omited consideration of triplet C_2H_2[25,52,53] as an initiation product.

The authors believed their mechanism and the rate constants proposed could provide satisfactory descriptions of the rates of appearance of the initial products. However, some problems, such as the identity and rates of the secondary reactions leading to polymer formation at low temperatures and carbon formation at high temperatures, and the role of falloff in the unimolecular reactions at low pressures, were not solved.

1-5-4. The molecular mechanism initiated by the isomerization of acetylene to form vinylidene

Duran, Amorebieta, and Colussi (DAC)[15] argued that the apparent success of previously proposed mechanisms relied critically on early data for the heats of formation of vinyl and ethynyl radicals, as well as on the arbitrary assignment of falloff effects for radical addition, decomposition, and combination reactions. They believed the heats of formation were seriously in error. Thus, they modeled a set of free radical chain reactions, which was very similar to Tanzawa and Gardiner's, and Back's free radical mechanisms, using updated thermodynamic data and considering the falloff effects on unimolecular reactions. By comparing their modeling results to the experimental results in yield plots and in Arrhenius plots, they concluded that the results did not agree at all. The modeled rates fell short by several orders of magnitude compared to the experimental values.

Hence, they believed that free radical mechanisms were qualitatively and quantitatively unacceptable as realistic descriptions of acetylene pyrolysis.

Therefore, DAC proposed a molecular mechanism. They suggested that the acetylene molecule could initially convert to an active species, singlet vinylidene, which was thermodynamically in equilibrium with the acetylene molecule, and then vinylidene could add to acetylene to form vinylacetylene. The scheme can be shown as follows,

$C_2H_2 \rightleftharpoons H_2C{=}C:$ [DAC1]

$H_2C{=}C: + C_2H_2 \rightarrow C_4H_4$ [DAC2]

The authors proposed three independent pieces of information to support their proposal. The first one was that *ab initio* calculations predicted the heat of formation of vinylidene to be 167 kJ/mol above that of acetylene, as required.[54,55] Next, DAC's studies[32] of the thermal reactions of acetylene with benzene or with toluene were said to reveal that the reactions were additions, instead of radical displacements, and the second order rate constants were almost identical with those measured in pure acetylene at the same temperatures. Finally, vinylidene was assumed to be formed in the high-temperature decomposition of methylenecyclopropane.[56]

1-5-5. The free radical chain mechanism initiated by acetone impurity in acetylene

This mechanism was proposed by Colket, Seery, and Palmer (CSP) in 1989.[13] They returned to a free radical chain mechanism, because they pointed out that the lifetime of

vinylidene was too short compared to the experimental auto-acceleration periods, although they could not disprove a contribution from vinylidene.

On the other hand, CSP reviewed TG's mechanism[12] and concluded that the initiation reaction, $C_2H_2 + C_2H_2 \rightarrow C_4H_3 + H$, was too slow. Therefore, they proposed initiation by acetone, an impurity in acetylene. The initiation rate from acetone was said to be several times larger than TG's initiation reaction even though the concentration of acetone in acetylene dropped to 0.1% after purification by different methods and by different workers. Thus, they believed a trace amount of acetone could readily generate enough methyl radicals, which in turn could easily convert to hydrogen atoms. Therefore, the pyrolysis of acetylene could be significantly accelerated by initiation from acetone. A new mechanism was given as,

$CH_3COCH_3 \rightarrow CH_3CO + CH_3$ [CSP1]

$CH_3CO \rightarrow CH_3 + CO$ [CSP2]

$CH_3 + C_2H_2 \rightarrow CH_3CHCH$ [CSP3]

$CH_3CHCH \rightarrow C_3H_5$ (allyl) [CSP4]

$C_3H_5 + C_2H_2 \rightarrow C_5H_7$ [CSP5]

$C_5H_7 \rightarrow C_5H_6 + H$ [CSP6]

$C_2H_2 + C_2H_2 \rightarrow C_4H_3 + H$ [CSP7]

$H + C_2H_2 \rightarrow C_2H_3$ [CSP8]

$C_2H_3 + C_2H_2 \rightarrow C_4H_4 + H$ [CSP9]

$C_2H_3 + C_2H_3 \rightarrow C_4H_6$ [CSP10]

$2C_3H_5 \rightarrow C_3H_6 + C_3H_4$ [CSP11]

$H + C_3H_4 \rightarrow CH_3CHCH$ [CSP12]

$H + C_3H_4 \rightarrow C_3H_5$ [CSP13]

$C_3H_5 + C_2H_3 \rightarrow C_5H_8$ [CSP14]

$C_3H_5 + H \rightarrow C_3H_6$ [CSP15]

$CH_3 + C_2H_2 \rightarrow CH_4 + C_2H$ [CSP16]

$2CH_3 \rightarrow C_2H_6$ [CSP17]

$2CH_3 \rightarrow C_2H_5 + H$ [CSP18]

$C_2H_6 + CH_3 \rightarrow C_2H_5 + CH_4$ [CSP19]

$C_2H_5 \rightarrow C_2H_4 + H$ [CSP20]

$CH_3 + CH_3COCH_3 \rightarrow CH_4 + CH_2CO + CH_3$ [CSP21]

$H + CH_3COCH_3 \rightarrow H_2 + CH_2CO + CH_3$ [CSP22]

$C_2H_3 + CH_3COCH_3 \rightarrow C_2H_4 + CH_2CO + CH_3$ [CSP23]

$CH_2CO \rightarrow CH_2 + CO$ [CSP24]

$CH_3 + H \rightarrow CH_2 + H_2$ [CSP25]

$CH_3 + CH_2 \rightarrow C_2H_4 + H$ [CSP26]

$2CH_2 \rightarrow C_2H_2 + H_2$ [CSP27]

$CH_2 + C_2H_2 \rightarrow C_3H_3 + H$ [CSP28]

$2C_3H_3 \rightarrow C_6H_6$ [CSP29]

$CH_2CO + H \rightarrow CH_3 + CO$ [CSP30]

$CH_2CO + CH_3 \rightarrow C_2H_5 + CO$ [CSP31]

With the above reactions, CSP modeled Munson and Anderson's experimental data in the temperature range of 973-1073 K. By combining the above reactions with 53 other

reactions at higher temperatures, they also modeled the shock tube experimental data of Ogura in the temperature range of 1000-1670 K,[41] and those of Wu, Singh and Kern over the temperature range of 1900-2500 K.[48] The modeling results were close to the experimental data. In addition, the modeling gave an activation energy of 167 kJ/mol and a steady-state analysis using reactions from [CSP1] to [CSP10] gave a reaction order of 1.5 for the overall reaction. The activation energy was consistent with previous experiments, while the reaction order was lower than the usually assumed value of 2. However, the results of CSP's literature review suggested the experimental reaction order should have been reported as 1.5 instead of 2.

Finally, the authors' conclusion was that acetone could dominate the initiation, although they could not rule out the participation of vinylidene or another nonchain mechanism.

1-5-6. The combined molecular/radical mechanism

In 1990 Kiefer and Von Drasek proposed a combined molecular/radical mechanism.[16] They criticized the proposal that the pyrolysis was dominated by free radical chain reactions at low temperatures because the initiation rate was said to be thermochemically too slow for the observed experimental results. Also, they did not believe acetone could initiate radical chain reactions because acetone deliberately added in a low-temperature experiment showed no effect on the pyrolysis of acetylene,[24] and the experimental results[20] with pure acetylene produced from water and metal carbide agreed with other

work. The inhibition by NO observed by many researchers made Kiefer and Von Drasek believe that a combined molecular and free radical mechanism was more reasonable.

At low temperatures (T < 1100 K), they proposed a revised molecular mechanism with radical character, which was similar to DAC's vinylidene mechanism.[15]

$$C_2H_2 \rightleftharpoons H_2C{=}C: \qquad [KV1]$$

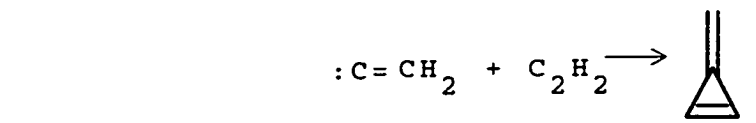

[KV2]

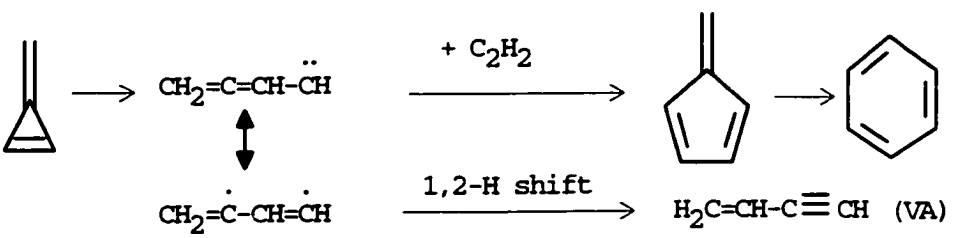

[KV3]

In the low temperature range, any free radical chain initiated by the following reaction,

$$2C_2H_2 \longrightarrow (\cdot C_4H_4 \cdot) \longrightarrow C_4H_3 + H \qquad [KV4]$$

was suppressed by stabilization of the intermediate $\cdot C_4H_4\cdot$. So, the molecular polymerization mechanism dominated in these conditions.

At intermediate temperatures (1100-1800 K), the reactions were still dominated by molecular reactions. Vinylacetylene, C_4H_4, was formed in the above molecular mechanism. Diacetylene, C_4H_2, was formed by the molecular mechanism,

$$C_2H_2 \rightleftharpoons H_2C{=}C: \qquad [KV1]$$

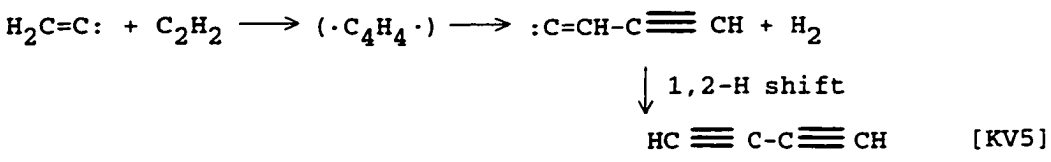

[KV5]

However, a free radical chain mechanism started to make a significant contribution for the formation of C_4H_4, C_2H_4 and C_6H_2 etc.,

$$2C_2H_2 \longrightarrow C_4H_3 + H \qquad [KV4]$$

$$C_2H_2 + H + M \longrightarrow C_2H_3 + M \qquad [KV6]$$

$$C_2H_3 + C_2H_2 \longrightarrow C_4H_4 + H \qquad [KV7]$$

The authors could not determine the contribution from the free radical mechanism because of uncertainties in key rates, especially termination rates, and the possibility of initiation by an impurity.

At high temperatures (T > 1800 K), the pyrolysis was dominated by a free radical chain mechanism carried by C_2H and H, and initiated by either,

$$2C_2H_2 \longrightarrow C_4H_3 + H \qquad [KV4]$$

or, for very high temperatures,

$$M + C_2H_2 \longrightarrow C_2H + H + M \qquad [KV8]$$

which was similar to Tanzawa and Gardiner's mechanism.[12] The principal remaining uncertainty in the modeling of this temperature range was the heat of formation of the ethynyl radical, C_2H.

Kiefer and Von Drasek used the above, combined molecular/radical mechanism, composed of 40 reactions, to model the shock-tube experimental results of Ogura from 1000 to 1670 K,[41,42] those of Colket at 1100-2300 K[47] and those of Wu, Singh and Kern

(WSK) at 1900-2500 K.[48] Ogura's results for the major products, C_4H_4 and C_4H_2, could be modeled well, but the modeling for the minor products, C_2H_4, allene, propyne and CH_4, seems very poor. Also, the modeling of the data of Colket[47] and of Wu et al.[48] was not satisfactory.

1-5-7. The free radical mechanism involving 1,4-diradicals

In 1992 Benson proposed a free radical mechanism dominated by 1,4-diradicals.[14] First of all, Benson ruled out the vinylidene mechanism due to the following difficulties: (1) Based on the mechanism of DAC, the derived concentration of vinylidene was too small to play a significant role in the pyrolysis of acetylene. (2) The vinylidene mechanism could not explain the auto-acceleration period and the effects of NO.

On the other hand, Benson argued that the free radical mechanism could not be initiated by the reaction [TG2],

$$C_2H_2 + C_2H_2 \rightarrow C_4H_3 + H \qquad \text{[TG2]}$$

due to the predicted low rate of this reaction. Based on the fact that vinylacetylene and styrene could accelerate the pyrolysis of acetylene,[57,58] Benson proposed that both acetylene and vinylacetylene (and other products at high conversions) could initiate the pyrolysis of acetylene. Thus, a new mechanism was proposed as,

(i) initiation

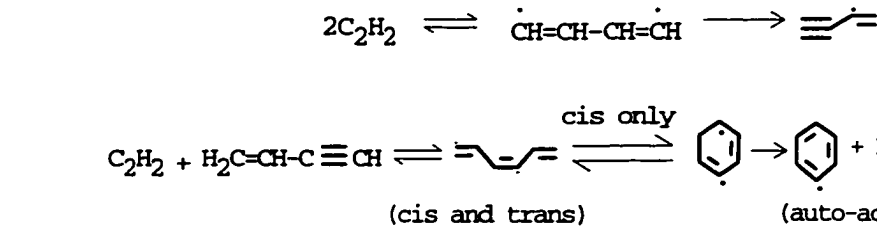

[B1]

[B2]

(cis and trans) (auto-acceleration)

(ii) propagation

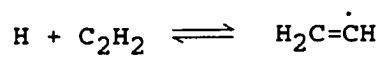

[B3]

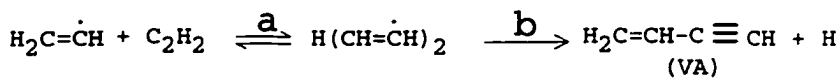

[B4]

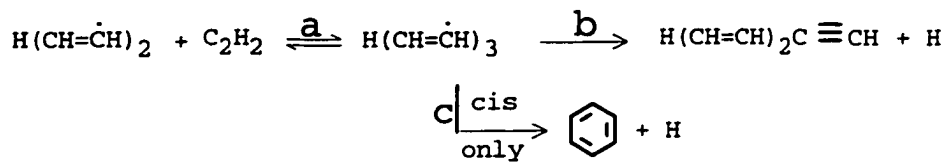

[B5]

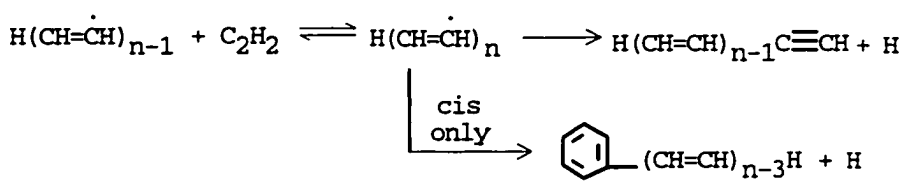

[B(n+2)]

(iii) termination

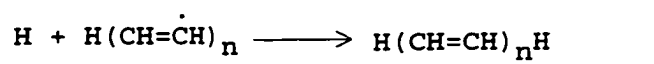

[Bt1]

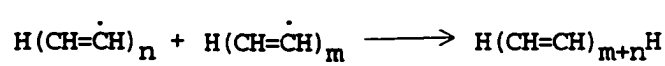

[Bt2]

In this mechanism, the radical chain was mainly carried by hydrogen atoms. In both of the initiation reactions, free radicals were formed through diradicals. Benson estimated the rate constant of initiation reaction [B2] was 10^5 times larger than that of reaction [B1] at 1000 K, so a trace amount of vinylacetylene would make reaction [B2] competitive with reaction [B1]. At higher conversions, Benson believed other polyenes could also produce radicals by bimolecular addition to acetylene. Thus, the reaction was accelerated by products.

Among the chain propagation reactions, two reactions could compete with the addition of a growing radical to acetylene. One is the dissociation of radicals to form hydrogen atoms and polyenes with a triple bond at one end. This reaction was said to be important above 900 K. Another competitive type of reaction would be the cyclization of radicals ($n > 3$) with cis geometry at the C_3-C_4 position. These reactions could regenerate H-atoms and would be important at all temperatures, since unimolecular cyclization is very fast compared to bimolecular propagation. Benson believed that above 700 K all cis radicals ($n > 3$) would cyclize rather than propagate.

Based on this mechanism, Benson estimated the rates of initiation and polymerization, the auto-acceleration period, and the chain length, using measured and estimated rate constants. Then he compared his results to experimental data. The general agreement between the estimated values and the reported data was good. However, the predicted reaction order for polymerization was 3/2 rather than the order of 2 reported by many workers. Benson predicted the actual reaction order would be close to 2, since he expected that the rate constant of reaction [B3] would be in its fall-off region and, hence, nearly proportional to the concentration of acetylene.

However, Kiefer[17] said that there were fatal problems in Benson's mechanism, mainly in the formation of vinylacetylene and in the initiation reaction. First, Kiefer pointed out that yields of vinylacetylene observed by Ogura[41] in shock-tube experiments were too high for Benson's mechanism to interpret. Secondly, Kiefer argued, based on thermochemical estimation, that Benson's second initiation step [B2] was too slow to play an important role. Although Benson suggested that in the initiation reaction [B2] the isomerization from the adduct C_6H_6 to benzene was exothermic enough to break the C-H bond and form C_6H_5 + H, Kiefer argued that "the most likely fate of the initial adduct C_6H_6 is a fast, highly exothermic isomerization to benzene....., followed by deactivation". In addition, Kiefer said that the auto-acceleration periods could be explained by a molecular reaction between acetylene and vinylacetylene to form benzene, and that the reaction between nitric oxide and acetylene was too complicated to serve as evidence for the involvement of free radicals.

1-6. Summary

The pyrolysis of acetylene has been studied for many years, but the reaction mechanism is not clear, especially at low temperatures.

Most of experimental studies using static and flow systems were performed between 1929 and 1965. Most of the experimental investigations using shock tube techniques occurred during the decades from 1960 to 1990. After 1990, many studies[13,16,59,60] have focused on kinetic modeling of experimental data to find the correct reaction mechanism.

At high temperatures, above 1500K, there is a consensus that the process has a free radical chain mechanism, although the proposed schemes are not exactly the same. However, the reaction mechanism at low temperatures is still a mystery. Both a free radical mechanism and a molecular mechanism have been proposed. Some researchers preferred a free radical chain mechanism. The proposed chain mechanisms have similar schemes, but the initiation reaction is the focus of controversy. Back's initiation reaction

$$C_2H_2 + C_2H_2 \rightarrow C_2H + C_2H_3 \qquad [MB1]$$

and Tanzawa and Gardiner's initiation reactions,

$$C_2H_2 + M \rightarrow C_2H + H + M \qquad [TG1]$$

$$C_2H_2 + C_2H_2 \rightarrow C_4H_3 + H \qquad [TG2]$$

were considered to be too slow, but those reactions may occur to some extent at certain experimental conditions. Initiation by acetone is uncertain and will be thoroughly studied in our work. The latest mechanism was proposed by Benson and seems more reasonable although Kiefer still argued vigorously against it. More experimental evidence is needed to test it. On the other hand, Kiefer, Colussi and Kern have supported a molecular mechanism. Vinylidene may be involved in the process, but may not play a predominant role. This suggestion could be tested by seeking an induction period, caused by the buildup of the steady-state concentrations of active intermediates. Minkoff's mechanism is too simple to account for the formation of various observed products.

The earlier experiments in the middle of last century did not provide enough high-quality data on the pyrolysis of acetylene at low temperatures.

Most workers used static reaction vessels combined with measurements of pressure change and gas analysis. The disadvantages of these vessels are the presence of large dead

volumes, and the time required for the temperature and pressure to reach equilibrium values and for valves to be turned to admit or remove gases. Thus, a static reaction vessel is only suitable for slow reactions at low temperatures, with reaction times greater than 1 minute. Measurements of pressure change alone can result in considerable errors due to assumptions regarding the products formed. In addition, the methods of gas analysis employed by the earlier workers were not accurate. The errors in the experimental data obtained with static vessels were much larger than those with flow reactors and shock tubes. Benson[14] said that the most extensive work which had been done at low temperatures (573-973K) was that of Frank-Kamenetzky.[22] However, the activation energy proposed by Frank-Kamenetzky, 125 kJ/mol, is much lower than most workers' values, which are between 167 and 188 kJ/mol. Moreover, Benson[14] found the rate constants proposed by Frank-Kamenetzky did not agree with others.

Flow reactors are suitable for studies of both fast reactions and slow reactions. Some workers used flow reactors and gas chromatography or mass spectrometry to study the pyrolysis of acetylene at low temperatures. Those experiments were carried out in the 1960s, when techniques of gas chromatography and mass spectrometry were not as well developed. This would cause difficulties in analysis of products from the very complicated process of acetylene pyrolysis. The lowest conversion was 0.6%, but typical conversions in these experiments were more than 10%. The more important fact is that no worker has deeply studied the pyrolysis of acetylene over wide ranges of pressure and temperature. This thesis is intended to fill this gap.

Until now, only Ogura[41] performed shock tube experiments at low conversions, but with a fixed reaction time of about 1 millisecond over the temperature range 1000-1670 K. Therefore, he could not observe any induction periods.

In the present work, surface reactions will be studied first, because any involvement of surface reactions will make the process of pyrolysis very complicated and will make it very difficult to measure reproducible data for homogeneous reactions. Many results obtained by previous workers were affected by surface reactions. Surface reactions could be more significant in the present work, because reactors of small diameters will be used extensively. After surface reactions are understood, procedures will be developed to suppress surface reactions.

After reliable, experimental methods are established, experiments will be carried out at low conversions, down to a few ppm, using micro-reactors to search for an induction period, of a few milliseconds, caused by the buildup of the steady-state concentrations of free radicals. Such an induction period would be completely different from the auto-acceleration periods observed by previous workers at 2-20% conversions and reaction times of 12 seconds and up. The former induction period would be crucial evidence to distinguish between free radical mechanisms and molecular mechanisms, because the induction period resulting from the gradual buildup of highly unstable intermediates such as vinylidene would be too short to be observed in flow systems. As well, if an induction period of a few milliseconds is observed, information regarding the order of initiation, the product of the rate constants for initiation and for termination, and rate constants for some key propagation steps will be obtained.

Study of the pyrolysis of acetylene doped with small amounts of neopentane or acetone, two known sources of free radicals, will provide more information regarding the mechanism. Similar acceleration factors for formation of vinylacetylene and benzene will be another key piece of evidence to support free radical mechanisms. The order and the rate constant of the initiation reaction could be measured, as well.

The last project will involve a search for minor products besides vinylacetylene and benzene. Different mechanisms predicted different products as primary and secondary products. A few workers observed various, minor products at high conversions, where it was very difficult to identify primary and secondary products. Experiments will be performed using micro-reactors and capillary GC and GC-MS at low conversions. A study of minor products should provide more information regarding mechanisms of the reaction.

In the rest of the thesis, flow systems and experimental procedures will be introduced first in Chapter 2. Surface reactions will be discussed in Chapter 3. A study of induction periods will be described in Chapter 4, and an acceleration by neopentane will be described in Chapter 5. A study of minor products will be detailed in Chapter 6. A summary of the thesis will be given in Chapter 7. Data obtained in the addition of small amounts of additives will be presented in the appendix.

References for Chapter 1

1. S.J.Harris and A.M.Weiner, *Annu.Rev.Phys.Chem.*, 1985, **36**, 31.
2. H.Bohm and H.Jander, *Phys.Chem.Chem.Phys.*, 1999, **1**, 3775.
3. M.Frenklach, D.W.Clary, W.C.Gardiner Jr., and S.E.Stein, *Twentieth Symposium (International) on Combustion, The Combustion Institute, Pittsburgh, PA*, 1985, 887.
4. M.Frenklach, *Twenty-Second Symposium (International) on Combustion, The Combustion Institute, Pittsburgh, PA*, 1988, 1075.
5. R.D.Kern and K.Xie, *Prog.Energy Combust.Sci.*, 1991, **17**, 191.
6. M.Terrones, W.K.Hsu, H.W.Kroto, and D.R.M.Walton, *Top Curr.Chem., Berlin, Springer-Verlag*, 1999, p. 189.
7. Z.W.Pan, S.S.Xie, B.H.Chang, L.F.Sun, W.Y.Zhou, and G.Wang, *Chem.Phys.Lett.*, 1999, **299**, 97.
8. X.Y.Zhang, L.D.Zhang, M.J.Zheng, G.H.Li, and L.X.Zhao, *J.Cryst.Growth*, 2001, **223**, 306.
9. C.J.Lee and J.Park, *J.Phys.Chem.B*, 2001, **105**, 2365.
10. R.N.Pease, *J.Am.Chem.Soc.*, 1929, **51**, 3470.
11. M.H.Back, *Can.J.Chem.*, 1971, **49**, 2199.
12. T.Tanzawa and W.C.Gardiner Jr., *J.Phys.Chem.*, 1980, **84**, 236.
13. M.B.Colket III, D.J.Seery, and H.B.Palmer, *Combustion and Flame*, 1989, **75**, 343.
14. S.W.Benson, *Int.J.Chem.Kinet.*, 1992, **24**, 217.
15. R.P.Duran, V.T.Amorebieta, and A.J.Colussi, *J.Phys.Chem.*, 1988, **92**, 636.
16. J.H.Kiefer and W.A.Von Drasek, *Int.J.Chem.Kinet.*, 1990, **22**, 747.
17. J.H.Kiefer, *Int.J.Chem.Kinet.*, 1993, **25**, 215.
18. H.B.Palmer and F.L.Dormish, *J.Phys.Chem.*, 1964, **68**, 1553.
19. S.T.Dimitrijevic, S.Paterson, and P.D.Pacey, *J.Anal.& Appl.Pyrolysis*, 2000, **53**, 107.
20. H.A.Taylor and A.von Hook, *J.Phys.Chem.*, 1935, **39**, 811.

21. H.D.Burnham and R.N.Pease, *J.Am.Chem.Soc.*, 1942, **64**, 1404.

22. D.A.Frank-Kamenetzky, *Acta Physicochim.U.R.S.S.*, 1943, **18**, 148.

23. C.G.Silcocks, *Proc.Roy.Soc.(London)*, 1957, **A242**, 411.

24. G.J.Minkoff, D.M.Newitt, and P.Rutledge, *J.Appl.Chem.*, 1957, **7**, 406.

25. G.J.Minkoff, *Can.J.Chem.*, 1958, **36**, 131.

26. C.F.Cullis, G.J.Minkoff, and M.A.Nettleton, *Trans.Faraday Soc.*, 1962, **58**, 1117.

27. F.G.Stehling, J.D.Frazee, and R.C.Anderson, *8th Symp.(Int.) on Combust., Williams and Wilkins, Baltimore*, 1962, p. 774.

28. M.S.B.Munson and R.C.Anderson, *J.Phys.Chem.*, 1963, **67**, 1582.

29. M.S.B.Munson and R.C.Anderson, *Carbon*, 1963, **1**, 51.

30. K.C.Hou and R.C.Anderson, *J.Phys.Chem.*, 1963, **67**, 1579.

31. C.F.Cullis and N.H.Franklin, *Roy.Soc.(London)*, 1964, **A280**, 139.

32. R.P.Duran, V.T.Amorebieta, and A.J.Colussi, *J.Am.Chem.Soc.*, 1987, **109**, 3154.

33. A.Becker and K.J.Huttinger, *Carbon*, 1998, **36**, 177.

34. W.J.Hooker, *7th Symp.(Int.) on Combust., Butterworths, London*, 1959, p. 949.

35. T.Kruse and P.Roth, *J.Phys.Chem.A* , 1997, **101**, 2138.

36. G.B.Skinner and E.M.Sokoloski, *J.Phys.Chem.*, 1960, **64**, 1952.

37. C.F.Aten and E.F.Greene, *Combust.Flame*, 1961, **5**, 55.

38. I.D.Gay, G.B.Kistiakowsky, J.V.Michael, and H.Niki, *J.Chem.Phys.*, 1965, **43**, 1720.

39. C.F.Cullis and I.A.Read, *Trans.Faraday Soc.*, 1970, **66**, 920.

40. A.F.Bopp and R.D.Kern, *J.Phys.Chem.*, 1975, **79**, 2579.

41. H.Ogura, *Bull.Chem.Soc.Jpn.*, 1977, **50**, 1044.

42. H.Ogura, *Bull.Chem.Soc.Jpn.*, 1977, **50**, 2051.

43. T.Tanzawa and W.C.Gardiner Jr., *17th Symp.(Int.) on Combust., The Combustion Institute, Pittsburgh*, 1978, p. 563.

44. R.B.Cundall, D.E.Fussey, A.J.Harrison, and F.Lampard, *J.Chem.Soc.Faraday Trans.1*, 1978, **74**, 1403.

45. P.Frank and Th.Just, *Combustion and Flame*, 1980, **38**, 231.

46. A.Bar-Nun and J.E.Dove, *12th Symp.on Shock Tubes and Waves, Magnes Press, Jerusalem*, 1980, p. 457.

47. M.B.Colket III, *Twenty-First Symposium (International) on Combustion, The Combustion Institute, Pittsburgh, PA*, 1986, 851.

48. C.H.Wu, H.J.Singh, and R.D.Kern, *Int.J.Chem.Kinet.*, 1987, **19**, 975.

49. P.D.Pacey, S.Paterson, and S.T.Dimitrijevic, *23rd Biennial Conference on Carbon, The American Carbon Society, University Park, PA*, 1997, **II**, 320.

50. P.J.Flory, *J.Am.Chem.Soc.*, 1937, **59**, 241.

51. M.L.Boyd, T.M.Wu, and M.H.Back, *Can.J.Chem.*, 1968, **46**, 2415.

52. C.S.Burton and H.Hunziker, *J.Chem.Phys.*, 1972, **57**, 399.

53. R.W.Wetmore and III H.F.Schaefer, *J.Chem.Phys.*, 1978, **69**, 164.

54. J.S.Binkley, *J.Am.Chem.Soc.*, 1984, **106**, 603.

55. A.C.Scheiner and H.F.Schaefer III, *J.Am.Chem.Soc.*, 1985, **107**, 4451.

56. P.Davison, H.M.Frey, and R.Walsh, *Chem.Phys.Lett.*, 1985, **120**, 227.

57. C.Chanmugathas and J.Heicklen, *Int.J.Chem.Kinet.*, 1986, **18**, 701.

58. C.Chanmugathas and J.Heicklen, *Int.J.Chem.Kinet.*, 1987, **19**, 659.

59. J.H.Kiefer, S.S.Sidhu, R.D.Kern, K.Xie, H.Chen, and L.B.Harding, *Combust.Sci.Technol.*, 1992, **82**, 101.

60. J.N.Bradley and K.O.West, *J.Chem.Soc.Faraday Trans.1*, 1976, **72**, 8.

CHAPTER 2. EXPERIMENTAL TECHNIQUE AND APPARATUS

2-1. Linear flow technique

The linear flow technique is a very important laboratory method for pyrolysis reactions and has been used by various researchers.[1,2] In this technique, a reactant flows through a heated tubular reactor, in which the temperature, the pressure and the flow rate of gas are well controlled. The residence time of the gas can be calculated by dividing the amount of gas in the reactor by the flow rate of the gas entering the reactor. The products coming from the reactor can by analyzed by chromatography and other methods.

In the use of this kind of reactor, it is customary to assume that (a) gas entering the reactor can be warmed up to the reaction temperature instantaneously, (b) the gas mixture coming from the reactor can be quenched instantaneously at the outlet of the reactor, (c) all the molecules have the same residence time in the reactor, and (d) there is no pressure drop along the reactor. It is necessary to make these assumptions because of the complexity of many reactions. In fact, gas cannot warm up at the inlet and quench at the outlet instantaneously, due to incomplete radial heat transfer. Also, molecules have different residence times because of the axial and radial diffusion. In addition, the pressure drop is significant at a high flow rate or in a long and narrow reactor. However, those disadvantages can be minimized to an acceptable extent. We will discuss the disadvantages in turn.

2-1-1. Incomplete radial heat transfer

The temperature at the surface of the reactor can be controlled very well. However, when a gas flows into a tubular reactor, it will travel a distance from the inlet of the reactor before it reaches the reaction temperature, and a distance to cool down and stop the reaction at the outlet. This is caused by incomplete radial heat transfer. When an experiment is carried out, this is a source of error.

This question has been studied by some researchers.[2,3] Mulcahy and Pethard[3] derived an equation for a first order reaction,

$$\frac{k_{app}}{k} = \{1 - \frac{r^2}{3.658\kappa\ t}[0.577 + \ln(\frac{0.82E_A(T_s - T_0)}{RT_s^2})]\} \qquad \text{(E2-1)}$$

Here, k_{app} is the apparent first order rate constant with incomplete radial heat transfer; k, the true first order rate constant without the influence of incomplete radial heat transfer; r, the radius of the reactor; κ, the coefficient of thermal diffusivity; t, the residence time; E_A, the activation energy; T_s, the temperature of the reactor wall; and T_0, the temperature of the entering reactant.

The flow rate of the reactant A, $\Delta n/\Delta t$, can be calculated as,

$$\frac{\Delta n}{\Delta t} = \frac{n}{t} = \frac{[A] \times \pi\ r^2 L}{t} \qquad \text{(E2-2)}$$

where, n is the number of moles of the reactant in the reactor; L, the length of the reactor; and $[A]$, the concentration of the reactant A in the reactor.

The coefficient of thermal diffusivity is given by,

$$\kappa = \frac{\lambda}{[A]C_p} \tag{E2-3}$$

where C_p is the molar heat capacity at constant pressure; and λ, the thermal conductivity of the gas.

Combining equations (E2-2) and (E2-3) to cancel [*A*] gives,

$$\frac{r^2}{\kappa\, t} = \frac{\Delta n}{\Delta t} \times \frac{C_p}{\pi\ \lambda\ L} \tag{E2-4}$$

Substitution of equation (E2-4) in (E2-1) gives,

$$\frac{k - k_{app}}{k} = \frac{\Delta n}{\Delta t} \times \frac{C_p}{3.658\pi\ \lambda\ L} \times [0.577 + \ln\frac{0.82(T_s - T_0)E_A}{RT_s^2}] \tag{E2-5}$$

The fractional experimental error caused by incomplete radial heat transfer, $(k\text{-}k_{app})/k$, should be less than 5%. Thus,

$$\frac{\Delta n}{\Delta t} \times \frac{C_p}{3.658\pi\ \lambda\ L}[0.577 + \ln\frac{0.82(T_s - T_0)E_A}{RT_s^2}] \le 5\%$$

That is,

$$\frac{\Delta n}{\Delta t} \le \frac{5\% \times 3.658\pi\ \lambda\ L}{C_p[0.577 + \ln\frac{0.82(T_s - T_0)E_A}{RT_s^2}]} \tag{E2-6}$$

A typical reaction temperature in this work is 981.6 K. The ratio of λ/C_p at 981.6 K, 1.633×10^{-3} mol $m^{-1}s^{-1}$, can be estimated by extrapolating the λ/C_p values[4] at 300K-600 K to that at 981.6 K. The length of our reactor, *L*, is 0.1 meter. The activation energy, E_A, is 155 kJ/mol.[5] The values of T_s and T_0 are 981.6 K and 298 K, respectively. Substitution of those parameters in equation (2-6) leads to,

$$\frac{\Delta n}{\Delta t} \le \frac{5\% \times 3.658\pi \times 1.633 \times 10^{-3} \times 0.10}{[0.577 + \ln \frac{0.82(981.6K - 298K) \times 154800}{8.314 \times 981.6^2}]} \quad \text{(E2-7)}$$

$= 3.16 \times 10^{-5}$ (mol.s^{-1}) = 42.5 (sccm) = 73.3 (sccm, N_2 equivalent)

Here, sccm is the unit for the flow rate of a gas in standard cubic centimeter per minute.

The flow rate range of our mass flow controller is 0-50 sccm (N_2, equivalent), which is much less than 73.3 (sccm, N_2 equivalent), so incomplete radial heat transfer is negligible in our experiments.

2-1-2. Mass transfer

As mentioned above, when the reactant passes through a reactor, it is assumed that all the gas molecules spend the same length of time in the reactor. Actually, the occurrence of the reaction causes a decrease in the concentration of reactant along the reactor. Thus, a concentration gradient of the reactant can be formed in the reactor, which in turn causes axial diffusion of the reactant toward the exit. The residence time for the reactant would be shorter than the calculated value from equation (E2-2).

On the other hand, the parabolic velocity profile in the reactor could cause radial diffusion of the reactant.

Furue and Pacey[2] investigated the effect of mass transfer in the pyrolysis of cyclopropane in cylindrical flow reactors and found that the apparent first order rate constant could be reduced by 10% only at a conversion of 83% or more. Hence, effect of the mass transfer is negligible at very low conversions.

2-1-3. Volume contraction

When a reaction occurs in a reactor, the total number of moles of gas in the reactor may change. Any decrease in the number of moles would result in a volume contraction. In this case, the molecules in the reactor would leave the reactor slower. Thus, the actual residence time of molecules in the reactor would be longer than the value calculated from the flow rate, pressure, and temperature in the reactor. Therefore, volume contraction can cause errors, especially at high conversions, in which the residence time would be multiplied by a correction factor. However, the effect of volume contraction is negligible at very low conversions. Therefore, it is not necessary to worry about this in our low conversion experiments.

2-1-4. Pressure drop

Flowing a gas through a reactor can cause a pressure drop along the reactor, because there is friction between the reactor wall and a moving gas, especially at high flow rates. The magnitude of the pressure drop, which can be measured readily by measuring pressures prior to and after a reactor, mainly depends on the temperature, the pressure, the flow rate, and the structure of a reactor.

The flow rate of a gas in a cylindrical tube can be expressed as,[6]

$$\frac{\Delta n}{\Delta t} = \pi \, r^4 \frac{P_o^2 - P_i^2}{16 L \eta \, RT} \qquad \text{(E2-8)}$$

Here, P_i and P_o are pressures at the inlet and outlet of the reactor, respectively; and η is the coefficient of viscosity.

The pressure drop, $\Delta P = P_o - P_i$, and the average of pressures prior to and after the reactor, $P = (P_i+P_o)/2$, can be substituted in equation (E2-8) to give,

$$\frac{\Delta n}{\Delta t} = \frac{\pi r^4 P \Delta P}{8 L \eta RT}$$

That is,

$$\frac{\Delta P}{P} = \frac{8 L \eta RT}{\pi r^4 P^2} \frac{\Delta n}{\Delta t} \qquad \text{(E2-9)}$$

The residence time, t, is defined by,

$$t = \frac{n}{(\frac{\Delta n}{\Delta t})} = \frac{PV}{RT(\frac{\Delta n}{\Delta t})} \qquad \text{(E2-10)}$$

Substitution of equation (E2-10) and replacing V by $\pi r^2 L$ into (E2-9) and rearranging gives,

$$\frac{\Delta P}{P} = \frac{8 L^2 \eta}{r^2 Pt} \qquad \text{(E2-11)}$$

Therefore, in our experiments at very low conversions and very short residence times, the pressure drop is minimized by using a short reactor; more details about the structure of the reactor are given in section 2-2.

The expression (E2-10) for residence time above is only applicable for the case of very small pressure drops. Usually, pressure drops within 10% are acceptable. When the pressure drop is significant, by considering the pressure drop and assuming conversions

are very small and pressure drops are in the hot zone of the reactor, a more accurate equation[7] is given as,

$$t = \frac{2\pi\ r^2 L(P_i^3 - P_o^3)}{3RT(\frac{\Delta n}{\Delta t})(P_i^2 - P_o^2)} \qquad \text{(E2-12)}$$

For a product, x, formed in a reaction with a rate constant, k_x, stoichiometric coefficient for x of γ_x and order of n_x, with an initial pressure of P_{xi}, the measured partial pressure P_{xf} could be expressed[7] as,

$$P_{xf} = P_{xi} + \frac{2\gamma_x k_x P_o \pi\ r^2 L(P_i^{n_x+2} - P_o^{n_x+2})}{(n_x+2)(RT)^{n_x}(\frac{\Delta n}{\Delta t})(P_i^2 - P_o^2)} \qquad \text{(E2-13)}$$

The rate constant, k_x, could be calculated using equation (E2-13).

In addition, the chordal rate of formation of a product equals the concentration of the product at the exit of the reactor divided by the residence time.

In this work, equations (E2-12) and (E2-13) will be used to calculated the residence times and rate constants for formation of products when the pressure drop is significant.

2-2. Materials and apparatus

2-2-1. Reagent

Acetylene (Canox, <30,000 ppm acetone) was passed through an isopropanol/dry ice trap, which reduced the mole fraction of impurities to less than 120 ppm of acetone, less

than 270 ppm of ethane, less than 250 ppm of propane, and less than 80 ppm of propylene.

2-2-2. The design of the micro-reactor

The most important part of the apparatus is the reactor, the "heart" of the system. To observe an early stage of the pyrolysis of acetylene, its residence time in the reactor should be very short, which means the volume of the reactor should be very small. Cylindrical quartz tubes (Quartz Scientific, Inc., USA) of 27 cm in length and 0.969, 1.96, and 3.96 mm internal diameter (calculated by measuring the weights of each capillary empty and of each capillary filled with distilled water) were used as reactors. (The surface-to-volume ratios, S/V, were 40, 20, and 10 cm^{-1}, respectively.) The chemical composition of the quartz was 16 ppm Al, < 0.4 ppm As, < 0.1 ppm B, 0.6 ppm Ca, < 0.01 ppm Cd, 0.05 ppm Cr, < 0.1 ppm Cu, 0.3 ppm Fe, 0.7 ppm K, 1.0 ppm Li, 0.1 ppm Mg, 0.1 ppm Mn, 1.0 ppm Na, < 0.1 ppm Ni, 1.5 ppm P, < 0.4 ppm Sb, 1.1 ppm Ti, 1.5 ppm Zr, and < 5 ppm OH.[8] These are called micro-reactors, because sizes of popular reactors are 4-20 mm i.d. and 40-80 cm in length. Also, the small internal diameter in the micro-reactor can effectively reduce incomplete radial heat transfer according to (E2-1); and the short length can significantly lower the pressure drop in the reactor according to (E2-11). As far as we know, this kind of micro-reactor was used herein for the first time.

Usually, the length of a furnace should be at least 20 times as great as its diameter, to limit end effects and ensure a simple temperature profile. However, the diameter of the furnace must also be large enough to hold two thermocouples and the reactor. Therefore, a metal rod (10 cm long × 14 mm o.d.) with three holes of different sizes was placed inside the furnace to increase the thermal conduction, which in turn effectively improves the temperature profile of the micro-reactor. The schematic diagram is shown in Figure 2-1. After several different metals including brass, nickel, 316 stainless steel, etc., were tested for this purpose, 316 stainless steel was found to be the most suitable. Brass and nickel have very good thermal conductivity, but were oxidized at the high temperatures.

The quartz capillary reactor was inserted in one hole in the stainless steel rod, and two platinum/87%platinum - 13% rhodium thermocouples were put in the other two holes. One thermocouple with a quartz sleeve served to measure the temperature profile of the micro-reactor, while the other thermocouple connected to the temperature controller. The 316 stainless steel rod was inserted into a quartz tube (12 cm long × 15 mm id.) wound with nichrome wire. The furnace was 1 cm longer than the 316 SS rod at each end, so the end effect of the micro-reactor could be effectively minimized. Furnace cement (Mastercraft, Canadian Tire Ltd.) was put on the nichrome heating wire as insulation.

2-2-3. The design of the flow system

A new flow system was designed for this work. The schematic diagram of the system is shown in Figure 2-2. The system mainly consisted of a mass flow-controlling part, a

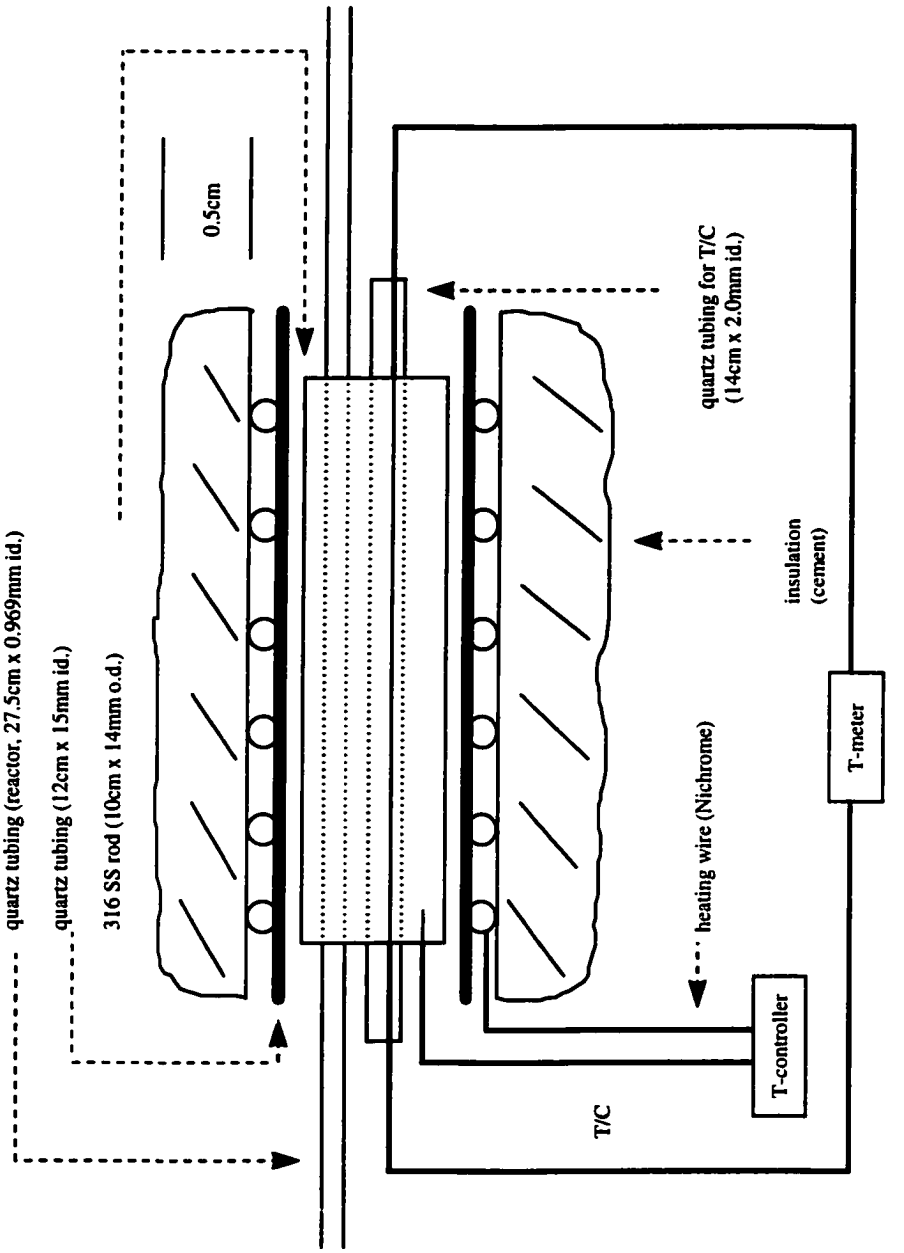

Figure 2-1. The schematic diagram of a micro-reactor.

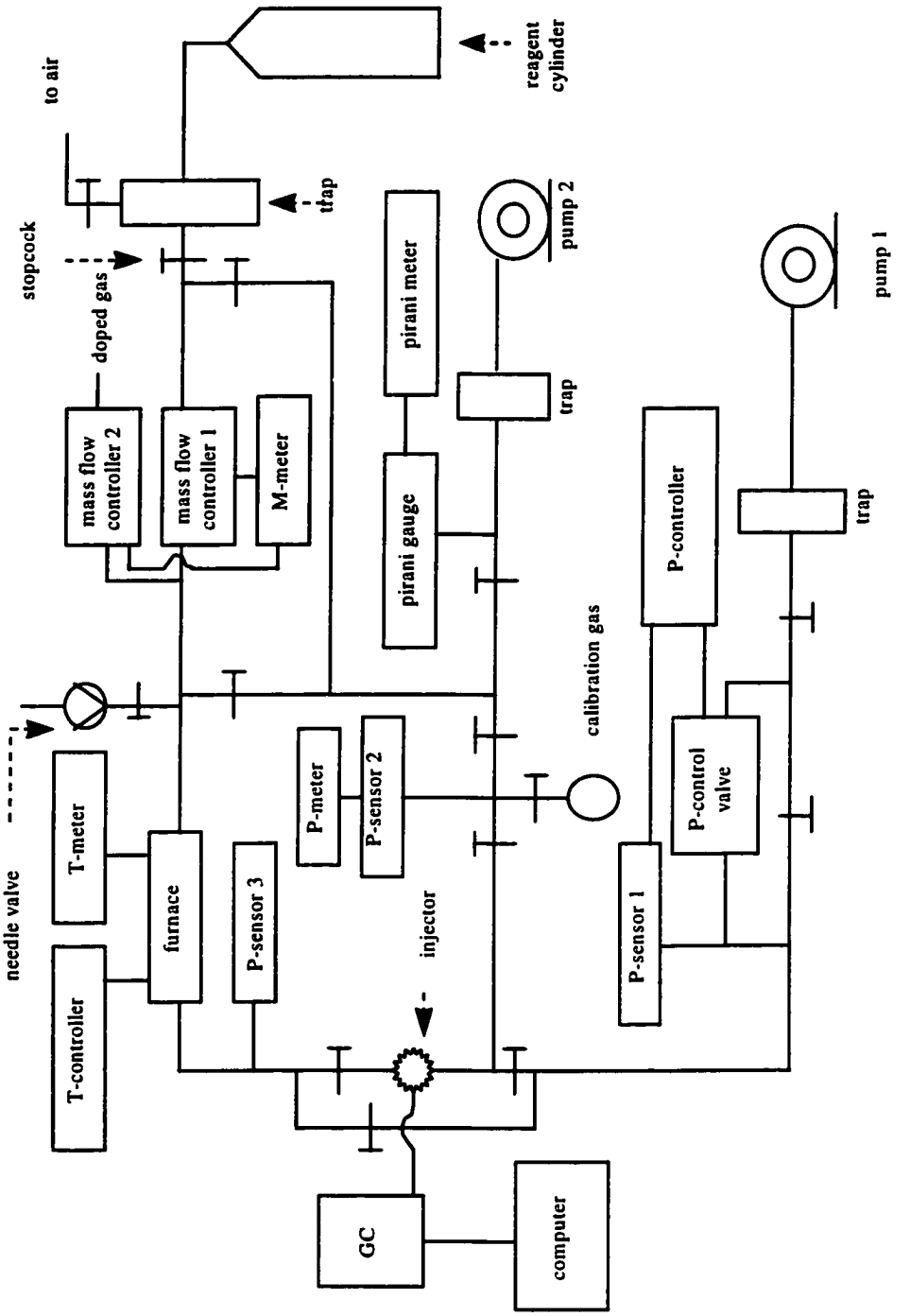

Figure 2-2. The schematic diagram of the system.

temperature-controlling part, a pressure-controlling part, and a product-analyzing part.

Under the control of the regulator, acetylene flowed from a cylinder into a dry ice/isopropanol trap, in which narrow Pyrex tubes were packed to increase the surface area of glass or the contact area between acetylene and glass. Thus, most of impurities could be effectively removed. This kind of "on line" purification system was used in the study of pyrolysis of acetylene previously in this laboratory.[7] The flow rate through the micro-reactor was very small, so a mass flow controller (MKS, Type 1179 A, 50 sccm), and a flow rate readout (MKS, Type 179 A) were used to accurately control the flow rate of acetylene. The control range of flow rates accessible on the controller was 0-50 sccm. Another mass flow controller (MKS, Type 1179 A, 20 sccm) was used to flow the mixtures of doped gases and acetylene.

Then, the gas flowed into the micro-reactor. A proportional-integral-differential (PID) temperature controller (ECS, Model 6820) and a digital multimeter (Dana, Model 4200) were used to control the temperature of the reactor. The needle valve prior to the reactor served to release air into the reactor to burn out the carbon deposited at high temperatures.

Products from the micro-reactor flowed through an injection valve to the pressure-controlling part; and then were evacuated to the atmosphere by the first mechanical pump, pump 1. The first pressure transducer (P-sensor 1, DATAMETRICS, Type 590A-1000T-201-H5X-4D), an auto-tune PID process/temperature controller (Omega, CN8500), a pressure control valve (MKS, Type 248A) and the pump 1 served together to control the pressure of the system. The second pressure transducer (P-sensor 2, Omega, PX 302) and a pressure meter (Omega, DP460-S) were used to measure the pressures prior to and after

the reactor by adjusting the stopcocks around P-sensor 2. A Pirani gauge (homemade) and a Pirani meter (homemade) were used to measure the vacuum in the system.

Two gas chromatographs (GC) were used to analyze products, including a packed column GC (Tracor, 550) and a capillary GC (Hewlett Packard, 5890). A triple quadrupole mass spectrometer (VG Quattro) was coupled to the capillary GC for GC-MS analysis. More details will be given in section 2-2-4. A six-way linear gas injection valve (Varian, Model 57-000034-00) was connected to each GC. In previous flow systems designed in this laboratory,[2,7] products from a reactor always flowed into a "manifold" with a big volume. The injection valve was put in a branch line connected to the manifold (off line), to minimize the perturbation to the system pressure caused by withdrawing products into the injector. However, the disadvantage of this design is that it took a long time to fill the manifold with new products after the conditions of pyrolysis were changed, especially when the flow rate was low.

To avoid this problem, a new design of the "on line" injection valve was used here. Thus, products flowed through the injection loop all the time when the injection valve was in the "load" position. A bypass near the injection valve was included because the flow of products would be cut off when the injection valve was in the "inject" position. When the pressure was very low and the flow rate of acetylene was fast, the pressure drop across the injector could be very high. In this situation, a sample was collected by partially opening the bypass to lower a high pressure drop to about 4 Torr. A pressure transducer (P-sensor 3, Omega, PX 302) was employed to measure the pressure between the reactor and the injector.

The gas line from the injection valve via P-sensor 2 to pump 2 served to pump out the GC carrier gas in the injection valve after each injection. The pressure transducer, P-sensor 2, could be used to measure the pressure in the injection valve after the stopcock between it and the Pirani gauge was closed. To minimize the filling time for products from the micro-reactor via the injection valve to P-sensor 2 after an injection, the volume between the micro-reactor and P-sensor 2 was reduced with some small volume stopcocks and a special design of connections of glass tubes.

2-2-4. Experimental procedure

2-2-4-1. General experimental procedure

Experiments were carried out by flowing acetylene through the heated micro-reactor. First, acetylene slowly flowed through the dry ice/isopropanol trap at a pressure slightly higher than 1 atmosphere to remove acetone and some other impurities, and filled the space between the acetylene cylinder and the flow controller while the flow rate was set at zero on the controller. This continued for at least 30 minutes to trap most of the impurities. Then, the purified acetylene flowed into the heated micro-reactor under the control of the mass flow controller. The pressure in the system was accurately controlled by the auto-tune process controller. Products coming from the micro-reactor were analyzed by gas chromatography.

The temperature in the micro-reactor was accurately controlled by a PID temperature controller. During an experiment, the temperature profile was measured at 1.0 cm intervals along the reactor, using a platinum/ platinum - 13% rhodium thermocouple. The temperature data were processed with a computer program,[9] which assigned each datum a weight, proportional to the rate of reaction at that temperature. Thus, an average reaction temperature and an effective length of the reaction zone were calculated by the program. During a typical experiment, calculations indicate that more than 90% of the reaction occurred within ± 4 K of the average temperature. Thus, a very good temperature profile was achieved.

All reactors were immersed in concentrated HNO_3 overnight to remove organic and inorganic impurities. Then, reactors were washed with a 25% HF solution, rinsed with distilled water, and dried. Carbon deposited in the reactor, which had been found to inhibit the gas phase reaction in an early stage of this study[10], was burned off between injections by flowing purified air through the reactor at 200 Torr. Injections were made when the acetylene had flowed for only 5 minutes, so as to limit any buildup of carbon.

Calibrations were carried out before and after each experiment using mixtures of nitrogen and hydrocarbons. The concentrations of the hydrocarbons were similar to those in the reaction products. Each hydrocarbon was degassed at the boiling point of liquid nitrogen to remove any impurities before it was used to prepare the calibration mixture. Each hydrocarbon was released into a high vacuum flask to a calculated pressure. At last, nitrogen was admitted into the flask to a pressure above an atmosphere. After the hydrocarbons mixed well for two hours, the gases in the flask were pumped to a calculated low pressure. Then, nitrogen flowed into the flask again to a final pressure

above an atmosphere. After two dilutions with nitrogen, a mixture of hydrocarbons with very low concentrations was prepared. Some typical mole fractions in a calibration mixture were: 0.0124%, 0.0101%, and 0.0115% for butene-1, acetone and benzene, respectively.

Butene-1 (Matheson, C. P.), acetone (Fisher, A. R.), and benzene (Fisher, A. R.) were used to prepare calibration mixtures to determine the concentrations of products and acetone. Here, butene-1 was used to calibrate vinylacetylene (VA) due to the lack of suppliers of vinylacetylene. To estimate the systematic error caused by calibration, GC sensitivities of butene-1 and 1,3-butadiene were compared; the former sensitivity was 6% higher than the latter value. Therefore, the systematic error resulting from the replacement for vinylacetylene by butene-1 for calibration should be very small.

2-2-4-2. Experimental procedure used in chapters 3 and 4

A few reactors were coated with a solution of 0.5M LiOH (BDH, ACS), 0.5M KOH (BDH, ACS), and 1.0M H_3BO_3 (Fisher, A. R.), then dried. Some reactors were coated with 0.06M Li_3PO_4 (Fisher, A. R.)/0.04M K_3PO_4 (Fisher, A. R.) solution and dried. These reactors were used to study the surface reactions in the experiments described in chapter 3. Other reactors were washed with 25% HF solution, rinsed with distilled water, and dried, and used in experiments described in all chapters.

In most cases, the carbon deposited in the reactor was burned off between injections by flowing purified air at 200 Torr through the reactor. The typical burning times (t_b) were 5

and 10 minutes. The typical deposition times (t_d) of carbon in the reactor were 5-10 minutes.

In certain experiments, a 670 nm beam from a diode laser passed along the axis of a 4-mm id reactor and through a semicircular, quartz disk placed in the middle of the hot zone. These experiments were performed to detect extinction of the laser radiation by carbon deposited on the disk, and to analyze gaseous products at the same time. Half of laser beam didn't pass through the window, thus the observed percentage of the light attenuated was doubled to determine the attenuation of the portion of the beam passing through the disk.

To examine the structure of carbon deposited in the reactor, thin quartz wires (< 0.3 mm o.d.) were treated by the same procedure as the reactor surfaces, and then were inserted into the hot zones of reactors. After experiments, the wires were carefully removed from the reactors. Some of them were examined by SEM (Bausch & Lomb, Nanolab 2000). The others were ultrasonicated in acetone for 15 minutes to disperse the deposit. A few drops of the suspension were placed on TEM grids (gold grids coated with carbon films, 200-A050, EMS). The samples were examined by TEM (Phillips, EM201).

A gas chromatograph (Tracor 550) with a Hayesep D column (3.1 m, Alltech) and a flame ionization detector was used to analyze products at a temperature of 210 °C. Nitrogen (extra dry, Praxair) was used as carrier gas.

2-2-4-3. Experimental procedure used in chapter 5

The flow rates of a (0.1968-5.238%) neopentane/acetylene mixture and of pure acetylene were controlled by two mass flow controllers (MKS, Type 1179A) and displayed by a readout of flow (MKS, Type 179A).

A gas chromatograph (Hewlett Packard 5890), equipped with an alumina capillary column (50 m length × 0.32 mm internal diameter × 8 μm film thickness, Hewlett Packard) and a flame ionization detector, was used to analyze products. The temperature gradient was: 20 ^{0}C per minute increasing from 35 ^{0}C to 180 ^{0}C, and then maintained at 180 ^{0}C for 10 minutes. Nitrogen (extra dry, Praxair) was used as carrier gas.

2-2-4-4. Experimental procedure used in chapter 6

The same flow system and capillary GC as in chapter 5 were used to observe the formation of products lighter than styrene. Nitrogen (Praxair, extra dry) was used as carrier gas. The column temperature gradient was: 35 ^{0}C for 5 minutes, followed by a gradient of 5 ^{0}C per minute to 100 ^{0}C, then 10 ^{0}C per minute to 180 ^{0}C, and held at 180 ^{0}C for 34 minutes. A triple quadrupole mass spectrometer (VG Quattro) was coupled to the GC for GC-MS analysis. Software, MassLynx (Fisons Instrument, version 2.1), was installed in a computer to collect mass spectra and to search candidates for unknown compounds in a database by comparing profiles of mass spectra for unknown compounds

and known compounds saved in the database. Helium (Praxair, Prepurified) was used as carrier gas for GC-MS analysis.

To study the formation of products heavier than styrene, a 3.96-mm (i.d.) reactor of the same design as in Figure 2-1 and a high temperature injection valve (Valco Instruments Co. Inc., VICI C6UWE) were installed in the oven of a gas chromatograph (Tracor, 550) with a Porapak Q column (Alltech, 2 m) and a flame ionization detector. (This will be referred to as furnace design II.) The temperature of the GC oven was maintained at 210 ^{0}C, so heavier products would not condense in the transfer line from the reactor to the GC.

Ethane (Matheson, C. P.), ethylene (Matheson, C. P.), propylene (Matheson, C. P.), propyne (Matheson, C. P.), butene-1 (Matheson, C. P.), neopentane (Matheson, C. P.), 1,3-butadiene (Matheson, C. P.), benzene (Fisher, A. R.), toluene (BDH, C. P.), and styrene (Fisher, A. R.) were used to prepare calibration mixtures to determine the concentrations of products and of neopentane. Other unknown products were calibrated using the sensitivities for known products of similar masses. Following compounds were injected in the GC-MS to identify minor products: 2,4-hexadiyne (Farchan Laboratories, Inc.), 1,3-cyclohexadiene (Aldrich, 97%), 1,4-cyclohexadiene (Aldrich, 95%), 1,3,5-hexatriene (Aldrich, 97%), ethylbenzene (BDH, laboratory reagent), o-xylene (BDH, laboratory reagent), m-xylene (BDH, laboratory reagent), p-xylene (BDH, laboratory reagent), divinylbenzene (Aldrich, 80%) and naphthalene (Aldrich, 98%), 1,3-cyclopentadiene (Aldrich), 2-methyl-1-buten-3-yne (Aldrich, 99%), 1,5-hexadiyne (GFS Chemicals, Inc., 50% in pentane), dimethylfulvene (Aldrich, 98%).

References for Chapter 2

1. C.F.Cullis and N.H.Franklin, *Roy.Soc.(London)*, 1964, **A280**, 139.
2. H.Furue and P.D.Pacey, *J.Phys.Chem.*, 1980, **84**, 3139.
3. M.F.R.Mulcahy and M.R.Pethard, *Australian J.Chem.*, 1963, **16**, 527.
4. R.C.Weast and M.J.Astle, *CRC Handbook of Chemistry and Physics*, 1997, 5-65, 6-214.
5. R.P.Duran, V.T.Amorebieta, and A.J.Colussi, *Int.J.Chem.Kinet.*, 1989, **21**, 947.
6. P.W.Atkins, *Physical Chemistry, 6th Edition, Freeman, New York*, 1998, p. 731.
7. S.T.Dimitrijevic, S.Paterson, and P.D.Pacey, *J.Anal.& Appl.Pyrolysis*, 2000, **53**, 107.
8. Quartz Scientific Inc., *Catalogue*, 1999, p. 16.
9. P.D.Pacey and J.H.Purnell, *J.Chem.Soc.Faraday Trans.I*, 1972, **68**, 1462.
10. X.Xu and P.D.Pacey, *Carbon*, 2001, **39**, 1839.

CHAPTER 3. INTERACTIONS BETWEEN ACETYLENE AND CARBON NANOTUBES AT 893 AND 1019 K

3-1. Introduction

Carbon nanotubes have often been synthesized by the pyrolysis of acetylene. However, both the mechanisms for the formation of nanotubes on the substrate and for the gas phase reactions of acetylene are not clear. More kinetic data are needed to resolve these issues.

Carbon can be formed in the pyrolysis of hydrocarbons by catalytic or noncatalytic processes.[1,2] Catalytic carbon is formed on metals, such as iron, cobalt and nickel, and tends to form as filaments with metal particles in the tips. Carbon filaments exist in various forms, depending on such experimental conditions as the nature and the dimensions of the metal catalyst, the identity of the hydrocarbon, and the temperature. Filaments consisting of a well-ordered graphitic wall and a hollow core are usually termed carbon nanotubes.[3,4] Filaments may also consist of a graphitic wall surrounding an amorphous core.[5] Some filaments, termed carbon nanofibers,[4] consist of graphitic sheets oriented in different directions with respect to the filament axis and have a solid, graphitic core. Noncatalytic carbon includes soot and pyrolytic carbon deposited on the surface of a reactor.

Carbon filaments were observed half a century ago,[2] but the comprehensive study of carbon nanotubes started in the early 1990s,[6] when their potential significance was widely recognized. Carbon nanotubes were predicted to possess remarkable chemical and physical properties, which could result in applications in nano-scale engineering and electronics. Several methods were successfully developed to prepare carbon nanotubes, including the arc discharge technique,[6,7] the catalytic pyrolysis of hydrocarbons,[8] laser vaporization,[9] and electrolysis.[10] Among these, catalytic pyrolysis is a technique with a low cost and a high yield. Hydrocarbons such as acetylene, ethylene, benzene, and naphthalene have been pyrolysed in the presence of Fe, Co, and Ni. Different reaction conditions have been studied.[11-13] Several mechanisms have been proposed to describe the formation of carbon nanotubes and filaments. The mechanisms of "tip growth"[2,5,14,15] and "root growth"[2,16] have been widely discussed. However, few studies have been carried out to identify the direct precursors of carbon nanotubes and filaments.

As indicated in Chapter 1, acetylene is believed to be a precursor of polycyclic aromatic hydrocarbons (PAHs) and carbon when various hydrocarbons are pyrolysed without the presence of a catalyst.[17-20] Therefore, it is important to understand the mechanism of the pyrolysis of acetylene. The mechanism at temperatures above 1500 K is believed to be a free radical process. However, the mechanism below 1500 K is still not clear. Both a free radical mechanism[21] and a molecular mechanism[22] have been proposed, mainly based on the results of early experiments performed at very high conversions, and on some computational results. Those results are limited and are subject to interference by secondary and even tertiary reactions, so neither proposed mechanism can be

eliminated. Study of the pyrolysis of acetylene at low conversions should provide crucial information regarding the mechanism.

Carbon forms readily in the pyrolysis of acetylene, and gradually builds up on the surface of the reactor. Taylor and van Hook[23] found that gas-phase reaction rates were reproducible when a carbon deposit was present in their reaction vessel at temperatures between 768 and 808 K. Cullis and Franklin[24] found that reproducible results were obtained after they performed many runs in their reactor in the temperature range of 773 K to 1272 K.

The present chapter has two purposes. One is to study the effect of carbon deposits on the rate of pyrolysis of acetylene in the gas phase. Another is to study the effects of the composition in the gas phase and of surface treatments on the rate of formation of carbon. Experiments have been performed at low conversions. Experimental conditions have been varied, including the residence time, the deposition time, the pressure, the temperature, and various treatments of reactor surfaces. The formation of carbon has been monitored by laser extinction, and the gaseous products have been determined by gas chromatography. The structure of carbon has been examined by scanning electron microscopy (SEM), and transmission electron microscopy (TEM).

3-2. Results

3-2-1. Deposition of carbon on the surfaces of reactors

To study the formation of carbon in the reactor, a series of experiments were performed at 1016 K and 56 Torr at a residence time, t_{res}, of gases in the reactor of 55 ms. The residence times of gases in the reactor were calculated from the reactor temperature and volume and from the gas pressure and flow rate. The residence times of gases at the semicircular window was only half of the total residence time in the reactor because the window was placed in the middle of the hot zone. Some results are shown in Figure 3-1. Curve (A) shows that the deposition of carbon started with a slight induction period (from the origin to the first, horizontal arrow), then proceeded to an acceleration period (between the first two arrows) and finally entered a constant growth period (between the last two arrows). The spikes in the curves were caused by the trigger pulses coinciding with GC injections. Curve (B) shows that the deposition of carbon at a greater mole fraction of acetone ($X_{acetone}$) was much faster than at the lower $X_{acetone}$. Curve (C) shows that the deposition of carbon in a reactor washed with HF was much slower in the early stages. The extinction reached a plateau after one hour in this case.

The rates of deposition of carbon were estimated from the slopes of graphs like Figure 3-1 with a linear regression program. The residence time was varied at 1016 K and 56 Torr in a 4-mm id reactor treated with HNO_3 to observe the rates of deposition of carbon

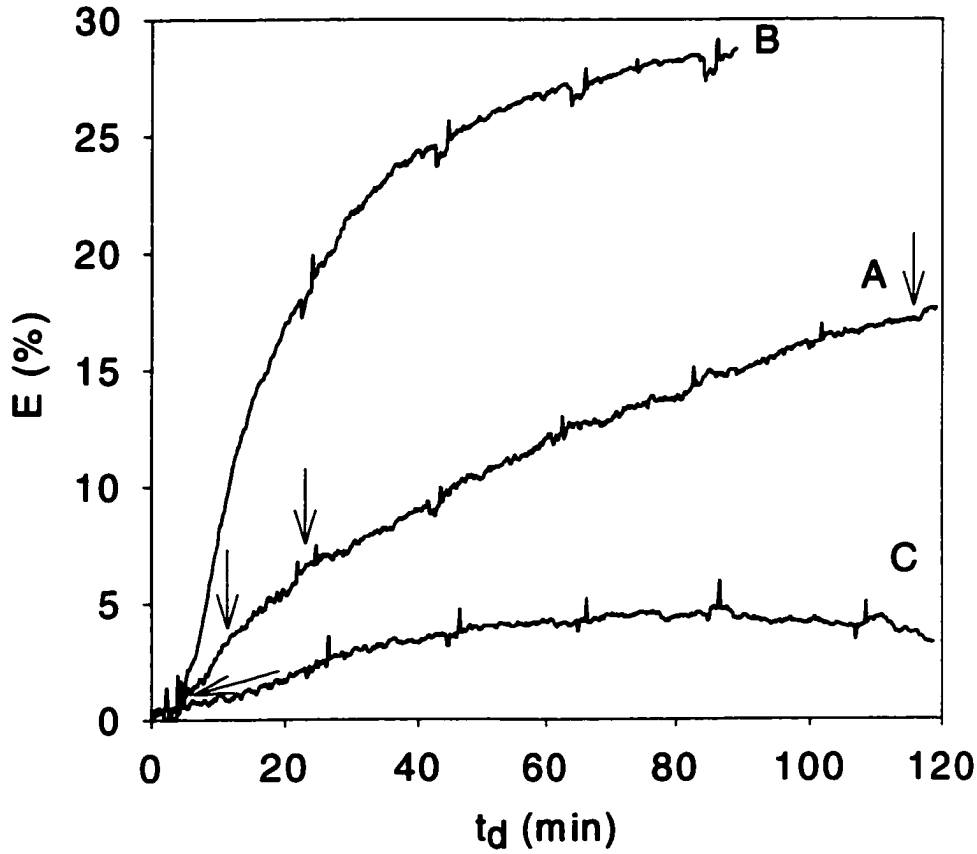

Figure 3-1. Dependence of the extinction (E) of the laser beam by carbon on the deposition time (t_d) at 1016 K and 56 Torr at a residence time of 55 ms in 4-mm id reactor. A, quartz surface treated with HNO_3, $X_{acetone}$ = 35 ppm; B, surface treated with HNO_3, $X_{acetone}$ = 28000 ppm; C, surface treated with HF, $X_{acetone}$ = 103 ppm. The arrows indicate the beginnings and ends of the acceleration period and of the constant growth period.

in the acceleration period and in the constant growth period. Figure 3-2 shows that the rates of deposition of carbon were independent of the residence time.

Table 3-1 summarizes the rates of deposition of carbon at 1016 K and 895 K. The conversion of acetylene was estimated from the concentrations of vinylacetylene and benzene, and turned out to be very low (less than 1.5%), so the concentration of acetylene did not change significantly during the reaction. The rates of carbon formation almost doubled when the pressure was almost doubled from 57.5 to 108 Torr. So the rate of formation of carbon was directly proportional to the pressure of acetylene.

The first and third lines of Table 3-1 show that the rate of deposition of carbon in the presence of a high concentration of acetone (28000 ppm) was 3.2 times the rate in the presence of a low concentration of acetone (35 ppm) in the acceleration periods, and 1.6 times in the constant growth periods. When the concentration of acetone was changed by the amount described above, the rates of formation of vinylacetylene and benzene were accelerated by a factor of 5 in the acceleration periods and by a factor of 6 in the constant growth periods.

As noted in Figure 3-1, treatment of the reactor with HF was found to significantly inhibit the deposition of carbon. The first and fourth lines of Table 3-1 show that the rate of deposition of carbon in the HF-washed reactor was only one-third of that in the HNO_3-washed reactor in the acceleration period. The constant growth period was replaced by a plateau in the reactor washed with HF.

It was also found that the rate of formation of carbon was four times greater at 1016 K than at 895 K at otherwise identical conditions. The activation energy for carbon

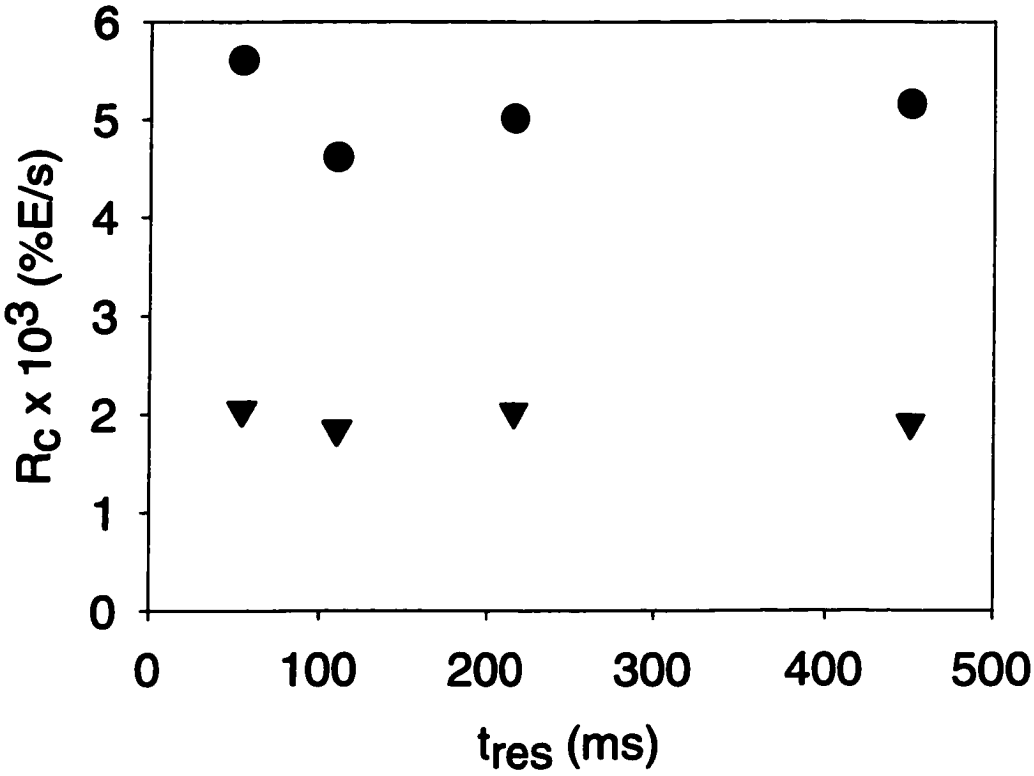

Figure 3-2. Dependence of the rates of deposition of carbon, measured as the slopes of graphs like Figure 3-1, on the residence time at 1016 K and 56 Torr in a 4-mm id reactor treated with HNO_3. ●, the rates in the acceleration periods; ▼, the rates in the constant growth periods.

Table 3-1. Rates of carbon deposition in 4-mm id reactors

T (K)	P (Torr)	t_{res} (ms)	$X_{acetone}$ (ppm)	$R_c^a \times 10^3$ (%E s^{-1})	$R_c^b \times 10^3$ (%E s^{-1})
1016	57.5	54.8	35	5.61	2.0
1016	108	211	32	9.7	3.8
1015	56.1	53.3	28000	18	3.1
1016[c]	56.1	55.3	103	1.9	0
895	108	215	58	-	0.9

a; The rates of carbon deposition in the acceleration periods

b; The rates of carbon deposition in the constant growth periods

c; An HF-washed reactor was used here; the reactor was washed with HNO_3 in the other cases.

deposition was estimated to be 84 kJ mol^{-1}.

Induction and acceleration periods were not observed at 895 K. Changes in the rates of carbon deposition in the induction and acceleration periods were too small to be observed at this temperature.

3-2-2. The structure of the carbon deposit

A series of experiments were carried out at 1019 K and 56.5 Torr at a residence time of 22 ms using small diameter reactors (1-mm id) to study the structure of the carbon deposits. Thin quartz wires were inserted into the hot zone of the reactors to collect samples for SEM and TEM tests. Some SEM and TEM images are shown in Figure 3-3. Figure 3-3a shows carbon deposited on a quartz thread treated with HNO_3. Carbon filaments were observed to predominate. Some microparticles were also observed in certain areas.

Figure 3-3b shows the surface structure of a substrate rinsed with HF solution and deposited with carbon. Less carbon was observed in Figure 3-3b than in Figure 3-3a, which confirms that treating the surface of a reactor with HF effectively reduced the amount of carbon formed. A few small pits with diameters less than 1 μm were observed; these pits apparently were etched in the quartz by HF.

Experiments were also carried out at 1016 K and 57.5 Torr at a residence time of 216 ms in a 4-mm id reactor with a thin quartz substrate treated with HNO_3. A TEM scan of the structure of the ultrasonicated carbon deposit is shown in Figure 3-3c. Carbon

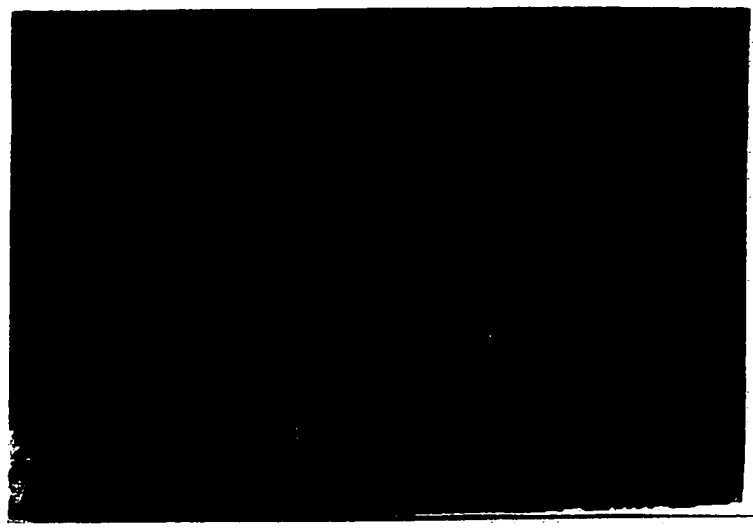

Fig. 3-3a

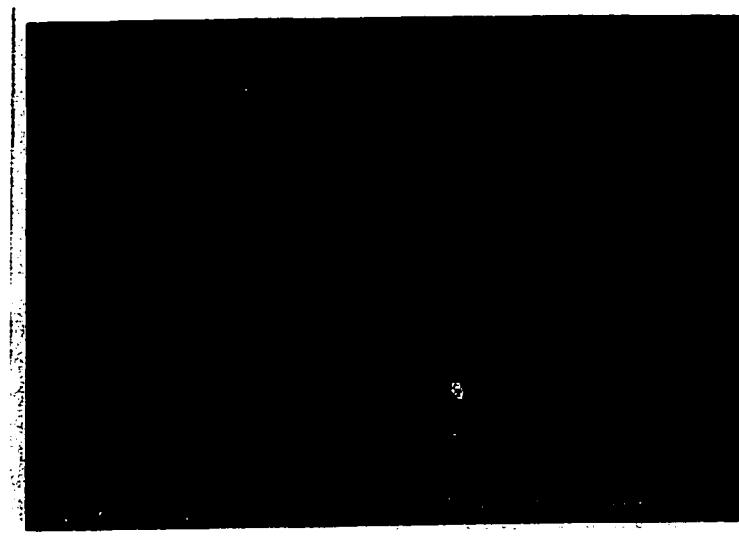

Fig. 3-3b

Fig. 3-3c

Figure 3-3.a, SEM image of carbon deposited on an HNO_3-treated surface; b, SEM image of carbon deposited on an HF-treated surface; c, TEM image of carbon deposited on an HNO_3-treated surface, magnification = 14760. Experimental conditions, 1019 K and 56.5 Torr at a residence time of 22 ms in 1-mm id reactors, $X_{acetone}$ = 90 ppm, t_d = 10 min, t_b = 5 min.

nanotubes were observed. Most nanotubes had internal diameters of 30 nm, outer diameters of 80 nm, and lengths of more than 1 μm. Some smaller particles were also observed in the images. These particles could be soot formed in the reactor or debris formed by the ultrasonication of samples. Metal particles were not found in the nanotubes examined. A gold TEM grid coated with carbon was directly inserted into the hot zone of a 4-mm id reactor to collect a TEM sample at the same conditions. The TEM images obtained showed similar carbon nanotubes. No amorphous materials were observed in this case.

3-2-3. Effect of surface on the gaseous products

Surface effects on the gas phase reaction were tested using reactors with different diameters. Experiments were performed at 895 K using two reactors with internal diameters of 4 mm and 2 mm. The results are presented in Table 3-2. (Quoted uncertainties are standard deviations). The average rates of formation of vinylacetylene (R_{VA}) and benzene (R_B) were calculated by dividing the yields by the residence times. The mole fractions of acetone were less than 70 ppm. When the surfaces were freshly washed with HNO_3, the rates measured with reactors of different diameters agreed reasonably well. In some cases changes of rates were greater than the standard deviations, because slight changes of temperature and pressure may have existed when reactors with different diameters were used. All the reactors used to obtain the results reported in the first six lines of the table were checked after the experiments. It was found that all of them were transparent.

Table 3-2. Rates of formation of vinylacetylene and benzene at 895 K.

Treatments of reactors	P (Torr)	t_{res} (ms)	id (mm)	$R_{VA} \times 10^6$ (mol L^{-1} s^{-1})	$R_B \times 10^7$ (mol L^{-1} s^{-1})
HNO_3	109	110	2	3.8±0.4	20±1
HNO_3	109	110	4	3.6±0.6	18±1
HNO_3	60.4	110	2	1.6±0.1	5.2±0.1
HNO_3	60.3	110	4	1.4±0.1	4.6±0.1
HNO_3	31.5	121	2	0.25±0.01	0.050±0.003
HNO_3	31.5	121	4	0.27±0.01	0.053±0.004
carbon coated	31.5	121	2	0.057±0.001	0.019±0.003
carbon coated	31.5	121	4	0.081±0.002	0.027±0.001

Carbon deposits were prepared on the surfaces of the reactors by pyrolysing acetylene at 1019 K and 100 Torr at a residence time of 590 ms ($X_{acetone}$ = 56 ppm) for one hour to form a uniform layer of carbon. When the temperature and pressure were lowered again to 895 K and 31.5 Torr, rates of formation of the two main products were lowered by factors between 2 and 5, as shown by comparing the last two lines of Table 3-2 with the two lines above them. The rate was slower in the reactor with the smaller diameter. This reflects a significant surface inhibition in the reactors coated with carbon.

A surface effect caused by the deposition of carbon was also observed at 1016 K. Figure 3-4 shows the results obtained by repeating injections at the same conditions without burning off the carbon in the reactor between injections. The time between consecutive injections was about 17 minutes, so the deposition of carbon on the semicircular window in a reactor could be monitored by laser extinction while the concentrations of vinylacetylene and benzene were detected at the same time. The results show that the values of R_{VA} and R_B clearly declined with an increase in the deposition time of carbon, while the laser extinction by carbon significantly increased with the deposition time.

The rates of formation of vinylacetylene were measured at 1018 K and 58 Torr at residence times between 24 and 55 ms in 1-mm, 2-mm, and 4-mm id reactors, which had been previously coated with carbon for 110 minutes at the same conditions. These rates were 4.24×10^{-6}, 6.51×10^{-6}, and 9.76×10^{-6} mol L^{-1} s^{-1}, respectively, increasing as the reactor diameter increased.

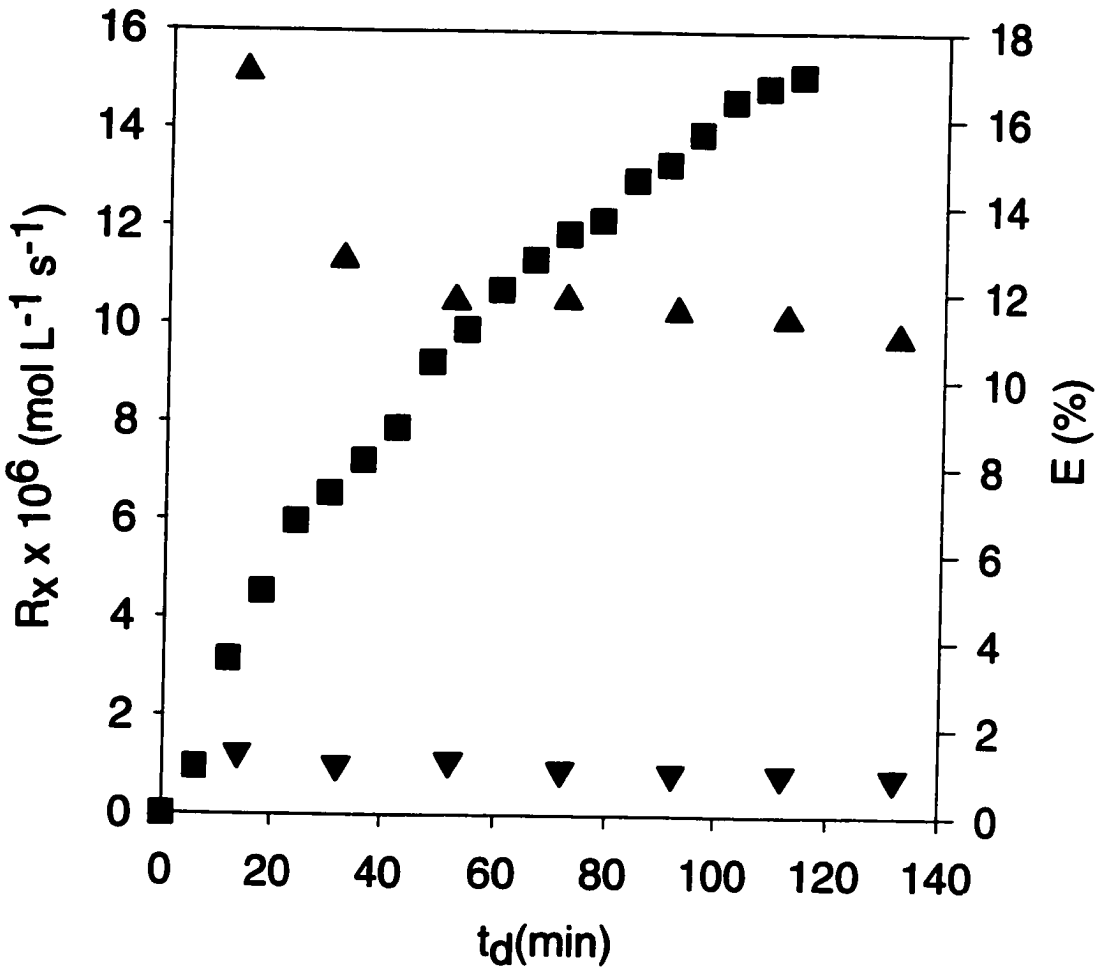

Figure 3-4. Dependence of the rates of formation of vinylacetylene and benzene (left axis), and of the laser extinction (E) due to carbon deposition (right axis) on the deposition time at 1016 K and 57.5 Torr at a residence time of 55 ms in a 4-mm id reactor treated with HNO_3, x = vinylacetylene or benzene; ■, extinction; ▲, vinylacetylene; ▼, benzene.

3-2-4. Treating the surfaces of the reactors

To minimize the surface effect caused by the deposition of carbon on the wall of the reactor, air filtered through a 1-cm thick plug of glass wool was then flowed through the hot reactor at 200 Torr to burn off the carbon deposit. The burning time, t_b, was changed from 5 to 10 minutes to check if all the carbon had been burned off. The time of carbon deposition after burning and before sample injection was changed from 5 to 10 minutes to observe how quickly carbon deposition affected the pyrolysis of acetylene. Experiments were performed at two temperatures and two pressures with three reactors of different internal diameters.

At 895 K, R_{VA} and R_B did not change when either t_b or t_d was varied from 5 to 10 minutes.

The results achieved at 1018±1 K and with different treatments of the surfaces of the reactors are given in Table 3-3. The results obtained with reactors of different diameters treated with HNO_3 disagreed with each other, especially at the lower pressure. The larger diameter reactor gave a larger R_{VA} and a larger R_B, which indicates that surface inhibition was very strong at high temperature, especially in the small diameter reactor. In the small diameter reactor, 10 minutes of deposition gave slightly smaller R_{VA} and R_B values than 5 minutes did, which indicates the amount of carbon deposition affected the results. Five minutes was long enough to burn off all the carbon on the reactor, because doubling t_b from 5 to 10 minutes gave similar R_{VA} and R_B values. After the experiments, most of the reactors appeared transparent, except that the wall of the small diameter reactor (1-mm id) used at 58.4 Torr was gray because of a thin layer of carbon.

Table 3-3. Rates of formation of vinylacetylene and benzene at 1018±1 K, and at two pressures, after burning off the carbonaceous deposits for times, t_b, in reactors with different surface treatments

Treatment of reactors	P (Torr)	t_{res} (ms)	id (mm)	$R_{VA} \times 10^6$ (mol L^{-1} s^{-1})			$R_B \times 10^7$ (mol L^{-1} s^{-1})		
				t_b=5 min	5 min	10 min	5 min	5 min	10 min
				t_d=5 min	10 min	5 min	5 min	10 min	5 min
HNO_3	108	34	2	52±5	45	46	95±12	82	81
HNO_3	108	36	1	44±2	41	43	77±5	72	74
HNO_3	56.4	23	2	17±3	14	16	18±4	15	17
HNO_3	58.4	23	1	7.1±0.6	6.3	6.9	6.9±0.9	5.7	6.5
HF	58.0	23	1	15.8±0.7	12.5	15.1	17.0±0.1	13	17
Li_3PO_4/K_3PO_4	58.0	23	1	9.4±0.3	7.9	9.1	8.0±0.4	6.6	7.6
$LiOH/KOH/H_3BO_3$	58.0	23	1	1.9±0.4	2.4	2.2	1.3±0.3	1.7	1.5

Different treatments of the reactor wall were tested, including rinsing the wall with HF solution and coating with Li_3PO_4/K_3PO_4 or $LiOH/KOH/H_3BO_3$. Experiments were performed with a series of small diameter reactors (1-mm id) treated in different ways. The results are listed in Table 3-3. The values for R_{VA} and R_B in the HF-washed reactor (in the fifth line) were very close to those in the 2-mm id reactor washed only with HNO_3 (in the third line). Comparing the fourth and fifth lines in the table, washing only with HNO_3 decelerated the formation of vinylacetylene and benzene compared to washing with HF. Comparing the fourth and sixth lines, the coating of Li_3PO_4/K_3PO_4 decelerated the reaction slightly less than the HNO_3-washed surface.

Another coating, $LiOH/KOH/H_3BO_3$, strongly inhibited the reaction. The rates measured on this surface were about one order of magnitude slower than those listed in the third line of Table 3-3. Doubling the deposition time from 5 to 10 minutes gave slightly faster R_{VA} and R_B on this surface, which was an exception among all the treatments. To explore the reason, experiments were performed without burning off the carbon in the reactor between consecutive injections. The results are shown in Figure 3-5. The values of R_{VA} and R_B gradually increased with the deposition of carbon, and reached maxima after 60 minutes deposition, then slightly decreased and approached plateau values.

Experiments were performed at similar temperatures and pressures to those in Tables 3-2 and 3-3 using reactors washed with HF solution to check the reduction in the surface effect. The results are presented in Table 3-4. Both R_{VA} and R_B were independent of the reactor diameter at several conditions when the deposition time was 5 minutes, which indicates that the surface effect was removed. The values of R_{VA} and R_B at 894-896 K

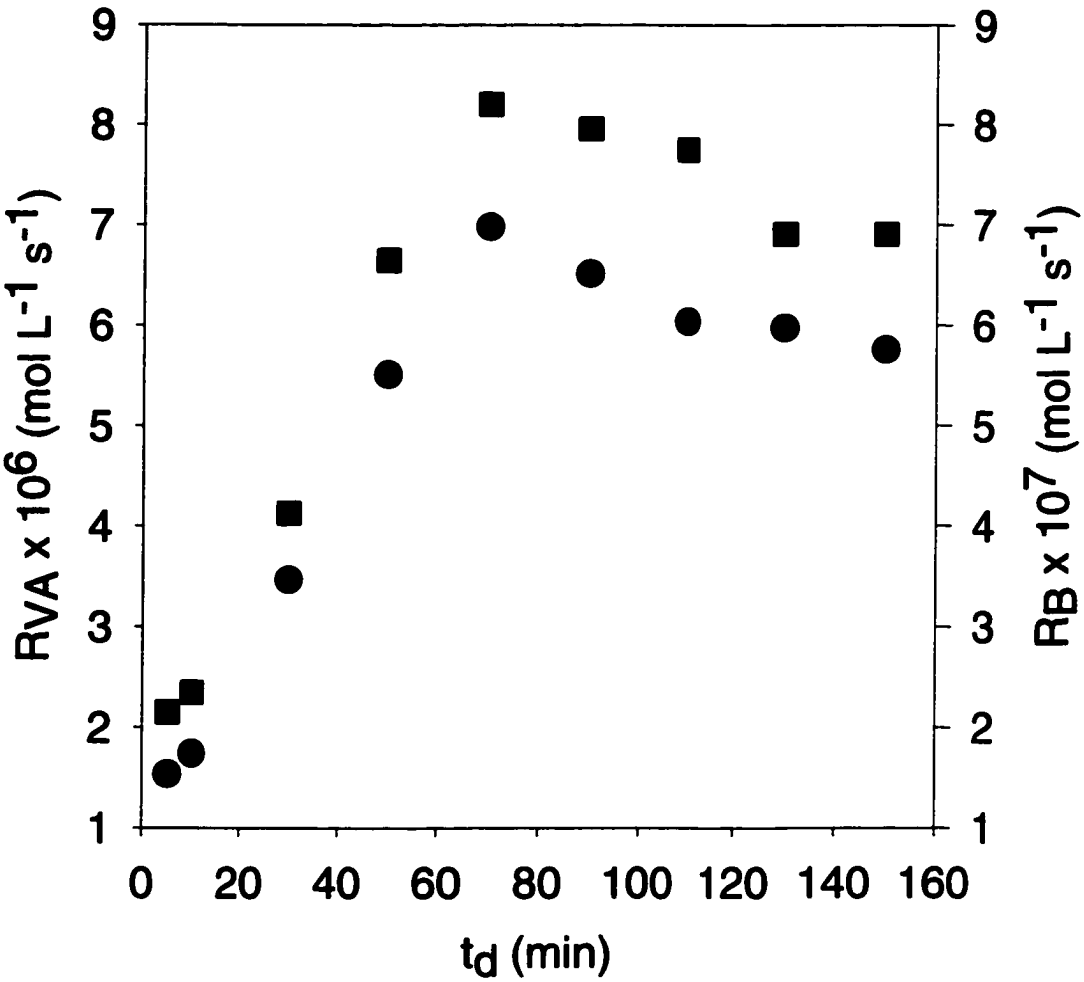

Figure 3-5. Dependence of the rates of formation of vinylacetylene and benzene on the deposition time at 1017 K and 58.6 Torr at a residence time of 22 ms in a 1-mm id reactor coated with LiOH/KOH/H_3BO_3; ■, vinylacetylene; ●, benzene.

Table 3-4. Rates of vinylacetylene and benzene formation in three reactors washed with HF solution. Carbon was burned off for 5 minutes between injections.

T (K)	P (Torr)	t_{res} (ms)	id (mm)	$R_{VA} \times 10^6$ (mol L^{-1} s^{-1})		$R_B \times 10^7$ (mol L^{-1} s^{-1})	
				t_d=5 min	10 min	5 min	10 min
895	60.5	114	2	1.6±0.1	1.54	4.8±0.1	4.8
894	60.2	118	4	1.5±0.1	1.49	4.6±0.2	4.8
895	109	114	2	4.7±0.1	4.6	21±1	21.4
896	109	122	4	4.3±0.1	4.4	18±1	18.4
1020	58.3	24	1	13±2	10.8	12±3	9.5
1021	56.5	22	2	15±1	9.7	14±1	8.1
1018	108	36	1	49±3	43	87±6	73
1018	107	35	2	53±1	43	96±2	74

were very close to those in Table 3-2, where the surface had only been washed with HNO_3. The values of R_{VA} and R_B measured at 1018-1021 K and 10 minutes of deposition were slower than those measured at 5 minutes of deposition, which reflects a slight inhibition by carbon at longer deposition times. All the reactors appeared transparent after the experiments.

3-3. Discussion

3-3-1. The formation of carbon nanotubes

A number of workers have reported the preparation of carbon nanotubes by pyrolysing acetylene in the presence of metal catalysts, e.g., iron, cobalt, or nickel particles. The present work reports the formation of carbon nanotubes and nanoparticles without adding metal catalyst on purpose. Probably, the trace amounts of metals in the quartz were not easily removed by treatment with HNO_3. Thus, these metal residues could have catalyzed the formation of carbon nanotubes.

Carbon nanotubes with metal particles in the tips[13,25] or metal particles at the bases[8,16,26] have been observed by previous workers. Different models, "tip growth" and "root growth", were proposed to interpret the growth of these nanotubes. In the "tip growth" model, a hydrocarbon was assumed to decompose on the upper, exposed surface of a metal particle to form hydrogen and carbon atoms. Then carbon atoms could diffuse through the metal particle,[2,25] or on the surface of the metal particle[14,15,25] and finally deposit on the lower surface to form nanotubes. The metal particle would stay in the tip of

the nanotube during its growth and would be observed in the tip by electron microscopy. In the "root growth" model,[2,16,26] a hydrocarbon was postulated to decompose on the side surfaces of a metal particle. The carbon atoms formed could diffuse in the metal particle and then form nanotubes on the upper surface of the metal. In this case, the metal particle would remain on the supporting surface during the growth of the nanotube. After such nanotubes were removed from supporting surfaces, usually no catalyst particles were observed in the tips.[8,16,26] The different growth mechanisms are dependent on the interaction between metal particles and the surface of the substrate. When the interaction is weak, the metal particles may separate from the substrate and be lifted up in the tips of the nanotubes. Contrarily, when the metal-substrate interaction is strong, the nanotubes may grow out from the metal particles fixed in the substrate.[5]

In the present work, no metal particles were found in any observed nanotubes. The open ends could have been attached to the surface of the reactor before ultrasonication removed them. This is consistent with formation by the "root growth" model.

Carbon nanotubes with similar dimensions to those in the present work have been reported previously.[27]

3-3-2. The rate of deposition of carbon

Similar curves to those in Figure 3-1 were obtained by Baker et al.[28] when acetylene was pyrolysed at 1010 K in contact with metals. They suggested that the induction periods were caused by the activation of growth centers on the metal surface. The

maximum rate of carbon deposition would coincide with the presence of a large number of active growth centers. The rate of carbon deposition would then slow down because excess carbon could gradually block the active surface.

The effect of HF-washing on the formation of carbon has been observed for the first time. The slower rates of carbon deposition on the HF-washed surface probably resulted from a smaller number of active growth sites on this surface. This is consistent with the lower surface coverage by carbon observed in the SEM images in Figure 3-3. The plateau in the rate of carbon deposition on the HF-washed surface in Figure 3-1 could have resulted from the blocking of active centers at long deposition times, as suggested for metal surfaces by Baker and Harris.[2]

The activation energy for the deposition of carbon in the pyrolysis of acetylene has been estimated to be 145 kJ mol^{-1} between 550 K and 875 K in the presence of nickel,[29] 67 ± 5 kJ mol^{-1} between 785 and 1245 K in the presence of α-iron,[28] and 139 ± 7 kJ mol^{-1} between 800 and 1200 K in the presence of cobalt.[28] Arefieva and Tesner reported a value of 138 kJ mol^{-1} between 823 K and 1373 K when acetylene was pyrolysed on the surface of quartz.[30] A value of 84 kJ mol^{-1} was obtained in the present work.

3-3-3. The precursor to the formation of carbon nanotubes

There is considerable interest in the mechanism of the formation of carbon nanotubes in the pyrolysis of hydrocarbons. The reactant or an intermediate, or a product, could be the direct precursor of carbon nanotubes. However, there has been no direct experimental

evidence to distinguish between these possible precursors. The results in the present work provide direct evidence regarding the precursor of carbon nanotubes for the first time.

Figure 3-2 shows that the rate of carbon formation was independent of the residence time; carbon was a primary product. The concentrations of acetylene and of primary radicals should have been independent of residence time when the reaction was in a steady state and when the conversions were very low (0.1-1.5%). On the other hand, the concentrations of the primary products, vinylacetylene and benzene, increased linearly with increasing residence time. If these products were precursors of carbon, the rate of carbon formation would have been expected to increase with increasing residence time, contrary to the behavior observed here. The present results are consistent with acetylene or a radical formed directly from acetylene acting as a precursor of carbon.

The deposition of pyrolytic carbon on the surface of alumina was studied recently by Becker and Huttinger[31] from the pyrolysis of acetylene at 1273 K and at much higher conversions (13-75% at 30 Torr) by weighing the amount of carbon deposited on the surface of the reactor. Their results showed that the rate of deposition of pyrolytic carbon was independent of residence time at about 13% conversion, and that the rate of formation of pyrolytic carbon increased in the later stages. However, they didn't report the existence of carbon nanotubes.

Table 3-1 shows that the rate of formation of carbon nanotubes was proportional to the pressure of acetylene. This is also consistent with acetylene or a radical formed directly from acetylene acting as the precursor of carbon. In the growth of carbon nanotubes, the diffusion of carbon atoms through metal particles was suggested to be the rate-determining step.[2] This would lead to an order of one-half with respect to the

concentration of acetylene, which is contrary to the observation in this work. Our results support a different mechanism for the growth of carbon nanotubes.

Tesner and his coworkers[29] gravimetrically investigated the formation of carbon filaments by pyrolysing acetylene in mixtures with nitrogen and hydrogen in contact with nichrome wires at 723-973 K (conversions, 1-50%). They didn't determine the reaction order, but an order of approximately unity can be calculated using their results.

The correlation between the rate of deposition of pyrolytic carbon and the initial pressure of acetylene was studied in the absence of catalyst by some workers. Tesner and his coworkers[30,32-34] measured the deposition of pyrolytic carbon on quartz by acetylene at 1000-1500 K. They found that the rate of deposition of pyrolytic carbon was directly proportional to the concentration of acetylene at low pressures, and exponentially increased with the concentration of acetylene at high pressures. They didn't report the observation of carbon nanotubes. Becker and Huttinger[31] found that, at low acetylene pressures, pyrolytic carbon was formed by a first order reaction, and that carbon was formed by a third order reaction at high acetylene pressures.

The acceleration by acetone of the formation of carbon nanotubes from the pyrolysis of acetylene was studied in this work for the first time. The presence of acetone in acetylene provided an additional source of free radicals.[35] The acceleration of the formation of carbon by acetone, as shown in Table 3-1, indicates that free radicals were involved in the formation of carbon nanotubes. The larger acceleration in the formation of vinylacetylene or benzene than in the formation of carbon suggests that both free radicals and acetylene could be precursors to the formation of carbon.

Arefieva and Tesner[30] suggested that free radicals might be involved in the formation of pyrolytic carbon from acetylene on a quartz surface when the temperature was over 1373 K, as the activation energy was observed to gradually increase between 1373 K and 1723 K, possibly indicating that the rupture of the strong C-H bonds in acetylene molecules might start to provide free radicals at high temperatures. By pyrolysing methane at 773 K, the acceleration of the formation of carbon nanotubes by acetone was observed by Evans et al.[36] They assumed that the formation of carbon was associated with the decomposition of CH_4, CH_3 and some secondary products, such as C_2H_6, C_2H_4 and C_2H_2, but they didn't have direct, experimental evidence to support this proposal.

In Figure 3-1 the slower rate of deposition of carbon in the constant growth period could have resulted from the gradual blockage of the active surface.[28] Another explanation is that the lower concentration of free radicals in the gas phase in the constant growth period may produce carbon at a slower rate.

3-3-4. Diffusion of species to the surface of the reactor

The maximum possible rates of surface deposition of carbon by diffusion of species to the surface were estimated using equation (E3-1).[37]

$$R_D = rk_D C_i M_i/2 \qquad \text{(E3-1)}$$

Here r is the radius of the reactor; k_D, the rate constant for radial diffusion to the surface of the reactor; C_i, the molar concentration of species i; and M_i, the molar mass (kg mol^{-1})

of carbon in species *i*. The rate constant for diffusion to a cylindrical surface in laminar flow may be calculated using equation (E3-2).[37]

$$k_D = 3.6D_{mi}/r^2 \qquad \text{(E3-2)}$$

Here, D_{mi} is the diffusion coefficient for a binary mixture of rigid spheres, which could be calculated using equation (E3-3).[38]

$$D_{mi} = (k_b^3 T^3 L(M_m+M_i)/(\pi^3 2M_m M_i))^{1/2}/(P\sigma_{mi}^2) \qquad \text{(E3-3)}$$

In equation (E3-3), k_b is the Boltzmann constant; T, the temperature, L, Avogadro's constant; m, the medium, acetylene; P, the pressure and σ, the average collision diameter.

The vinyl radical has been suggested to act as the main chain transfer radical.[21] The collision diameter of ethylene[38] was used for that of vinyl radicals. The rates of diffusion for acetylene and vinyl radicals at 1016 K and 57.5 Torr were estimated. Average collision diameters, σ_{mi}, were calculated as the arithmetic mean of σ_m and σ_i.

To estimate the concentration of vinyl radicals, the rate constant for the second order termination (k_t) of vinyl radicals in the gas phase was taken as 1.06×10^{10} L mol^{-1} s^{-1} [39] and the rate constant of the initiation reaction (k_i) was calculated using the pre-exponential value of $10^{10.4}$ L mol^{-1} s^{-1} and the activation energy of 221 kJ mol^{-1}.[35] The concentration of vinyl radicals was calculated using equation (E3-4),

$$[C_2H_3] = (k_i/k_t)^{1/2}[C_2H_2] \qquad \text{(E3-4)}$$

Table 3-5 lists the calculated rates of diffusion for acetylene and for vinyl radicals in a 4-mm id reactor.

The relation, reported by Chen and Back,[40] between the amount of carbon deposited and the laser extinction by a carbon deposit was used in this work to estimate the amount of carbon formed. Table 3-5 also lists the rates of formation of carbon in the acceleration

Table 3-5. The rates of diffusion of species to the surface of the reactor at 1016 K and 57.5 Torr at a residence time of 55 ms in a 4-mm id reactor.

Species	rates of diffusion $\times 10^{10}$ (kg m^{-2} s^{-1})
acetylene	2.62E+08
vinyl radical	737
R_c[a]	18
R_c[b]	7.2

a: the rate of formation of carbon in the acceleration period

b: the rate of formation of carbon in the constant growth period

and constant growth periods, again using the extinction coefficient from the literature.[40] The results show that the rates of diffusion of acetylene and of vinyl radicals were great enough to account for the formation of the carbon nanotubes in the reactor. Therefore, both acetylene and vinyl radicals are capable of acting as the main, direct precursors of the formation of carbon nanotubes.

The rate constant for the first-order deposition of carbon from acetylene was calculated to be 2.40×10^{-13} kg m^{-2} s^{-1} Pa^{-1} during the acceleration period and 0.962×10^{-13} kg m^{-2} s^{-1} Pa^{-1} during the constant growth period at 1016 K and 57.5 Torr at a residence time of 55 ms. These values are an order of magnitude less than the value of 6.56×10^{-13} kg m^{-2} s^{-1} Pa^{-1} reported by Borodina and Tesner.[32]

At the same conditions and at a deposition time of 114 minutes, the rates of formation of vinylacetylene, benzene and carbon were calculated to be 1.8×10^{-8} mol s^{-1}, 1.4×10^{-9} mol s^{-1}, and 7.6×10^{-11} mol s^{-1}, respectively. The selectivity for carbon was 0.4%. Carbon has a lower order and lower activation energy (one and 84 kJ mol^{-1}, respectively) than those for vinylacetylene and benzene, which are reported to be two and 208 kJ mol^{-1} for vinylacetylene, and three and 164 kJ mol^{-1} for benzene.[35] The selectivity for carbon increased at low pressures, low temperatures and short residence times.

3-3-5. The effect of the carbon deposit on the pyrolysis of acetylene

The elucidation of the mechanism of the pyrolysis of acetylene at temperatures less than 1500 K is an unsolved problem. The divergent proposals involve free radical

processes or molecular processes. The free radical mechanism was experimentally supported by recent work in this laboratory.[35]

Figure 3-4 shows that the rates of formation of vinylacetylene and benzene decreased during the acceleration period for the formation of carbon nanotubes. The gas-phase rate approached a constant value at longer deposition times, when the slope of the plot of %E as a function of deposition time was also constant.

Figures 3-4 and 3-5 and Tables 3-2, 3-3 and 3-4 show that the relative yields of the products, vinylacetylene and benzene, were very similar with and without carbon on the surface of reactor. This indicates that the reaction retained its radical nature in the presence of carbon. Participation of the surface in initiation or propagation steps would be expected to lead to an acceleration of the reaction at high S/V, which was the reverse of the experimental observation. The results were consistent with an additional chain termination step occurring on the surface of the reactor.

It can be seen in Figure 3-4 that plateau rates of formation of vinylacetylene and benzene were obtained when sufficient carbon was deposited on the surface of a reactor. Earlier workers[23,24] also found that they obtained consistent results when they coated the surface with carbon. These early results may not have involved homogenous, gaseous processes, but instead, gaseous, radical, initiation and propagation processes limited by a heterogeneous termination reaction.

An effect from the deposition of pyrolytic carbon was previously observed in the pyrolysis of other hydrocarbons. Pacey and Wimalasena[41] found that, when ethane was pyrolysed at 904 K, the rates of formation of products could be lowered by a termination

reaction on a surface coated with carbon. A clean quartz surface was found to minimize surface termination. Their observation was similar to that in the present work.

Venkateswaran et al.[42] studied the effects of pyrolytic carbon on the pyrolysis of methane at temperatures from 873 to 1023 K in a static system. They found the rate of decomposition of methane gradually increased with the deposition of carbon on the surface of the reaction vessel, and reached a plateau value when the amount of carbon was larger than that of a monolayer. The conversion of methane accelerated by carbon could be as much as 40 times greater than that without any acceleration by carbon. They attributed the acceleration by carbon to a heterogeneous initiation process. It was suggested that various radical sites on the surface of carbon could assist in breaking C-H bonds in methane molecules. Free radicals, H and CH_3, formed on the carbon surface, could accelerate the reaction. However, there was no evidence for a similar heterogeneous initiation in the present work. We note that the strength of a C-H bond in acetylene is much greater than that in methane.[43]

Ismail et al.[44] studied the chemical vapor deposition (CVD) of pyrolytic carbon on different carbon substrates by pyrolysing 10% methane in argon in a flow system at 1273-1338 K. They found the deposition rate of carbon mainly depended on two factors, i.e., the active surface area and the total surface area. The existence of active sites on the surface of the carbon substrate was observed to significantly accelerate the deposition of carbon from the gas phase decomposition of methane. The deposition rate of carbon increased with an increase in the total surface area.

Treatment of the surface of a reaction vessel with HF has been reported by several workers. Minkoff et al.[45] treated the surface of their reaction vessel with 30% HF, and

found the rate of decomposition of acetylene increased by about 30% and that the acceleration period was shortened at 773 K. Camilleri et al.[46] found that a reactor washed with 25% HF solution could minimize the heterogeneous termination reaction of hydrogen atoms between 503 and 753 K at pressures of ethane between 8 and 16 Torr in a flow-discharge system. However, these workers didn't report the mechanism of HF treatment. We believe that treatment with HF solution removed most of the active sites on the wall of the reactor. Those active sites could be metal atoms (M) bound to the surface of the quartz, or unsaturated oxygen atoms on the surface. The reactions occurring on the surface of a quartz reactor during treatment with HF could be described as follows,

$$SiO_{2(s)} + 4HF = SiF_4\uparrow + 2H_2O \qquad [3\text{-}1]$$

$$M^{n+}\text{-quartz} + nHF = MF_n + nH^+\text{-quartz} \qquad [3\text{-}2]$$

3-3-6. The behavior of coatings of $LiOH/KOH/H_3BO_3$ and Li_3PO_4/K_3PO_4

In industrial research, coatings of Li_3PO_4/K_3PO_4 and $LiOH/KOH/H_3BO_3$ have been shown to lower the buildup of carbon on the surface of a reaction vessel, and to make it easier to burn off the carbon in the reactor.[47] It was proposed[47] that a mixture of 0.5M LiOH/0.5M KOH/1.0M H_3BO_3 would convert to a melt of $Li_2O/K_2O/B_2O_3$ (1:1:1) when it was heated above the melting point of this mixture at 850 K. The network structure formed by B_2O_3 could be partially broken by Li_2O and K_2O to form linear chains. The latter could interact with carbon formed and take it into the melt, so the carbon would not float and build up on the surface of the reactor. Also, carbon could be burned off much

more easily from the melt when oxygen or steam flowed through reactors. Therefore, Figure 3-5 could be interpreted from two points of view. First, a trace amount of oxygen may have been dissolved in the melt and would inhibit the pyrolysis at the beginning of the reaction. With the formation of carbon in the reaction, oxygen would be gradually consumed to form carbon dioxide, so R_{VA} and R_B gradually increased to their maxima. When all of the oxygen was used up, carbon trapped in the melt could slightly inhibit the reaction, so R_{VA} and R_B slightly decreased and approached plateau values.

The melting point of a 3:2 molar ratio of Li_3PO_4 and K_3PO_4 is 820 K,[48] so this coating was also a liquid at 1019 K. It was found to slightly reduce the surface effect compared to that in a similar, HNO_3-washed reactor.

3-3-7. Estimation of rate constants for surface reactions

The rate constants for the termination of radicals on different surfaces may be estimated from the inhibition observed, using equation (E3-5) suggested in the literature.[41]

$$R^{VA}_{g+s}/R^{VA}_{g} = [C_2H_3]_{g+s}/[C_2H_3]_{g} = (1+k_s^2/a^2)^{1/2} - k_s/a \qquad \text{(E3-5)}$$

Here, R^{VA}_{g+s} is the rate of formation of vinylacetylene with termination in the gas phase and on the surface; R^{VA}_{g}, the rate of formation of vinylacetylene without surface termination; $[C_2H_3]_{g+s}$, the concentration of vinyl radicals with gas and surface termination; $[C_2H_3]_{g}$, the concentration of vinyl radicals without surface termination; k_s,

the rate constant of surface termination; and $a = (4k_ik_t[C_2H_2]^2)^{1/2}$, where k_i is the rate constant for initiation; and k_t, the rate constant for termination in the gas phase.

Table 3-3 shows that the rate of formation of vinylacetylene in the 2-mm id reactor agreed very well with that measured in the HF-treated 1-mm id reactor, so the former rate (17×10^{-6} mol L^{-1} s^{-1}) was assumed to be free of surface termination. It provided the value of R^{VA}_g. The rate constant of the initiation step was calculated using Arrhenius parameters reported assuming second-order termination.[35] The rate constant for recombination of vinyl radicals in the gas phase was 1.06×10^{10} L mol^{-1} s^{-1}.[39]

The relation between k_s and S/V was checked using the rates of vinylacetylene formation measured at 1018 K and 58 Torr in 1-mm, 2-mm, and 4-mm id reactors coated with carbon when the deposition time was 110 minutes. Figure 3-6 shows the calculated results. The values of k_s were directly proportional to the values of S/V. This is consistent with kinetic control of surface termination[41] according to equation (E3-6),

$$k_s = \gamma c(S/V)/4 \qquad \text{(E3-6)}$$

Here γ is the probability of reaction on each collision, and c is the average molecular velocity of vinyl radicals.

The rate constants for surface termination and the probabilities of reaction of vinyl radicals on different surfaces were estimated using the data listed in Tables 3-2 and 3-3. The calculated rate constants are listed in Table 3-6. The rate constant for surface termination on the HF-treated reactor was the lowest. The surface coated by carbon showed the second greatest surface effect. The value of γ on carbon was smaller at 894 K than at 1018 K. The value of γ of 0.32×10^{-4} obtained on a carbon surface (in the last line of Table 3-6) at 894 K and 31 Torr was smaller than the value of 0.6×10^{-4} for ethyl

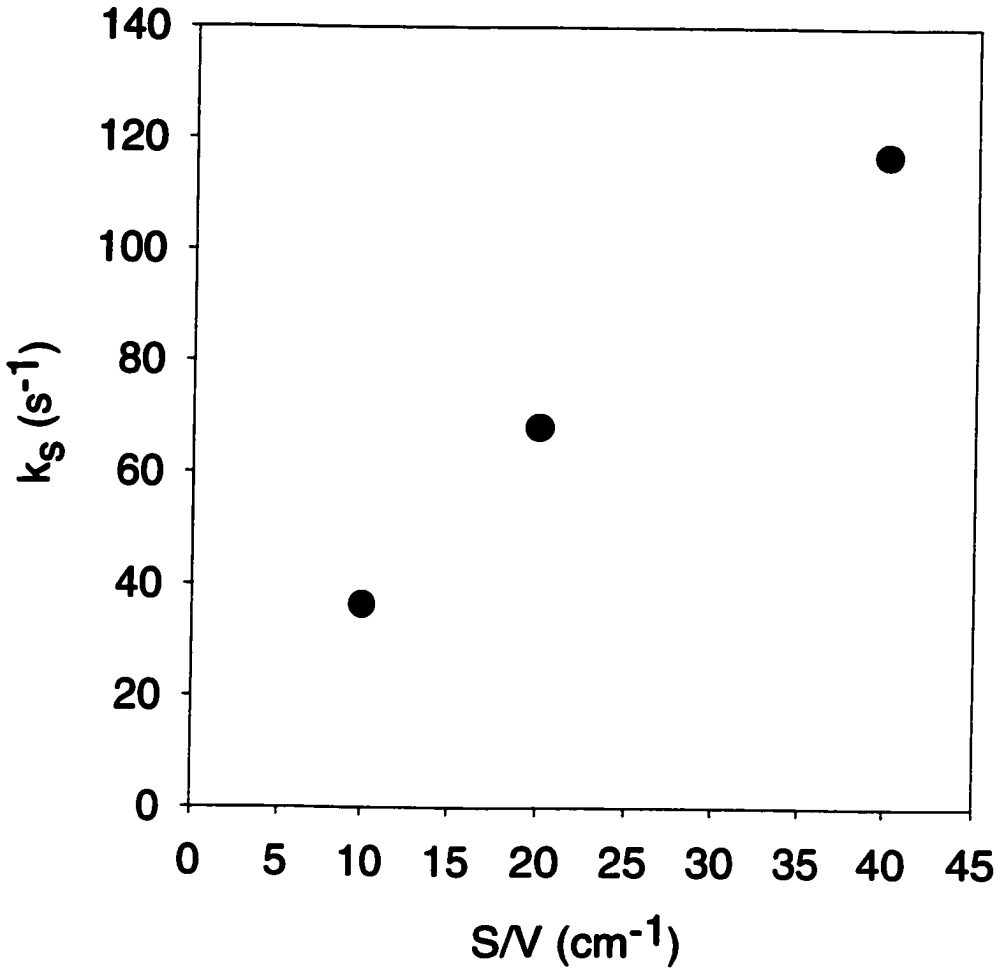

Figure 3-6. Dependence of the rate constant for the surface termination of free radicals (at 1016-1018 K and 58 Torr at residence times of 24-55 ms) on the surface-to-volume ratio. The reactors were coated with carbon at these conditions for 110 minutes.

Table 3-6. The estimated rate constants of surface termination on different surfaces at 1018 and 894 K.

Treatments of surfaces	T (K)	P (Torr)	id (mm)	t_d (min)	k_s (s^{-1})	$\gamma \times 10^4$
HF	1018	58	1	5	5	0.05
Li_3PO_4/K_3PO_4	1018	58	1	5	39	0.44
HNO_3	1018	58	1	5	61	0.69
$LiOH/KOH/H_3BO_3$	1018	58	1	5	270	3.0
Carbon	1018	57	1	110	120	1.3
Carbon	894	31	2	*	13	0.32

* The surface was coated with carbon at 1019 K and 100 Torr at a residence time of 590 ms for 60 min. Then, the temperature was lowered to 894 K.

radicals on a carbon-coated surface at 902 K and 16 Torr[41] and was also smaller than the value of 1.1×10^{-4} for methyl radicals at 729 K and 30-143 Torr.[49]

Values of k_s were also calculated by comparing the rates of formation of vinylacetylene at various deposition times in a reactor washed with HNO_3, from Figure 3-4, with the corresponding rate in a 1-mm id, HF-washed reactor, from Table 3-4. The relation between k_s and the laser extinction by carbon is shown in Figure 3-7. The value of k_s increased in the acceleration period for the deposition of carbon, and became almost constant in the constant growth period.

The maximum possible rate of formation of carbon from the termination of vinyl radicals on the surface of the reactor could be estimated to be 84×10^{-10} kg m^{-2} s^{-1} at 1016 K and 57.5 Torr in a 4-mm id reactor using the rate constant of surface termination of vinyl radicals listed in Table 3-6 (the fifth line), and the concentration of vinyl radicals estimated using equation (E3-4). This value is greater than the deposition rates of carbon determined by laser extinction, 18×10^{-10} kg m^{-2} s^{-1} in the acceleration period and 7.2×10^{-10} kg m^{-2} s^{-1} in the constant growth period. It is smaller than the diffusion rate of vinyl radicals to the surface, 737×10^{-10} kg m^{-2} s^{-1}. This supports the idea that some vinyl radicals reacted on the surface and that some of the products then left for the gas phase.

To minimize the surface effect caused by the deposition of carbon, we recommend that an HF-treated reactor should be used, and that the carbon deposit on the surface should be burned off between injections.

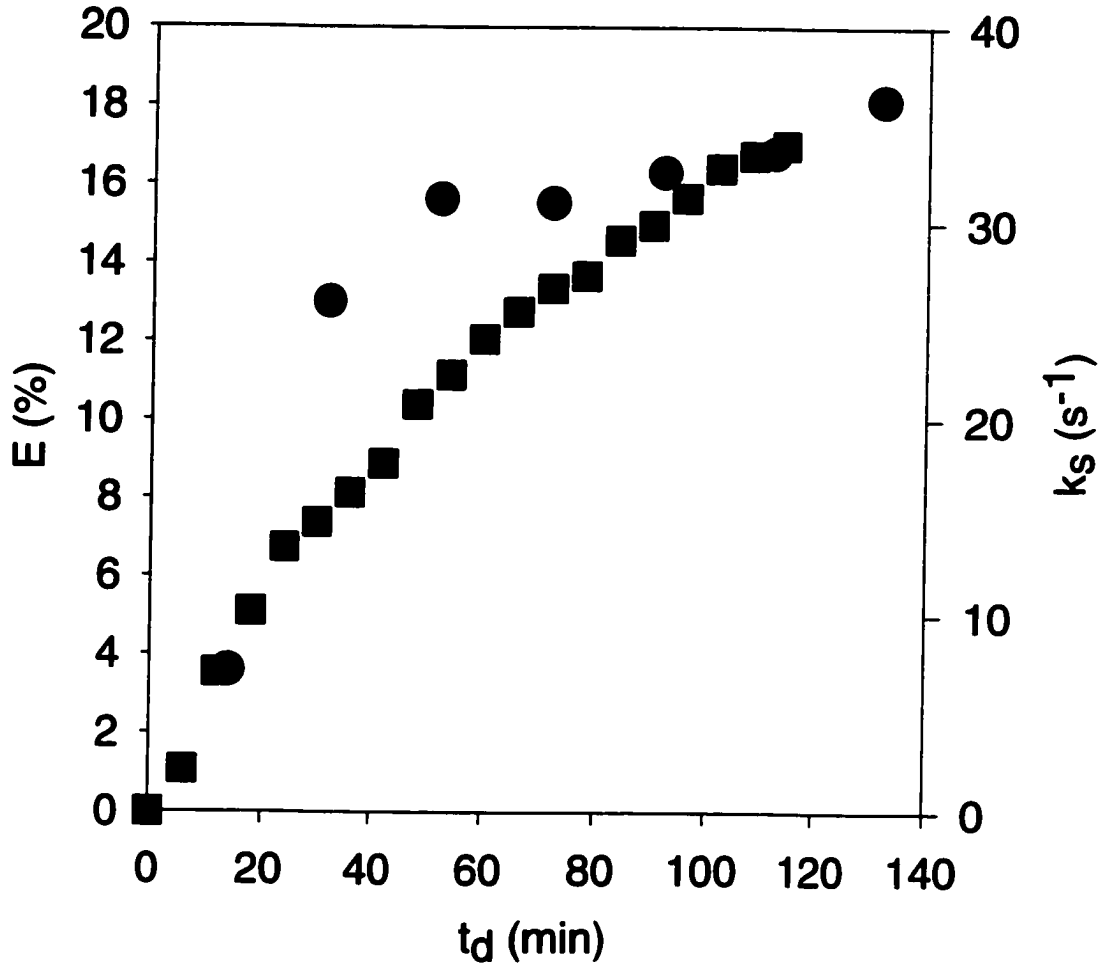

Figure 3-7. Dependence of the extinction (■) of a laser beam by carbon (left axis) and of the rate constant (●) for surface termination (right axis) on the deposition time at 1016 K and 57.5 Torr at a residence time of 55 ms in a 4-mm id reactor washed with HNO_3.

3-3-8. A new mechanism for the formation of carbon nanotubes

In the present work, washing the surfaces of the reactors with an HF solution significantly inhibited the formation of carbon nanotubes. This observation is consistent with the presence of small amounts of metal oxides embedded in the surface of the reactors. These metal oxides could not be easily removed by an HNO_3 solution, but could be removed by HF. At high temperatures and in the presence of acetylene, these metal oxides could be converted to metals, forming the induction period shown in Figure 3-1. The metals then could catalyze the formation of carbon nanotubes. The metals appear to remain in the surface of the reactor during the growth of carbon nanotubes, because no metal particles were observed in the nanotubes examined using TEM.

An order of unity was observed in this work for the formation of carbon nanotubes. This order is different from the order of one-half predicted using the assumption that the rate-determining step was the diffusion of carbon atoms through metal catalysts. This may suggest a different mechanism in addition to the proposed "root" growth and "tip" growth" mechanisms.

In the present work, carbon nanotubes may start to grow on the upper faces of metal particles embedded in the surface of the reactor, because removal of the metals by HF solution inhibited the formation of carbon nanotubes. Evidence for the involvement of radicals has been obtained in this work. Free radicals might precipitate on the surface of the metal particles to form the tubular, hexagonal structures of carbon nanotubes, with hydrogen atoms attached to the carbon atoms at the edges. Radicals in the gas phase might abstract these hydrogen atoms and leave radical sites on carbon nanotubes in a

process similar to the H-abstraction-C_2H_2-addition (HACA) model of formation of PAHs and soot due to Frenklach et al.[18,19] Most acetylene molecules striking carbon nanotubes returned to the gas phase without any changes, because the rate of collision for acetylene on the surface of the reactor was significantly greater than the rate of formation of carbon nanotubes, as indicated in Table 3-5. A few acetylene molecules could add to these radical sites. Thus, carbon nanotubes could grow to the dimensions observed.

3-4. Conclusion

Carbon nanotubes were observed to be formed in the pyrolysis of acetylene with catalysis by small amounts of metals and metal oxides embedded in the surface of the reactor. Washing the surface of the reactor with an HF solution could significantly inhibit the formation of carbon nanotubes. Boosting the concentration of free radicals by introducing small amounts of acetone in acetylene could significantly accelerate the formation of carbon nanotubes. An order of unity was measured for the formation of carbon nanotubes, which is different from the order of one-half, predicted using normal "tip" growth and "root" growth mechanisms. A new mechanism has been proposed to interpret the formation of carbon nanotubes.

On the other hand, the formation of carbon nanotubes on the surface of the reactor significantly lowered the rates of the formation of vinylacetylene and benzene, by a new surface termination step. The gas-phase process and the surface process interact with each other.

References for Chapter 3

1. J.C.Bokros in P.L.Walker Jr., editor, *Chemistry and Physics of Carbon, Vol.5, New York, Marcel Dekker*, 1969, p. 1.

2. R.T.K.Baker, P.S.Harris, In P.L.Walker Jr.and P.A.Thrower, editors, *Chemistry and Physics of Carbon, Vol.14, New York, Marcel Dekker*, 1978, p. 83.

3. M.Endo and H.W.Kroto, *J.Phys.Chem.* , 1992, **96**, 6941.

4. N.M.Rodriguez, A.Chambers, and R.T.K.Baker, *Langmuir*, 1995, **11**, 3862.

5. R.T.K.Baker, *Carbon*, 1989, **27**, 315.

6. S.Iijima, *Nature*, 1991, **56**, 354.

7. E.F.Kukovitsky, S.G.L'vov, and N.A.Sainov, *Chem.Phys.Lett.*, 2000, **317**, 65.

8. S.Fan, M.G.Chapline, N.R.Franklin, T.W.Tombler, A.M.Cassell, and H.Dai, *Science*, 1999, **283** , 512.

9. T.Guo, P.Nikoleav, A.G.Rinzler, D.Tomanek, D.T.Colbert, and R.E.Smalley, *J.Phys.Chem.*, 1995, **99**, 10694.

10. W.K.Hsu, J.P.Hare, M.Terrones, P.F.J.Harris, H.W.Kroto, and D.R.M.Walton, *Nature*, 1995, **377**, 687.

11. M.J.Yacaman, M.M.Yoshida, L.Rendon, and J.G.Santiesteban, *Appl.Phys.Lett.*, 1993, **62**, 202.

12. V.Ivanov, A.Fonseca, J.B.Nagy, D.Bernaerts, A.Fudala, and A.A.Lucas, *Zeolites*, 1995, **17**, 416.

13. S.B.Sinnott, R.Andrews, D.Qian, A.M.Rao, Z.Mao, E.C.Dickey, and F.Derbyshire, *Chem.Phys.Lett.*, 1999, **315**, 25.

14. T.Baird and J.R.Fryer, *Carbon*, 1974, **12**, 591.

15. A.Oberlin, M.Endo, and T.Koyama, *J.Cryst.Growth*, 1976, **32**, 335.

16. S.Amelinckx, X.B.Zhang, D.Bernaerts, X.F.Zhang, V.Ivanov, and J.B.Nagy, *Science*, 1994, **265**, 635.

17. S.J.Harris and A.M.Weiner, *Annu.Rev.Phys.Chem.*, 1985, **36**, 31.

18. M.Frenklach, D.W.Clary, W.C.Gardiner Jr., and S.E.Stein, *Twentieth Symposium (International) on Combustion, The Combustion Institute, Pittsburgh, PA*, 1985, 887.

19. M.Frenklach, *Twenty-Second Symposium (International) on Combustion, The Combustion Institute, Pittsburgh, PA*, 1988, 1075.

20. R.D.Kern and K.Xie, *Prog.Energy Combust.Sci.*, 1991, **17**, 191.

21. S.W.Benson, *Int.J.Chem.Kinet.*, 1992, **24**, 217.

22. R.P.Duran, V.T.Amorebieta, and A.J.Colussi, *J.Phys.Chem.*, 1988, **92**, 636.

23. H.A.Taylor and A.von Hook, *J.Phys.Chem.*, 1935, **39**, 811.

24. C.F.Cullis and N.H.Franklin, *Roy.Soc.(London)*, 1964, **A280**, 139.

25. M.Terrones, W.K.Hsu, H.W.Kroto, and D.R.M.Walton, *Top Curr.Chem., Berlin, Springer-Verlag*, 1999, p. 189.

26. W.Z.Li, S.S.Xie, L.X.Qian, B.H.Chang, B.S.Zou, W.Y.Zhou, R.A.Zhao, and G.Wang, *Science*, 1996, **274**, 1701.

27. D.C.Li, L.Dai, S.Huang, A.W.H.Mau, and Z.L.Wang, *Chem.Phys.Lett.*, 2000, **316**, 349.

28. R.T.K.Baker, P.S.Harris, R.B.Thomas, and R.J.Waite, *J.Catal.*, 1973, **30**, 86.

29. P.A.Tesner, E.Y.Robinovich, I.S.Rafalkes, and E.F.Arefieva, *Carbon*, 1970, **8**, 435.

30. E.F.Arefieva and P.A.Tesner, *Fizika Goreniya i Vzryva*, 1986, **22**, 73.

31. A.Becker and K.J.Huttinger, *Carbon*, 1998, **36**, 177.

32. L.M.Borodina and P.A.Tesner, *Khimiya Tverdogo Topliva*, 1983, **17**, 157.

33. P.A.Tesner, In P.A.Thrower, editor, *Chemistry and Physics of Carbon, Vol.19, New York, Marcel Dekker*, 1984, p. 65.

34. P.A.Tesner, I.M.Gutor, V.G.Knorre, N.V.Lutsik, and M.P.Mulyava, *Sov.J.Chem.Phys.*, 1985, **2** , 1837.

35. S.T.Dimitrijevic, S.Paterson, and P.D.Pacey, *J.Anal.& Appl.Pyrolysis*, 2000, **53**, 107.

36. E.L.Evans, J.M.Thomas, P.A.Thrower, and P.L.Walker, *Carbon*, 1973, **11**, 441.

37. J.Lede and J.Villermaux, *J.Chim.Phys.*, 1974, **85**, 71.

38. J.O.Hirschfelder, C.F.Curtiss, and R.B.Bird, *Molecular Theory of Gases and Liquids, 2nd Edition, New York, John Wiley and Sons, Inc.*, 1964, p. 14, p. 1112.

39. W.Tsang and R.F.Hampson, *J.Phys.Chem.Ref.Data*, 1986, **15**, 1087.

40. C.J.Chen, M.H.Back, and B.A.Back, *Can.J.Chem.*, 1976, **54**, 3175.

41. P.D.Pacey and J.H.Wimalasena, *Can.J.Chem.*, 1983, **61**, 1086.

42. R.Venkateswaran, M.H.Back, and G.Scacchi, *Carbon*, 1994, **32**, 911.

43. D.R.Lide, *Handbook of Chemistry and Physics, 77th Ed., CRC Press*, 1996, 9-64.

44. I.M.K.Ismail, M.M.Rose, and M.A.Mahowald, *Carbon*, 1991, **29**, 575.

45. G.J.Minkoff, D.M.Dewitt, and P.V.Rutledge, *J.Appl.Chem.(London)*, 1957, **7**, 412.

46. P.Camilleri, R.M.Marshall, and J.H.Purnell, *J.Chem.Soc.Faraday Trans.I*, 1974, **70**, 1434.

47. J.J.Dugan, J.P.Higgins, J.M.Salva, I.S.Pasternak, J.G.Evans, and P.D.Pacey, *US Patent*, 1971, 1414779.

48. E.M.Levin, C.R.Robbins, and H.F.McMurdie, *Phase Diagrams for Ceramists, The American Ceramic Society*, 1964, p. 145.

49. I.S.Jayaweera and P.D.Pacey, *J.Chim.Phys.*, 1987, **84**, 13.

CHAPTER 4. AN INDUCTION PERIOD IN THE PYROLYSIS OF ACETYLENE

4-1. Introduction

As indicated in Chapter 1, several mechanisms have been proposed for the pyrolysis of acetylene. The mechanism at temperatures above 1500 K is believed to be a free radical process.[1,2] However, the mechanism below 1500 K is still the subject of sharp controversy. Published experimental results are limited and are subject to interference by secondary and even tertiary reactions, so neither proposed mechanism could be eliminated. Study of the pyrolysis of acetylene at low conversions should provide crucial information regarding the mechanism.

When a free radical reaction starts, it takes a short time for free radicals to be formed and to reach their steady concentration. This period of time is usually called the induction period. Induction periods were observed in free radical polymerizations in the liquid phase using the viscosity method,[3] the rotating-sector technique[4] and the emulsion technique.[5] A mathematical theory was proposed by Come[6] for induction periods in the pyrolysis of hydrocarbons. Induction periods have been observed in the pyrolysis of ethane,[7] ethylene,[8] neopentane,[9,10] acetone[11], and 1,2-dichloroethane.[12] Such induction periods were usually observed in flow systems.

An equation was derived for the rate of formation of methane in neopentane pyrolysis in a plug flow system.[9] A similar equation applies to other cases where the key radicals are removed in a bimolecular, chain termination.

$$[P]/t = [(b_P/t)ln\{[1+exp(a_Pt)]/2\}-a_Pb_P/2](1-c_Pt) \quad \text{(E4-1)}$$

Here, $[P]$ is the concentration of a product leaving the reactor; t, the residence time of gases in the reactor; a_Pb_P equals $2R_p^{ss}$; R_p^{ss} is the steady-state rate of product formation; a_P equals $4(R_ik_t)^{1/2}$; R_i is the initiation rate; k_t, the termination rate constant; and c_P, a parameter associated with secondary reactions.

The relation between the induction period, τ, and the parameter, a_p, was derived as equation (E4-2),[6] assuming the termination step was second order.

$$\tau = 1/(k_ik_t[C_2H_2]^n)^{1/2} = 2ln2/a_p \quad \text{(E4-2)}$$

Here, k_i is the rate constant for the initiation reaction and n is the order of the initiation reaction.

Vinylidene was proposed to be a key intermediate in the molecular mechanism. The induction period caused by the delay in establishing the steady-state concentration of vinylidene should be its lifetime, 3.5 μs, a recent, experimental result by Levin et al. using coulomb explosion imaging techniques.[13] This is too fast to be observed in a flow system. Therefore, the observation of an induction period at low temperatures would be an excellent method to distinguish between a free radical mechanism and a molecular mechanism.

In the present work, we will search for an induction period of a few milliseconds at very low conversions.

4-2. Results

4-2-1. Observation of induction periods for the formation of vinylacetylene and benzene

Acetylene was pyrolysed in a flow system between 854 and 970 K, at pressures between 27 and 127 Torr, and at residence times between 8 and 1520 ms. Only vinylacetylene and benzene were observed as products at these conditions. The flow rates of acetylene into the reactors and the diameters of the reactors were varied to attempt to detect an induction period in the formation of vinylacetylene and benzene. The residence time of gas in the reactor was calculated from the reactor temperature and volume, and from the gas pressure and flow rate. The average rates of formation of vinylacetylene (R_{VA}) and benzene (R_B) were calculated by dividing their concentrations at the reactor exit by the residence times. Conversions were calculated to be in a range between 0.0022% and 1.4%. Reactors with smaller inner diameters were used at high pressures or high temperatures.

Figure 4-1 shows the average rates observed for vinylacetylene and benzene at 27 Torr and 935 K in a 3.96-mm-id reactor at residence times between 0.027 and 0.39 s. At residence times greater than 0.2 s, the rates of formation of vinylacetylene and benzene were almost independent of the reaction time; this behavior would be characteristic of a primary reaction occurring with the concentrations of intermediates at their steady state

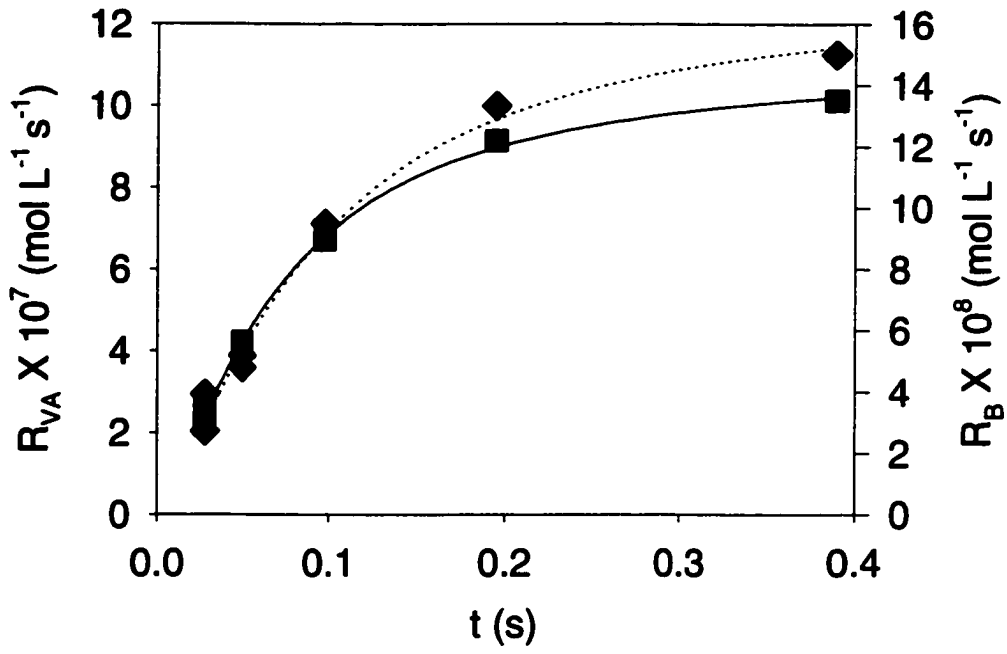

Figure 4-1. Dependence of the rates of formation of vinylacetylene and benzene on the residence time at 27 Torr and 935 K in a 4-mm-id reactor; ■, vinylacetylene; ▲, benzene; solid curve, non-linear least-squares fit of equation (E4-1) to the data for vinylacetylene; dotted curve, non-linear least-squares fit for benzene.

values. At shorter residence times, the rates of product formation were much less. At the shortest residence time, the rates of formation of vinylacetylene and benzene were only 24% and 21%, respectively, of their values at 0.4 s. This behavior is characteristic of an induction period. The increases in the rates of formation for vinylacetylene and benzene were almost parallel to each other; indicating their induction periods were similar.

Figure 4-2 shows typical induction periods observed at 68 Torr and 936 K in a 1.96-mm-id reactor. The rate of formation of vinylacetylene increased with increasing residence time to a maximum value, and then gradually fell off. On the other hand, the rate of formation of benzene increased with the residence time to a shoulder value, and then continued to increase more gradually.

4-2-2. Results of fitting the induction periods for vinylacetylene and benzene

Equation (E4-1) was fitted to the data for vinylacetylene and benzene by non-linear least squares.[14] Figures 4-1 and 4-2 show examples of the fitted curves. Table 4-1 lists the values of the parameters obtained from the fits. Quoted uncertainties are standard deviations. The values of the induction period, τ, obtained from the vinylacetylene data and from the benzene data agreed within 9% in most cases. There were differences in a few cases at low pressures because of the larger errors in the benzene data, associated with the much smaller peaks for benzene. The steady state rates obtained for vinylacetylene were greater than those obtained for benzene. The parameters, c, obtained

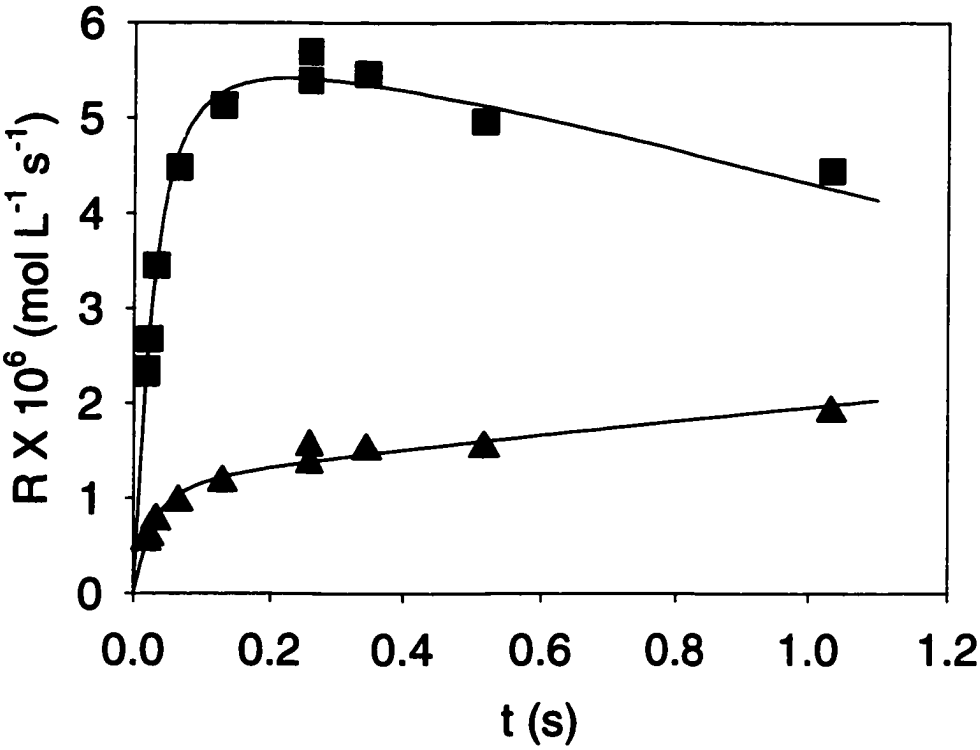

Figure 4-2. Dependence of the rates of formation of vinylacetylene and benzene on the residence time at 68 Torr and 936 K in a 2-mm-id reactor; ■, vinylacetylene; ▲, benzene; solid lines, non-linear least-square fits of equation (E4-1) to the data.

Table 4-1. Parameters of the progress curves for vinylacetylene and benzene obtained by nonlinear least-squares fits of equation (E4-1) to experimental data.

T (K)	P (Torr)	reactor id (mm)	τ_{VA} (s)	τ_B (s)	$R_{VA}^{ss} \times 10^7$ (mol L^{-1} s^{-1})	$R_B^{ss} \times 10^7$ (mol L^{-1} s^{-1})	c_{VA} (s^{-1})	c_B (s^{-1})
970	53	1.96	0.035±0.002	0.038±0.006	67.5±1.5	8.5±0.5	0.44±0.04	-1.03±0.16
970	36	0.969	0.049±0.005	0.086±0.018	30.1±1.1	4.03±0.25	*	*
938	126	0.969	*	*	195±8	65±5	*	*
936	69	1.96	0.045±0.003	0.041±0.008	63±3	12.8±1.1	0.30±0.09	-0.55±0.27
934	52	3.96	0.056±0.007	0.057±0.006	40.6±1.7	7.0±0.3	0.34±0.06	-0.37±0.07
934	34	3.96	0.096±0.012	0.072±0.006	20.8±1.3	2.33±0.10	0.36±0.07	-0.60±0.09
935	27	3.96	0.121±0.005	0.151±0.014	11.5±0.2	1.76±0.07	*	*
895	60	3.96	0.118±0.008	0.105±0.003	22.7±0.8	6.9±0.1	0.20±0.04	*
854	120	3.96	0.121±0.003	0.121±0.009	28.1±2.0	16.9±0.4	0.090±0.001	*

* There was insufficient data to reliably obtain the missing parameters.

from the secondary processes for vinylacetylene and for benzene were similar in absolute magnitude, but opposite in sign.

The orders of the parameters were calculated from their pressure dependences at 934-936 K. Figure 4-3 shows an order plot for the induction period, τ. The order for τ_{VA} was -1.09±0.07. The order for τ_B was -1.2±0.3, and the order for the combination of τ_{VA} and τ_B was -1.1±0.1. In determining these orders, individual points were given weights proportional to the inverse squares of their fractional standard deviations. All these values are consistent with an order of -1, indicating that the value of n (the order of the initiation reaction) in equation (E4-2) is two. Figure 4-4 shows that the order for the steady-state rate of formation of vinylacetylene, R_{VA}^{ss}, was 1.8±0.1, and that the order for the formation of benzene, R_B^{ss}, was 2.4±0.1. The parameters, c_{VA} and c_B, were found to be almost independent of the pressure.

Arrhenius plots for $k_i k_t$ *(equal to* $(\tau[C_2H_2])^{-2}$ from equation *(E4-2))* are shown in Figure 4-5. Similar parameters (E4-3)-(E4-5) were derived from different sets of data.

$$(k_i k_t)_{VA} = 10^{23.5\pm0.5}\, L^2\, mol^{-2}\, s^{-2} exp[(-268\pm8)\, kJ\, mol^{-1}/RT] \quad \text{(E4-3)}$$

$$(k_i k_t)_B = 10^{21.4\pm1.9}\, L^2\, mol^{-2}\, s^{-2} exp\,[-(231\pm34) kJ\, mol^{-1}/RT] \quad \text{(E4-4)}$$

$$(k_i k_t)_{VA+B} = 10^{23.1\pm0.5}\, L^2\, mol^{-2}\, s^{-2} exp[\,-(261\pm7) kJ\, mol^{-1}/RT] \quad \text{(E4-5)}$$

Here, equation (E4-5) was obtained from the data for both vinylacetylene and benzene.

Arrhenius plots for k_{VA} $(= R_{VA}^{ss}/[C_2H_2]^2)$, *and* k_B $(= R_B^{ss}/[C_2H_2]^{2.4})$ are shown in Figure 4-6. Here the order for R_{VA}^{ss} was rounded to two, but the order for R_B^{ss} was kept as a

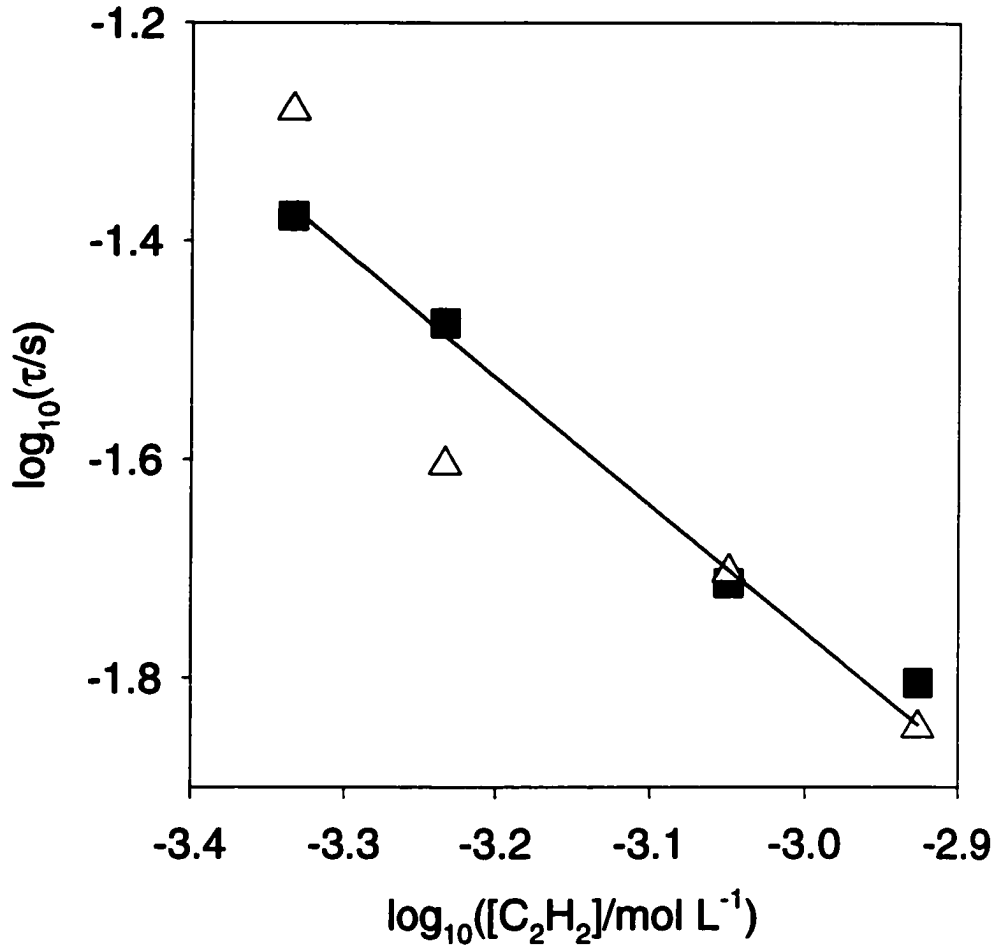

Figure 4-3. Dependence of the induction period, τ, on the acetylene concentration at 934-936 K; solid squares, results for vinylacetylene; hollow triangles, results for benzene; solid line, weighted least-squares fit to the data for both vinylacetylene and benzene.

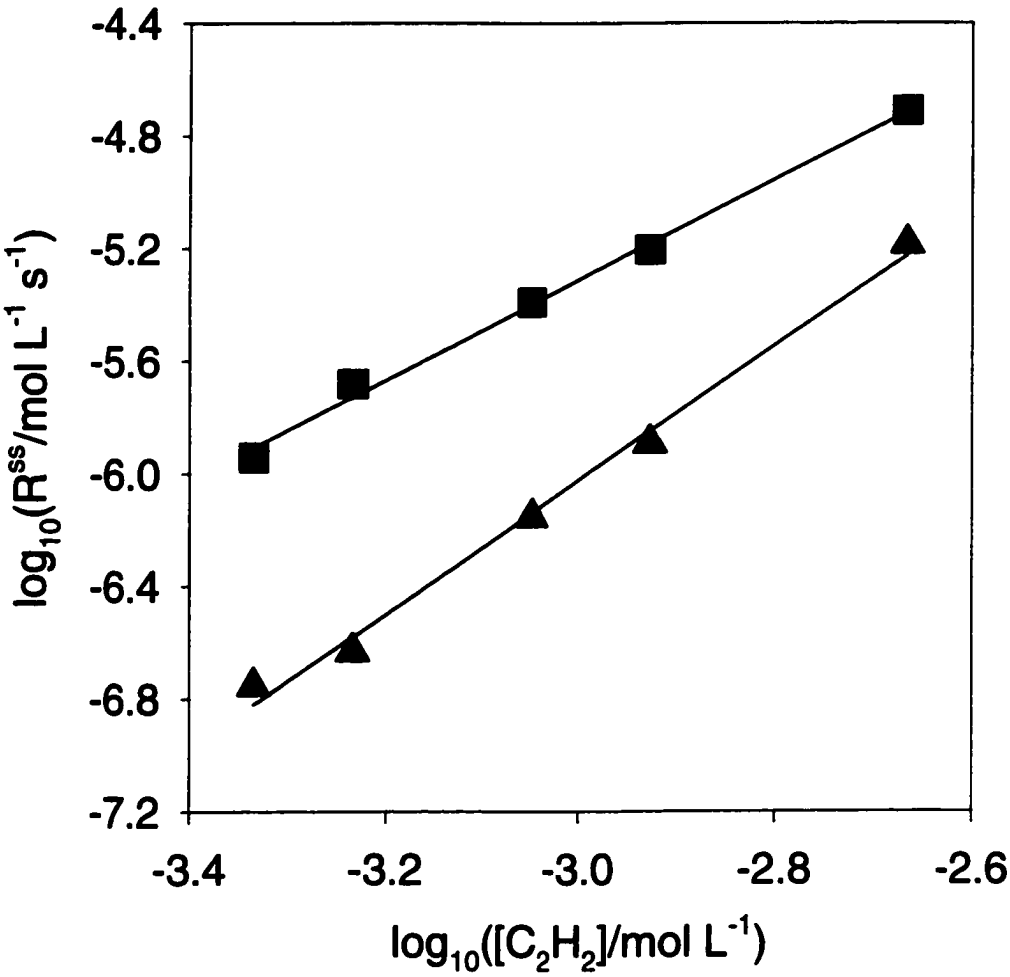

Figure 4-4. Dependence of the steady-state rates, R^{ss}, on the acetylene concentration at 934-936 K; squares, results for vinylacetylene; triangles, results for benzene.

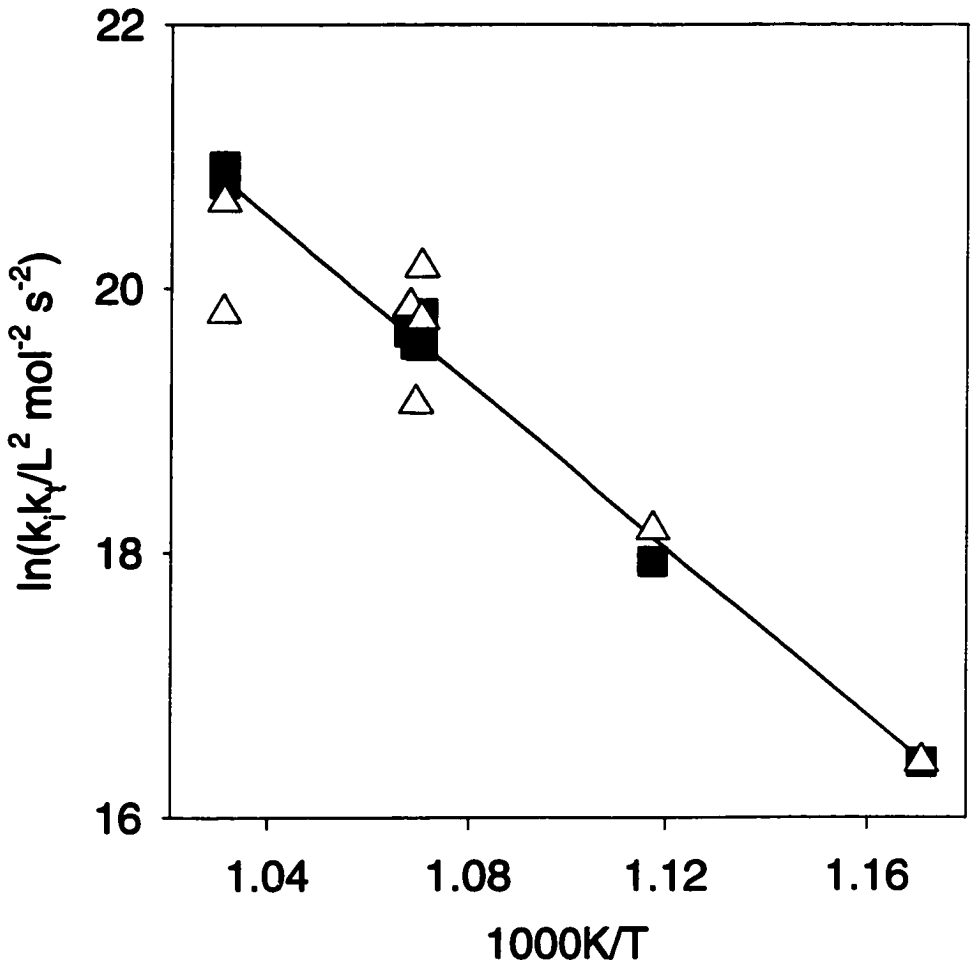

Figure 4-5. Arrhenius plot of $k_i k_t$; solid squares, results for vinylacetylene; hollow triangles, results for benzene; solid line, weighted least-squares fit to the data for both vinylacetylene and benzene.

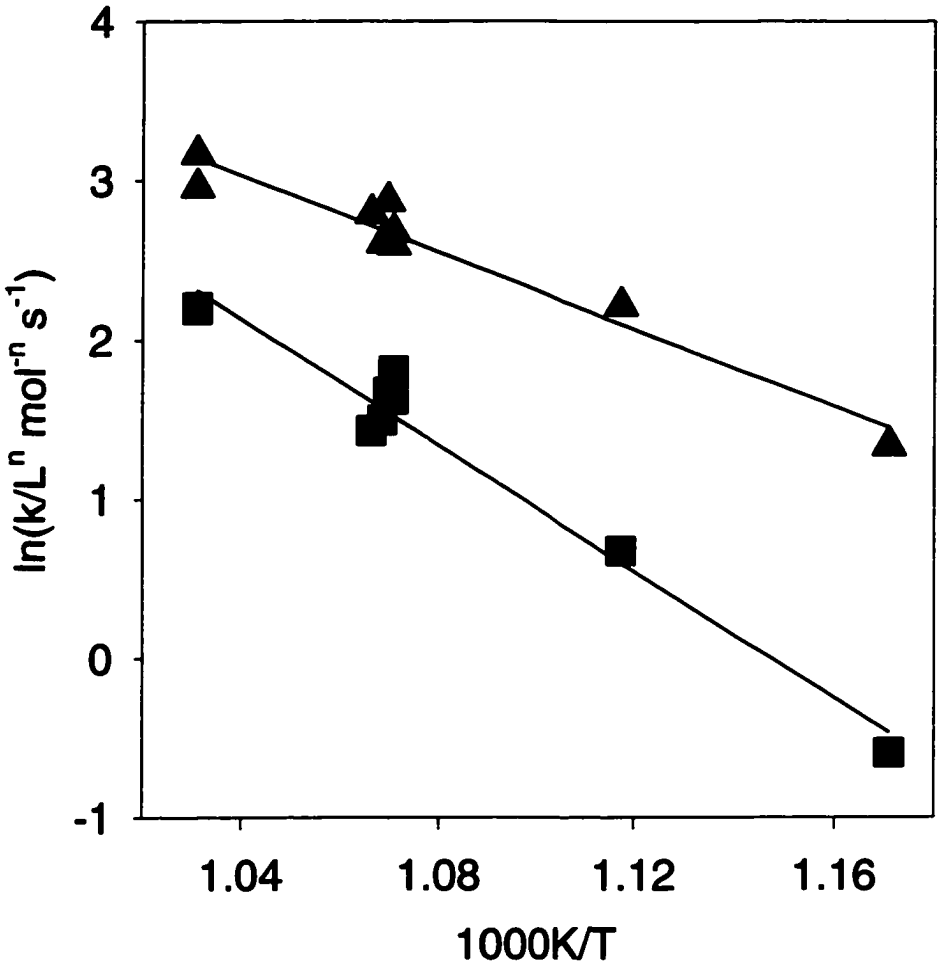

Figure 4-6. Arrhenius plots for $k/L^n\ mol^n\ s^{-1}$ (n = 1 for vinylacetylene, and 1.4 for benzene), the effective rate constants in the steady-state regime; squares, results for vinylacetylene; triangles, results for benzene.

fraction. Equations (E4-6) and (E4-7) were obtained from the data on vinylacetylene and benzene, respectively.

$$k_{VA} = 10^{9.86\pm0.65}\ L\ mol^{-1}\ s^{-1} exp[\ -(165\pm11)kJ\ mol^{-1}/RT] \quad \text{(E4-6)}$$

$$k_B = 10^{6.77\pm0.48}\ L^{1.4}\ mol^{-1.4}\ s^{-1}\ exp\ [-(100\pm9)kJ\ mol^{-1}/RT] \quad \text{(E4-7)}$$

Figure 4-7 shows the Arrhenius plots for the parameters, c_{VA} and c_B. The following equations were derived,

$$c_{VA} = 10^{4.82\pm0.52}\ s^{-1}\ exp\ [-(95.4\pm9.3)kJ\ mol^{-1}/RT] \quad \text{(E4-8)}$$

$$c_B = -10^{3.56\pm0.78}\ s^{-1}\ exp\ [-(67.0\pm14.1)kJ\ mol^{-1}/RT] \quad \text{(E4-9)}$$

4-3. Discussion

The observations reported in the previous section will be discussed in this section. We will start by considering whether there may be systematic errors interfering with the results reported. We will consider first various physical interferences, such as heat, momentum and mass transfer, and then various chemical processes, such as surface reactions and possible parallel processes. We will then consider the lessons to be drawn from these experiments, and compare the results with theoretical predictions and with the results of earlier experiments, where appropriate.

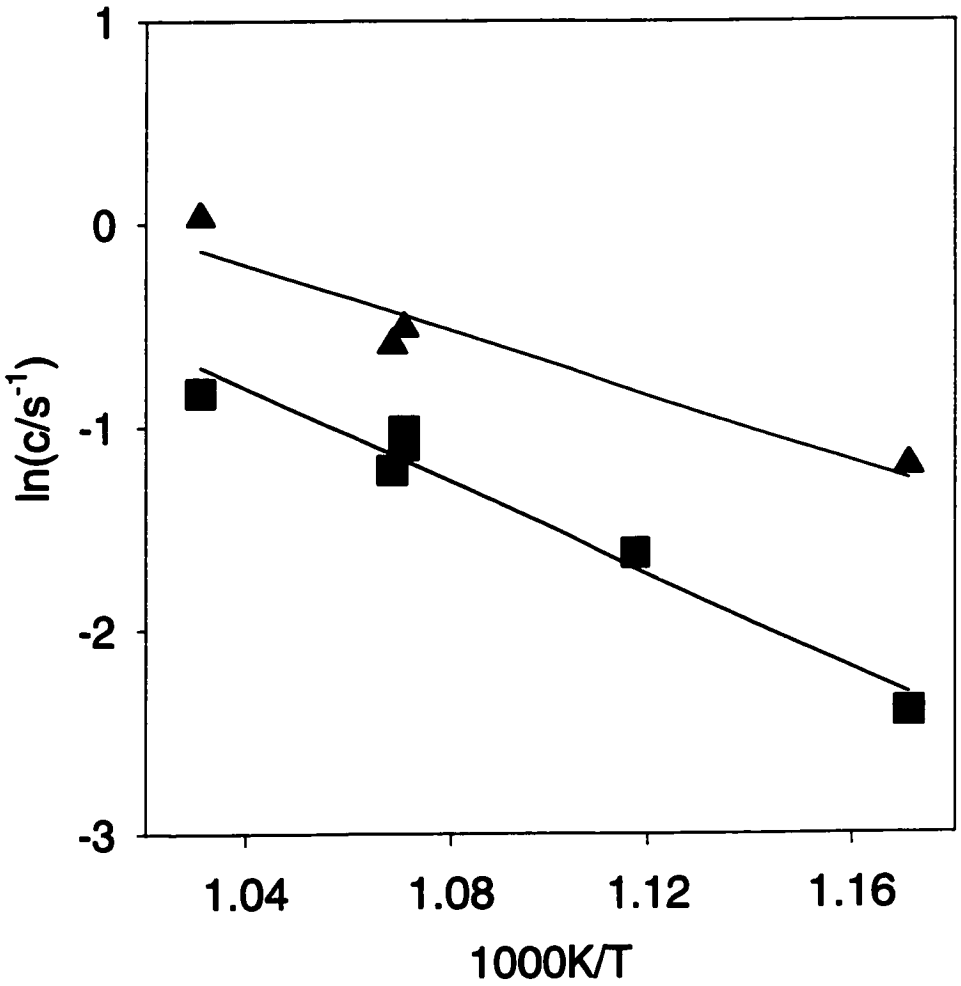

Figure 4-7. Arrhenius plots for the absolute values of the parameters, *c*, for secondary reactions; squares, results for vinylacetylene; triangles, results for benzene.

4-3-1. Effect of incomplete radial heat transfer

This effect has been discussed in section 2-1. Thermal properties of acetylene were obtained from the literature.[15] Using the activation energies and the reactor radii, residence times and temperatures from the present work, the maximum reduction in k_{app} because of incomplete radial heat transfer was calculated to be 4%. This may be compared to the experimental reductions in rates of between 60% and 80% observed in Figures 4-1 and 4-2. We conclude that the induction periods observed were not caused by incomplete radial heat transfer.

4-3-2. Pressure drop, axial diffusion and volume contraction

The Reynolds number was estimated to be in the range between 0.20 and 24, so laminar flow was established in the present work. The pressure drop in the present work was minimized by using short reactors. Measured pressure drops were always less than 10%, so the effect of pressure drop was negligible.

Furue and Pacey[16] investigated the effect of mass transfer in the pyrolysis of cyclopropane in cylindrical flow reactors and found that the apparent first order rate constant was reduced by 10% only at conversions of 83% or more. Hence, the effect of mass transfer was not significant at the low conversions of less than 1.4% in the present work. The Peclet number was calculated to be between 4 and 1800, also indicating that

diffusion was insignificant compared to convection. In addition, the low conversions in this work should not have resulted in a significant volume contraction.

4-3-3. Surface reaction and the effect of impurities

A possible source of error is a surface reaction, which would vary in importance in reactors with different diameters. A carbon deposit on the surface was found in the previous chapter[17] to inhibit the formation of gaseous products by a heterogeneous termination process. Washing the reactor with HF and burning off the carbon deposit almost eliminated this inhibition. These procedures were followed in the present chapter.

Equation (E4-1) applies to a mechanism with a bimolecular termination process. It has been shown elsewhere[18] that, if termination occurs by a unimolecular, surface process, the induction period is inversely proportional to k_t. If a surface reaction is limited by the first-order rate of reaction of radicals at the surface, the induction period would be independent of $[C_2H_2]$. If a surface reaction is limited by diffusion, the induction period would be proportional to the gas pressure. Neither of these hypotheses would predict the inverse proportionality between τ and $[C_2H_2]$ observed in Figure 4-3. It is concluded that chain termination in the present system occurs in the gas phase. If the termination occurs by a bimolecular removal of two intermediates, equations (E4-1) and (E4-2) in the introduction are appropriate. If termination occurs by a collision between the key intermediate and acetylene, the induction period would be equal to $(k_t[C_2H_2])^{-1}$.[18] This

possibility also agrees with the observed order in Figure 4-3, and will be considered further in the next two sections.

The results at the highest concentrations in Table 4-1 and Figures 4-3 and 4-4 were obtained using reactors of different diameters. These results agreed very well with the trends established at lower concentrations in the large reactor.

The main impurity in acetylene was acetone, which is a source of free radicals at high temperatures. It was previously found that acetone had no significant effect on the pyrolysis of acetylene when its mole fraction was less than 400 ppm.[19] In the present work, its mole fraction was controlled to be less than 120 ppm. The rates of initiation reactions from acetone, propylene, propane, and ethane impurities in the purified acetylene were estimated from the concentrations in section 2-2 and from rate constants in the literature[11,20-22] to be 5.9×10^{-9} mol L^{-1} s^{-1}, 4.7×10^{-16} mol L^{-1} s^{-1}, 1.4×10^{-9} mol L^{-1} s^{-1}, and 2.3×10^{-11} mol L^{-1} s^{-1}, respectively. The value for initiation by acetone was the largest of these, so initiation by propylene, propane, and ethane should also be negligible.

4-3-4. Mechanism of the reaction

As mentioned in Chapter 1, molecular mechanisms involving vinylidene and free radical mechanisms have both been proposed to interpret the pyrolysis of acetylene. The lifetime for vinylidene in a vacuum was determined to be 3.5 μs by Levin et al.[13] A multiple barrier recrossing between vibrationally excited acetylene and vinylidene was

simulated by Hayes et al. using *ab initio* molecular dynamics methods.[23] At the gas pressures used in the present work, the lifetime of vinylidene would be determined by its deactivation by collision with other molecules. Assuming deactivation on every collision, the lifetime is estimated to be 1-5 ns in our system, seven orders of magnitude shorter than the induction periods observed.

The lifetime of the propargylmethylene intermediate, CH_2CCHCH, proposed by Kiefer and Von Drasek,[24] was estimated to be between 10^{-11} and 10^{-12} s at 854-970 K, using the rate constant for its conversion to vinylacetylene suggested by Benson.[25]

The contribution of a molecular mechanism should be independent of the residence times used in the present work. When a term, d, representing the contribution of a molecular mechanism is added into equation (E4-1), we obtain,

$$[P]/t = d + [(b_P/t)ln\{[1+exp(a_Pt)]/2\}-a_Pb_P/2](1-c_Pt) \qquad \text{(E4-10)}$$

Table 4-2 shows the ratio, d/R^{ss}, of the rate of a possible molecular process to the full steady-state rate, obtained by fitting (E4-10) to the data for vinylacetylene and for benzene. The uncertainties in the parameters a, b, and c, increased by factors between 2 and 5. Uncertainties greater than 50% in most cases, and negative values in some cases, were obtained for the parameter, d. The average value of d_{VA}/R_{VA}^{ss}, expressed as a percentage, was (2.6±7.7)%. Therefore, the contribution from a molecular mechanism to the formation of vinylacetylene (d_{VA}/R_{VA}^{ss}) was negligible. At 934-936 K, the maximum contributions from a molecular mechanism to the formation of benzene (d_B/R_B^{ss}) were about 30%. The average value of d_B/R_B^{ss} in the table was (15±15)%. This leaves open the possibility of a minor, molecular pathway leading to the formation of benzene.

Table 4-2. Estimated fractional rates of formation of vinylacetylene and benzene from a possible, parallel, molecular pathway obtained by nonlinear least-squares fits of equation (E4-10) to the experimental data. *

T (K)	P (Torr)	d_{VA}/R_{VA}^{ss}	d_B/R_B^{ss}
970	53	0.059±0.082	0.18±0.09
970	36	0.070±0.071	0.10±0.02
936	69	0.13±0.07	0.30±0.08
934	34	-0.087±0.006	0.27±0.05
935	27	-0.0008±0.0312	-0.019±0.004
895	60	0.066±0.116	-0.072±0.126
854	120	-0.053±0.181	0.30±0.48

*Non-linear least-squares fits didn't converge at 938 K and 126 Torr, and at 934 K and 52 Torr.

It is necessary to distinguish the present induction period from another period of time, the auto-acceleration period, which has sometimes been called an induction period in previous work. When significant amounts of products have been formed, one or more of these products could introduce new sources of free radicals. Therefore, the entire reaction could be accelerated. Auto-acceleration has been observed at higher conversions in the pyrolysis of acetylene by some previous workers. Frank-Kamenetzky[26] found an auto-acceleration period of 12 seconds at 192 Torr and 877 K in a flow system. He found the auto-acceleration period was proportional to the inverse square of $[C_2H_2]$ at temperatures above 773 K. Minkoff et al.[27] observed an auto-acceleration period of 48 seconds at 236 Torr and 773 K in a static reactor. Cullis and Franklin[28] observed an auto-acceleration period between 10 and 20 seconds at pressures from 270 to 370 Torr over the temperature range of 828-938 K. These auto-acceleration periods were two or three orders of magnitude longer than the induction periods observed in the present work, and represent a distinct chemical phenomenon. The rates at short residence times in Figures 4-1 and 4-2 in the present work appeared to approach zero, whereas a finite rate was observed at short residence times in the previous studies. Auto-acceleration was observed for benzene in the present work. If the data at residence times less than 0.2 s were deleted from Figure 4-2, we would have a similar situation to that reported by the earlier workers.[26-28] The rate of benzene formation would increase with increasing residence time, but, without the first few data points, there would appear to be a finite initial rate. Benson[25] interpreted auto-acceleration as the result of the build-up of vinylacetylene concentration in the system.

In the present work, both vinylacetylene and benzene were found to be primary products. The induction periods in Table 4-1 were between 35 and 150 ms. These are seven orders of magnitude slower than the relaxation time for vinylidene, and nine orders of magnitude slower than the lifetime for propargylmethylene. They are one or two orders of magnitude slower than radial heat transfer. They are two or three orders of magnitude faster than auto-acceleration.[26-28] They are similar to the induction periods caused by the establishment of free radical concentrations in other pyrolysis systems.[7-11] This is crucial evidence for a free radical mechanism in the pyrolysis of acetylene. Molecular mechanisms involving vinylidene[24,29] do not appear to play a dominant role in the present work. However, we cannot rule out a minor contribution from a molecular mechanism to the formation of benzene.

The similarity of the induction periods for vinylacetylene and for benzene indicates that both vinylacetylene and benzene were formed from the same free radicals or from free radicals which could rapidly interconvert.

4-3-5. Properties of the initiation and termination reactions

The order of the initiation reaction may be estimated using equation (E4-2). It is twice the absolute value of the slope of a graph of $log_{10}\tau$ versus $log_{10}[C_2H_2]$, as shown in Figure 4-3. The order of the initiation reaction can be calculated to be 2.18±0.14 from the

vinylacetylene data, 2.4±0.6 from the benzene data, and 2.2±0.2 from the data for both vinylacetylene and benzene. A second-order initiation reaction was supported.

Most radical recombination reactions have rates which are almost independent of temperature. Sometimes there is a dependence on $T^{1/2}$ or $T^{-1/2}$, corresponding to an activation energy of ±0.5 RT, or ±4 kJ mol^{-1} at the temperatures of this work. Therefore, the temperature dependence of the product, $k_i k_t$, in equations (E4-3) to (E4-5) must be almost entirely associated with k_i. The activation energy for the initiation reaction may be derived to be 268±12 kJ mol^{-1} from the data for vinylacetylene, 231±38 kJ mol^{-1} from the data for benzene, and 261±11 kJ mol^{-1} from the combined data.

The singlet-triplet gap for acetylene was experimentally determined to be 346 kJ mol^{-1},[30] which is much higher than the activation energy for initiation in the present paper. Therefore, Minkoff's triplet-initiation mechanism can be ruled out.

Back's initiation reaction,[31]

$$2C_2H_2 \rightarrow C_2H + C_2H_3 \qquad \text{[MB1]}$$

can be ruled out, because its activation energy was calculated using *ab initio methods*[29] to be 370 kJ mol^{-1}, which is again much higher than the activation energy determined in the present work.

Unimolecular initiation by the rupture of a C-H bond in acetylene,

$$C_2H_2 + M \rightarrow C_2H + H + M \qquad \text{[MB2]}$$

was important at much higher temperatures.[31,32] The activation energy for this reaction was calculated to be 508 kJ mol^{-1} at 1000 K, using recent experimental results reported by

Kruse and Roth[32] at 2580 to 4650 K. This energy is almost twice as great as our activation energy, so unimolecular initiation was not important in this work.

The rate constant for an initiation reaction involving the formation of C_4H_3 and H,

$$2C_2H_2 \rightarrow C_4H_4^* \rightarrow C_4H_3 + H \qquad [B1]$$

has been estimated by some previous workers using thermochemical methods. Tanzawa and Gardiner[33] suggested a rate constant of 2×10^9L mol^{-1} s^{-1}exp(-192 kJ mol^{-1}/RT). Wu and co-workers[34] estimated an expression of 2×10^{10}L mol^{-1} s^{-1}exp(-186 kJ mol^{-1}/RT). Kiefer et al.[2] predicted an expression of 1.5×10^{11}L mol^{-1} s^{-1}exp(-234 kJ mol^{-1}/RT). Melius et al.[35] calculated an activation energy of 231±15 kJ mol^{-1} for this reaction by *ab initio* methods. The values estimated by Kiefer et al. and by Melius et al. are very close to the value determined from the benzene data in this work. The lowest energy form of C_4H_3 plus H was calculated to be 179.7 kJ mol^{-1} more stable than C(^{3}P) plus allene using *ab initio MO* methods.[36] Combining this result with the enthalpies of formation of the latter species and of acetylene,[37] the activation energy for reaction [B1] could be calculated to be 273 kJ mol^{-1}. This value is very close to that determined from the data for vinylacetylene in the present work.

The rate constant of this initiation reaction may also have been experimentally measured. One of the possible products of the initiation reaction, C_4H_3, was observed in a shock tube at 1600-2400 K by Gay et al.[1] They assumed that the rate of the initiation reaction was equal to the rate of formation of diacetylene, for which an induction period was observed in their system. The Arrhenius expression for initiation was calculated to be 2.95×10^{10} L mol^{-1} s^{-1}exp(-162 kJ mol^{-1}/RT). Frank and Just[38] observed another possible

product of the initiation reaction, H, in a shock tube at 1850-3000 K. The concentration of H built up to a steady-state value following an induction period. They first assumed that the only source of H atoms was reaction [MB2], but the Arrhenius curve for this reaction was found to bend up at their lowest temperatures, 1850-2000 K, indicating that there was an additional source of H atoms, which was suggested to be reaction [B1]. However, they didn't propose an Arrhenius expression for this initiation reaction because of the narrow range of temperatures. They found that their rate constant was 12 times slower than that reported by Gay et al.,[1] and suggested that a chain reaction might have been involved in the earlier experiments.

Dimitrijevic et al.[19] obtained an Arrhenius expression of $10^{12.7\pm0.9}$L mol^{-1} s^{-1}exp(-253±15 kJ mol^{-1}/RT) for a bimolecular, initiation reaction, assuming a first-order, surface termination, by studying the acceleration of the pyrolysis of acetylene by acetone at 914-1039 K.

A C_4H_4 triplet, $H_2^{\bullet}CCCC^{\bullet}H_2$, was calculated using *ab initio MO* methods[36] to be 224.7 kJ mol^{-1} more stable than C_4H_3 plus H. Using the *ab initio* enthalpy of C_4H_3 above,[35] the enthalpy change for the formation of C_4H_4 triplet from acetylene would be only 6±15 kJ mol^{-1}. The original authors[36] didn't suggest this triplet would participate in acetylene pyrolysis, but it is energetically accessible, so it must be considered further.

If the triplet, C_4H_4, was the main chain carrier, net removal of the triplet species could occur by three possible pathways, i.e. unimolecular intersystem crossing to a singlet, bimolecular quenching to a singlet, or bimolecular triplet-triplet annihilation. The first, unimolecular process would lead to an induction period independent of $[C_2H_2]$, contrary

to the experimental observations. Bimolecular quenching and triplet-triplet annihilation would agree with the observed concentration dependence.

In the case of bimolecular quenching between a triplet and an acetylene molecule, the expression for the induction period could be derived as,

$$\tau = 1/(k_q[C_2H_2]) \qquad \text{(E4-11)}$$

Here, k_q is the rate constant of bimolecular quenching. To agree with the experiments, this quenching process would need to have a pre-exponential factor equal to the square root of $10^{23.1\pm0.4}$ L^2 mol^{-2} s^{-2}, i.e. 3.6×10^{11} L mol^{-1} s^{-1}, and an activation energy of 130±4 kJ mol^{-1}. The Arrhenius parameters for k_q could be estimated from the parameters for similar processes. The pre-exponential factor and the activation energy for the quenching of triplet acetophenone by singlet acetophenone were reported to be 2.5×10^{8} L mol^{-1} s^{-1} and 1.3 kJ mol^{-1} in the gas phase, and 6.3×10^{6} L mol^{-1} s^{-1} and 2.1 kJ mol^{-1} in solution, respectively.[39] Typical pre-exponential factors for quenching of various triplet species in solution were determined to lie between 10^6 and 10^{10} L mol^{-1} s^{-1}.[40] We can find no precedent for an activation energy for quenching as high as 130 kJ mol^{-1}, nor for a pre-exponential factor as high as 3.6×10^{11} L mol^{-1} s^{-1} for this spin-forbidden process. Therefore, we can rule out bimolecular quenching of a triplet as the process responsible for the observed induction periods.

In the case of triplet-triplet annihilation, by analogy with equation (E4-2) an expression for the induction period could be derived, as follows:

$$\tau = 1/(k_{SS}k_{TT}[C_2H_2]^2)^{0.5} \qquad \text{(E4-12)}$$

Here, k_{SS} is the rate constant for the formation of C_4H_4 triplet from two singlet acetylene molecules, and k_{TT} is the rate constant for the triplet-triplet annihilation. To agree with the constant term in equation (E4-5), these processes would need to have the product of their pre-exponential factors equal to $10^{23.1\pm0.4}$ L^2 mol^{-2} s^{-2}. The pre-exponential factor for the bimolecular interaction of singlet methylene and singlet acetylene to form triplet methylene and singlet acetylene in the gas phase was reported to be 4.8×10^{10} L mol^{-1} s^{-1}.[41] The pre-exponential factor for the bimolecular removal of two triplet methylenes in the gas phase was reported to be 1.2×10^{10} L mol^{-1} s^{-1}.[41] The product of these two numbers is 5.8×10^{20} L^2 mol^{-2} s^{-2}, more than two orders of magnitude less than the value determined in the present work. Slow pre-exponential factors from 10^8 to 10^{10} L mol^{-1} s^{-1} were also found for deactivation of large organic triplets by triplet oxygen in solution.[40]

Furthermore, the deactivation of C_4H_4 triplet, $H_2^{\bullet}CCCC^{\bullet}H_2$, should produce butatriene, which was not observed experimentally. *Ab initio* calculation showed that butatriene was only 26.7 kJ mol^{-1} less stable than vinylacetylene, and that there was a high barrier, 320 kJ mol^{-1}, for the conversion of butatriene to vinylacetylene.[35] The conversion from butatriene to vinylacetylene should not be significant in the present work. Therefore, no significant amount of C_4H_4 triplet, $H_2^{\bullet}CCCC^{\bullet}H_2$, could have been formed in the present work.

In view of the foregoing, the only initiation reaction which is consistent with the order, activation energy and product distribution observed in the present work is reaction [B1]. Recent workers[35] suggest this reaction occurs by the isomerization of an acetylene molecule to vinylidene, which adds to another acetylene to give a vibrationally excited,

singlet C_4H_4 complex, which decomposes to C_4H_3 and H. These two radicals would then add to acetylene, producing further radicals which would participate in the main chain reaction.

The constant term in equation (E4-5) corresponds to a product of the pre-exponential factors, A_iA_t, for initiation and termination of $10^{23.1\pm0.4}$ L^2 mol^{-2} s^{-2}. Vinylidene, with three rotational degrees of freedom, would be expected to have a higher entropy than acetylene, which has only two rotational degrees of freedom. Provided the attack of vinylidene on acetylene and the radical recombination occur with pre-exponential factors near the collision limit, the magnitude of the product, A_iA_t, above can be explained.

4-3-6. Properties of the steady state rates

The order for the formation of vinylacetylene was determined by some previous workers; results are summarized in Table 4-3. Ogura[42] found an order of 2.35 while most other workers reported an order of two. When vinylacetylene was the main product, the order for the decomposition of acetylene would approximately equal the order for the formation of vinylacetylene. The order for the decomposition of acetylene was measured by many previous workers, and the results were reviewed by Colket et al.[43] Most orders were found to be between 1.5 and 2.0. Most workers favored an order of two.

The second-order rate constant for the formation of vinylacetylene has been measured by several groups. Arrhenius parameters are also summarized in Table 4-3. The large

Table 4-3. Orders and Arrhenius parameters measured for the formation of vinylacetylene.

Reference	Apparatus	T (K)	$\log_{10}(A/L^{n-1}\ mol^{1-n}\ s^{-1})$	E_A (kJ mol^{-1})	Order
Bradley and Kistiakowsky[45]	shock tube	1800-2700	11.56	185	2
Ogura[42]	shock tube	1000-1670	13.74±1.05	201±6	2.35±0.15
Kiefer et al.[46]	shock tube	1700-2400	10.77	187	2
Duran et al.[44]	static reactor	770-980	9.74±0.20	155	2
Dimitrijevic et al.[19]	flow reactor	914-1039	11.8±0.7	208±13	2
the present work	flow reactor	854-970	9.86±0.65	165±11	1.8±0.1

variations in these parameters may be caused by the presence of auto-acceleration in experiments at higher conversions and by the presence of surface reactions in earlier work in static and flow reactors. In shock tube studies, the dominant initiation reaction may be reaction [MB2]. The absolute rate constants are compared in Figure 4-8. The rate constants from the present work lie between the results of Dimitrijevic et al.[19] and those of Duran et al.[46] It should be pointed out that the rate constant determined in the present work may have a small systematic error, because 1-butene was used to calibrate the GC peaks for vinylacetylene.

Benzene was also found to be a primary product in the pyrolysis of acetylene at 1273 K by Becker and Huttinger.[47] The order for the formation of benzene was suggested to be a combination of first and third order, depending on the residence time. The rate of formation of benzene could be calculated from their results to be 8.60×10^{-5} mol L^{-1} s^{-1} at 60 Torr and 1273 K. This is five times faster than the value calculated using our equation (E4-7). The third-order rate constant for the formation of benzene was reported to be $10^{11.6\pm0.9} L^2$ mol^{-2} s^{-1}exp(-164±17 kJ mol^{-1}/RT) by Dimitrijevic et al.[19]

In the present work, expression (E4-7) has an order of 2.4, instead of an integer. There are various interpretations of the fractional order. One explanation could be that benzene was formed by two parallel pathways with different orders. Different free radicals might have been involved. Therefore, the order observed would be a combination of the two orders of the pathways. According to the polymerization mechanism suggested by Benson,[25] a series of free radicals of different lengths could be formed. A second

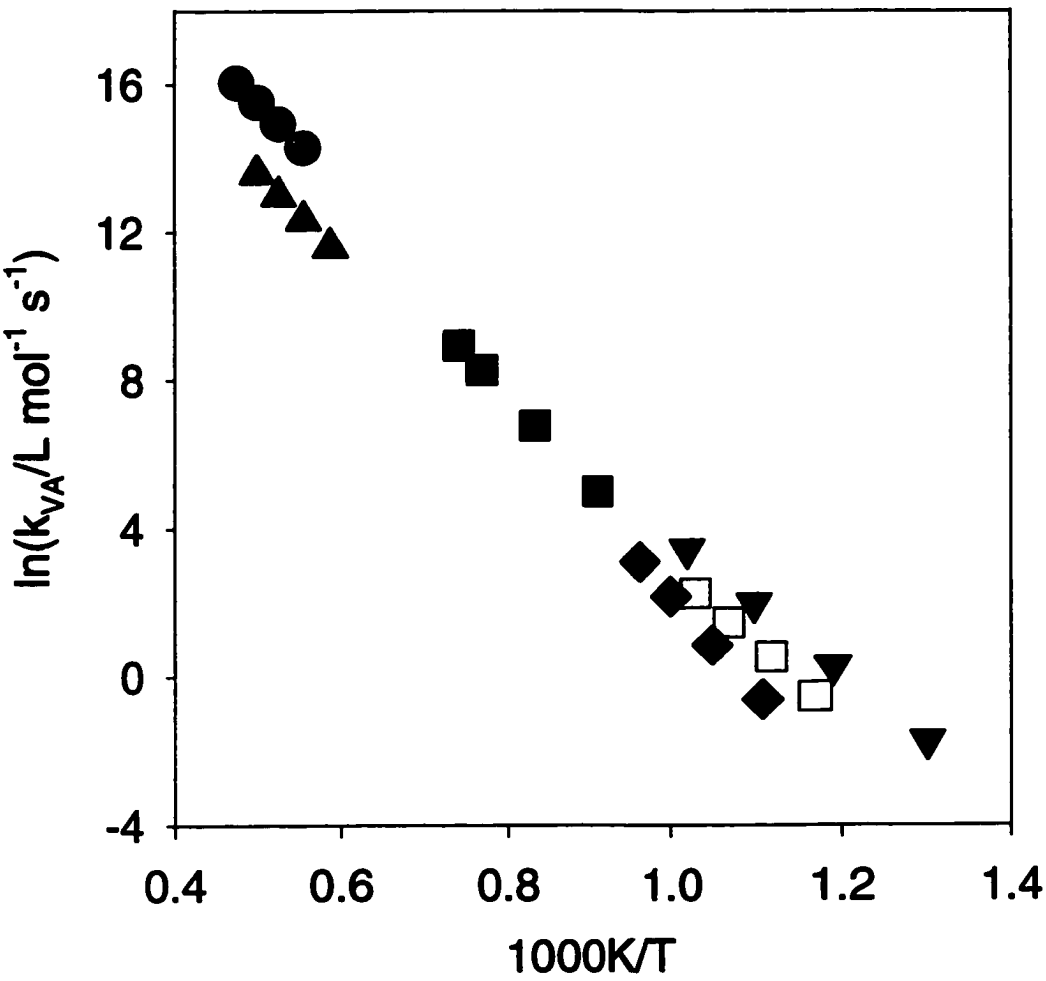

Figure 4-8. Arrhenius plot for $k_{VA}/L\ mol^{-1}\ s^{-1}$; ●, Bradley and Kistiakowsky[44]; ■, Ogura[42]; ▲, Kiefer et al.[45]; ▼, Duran et al.[46]; ◆, Dimitrijevic et al.[19]; □, this work.

explanation could be that benzene was limited by different, consecutive steps in a mechanism, e.g., the rate-determining step for the formation of benzene could be

$C_2H_2 + C_2H_3 \rightarrow C_4H_5$ [B4a]

at high pressures and

$C_2H_2 + C_4H_5 \rightarrow C_6H_7$ [B5a]

at low pressures. The combination of these two cases would lead to an order between 2 and 3. A third possibility is that two or more free radicals might be involved in termination reactions, which would also lead to a fractional order.

4-3-7. The parameters, b

Using equation (E4-2) and the definitions following equation (E4-1), it may be readily shown that the parameter b equals $R^{ss}\tau/ln2$. This parameter may be obtained by multiplying the parameters listed in the fourth and sixth columns of Table 4-1.

An expression for $ln(b/[C_2H_2])_{VA}$ can be derived from equations (E4-3) and (E4-6) as,

$$(b/[C_2H_2])_{VA} = 10^{-1.74\pm0.69}\ exp[-(31\pm12)kJ\ mol^{-1}/RT] \quad \text{(E4-13)}$$

Similarly, an expression for $ln(b/[C_2H_2]^{1.4})_{VA}$ can be derived from equations (E4-3) and (E4-7) as,

$$(b/[C_2H_2]^{1.4})_B = 10^{-4.82\pm0.52}\ mol^{0.4}\ L^{0.4}\ exp\ [(34\pm10)kJ\ mol^{-1}/RT] \quad \text{(E4-14)}$$

Now we know that both the initiation and termination reactions are bimolecular, it is possible to obtain an expression for the steady-state concentration of the radical, *X*, removed in the termination step.

$$[X]_{ss} = (k_i[C_2H_2]^2/k_t)^{1/2} \qquad \text{(E4-15)}$$

The case where there is more than one termination step has been considered by Come.[48] $[X]_{ss}$ depends on the first power of $[C_2H_2]$, whereas R_{VA}^{ss} has been shown to be approximately proportional to $[C_2H_2]^2$. So R_{VA}^{ss} can be related to $[X]_{ss}$ as follows:

$$R_{VA}^{ss} = k_p[X]_{ss}[C_2H_2] \qquad \text{(E4-16)}$$

Here, k_p is an effective rate constant for propagation. It may be that *X* does not lead to vinylacetylene in one step but by several steps involving the rapid interconversion of radicals. Combining equations (E4-2), (E4-15) and (E4-16), we find the quotient in equation (E4-13) is related to k_p and k_t.

$$b_{VA}/[C_2H_2] = k_p/(k_t ln2) \qquad \text{(E4-17)}$$

Again the termination rate constant, k_t, is likely to have only a weak temperature dependence, so the activation energy, 31 ± 12 kJ mol^{-1}, in equation (E4-13) must be similar to the activation energy for k_p. The constant term, -5.0 ± 1.6, indicates that k_p has a pre-exponential factor lower than that for k_t by about two orders of magnitude.

The activation energy for reaction [B4a] has been estimated to be 25 kJ mol^{-1} using a thermochemical method[49] and 36 kJ mol^{-1} from an *ab initio* calculation.[50] These values are within the range of uncertainties in equation (E4-13).

Because of the greater uncertainties in the benzene data, it is not possible to perform a similar analysis.

4-3-8. The parameters, c

Auto-acceleration was observed in the formation of benzene in the present time scale. (The parameter c_B was always positive.) This process might involve secondary reactions of vinylacetylene with free radicals. The amounts of vinylacetylene removed and of benzene formed by secondary reactions can be compared by examining the products $b_{VA}c_{VA}$ and $-b_Bc_B$. The fact that $b_{VA}c_{VA}$ values were two to seven times larger than b_Bc_B values indicates that vinylacetylene might have been involved in several secondary reactions, including its conversion to benzene and the continuous addition of C_2 units to form C_8 and higher species.

Vinylacetylene was reported to be a reactive species at high temperatures.[51] The first-order rate constant for the total removal of vinylacetylene in the pyrolysis of pure vinylacetylene in a shock tube[52] was reported to be $6.1\times10^{13}(s^{-1})\exp(-334\ kJ\ mol^{-1}/RT)$. This is about four orders of magnitude smaller than the value of c_{VA} from (E4-8) at 970 K in the present work. The activation energy reported was three times greater than the value measured in the present work. This indicates that the main secondary reaction of vinylacetylene in the present work was not the unimolecular decomposition of vinylacetylene.

The rate of vinylacetylene removal in the pyrolysis of an equimolar mixture of acetylene and vinylacetylene in a static vessel at 723 K[53] was shown to be 2.6×10^{-6} mol L^{-1} s^{-1}. This rate is about half as great as the value calculated using equation (E4-8). The results are consistent with an hypothesis that the main secondary reaction of

vinylacetylene in the present work is a bimolecular reaction between vinylacetylene and a radical whose concentration is almost independent of the pressure of acetylene. According to equation (E4-12) this radical is not the main, chain-terminating radical. The radical removing vinylacetylene is probably a smaller radical, such as a hydrogen atom.

4-4. Conclusion

Induction periods for the formation of vinylacetylene and benzene have been observed between 854 and 970 K. This is the first observation of an induction period, distinct from an auto-acceleration period, in acetylene pyrolysis below 1600 K. This is crucial evidence for a free radical mechanism. Any contribution from a parallel, molecular mechanism was too small to be reliably established. The initiation reaction was shown to involve two acetylene molecules. The termination reaction is a bimolecular, gas phase, radical combination. The product of the rate constants for the initiation and termination steps was determined from the induction periods. The initiation reaction was shown to have an activation energy of approximately 260 kJ mol^{-1}. The orders and the rate constants for the formation of vinylacetylene and benzene were determined. Vinylacetylene was formed from a reaction or series of reactions involving the main, chain-terminating radical, *X*, and an additional molecule of acetylene. These reactions have an overall activation energy of 31±12 kJ mol^{-1}. Benzene has an overall order of formation of 2.4. Its overall

activation energy of formation is only 100±9 kJ mol^{-1}, indicating it is formed from intermediates with a lower enthalpy than the main, chain-terminating radical.

To obtain more information regarding the mechanism of the pyrolysis of acetylene, more experiments will be described to investigate the acceleration of the reaction by additives, and to search for minor products.

References for Chapter 4

1. I.D.Gay, G.B.Kistiakowsky, J.V.Michael, and H.Niki, *J.Chem.Phys.*, 1965, **43**, 1720.
2. J.H.Kiefer, S.S.Sidhu, R.D.Kern, K.Xie, H.Chen, and L.B.Harding, *Combust.Sci.Technol.*, 1992, **82**, 101.
3. C.H.Bamford and M.J.S.Dewar, *Nature*, 1946, **158**, 380.
4. G.M.Burnett and H.W.Melville, *Proc.R.Soc.London, Ser.A*, 1947, **189**, 456.
5. M.V.Smith and R.H.Eward, *J.Chem.Phys.*, 1948, **16**, 592.
6. G.M.Come, *J.Phys.Chem.*, 1977, **81**, 2560.
7. P.D.Pacey and J.H.Wimalasena, *J.Phys.Chem.*, 1984, **88**, 5657.
8. A.L.MacKenzie, P.D.Pacey, and J.H.Wimalasena, *Can.J.Chem.*, 1983, **61**, 2033.
9. P.D.Pacey and J.H.Wimalasena, *J.Phys.Chem.*, 1980, **84**, 2221.
10. P.M.Marquaire and G.M.Come, *React.Kinet.Catal.Lett.*, 1978, **9**, 171.
11. H.Mousavipour and P.D.Pacey, *J.Phys.Chem.*, 1996, **100**, 3573.
12. M.Salouhi, P.M.Marquaire, and G.M.Come, *J.Chim.Phys.PCB*, 1999, **96**, 797.
13. J.Levin, H.Feldman, A.Baer, D.Ben-Hamu, O.Heber, D.Zajfman, and Z.Vager, *Phys.Rev.Lett.*, 1998, **81**, 3347.
14. Los Angeles CA BMDP Statistical Software Inc., *BMDP*, 1990, **vol. 1**.
15. D.R.Lide, *Handbook of Chemistry and Physics, 77th Ed., CRC Press*, 1996, 6-214.
16. H.Furue and P.D.Pacey, *J.Phys.Chem.*, 1980, **84**, 3139.
17. X.Xu and P.D.Pacey, *Carbon*, 2001, **39**, 1839.
18. P.D.Pacey and J.H.Wimalasena, *Can.J.Chem.*, 1983, **61**, 1086.
19. S.T.Dimitrijevic, S.Paterson, and P.D.Pacey, *J.Anal.& Appl.Pyrolysis*, 2000, **53**, 107.
20. W.Tsang, *J.Phys.Chem.Ref.Data*, 1991, **20**, 221.

21. C.Juste, G.Scacchi, and M.Niclause, *Int.J.Chem.Kinet.*, 1981, **13**, 855.

22. P.D.Pacey and J.H.Wimalasena, *Can.J.Chem.*, 1984, **62**, 293.

23. R.L.Hayes, E.Fattal, N.Govind, and E.A.Carter, *J.Am.Chem.Soc.*, 2001, **123**, 641.

24. J.H.Kiefer and W.A.Von Drasek, *Int.J.Chem.Kinet.*, 1990, **22**, 747.

25. S.W.Benson, *Int.J.Chem.Kinet.*, 1992, **24**, 217.

26. D.A.Frank-Kamenetzky, *Acta Physicochim.U.R.S.S.*, 1943, **18**, 148.

27. G.J.Minkoff, D.M.Newitt, and P.Rutledge, *J.Appl.Chem.*, 1957, **7**, 406.

28. C.F.Cullis and N.H.Franklin, *Roy.Soc.(London)*, 1964, **A280**, 139.

29. R.P.Duran, V.T.Amorebieta, and A.J.Colussi, *J.Phys.Chem.*, 1988, **92**, 636.

30. M.Ahmed, D.S.Peterka, and A.G.Suits, *J.Phys.Chem.*, 1999, **110**, 4248.

31. M.H.Back, *Can.J.Chem.*, 1971, **49**, 2199.

32. T.Kruse and P.Roth, *J.Phys.Chem.A* , 1997, **101**, 2138.

33. T.Tanzawa and W.C.Gardiner Jr., *J.Phys.Chem.*, 1980, **84**, 236.

34. C.H.Wu, H.J.Singh, and R.D.Kern, *Int.J.Chem.Kinet.*, 1987, **19**, 975.

35. C.F.Melius, J.A.Miller, and E.M.Evleth, *Proceedings of the 24th Symposium (International) on Combustion*, 1992, 621.

36. A.M.Mebel, R.I.Kaiser, and Y.T.Lee, *J.Am.Chem.Soc.*, 2000, **122**, 1776.

37. D.R.Lide, *Handbook of Chemistry and Physics, 81th Ed., CRC Press*, 2001, p. 5-1, p. 5-29, p. 5-32.

38. P.Frank and Th.Just, *Combustion and Flame*, 1980, **38**, 231.

39. J.A.Bell, M.Berger, and C.Steel, *Chem.Phys.Lett.*, 1974, **28**, 205.

40. E.A.Lissi and M.V.Encinas, *CRC Handbook of Organic Photochemistry, Ed.by J.C.Scaiano, CRC Press, Inc.*, 1989, **II**, 111.

41. D.L.Baulch, C.J.Cobos, R.A.Cox, C.Esser, P.Frank, Th.Just, J.A.Kerr, M.J.Pilling, J.Troe, R.W.Walker, and J.Warnatz, *J.Phys.Chem.Ref.Data*, 1992, **21**, 411.

42. H.Ogura, *Bull.Chem.Soc.Jpn.*, 1977, **50**, 1044.

43. M.B.Colket III, D.J.Seery, and H.B.Palmer, *Combustion and Flame*, 1989, **75**, 343.

44. J.N.Bradley and G.B.Kistiakowsky, *J.Chem.Phys.*, 1961, **35**, 264.

45. J.H.Kiefer, K.I.Mitchell, R.D.Kern, and J.N.Young, *J.Phys.Chem.*, 1988, **92**, 677.

46. R.P.Duran, V.T.Amorebieta, and A.J.Colussi, *Int.J.Chem.Kinet.*, 1989, **21**, 947.

47. A.Becker and K.J.Huttinger, *Carbon*, 1998, **36**, 177.

48. G.M.Come, J.F.Large, and J.A.Rondeau, *J.Chim.Phys.*, 1974, **71**, 1516.

49. S.W.Benson, *Int.J.Chem.Kinet.*, 1989, **21**, 233.

50. J.A.Miller, S.J.Klippenstein, and S.H.Robertson, *J.Phys.Chem.A*, 2000, **104**, 7525.

51. R.Lundgard and J.Heicklen, *Int.J.Chem.Kinet.*, 1984, **16**, 125.

52. Y.Hidaka, K.Tanaka, and M.Suga, *Chem.Phys.Lett.*, 1986, **130**, 195.

53. C.Chanmugathas and J.Heicklen, *Int.J.Chem.Kinet.*, 1986, **18**, 701.

CHAPTER 5. THE ACCELERATION OF THE PYROLYSIS OF ACETYLENE BY NEOPENTANE

5-1. Introduction

In the previous chapter, induction periods were reported for the formation of vinylacetylene (VA) and benzene (B).[1] This is crucial evidence for a free radical mechanism. However, it was not possible to directly measure the rate constants for elementary reactions.

A similar situation occurred in studies of the pyrolysis of ethylene.[2,3] A method involving the acceleration of the pyrolysis by an additive was developed to determine the rate constant for the initiation reaction. The method was initially proposed by Niclause et al.[4-8] and was further developed by Back and her co-workers.[2,3] Additives, such as oxygen,[9] butene-1,[2] neopentane and ethane,[3] were added to ethylene to accelerate the reaction. The initiation reaction of the additive should be fast enough to increase the steady-state concentration of the free radicals, and should be slow enough that the concentration of the additive does not decrease significantly during the residence time. The mole fraction of the additive was kept small, so that it would not be significantly involved in the propagation steps, but would only introduce a new initiation. Because of the weaker bonds in the additive, the total concentration of free radicals would be boosted, compared to the pyrolysis of pure ethylene, and thus the rate of the chain

reaction could be accelerated. The acceleration factor, Q, the ratio of the rate of reaction in the presence and in the absence of an additive, was related to the concentration of the additive according to the following equation, assuming that the chain length of the reaction was long,

$$Q^z = (R^{ss}_a/R^{ss})^z = 1 + (R^i_a/R^i) \qquad \text{(E5-1)}$$

Here, z is the order with respect to radicals of the termination step; R_a^{ss} and R^{ss} are the steady-state rates of formation of a primary, chain-propagation product in the presence and absence of an additive, respectively; R_a^i and R^i are the rates of the initiation introduced by the additive and of the initiation in the pure reactant, respectively. The rate constant for the latter initiation could be calculated if the rate constant for the initiation by the additive was well known.

Some workers have previously investigated the effects of various additives on the pyrolysis of acetylene. A trace amount of nitric oxide, a scavenger of free radicals, was found to significantly inhibit the decomposition of acetylene, as described in section 1-2-1.[10-15] Minkoff et al.[13] found that at 873 K and 350 Torr no significant effect was observed on the pyrolysis of acetylene in the presence of 0.1-1.5% of ketene, acetylacetone, acetonylacetone, dimethylfuran, acetic acid, formaldehyde, ethyl alcohol, tert-butyl hydroperoxide, peracetic acid, air, benzene, cyclo-octatetraene, or butadiene. They found that diacetyl and diacetylene could accelerate the reaction by a factor of about 1.5. Cullis and Franklin[16] didn't observe any effects at 998 K and 400 Torr in the presence of 1% of nitrogen, hydrogen, methane, ethane, ethylene or methylacetylene. Ogura[17] observed inhibition of the reaction by 0.5-2% of hydrogen chloride. The presence

of 18-70% of vinylacetylene in acetylene was observed by Chanmugathas and Heicklen[15] to significantly accelerate the reaction at 673-773 K and 30 Torr. Duran et al.[18] found that 10% of toluene accelerated the decomposition of acetylene, but 10% of benzene didn't change the reaction at temperatures from 820 to 970 K and pressures between 32 and 53 Torr. In another article, Duran et al.[19] observed significant acceleration by 20-80% neopentane and by 30-90% acetone at temperatures between 850 and 950 K, and at pressures from 10 to 200 Torr. Kern et al.[20] didn't observe acceleration by 30 ppm acetone at temperatures between 1880 and 2620 K. Dimitrijevic et al.[21] studied the acceleration by 0.7-1.7% acetone of the pyrolysis of acetylene at 914-1039 K and 45-354 Torr, and extracted possible rate constants for the initiation reaction, but their results were likely affected by a surface termination reaction.[22]

Most studies were performed in the presence of large amounts of additives (except nitric oxide), where the additives could have been involved in the initiation, propagation and termination reactions, and at low temperatures and high pressures, where the acceleration could be less significant. Therefore, it was difficult to obtain information regarding the initiation reaction. To avoid these problems, it is crucial to dope with small amounts of additive and to perform experiments at moderate temperatures and low pressures. In addition, most of previous work was performed at high conversions, where the reaction might have been accelerated by one of the products, vinylacetylene.

The purpose of the present work is to determine the rate constant for the initiation in the pyrolysis of pure acetylene, by using small amounts of neopentane as the additive.

The C-C bond is significantly weaker than the C-H bond in neopentane, so the predominant initiation reaction introduced should be

$C_5H_{12} \rightarrow CH_3 + C_4H_9$ [5-1]

Methyl radicals may be readily converted to one of the main chain transfer radicals, vinyl, through a pathway suggested by Colket, [CSP3]-[CSP6].[23] These reactions were previously discussed in section 1-5-5.

$CH_3 + C_2H_2 \rightarrow CH_3CHCH$ [CSP3]

$CH_3CHCH \rightarrow CH_2CHCH_2$ [CSP4]

$CH_2CHCH_2 + C_2H_2 \rightarrow C_5H_7$ [CSP5]

$C_5H_7 \rightarrow C_5H_6$ (cyclopentadiene) +H [CSP6]

$H + C_2H_2 \rightarrow C_2H_3$ [CSP8]

If we assume a bimolecular initiation by acetylene [TG2],

$C_2H_2 + C_2H_2 \rightarrow C_4H_3 + H$ [TG2]

as shown in Chapter 4, and a unimolecular initiation by neopentane [5-1],[24] Equation (E5-2) can be derived from equation (E5-1),

$$Q^2\text{-}1 = k_{i,C5H12}X_{C5H12}/(k_{i,C2H2}[C_2H_2]) \quad \text{(E5-2)}$$

Here, $k_{i,C5H12}$ and $k_{i,C2H2}$ are the rate constants for initiation by neopentane and by acetylene, respectively; X_{C5H12} is the mole fraction of neopentane; and $[C_2H_2]$ is the concentration of acetylene.

A cross initiation between an acetylene molecule and a neopentane molecule [5-2] could also be considered,

$C_2H_2 + C_5H_{12} \rightarrow C_2H_3 + C_5H_{11}$ [5-2]

To include initiation by reactions [5-1], [5-2], and [TG2], equation (E5-3) can be derived from (E5-1)

$(Q^2-1)/X_{C5H12} = (k_{i,C5H12}/[C_2H_2]+k_{i,cross})/k_{i,C2H2}$ (E5-3)

Here, $k_{i,cross}$ is the rate constant of the cross initiation.

An equation, (E4-1), has been introduced and applied in Chapter 4 to describe the rate of formation of a product, P, during induction periods observed in the pyrolysis of acetylene,

$[P]/t = [(b_P/t)ln\{[1+exp(a_Pt)]/2\}-a_Pb_P/2](1-c_Pt)$ (E4-1)

Here, $[P]$ is the concentration of a product leaving the reactor; t, the residence time of gases in the reactor; a_Pb_P equals $2R_p^{ss}$; R_p^{ss} is the steady-state rate of product formation; a_P equals $4(R_ik_t)^{1/2}$; R_i is the initiation rate; k_t, the termination rate constant; and c_P, a parameter associated with secondary reactions. An induction period could be described by equation (E4-2), derived in Chapter 4,

$\tau = 1/(k_ik_t[C_2H_2]^n)^{1/2} = 2(ln2)/a_p$ (E4-2)

Equation (E4-17) was also derived in Chapter 4,

$b_{VA}/[C_2H_2] = k_{p,VA}/(k_tln2)$ (E4-17)

Note that b is independent of the initiation rate and that the induction period is inversely proportional to a_p. Therefore, the acceleration factor, Q, could be derived as,

$Q = R^{ss}_a/R^{ss} = (a_Pb_P)_a/(a_Pb_P) = (a_P)_a/a_P = \tau/\tau_a$ (E5-4)

using the above equations. According to equation (E5-4), the acceleration factor could be calculated using either the steady-state rates or the induction periods.

This chapter will involve the study of acceleration effects by small amounts of neopentane. The residence time, concentration of neopentane, pressure of acetylene, and temperature will be varied. Reactors with various internal diameters will be employed. The steady-state rates and induction periods for the formation of vinylacetylene and benzene will be obtained by fitting equation (E4-1) to the rates of formation of vinylacetylene and benzene. Acceleration factors for vinylacetylene and benzene will be calculated, mainly using steady-state rates. The rate constant of the initiation reaction by acetylene, reaction (TG2), will be extracted using equation (E5-3). The possibility of the involvement of the cross initiation, reaction [5-2], will be discussed using equation (E5-3).

5-2. Results

5-2-1. Acceleration by neopentane

Acetylene was pyrolysed in a flow system between 856 and 972 K, at pressures between 20.4 and 120 Torr, and at residence times between 15 and 2009 ms. Vinylacetylene (VA) and benzene (B) were observed as products. As in the previous chapter,[1] the flow rates of acetylene into the reactors and the diameters of the reactors were varied to attempt to detect an induction period in the formation of vinylacetylene

and benzene. Neopentane was added to accelerate the reaction. No measurable decrease in the mole fraction of neopentane was observed after the reaction.

Figure 5-1 shows the rates of formation of vinylacetylene as a function of time when acetylene was pyrolysed pure and doped with 0.596 mole % neopentane, respectively, at 120 Torr and 856 K in a 3.962-mm-id reactor. Figure 5-2 shows the rates of formation of benzene under the same conditions. The neopentane was observed to accelerate the formation of vinylacetylene and benzene, and to shorten the induction periods. Also, the steady-state rates for vinylacetylene and for benzene produced from doped acetylene in Figures 5-1 and 5-2 gradually dropped with an increase in the residence time, indicating the involvement of secondary reactions, as discussed in Chapter 4.

As in Chapter 4, the steady-state rates of formation of vinylacetylene and benzene were extracted by fitting equation (E4-1) to the rates observed. Table 5-1 gives the results of least-squares fitting for the acceleration by neopentane at various mole percentages, experimental pressures, and temperatures. Quoted uncertainties are standard deviations. An acceleration factor (Q) was calculated by dividing the steady-state rate of formation of vinylacetylene or benzene in the presence of neopentane by the steady-state rate obtained at the same pressure and temperature in the absence of neopentane. Similar acceleration factors, Q_{VA} and Q_B, were determined for vinylacetylene and for benzene at each experimental condition. The ratio of acceleration factors, Q_{VA}/Q_B, was 1.0±0.1 for all the cases in Table 5-1.

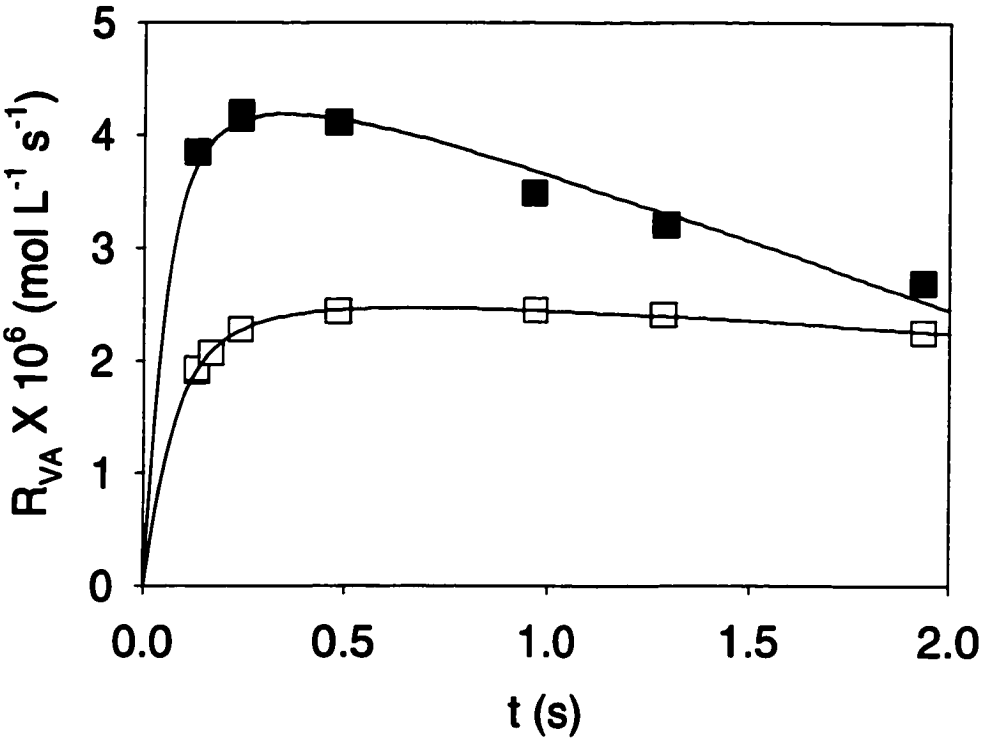

Figure 5-1. Dependence of the rates of formation of vinylacetylene on the residence times at 120 Torr and 856 K in a 3.96-mm-id reactor; ■, acetylene doped with 0.596% neopentane; ❐, purified acetylene; lines, non-linear least-square fits of equation (E4-1) to the data.

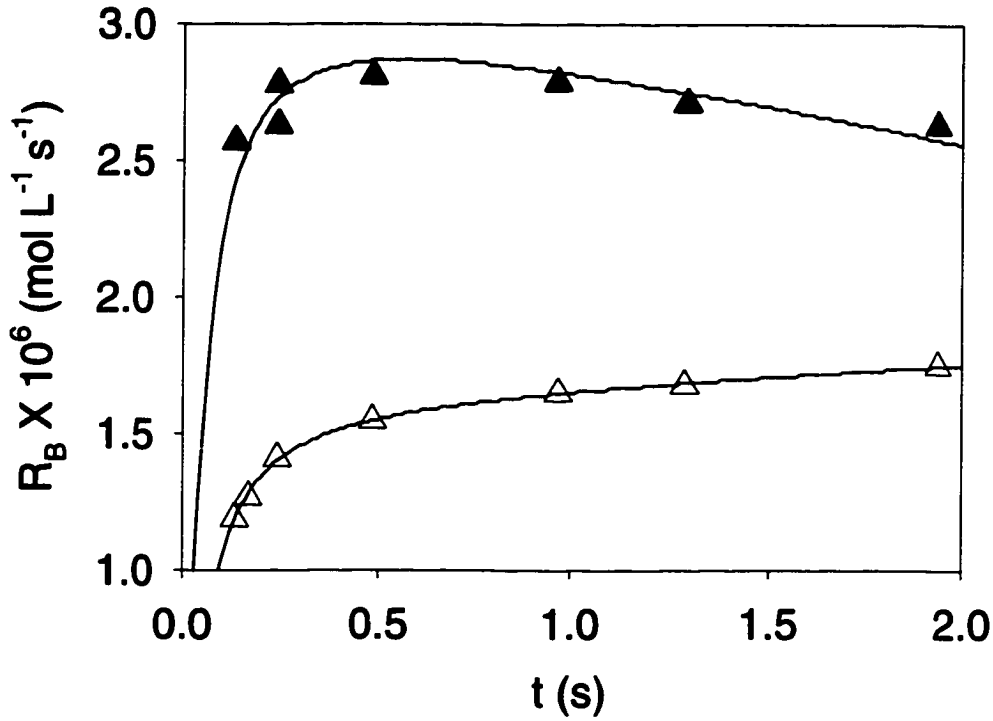

Figure 5-2. Dependence of the rates of formation of benzene on the residence times at 120 Torr and 856 K in a 3.96-mm-id reactor; ▲, acetylene doped with 0.596% neopentane; △, purified acetylene; lines, non-linear least-square fits of equation (E4-1) to the data.

Table 5-1. Acceleration by neopentane of the rates of formation of vinylacetylene and benzene.

T (K)	reactor diameter (mm)	P_{total} (Torr)	X_{C5H12} (%)	$R_{VA}^{*}\times10^{6}$ (mol L^{-1} s^{-1})	$R_{B}^{*}\times10^{7}$ (mol L^{-1} s^{-1})	Q_{VA}	Q_{B}
856	3.96	120.0	0.298	3.40±0.05	24.0±0.2	1.22±0.03	1.20±0.01
856	3.96	120.0	0.596	4.11±0.21	30.9±0.3	1.48±0.11	1.54±0.22
856	3.96	120.1	1.23	6.20±0.12	45.5±0.5	1.99±0.56	1.80±0.50
856	3.96	120.1	2.47	7.70±0.14	59.8±0.7	2.48±0.06	2.37±0.04
856	3.96	120.0	3.79	10.75±0.09	78.0±0.1	3.29±0.39	3.58±0.39
894	3.96	60.1	0.150	4.99±0.05	16.4±0.8	1.71±0.03	1.77±0.12
894	3.96	60.1	0.300	6.70±0.27	21.7±0.7	2.02±0.11	1.91±0.08
894	3.96	60.1	0.590	8.39±0.52	28.5±1.8	2.53±0.22	2.51±0.22
894	3.96	60.1	1.16	9.80±0.73	33.0±0.6	3.37±0.35	3.57±0.09
930	3.96	34.1	0.638	11.5±0.4	20.7±2.1	5.44±0.28	4.96±0.26
933	3.96	34.1	1.29	16.1±0.7	27.0±5.4	7.39±0.43	7.44±2.08
933	3.96	51.6	0.295	15.5±1.3	36.5±2.3	3.02±0.36	3.65±0.32
933	3.96	51.6	0.578	17.8±0.9	43.0±1.29	3.47±0.23	4.30±0.18
931	3.96	51.6	0.628	21.0±0.6	47.8±9.6	4.10±0.16	4.51±1.26
934	3.96	51.6	1.28	25.5±1.2	61.5±0.2	5.63±0.39	6.48±0.02
970	4.13	20.4	0.0629	3.00±0.36	3.18±0.35	2.52±0.31	2.54±0.41
969	1.96	35.0	0.0625	9.43±2.73	1.21±0.10	2.23±0.65	1.71±0.20
969	1.96	35.0	0.126	12.81±0.04	1.88±0.05	3.04±0.01	2.65±0.09
969	1.96	52.0	0.0643	16.9±3.4	2.98±0.60	2.00±0.56	1.75±0.49
969	1.96	52.0	0.126	22.6±0.5	4.13±0.66	2.68±0.08	2.49±0.56
972	1.96	51.8	0.301	34.5±3.5	6.30±0.60	4.15±0.05	4.17±0.56
972	1.96	51.7	0.604	42.0±0.4	7.90±0.07	5.05±0.07	5.23±0.06
969	0.969	104	0.0986	47.6±1.4	121±3.6	1.42±0.05	1.56±0.08
969	0.969	104	0.197	43.4±2.3	125±13	1.28±0.07	1.61±0.18

* Rates of formation of vinylacetylene and benzene in the presence of neopentane.

Table 5-2 shows the acceleration factors measured using steady-state rates and using induction periods. The addition of small amounts of neopentane was shown to increase steady-state rates, and to decrease induction periods. Acceleration factors measured using steady-state rates and using induction periods were reasonably consistent. However, acceleration factors measured using steady-state rates were more accurate than using induction periods. Acceleration factors measured using steady-state rates will be used to extract kinetic information.

Acceleration factors increased with an increase in mole fraction of neopentane and with a decrease in the pressure of acetylene. The mole fraction of neopentane was varied between 0.0625 and 3.79. Figure 5-3 shows the dependence of Q^2-1 on $X_{C5H12}/[C_2H_2]$ at 930-934 K. As a comparison, the dependence of Q-1 on $X_{C5H12}/[C_2H_2]$ at 930-934 K is shown in Figure 5-4. The least-squares straight line passes through the origin, as predicted by equation (E5-2), when the exponent, z, is two, but not when it is unity. This supports the proposal that the addition of neopentane mainly introduced a unimolecular initiation reaction, and that the effect of a cross initiation reaction between neopentane and acetylene was not significant. This also supports the idea that the termination reaction in the pyrolysis of acetylene is a bimolecular process involving two free radicals. Furthermore, the least-square fitting of the parameters in equation (E5-2) to the acceleration factors of vinylacetylene and benzene showed that at 930-934 K the exponent z was equal to 2.05±0.19, indicating a second-order termination reaction. According to equation (E5-1), the slope of a straight line obtained using linear regression (forcing the line to pass through the origin) in

Table 5-2. Acceleration factors measured using steady-state rates and using induction periods.

T (K)	reactor diameter (mm)	P_{total} (Torr)	X_{C5H12} (%)	Q_{VA}[a]	Q_B[a]	Q_{VA}[b]	Q_B[b]
856	3.96	120.0	0.596	1.48±0.11	1.54±0.22	1.34±0.14	1.22±0.11
969	0.969	104	0.0986	1.42±0.05	1.56±0.08	2.09±0.31	1.89±0.28

a, acceleration factors measured using steady-state rates.

b, acceleration factors measured using induction periods.

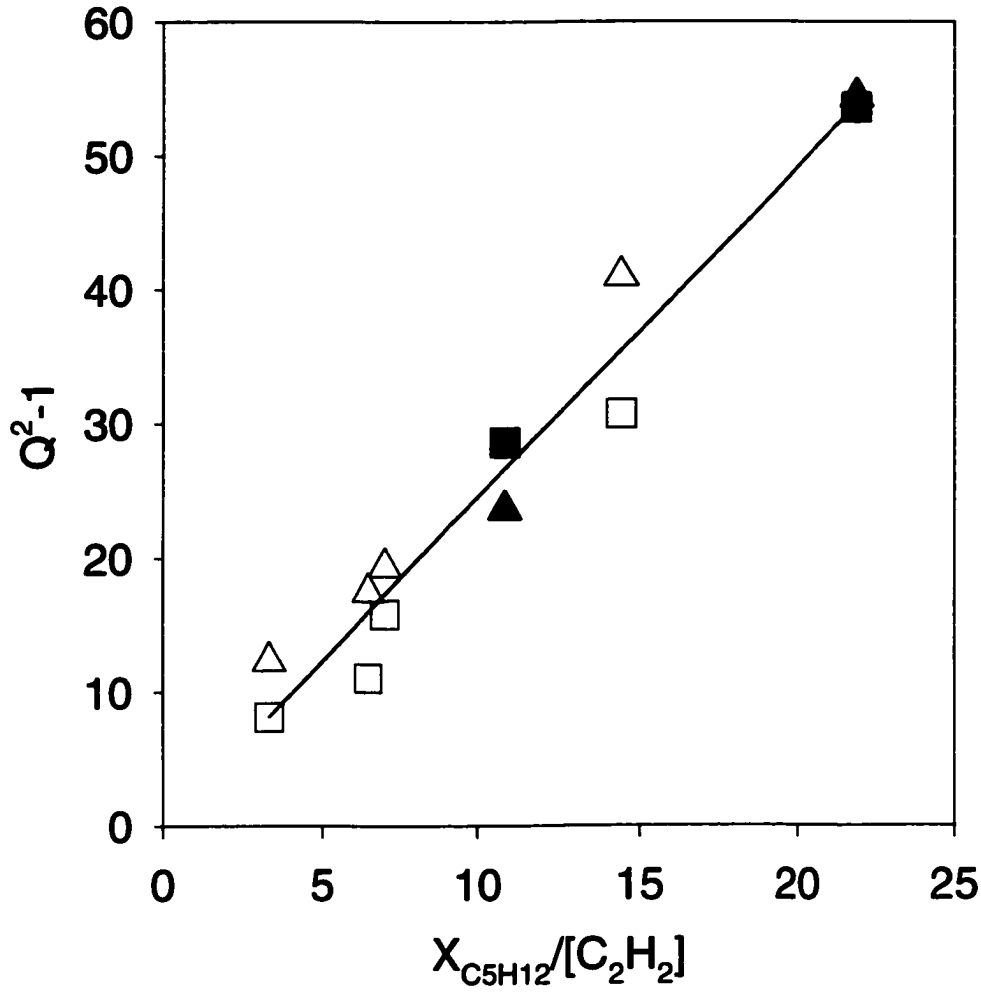

Figure 5-3. Dependence of Q^2-1 on $X_{C5H12}/[C_2H_2]$ (mol^{-1} L) at 930-934 K; ■, vinylacetylene at 34.1 Torr of acetylene; □, vinylacetylene at 51.6 Torr of acetylene; ▲, benzene at 34.1 Torr of acetylene; △, benzene at 51.6 Torr of acetylene; solid line, least-squares fit of equation (E5-2), assuming z = 2 and forcing the line to pass through the origin, to the data for both vinylacetylene and benzene.

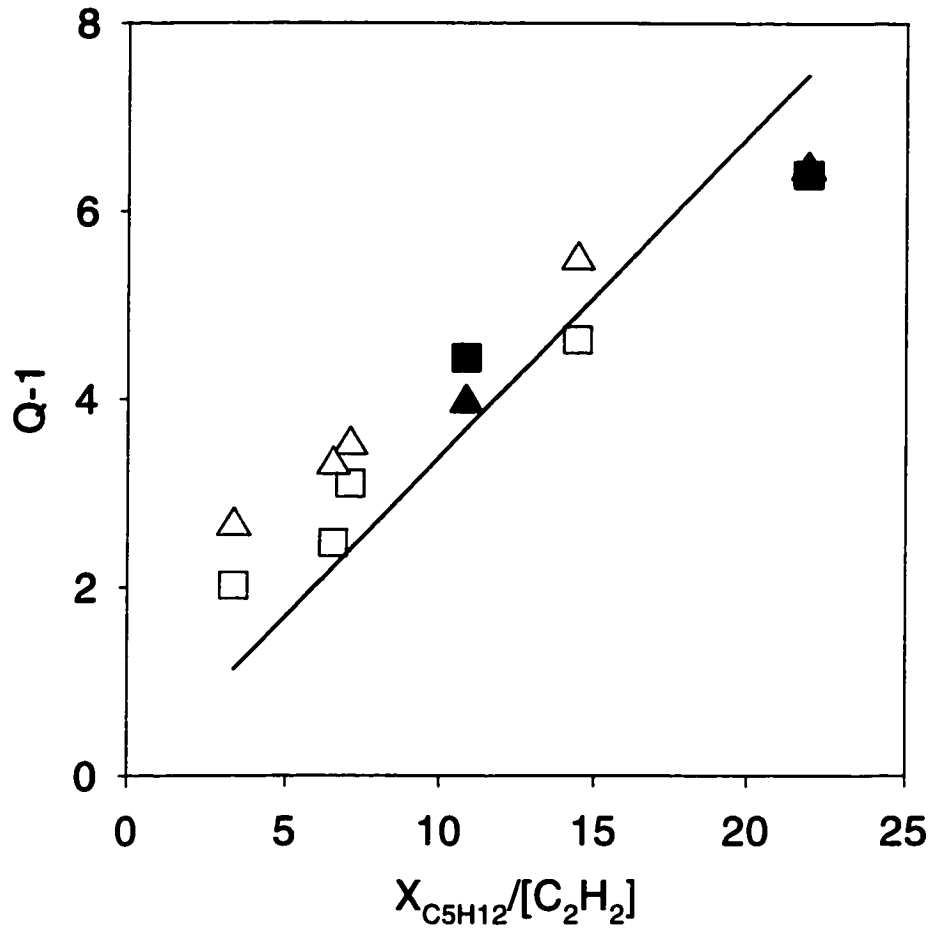

Figure 5-4. Dependence of *Q-1* on $X_{C5H12}/[C_2H_2]$ (mol^{-1} L) at 930-934 K; ■, vinylacetylene at 34.1 Torr of acetylene; ❐, vinylacetylene at 51.6 Torr of acetylene; ▲, benzene at 34.1 Torr of acetylene; △, benzene at 51.6 Torr of acetylene; solid line, least-squares fit of equation (E5-2), assuming z = 1 and forcing the line to pass through the origin, to the data for both vinylacetylene and benzene.

Figure 5-4 equals $k_{i,C5H12}/k_{i,C2H2}$. Good linearity was also observed at other temperatures for the dependence of Q^2-1 on $X_{C5H12}/[C_2H_2]$.

In addition, contributions of the unimolecular initiation reaction and the cross initiation reaction could be estimated by plotting curves of $(Q^2-1)/X_{C5H12}$ versus $1/[C_2H_2]$, providing contributions of the unimolecular initiation reaction in the slopes and contributions of the cross initiation reaction in the intercepts, according to equation (E5-3). Figures 5-5 and 5-6 show the dependence of $(Q^2-1)/X_{C5H12}$ on $1/[C_2H_2]$ at 930-934 K and 969-972 K, respectively. Intercepts were determined to be 428±845 at 930-934 K, and 232±626 at 969-972 K, respectively. Slopes were determined to be 2.18±0.63 mol L^{-1} at 930-934 K, and 3.00±0.41 mol L^{-1} at 969-972 K, respectively. The values of the intercepts were much smaller than the values of $(Q^2-1)/X_{C5H12}$ shown in Figures 5-5 and 5-6, respectively. Therefore, the contributions of the cross initiation reaction were not important in the present work.

Therefore, plots similar to Figure 5-3 were made at four temperatures; and the slopes were determined as the ratios of $k_{i,C5H12}/k_{i,C2H2}$ according to equation (E5-2) (z = 2). These values of $k_{i,C5H12}/k_{i,C2H2}$ are listed in Table 5-3. An Arrhenius plot for $k_{i,C5H12}/k_{i,C2H2}$ using results for vinylacetylene and benzene is shown in Figure 5-7. The Arrhenius expression was determined to be

$$k_{i,C5H12}/k_{i,C2H2} = 10^{7.02\pm0.35}\ mol\ L^{-1}\ exp\ [-(119\pm6)\ kJ\ mol^{-1}/RT] \qquad \text{(E5-5)}$$

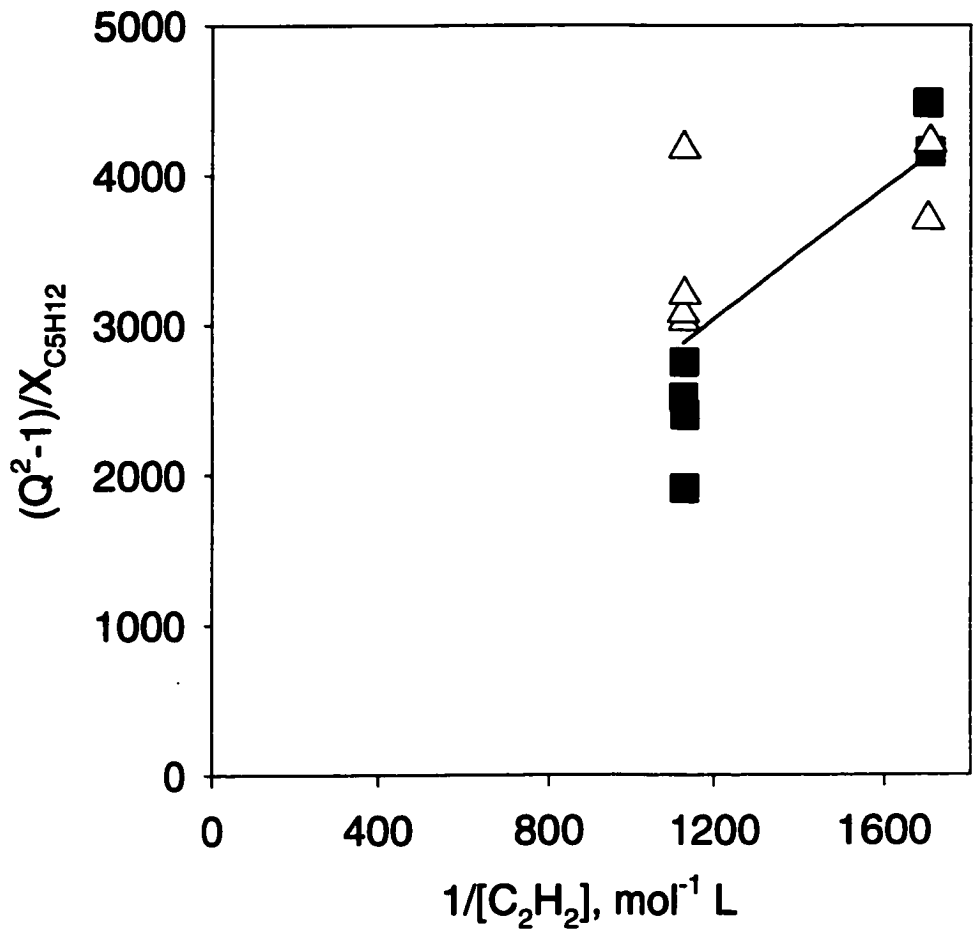

Figure 5-5. Dependence of $(Q^2-1)/X_{C5H12}$ on $1/[C_2H_2]$ at 930-934 K; ■, data for vinylacetylene; △, data for benzene; solid line, least-squares fit of equation (E5-3), assuming $z = 2$, to the data for both vinylacetylene and benzene.

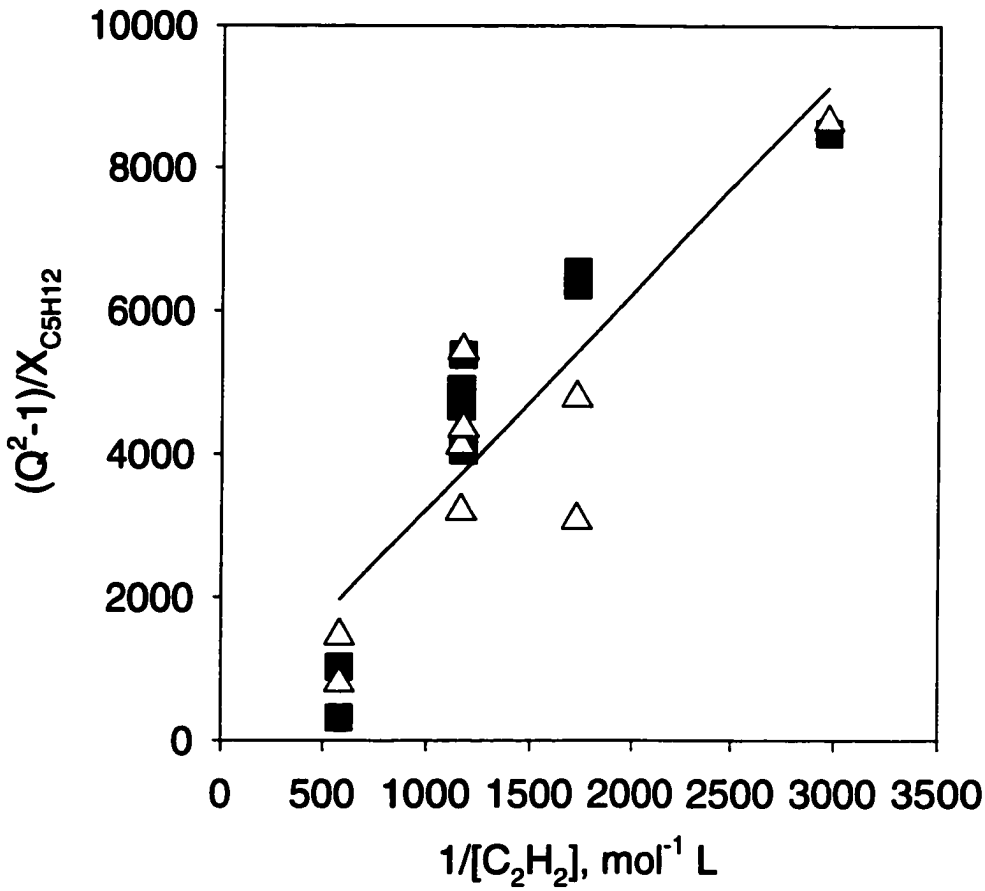

Figure 5-6. Dependence of $(Q^2-1)/X_{C5H12}$ on $1/[C_2H_2]$ at 969-972 K; ■, data for vinylacetylene; △, data for benzene; solid line, least-squares fit of equation (E5-3), assuming z = 2, to the data for both vinylacetylene and benzene.

Table 5-3. Ratios of $k_{i,C5H12}/k_{i,C2H2}$ determined at various temperatures.

T (K)	$(k_{i,C5H12}/k_{i,C2H2})_{VA}$ (mol L^{-1})	$(k_{i,C5H12}/k_{i,C2H2})_{B}$ (mol L^{-1})
856	0.547±0.026	0.602±0.067
894	0.980±0.032	1.07±0.04
932±1	2.35±0.10	2.56±0.11
970±1	3.72±0.20	3.78±0.24

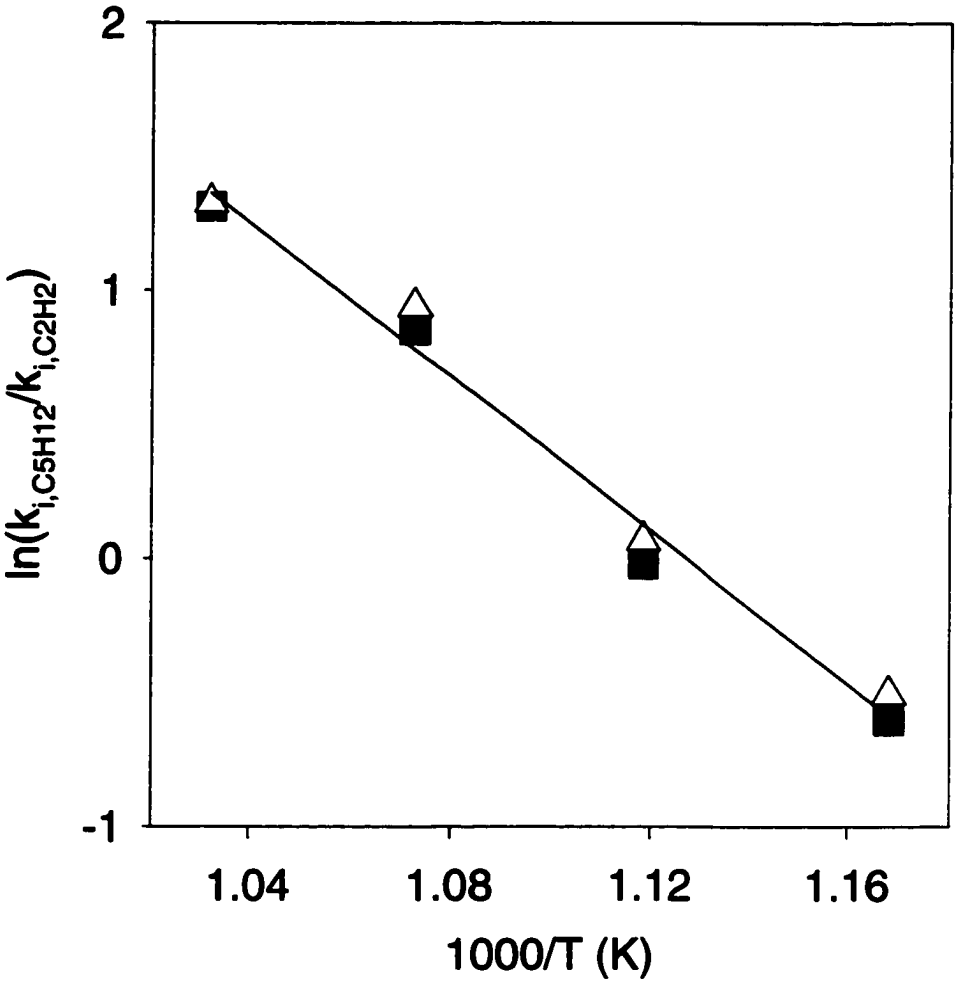

Figure 5-7. Arrhenius plot for $k_{i,C5H12}/k_{i,C2H2}$; ■, data from vinylacetylene and △, data from benzene.

5-3. Discussion

5-3-1. Possible sources of errors

As discussed in Chapter 2, the flow rates of gases were controlled to be less than 29 cc min^{-1}, so the maximum reduction in rate because of incomplete radial heat transfer was calculated to be 4%. The pressure drop along the reactor was controlled to be less than 10%. The maximum conversion was calculated to be 1.7%, so axial diffusion and volume contraction should be negligible.

The surface reaction and the effect of impurities were shown to be insignificant in Chapter 3. The order of the termination was also shown to be two instead of unity in Chapter 4.

5-3-2. Effect of neopentane on the induction periods and steady-state rates

Induction periods observed at 856 K and 120 Torr were shown in Figures 5-1 and 5-2. Addition of neopentane shortened the induction periods and increased the steady-state rates. Table 5-2 shows that similar acceleration factors were measured using steady-state rates and using induction periods, agreeing with equation (E5-4). This indicates that neopentane accelerated the pyrolysis of acetylene by introducing a new initiation reaction.

Acceleration factors were calculated using steady-state rates to determine the rate constant of the initiation reaction [TG2], because induction periods were not observed accurately in most experiments.

The involvement of neopentane in a propagation reaction would result in different acceleration factors for vinylacetylene and for benzene. If the concentration of neopentane were high, eventually it would be involved in propagation reactions. Neopentane would be likely to transfer hydrogen to C_4H_3 and C_6H_5 radicals to form vinylacetylene and benzene at different rates, so the acceleration factors, Q, for these two products would be different. No more than 3.8% neopentane was used in the present work. Similar acceleration factors were observed for vinylacetylene and benzene in Table 5-1, indicating that neopentane was not significantly involved in propagation reactions.

Table 5-1 also shows that the acceleration factors measured at similar X_{C5H12} and different pressures of acetylene were significantly different (lines 11 and 15, 16 and 18, 17 and 19). The acceleration factors determined at lower pressures of acetylene were higher than those measured at higher pressures, supporting the unimolecular initiation [5-1], according to the derived equation (E5-2).

5-3-3. The rate constant for the initiation reaction in the pyrolysis of pure acetylene

The rate constant for the unimolecular initiation in neopentane has been experimentally determined by various groups, and the Arrhenius parameters (including rate constants calculated at 900 K using these Arrhenius parameters for comparison) are listed in Table 5-4. The rate constant reported by Pacey[24] was determined in a similar temperature range to the present work,

$$k_{i,C5H12} = 10^{17.7\pm0.3}\ s^{-1}\ exp(-356\pm6\ kJ\ mol^{-1}/RT) \quad \text{(E5-6)}$$

The rate constant for the bimolecular initiation in pure acetylene could be derived by combining equation (E5-5) with (E5-6),

$$k_{i,C2H2} = 10^{10.68\pm0.46}\ L\ mol^{-1}\ s^{-1}\ exp(-237\pm9\ kJ\ mol^{-1}/RT) \quad \text{(E5-7)}$$

In the absence of neopentane, chain lengths were calculated to be 3.6×10^3 for vinylacetylene and 2.6×10^3 for benzene at 120 Torr and 854 K, and 1.6×10^3 for vinylacetylene and 2.6×10^2 for benzene at 35.0 Torr and 969 K. Therefore, the long chain assumption applies.

5-3-4. The mechanism of the reaction and the initiation reaction

A trace amount of neopentane was observed to accelerate the pyrolysis of acetylene by similar acceleration factors for both vinylacetylene and benzene, indicating they were

Table 5-4. Rate constants reported for the unimolecular initiation reaction of neopentane

T (K)	P (Torr)	technique	A (s^{-1})	E_A (kJ mol^{-1})	$k_{900K} \times 10^3$ (s^{-1})	reference
1000-1100	2280	shock tube	1.26×10^{16}	328	1.16	Tsang[25]
700-833	20-550	flow system	1.12×10^{18}	359	1.63	Halstead et al.[26]
923-1073	-	flow system	7.94×10^{16}	337	2.19	Taylor et al.[27]
723-803	25-200	flow system	6.31×10^{16}	343	0.78	Baronnet et al.[28]
793-953	20-400	flow system	$10^{17.7\pm0.3}$	356±6	1.09	Pacey[24]
1030-1300	2250-3000	shock tube	3.30×10^{16}	336	1.04	Bradley and West[29]
756-845	100-200	flow system	$10^{16.1\pm1.0}$	330±15	0.86	Marshall et al.[30]
703-743	50	stirred flow system	3.98×10^{17}	351	1.69	Marquaire and Come[31]
1000-1260	-	VLPP	2.00×10^{17}	338	4.82	Baldwin et al.[32]
1140-1300	1520-2280	shock tube	1.70×10^{17}	351	0.72	Bernfeld and Skinner[33]
1230-1455	266	shock tube	1.10×10^{13}	259	10.2	Rao and Skinner[34]

formed in a free radical process. Neopentane is well known to be a source of free radicals at high temperatures.[24] If a molecular mechanism involving vinylidene were important for formation of vinylacetylene or benzene, the addition of neopentane should have accelerated the formation of vinylacetylene and benzene to different extents.

The initiation reaction for the pyrolysis of acetylene was discussed in Chapter 4. The activation energy for an initiation involving the formation of a C_4H_3 radical and an H atom [B1],

$$2C_2H_2 \rightarrow C_4H_4^* \rightarrow C_4H_3 + H \qquad [B1]$$

was estimated by previous workers using *ab initio* methods. Arrhenius parameters suggested by previous workers are summarized in Table 5-5, and rate constants are compared in Figure 5-8. Some of the activation energies are very close to that observed in the present work, suggesting that the initiation [B1] played a dominant role in the present experiments. Table 5-5 shows that the activation energy determined in the present work is very close to the value estimated by Melius et al.[35] Also, Figure 5-8 shows that the extrapolated value of the rate constant for initiation determined in the present work reasonably agrees with that measured by Frank and Just.[38] A lower activation energy was determined by Gay et al.[37] in a shock tube at 1600-2400 K by assuming that the rate of the initiation reaction was equal to the rate of formation of diacetylene. It was later suggested[38] that a chain reaction was involved in these experiments. This would result in significant errors in determining the activation energy. The rate constant reported by Dimitrijevic et al.[21] likely was affected by a surface termination reaction caused by the deposition of carbon on the surface of the reactor.

Table 5-5. Arrhenius parameters estimated and measured for the initiation reaction C_2H_2 + $C_2H_2 \rightarrow C_4H_3 + H$

Reference	Method	T (K)	A (L mol^{-1} s^{-1})	E_A (kJ mol^{-1})
Melius et al.[35]	ab initio			231±15
Mebel et al.[36]	ab initio			273
Gay et al.[37]	shock tube	1600-2400	$10^{10.47}$	162
Dimitrijevic et al.[21]	flow reactor	914-1039	$10^{12.7\pm0.9}$	253±15
Chapter 4	flow reactor	854-970	-	261±7
present chapter	flow reactor	856-972	$10^{10.7\pm0.5}$	237±9

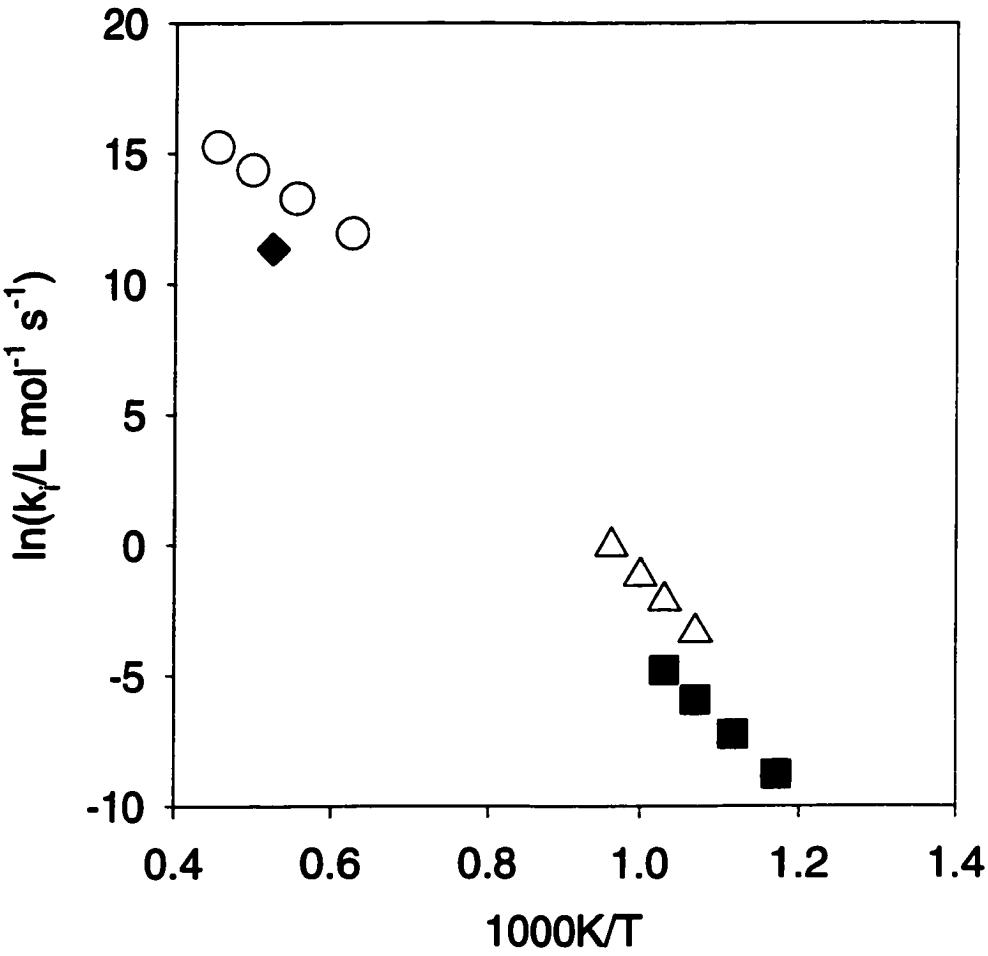

Figure 5-8.Arrhenius plot for the initiation reaction; ◆, Frank and Just;[38] ○, Gay et al.;[37] △, Dimitrijevic et al.;[21] ■, the present work.

5-3-5. The rate constants of termination and propagation steps

The rate constants of the termination reaction could be calculated as follows. Values of $k_{i,C2H2}k_t$ could be calculated using the data in Table 4-1 and equation (E4-2). Values of $k_{i,C2H2}$ could be calculated using the data in Table 5-1 and equation (E5-2) assuming z = 2. Then, using $k_{i,C2H2}k_t$ and $k_{i,C2H2}$ determined at similar temperatures and pressures, k_t was calculated and listed in Table 5-6. The average value of k_t was $(11\pm4) \times 10^{10}$ L mol^{-1} s^{-1} using data for vinylacetylene, $(11\pm7) \times 10^{10}$ L mol^{-1} s^{-1} using data for benzene, and $(11\pm6) \times 10^{10}$ L mol^{-1} s^{-1} using data for both vinylacetylene and benzene.

Vinylacetylene could be formed in a propagation reaction between a vinyl radical and an acetylene molecule,

$$C_2H_3 + C_2H_2 \rightarrow C_4H_4 + H \qquad [5\text{-}3]$$

The most abundant product was vinylacetylene, so the vinyl radicals should be the main chain-transfer radicals. The recombination of two vinyl radicals should be the main termination reaction in the present work. Table 5-7 lists the rate constants reported in the literature for the reaction,

$$C_2H_3 + C_2H_3 \rightarrow C_4H_6 \qquad [5\text{-}4]$$

Table 5-7 shows that the rate constant of the termination reaction measured in the present work is greater than the rate constants previously reported for reaction [5-4]. This could be caused by several possible reasons. First, the termination by C_2H_3 could proceed by both reactions [5-4] and [5-5],

Table 5-6. Rate constants of the termination reaction

T (K)	reactor id (mm)	P (Torr)	X_{C5H12} (%)	$k_{t,VA} \times 10^{-10}$ (L mol^{-1} s^{-1})	$k_{t,B} \times 10^{-10}$ (L mol^{-1} s^{-1})
856	3.96	120	0.298	5.3	4.7
856	3.96	120	0.596	6.4	7.4
856	3.96	120.1	1.23	7.7	5.9
856	3.96	120.1	2.47	6.7	6.0
856	3.96	120	3.79	8.3	10
894	3.96	60.1	0.150	11	15
894	3.96	60.1	0.300	8.6	9.4
894	3.96	60.1	0.590	7.7	9.6
894	3.96	60.1	1.16	7.5	11
930	3.96	34.1	0.638	16	25
933	3.96	34.1	1.29	13	24
933	3.96	51.6	0.295	17	24
933	3.96	51.6	0.578	12	18
931	3.96	51.6	0.628	17	20
934	3.96	51.6	1.28	14	18
970	4.13	20.4	0.0629	10	3.5
969	1.96	35	0.0625	14	2.2
969	1.96	35	0.126	14	3.5
969	1.96	52	0.0643	13.4	8.0
969	1.96	52	0.126	14	10
972	1.96	51.8	0.301	13	12
972	1.96	51.7	0.604	10	9.4
969	0.969	104	0.0986	5.9	7.3
969	0.969	104	0.197	1.7	4.0

Table 5-7. Rate constants estimated and measured for the reaction $C_2H_3 + C_2H_3 \rightarrow C_4H_6$.

Reference	Method	T (K)	$k \times 10^{-10}$ (L mol^{-1} s^{-1})
Fahr et al.[39]	flow reactor	298	7.23
Fahr and Laufer[40]	flow reactor	298	4.94
Colket et al.[23]	simulation	900-1100	2.00
this work*	flow reactor	856-972	11±6

* The rate constant of the termination reaction measured in the present work.

$C_2H_3 + C_2H_3 \rightarrow C_2H_4 + C_2H_2$ [5-5]

The rate constant of reaction [5-5] was reported[41] to be 31.3% of the rate constant of reaction [5-4], so a value of 2.26×10^{10} L mol^{-1} s^{-1} could be calculated using a reported[39] rate constant of 7.23×10^{10} L mol^{-1} s^{-1} for reaction [5-4]. Thus, the sum of these two rate constants would be 9.49×10^{10} L mol^{-1} s^{-1}, which agrees well with the rate constant determined in the present chapter.

C_4H_5 might also be involved in termination reactions by reactions [5-6] and [5-7],

$C_4H_5 + C_4H_5 \rightarrow C_8H_{10}$ [5-6]

$C_4H_5 + C_2H_3 \rightarrow C_6H_8$ [5-7]

The rate constant of reaction [5-6] was calculated to be $2.02 \times 10^{11}\exp(-4.157$ kJ mol^{-1} /RT) L mol^{-1} s^{-1} by DAC[42] using an *ab initio* method. The rate constant of reaction [5-7] was estimated to be 1.70×10^{10} L mol^{-1} s^{-1} by Westmoreland et al.[43] using thermochemistry.

The rate constant for the overall reaction [5-8],

$C_2H_3 + C_2H_3 \rightarrow$ products, [5-8]

the sum of reactions [5-4] and [5-5], was measured to be 8.49×10^{10} L mol^{-1} s^{-1} by Thorn et al.[44] using a discharge flow system coupled to a mass spectrometer at 298 K and 1 Torr, in good agreement with the present results at high temperatures.

In section 4-3-7 it was shown that vinylacetylene and benzene were formed from reactions between free radicals and acetylene, reactions [5-3] and [5-9],

$C_2H_3 + C_2H_2 \rightarrow C_4H_4 + H$ [5-3]

$C_4H_5 + C_2H_2 \rightarrow C_6H_6 + H$ [5-9]

The expression for the parameter, b, was derived to be

$$b = k_p^{prop}[C_2H_2]/(k_t \ln 2) \quad \text{(E5-8)}$$

Here, k_p^{prop} is the rate constant for the formation of product, p, which is vinylacetylene or benzene, from a propagation step or series of steps between a free radical and an acetylene molecule. The expression for k_p^{prop} was derived by combining the definitions of R_p^{ss} and a_p described in the introduction section with (E5-8)

$$k_p^{prop} = R_p^{ss}(k_t/k_i)^{1/2}/[C_2H_2]^2 \quad \text{(E5-9)}$$

Values of k_p^{prop} for vinylacetylene and benzene can be calculated using the data reported in Chapter 4,[1] and from the values of k_i and k_t in this chapter, and are listed in Table 5-8. The temperature dependences of these values were very weak. An expression for k_p^{prop} for vinylacetylene, k_{VA}^{prop}, was determined to be

$$k_{VA}^{prop} = 10^{9.2\pm0.7} L\ mol^{-1}\ s^{-1} exp[(-32\pm12) kJ\ mol^{-1}/RT] \quad \text{(E5-10)}$$

An expression for this rate constant was also determined by Knyazev et al.[45] using the flash photolysis technique at 630-980 K and 1.85-3.7 Torr,

$$k_{VA}^{prop} = 10^{9.3} L\ mol^{-1}\ s^{-1} exp(-25\ kJ\ mol^{-1}/RT) \quad \text{(E5-11)}$$

which agrees well with our expression (E5-10). An average value of k_B^{prop} for benzene was calculated to be $(5.7\pm2.1)\times10^6$ L mol^{-1} s^{-1}, because the values were too close to extract an Arrhenius expression. As shown in Table 5-8, k_{VA}^{prop} slightly decreased with an increase in the pressure at 934-938 K, indicating the order for the formation of

Table 5-8. Rate constants for the formation of vinylacetylene and benzene from propagation steps.

T (K)	P (Torr)	reactor id (mm)	$R_{VA}^{ss} \times 10^7$ (mol L^{-1} s^{-1})	$R_B^{ss} \times 10^7$ (mol L^{-1} s^{-1})	$k_{VA}^{prop} \times 10^7$ (L mol^{-1} s^{-1})	$k_B^{prop} \times 10^6$ (L mol^{-1} s^{-1})
970	53	1.96	67.5±1.5	8.5±0.5	3.4	4.3
970	36	0.969	30.1±1.1	4.03±0.25	3.3	4.4
938	126	0.969	195±8	65±5	2.5	8.5
936	69	1.96	63±3	12.8±1.1	2.8	5.7
934	52	3.96	40.6±1.7	7.0±0.3	3.3	5.6
934	34	3.96	20.8±1.3	2.33±0.10	3.9	4.4
935	27	3.96	11.5±0.2	1.76±0.07	3.4	5.2
895	60	3.96	22.7±0.8	6.9±0.1	2.3	7.0
854	120	3.96	28.1±2.0	16.9±0.4	1.28	7.70

vinylacetylene in reaction [5-3] was slightly lower than the value of two, which had been assumed in deriving equation (E5-9). As well, k_B^{prop} increased with an increase in the pressure at 934-938 K, indicating the order for the formation of benzene in reaction [5-9] was slightly greater than two.

5-4. Conclusion

Trace amounts of neopentane, a well known source of free radicals at high temperatures, were observed to accelerate the rates of formation of vinylacetylene and benzene by similar factors. This confirms that a free radical mechanism dominates the pyrolysis of acetylene. The order of the termination reaction was shown to be two. The rate constant for initiation in the pyrolysis of acetylene was experimentally determined for the first time in the present temperature range without effects by a surface termination. The rate constants for the termination reaction and for the formation of vinylacetylene and benzene from chain propagation steps were also determined.

Now that we have obtained insights into the chain initiation, propagation, and termination reactions, further work will involve the study of minor products including those formed in the termination reactions.

References for Chapter 5

1. X.Xu and P.D.Pacey, *Phys.Chem.Chem.Phys.*, 2001, **3**, 2836.
2. G.Ayranci and M.H.Back, *Int.J.Chem.Kinet.*, 1981, **13**, 897.
3. G.Ayranci and M.H.Back, *Int.J.Chem.Kinet.*, 1983, **15**, 83.
4. M.Niclause, R.Martin, F.Baronnet, and G.Scacchi, *Rev.Inst.Fr.Petrole*, 1966, **21**, 1724.
5. M.Niclause, F.Baronnet, G.Scacchi, J.Muller, and J.Y.Jezequel, In L. F. Albright and B. L. Crynes, editors, *Industrial and Laboratory Pyrolysis*, 1976, **ACS Symposium Series 32**, p.17.
6. R.Martin, M.Niclause, and G.Scacchi, In L. F. Albright and B. L. Crynes, editors, *Industrial and Laboratory Pyrolysis*, 1976, **ACS Series 32**, p. 37.
7. G.Scacchi, F.Baronnet, and M.Niclause, *Can.J.Chem.*, 1982, **60**, 249.
8. G.Scacchi, F.Baronnet, and M.Niclause, *Can.J.Chem.*, 1982, **60**, 257.
9. M.H.Back and R.Martin, *Int.J.Chem.Kinet.*, 1979, **XI**, 757.
10. R.N.Pease, *J.Am.Chem.Soc.*, 1929, **51**, 3470.
11. D.A.Frank-Kamenetzky, *Acta Physicochim.U.R.S.S.*, 1943, **18**, 148.
12. C.G.Silcocks, *Proc.Roy.Soc.(London)*, 1957, **A242**, 411.
13. G.J.Minkoff, D.M.Newitt, and P.Rutledge, *J.Appl.Chem.*, 1957, **7**, 406.
14. H.Ogura, *Bull.Chem.Soc.Jpn.*, 1978, **51**, 3418.
15. C.Chanmugathas and J.Heicklen, *Int.J.Chem.Kinet.*, 1986, **18**, 701.
16. C.F.Cullis and N.H.Franklin, *Roy.Soc.(London)*, 1964, **A280**, 139.
17. H.Ogura, *Bull.Chem.Soc.Jpn.*, 1980, **53**, 1210.
18. R.P.Duran, V.T.Amorebieta, and A.J.Colussi, *J.Am.Chem.Soc.*, 1987, **109**, 3154.
19. R.P.Duran, V.T.Amorebieta, and A.J.Colussi, *Int.J.Chem.Kinet.*, 1989, **21**, 947.

20. R.D.Kern, K.Xie, H.Chen, and J.H.Kiefer, *Twenty-Third Symposium (International) on Combustion, The Combustion Institute*, 1990, 69.

21. S.T.Dimitrijevic, S.Paterson, and P.D.Pacey, *J.Anal.& Appl.Pyrolysis*, 2000, **53**, 107.

22. X.Xu and P.D.Pacey, *Carbon*, 2001, **39**, 1839.

23. M.B.Colket III, D.J.Seery, and H.B.Palmer, *Combustion and Flame*, 1989, **75**, 343.

24. P.D.Pacey, *Can.J.Chem.*, 1973, **51**, 2415.

25. W.Tsang, *J.Chem.Phys.*, 1966, **44**, 4283.

26. M.P.Halstead, R.S.Konar, D.A.Leathard, R.M.Marshall, and J.H.Purnell, *Proc.R.Soc.London, A*, 1969, **310**, 525.

27. J.E.Taylor, D.A.Hutchings, and K.J.Frech, *J.Am.Chem.Soc.*, 1969, **91**, 2215.

28. F.Baronnet, M.Dzierzynski, G.M.Come, R.Martin, and M.Niclause, *Int.J.Chem.Kinet.*, 1971, **3** , 197.

29. J.N.Bradley and K.O.West, *J.Chem.Soc.Faraday Trans.1*, 1976, **72**, 8.

30. R.M.Marshall, J.H.Purnell, and P.D.Storey, *J.Chem.Soc.Faraday Trans.1*, 1976, **72**, 85.

31. P.M.Marquaire and G.M.Come, *React.Kinet.Catal.Lett.*, 1978, **9**, 171.

32. A.C.Baldman, K.E.Lewis, and D.M.Golden, *Int.J.Chem.Kinet.*, 1979, **11**, 529.

33. D.Bernfeld and G.B.Skinner, *J.Phys.Chem.*, 1983, **87**, 3732.

34. V.S.Rao and G.B.Skinner, *Int.J.Chem.Kinet.*, 1988, **20**, 165.

35. C.F.Melius, J.A.Miller, and E.M.Evleth, *Symp.Int.Combust.Proc.*, 1992, 621.

36. A.M.Mebel, R.I.Kaiser, and Y.T.Lee, *J.Am.Chem.Soc.*, 2000, **122**, 1776.

37. I.D.Gay, G.B.Kistiakowsky, J.V.Michael, and H.Niki, *J.Chem.Phys.*, 1965, **43**, 1720.

38. P.Frank and Th.Just, *Combustion and Flame*, 1980, **38**, 231.

39. A.Fahr, A.Laufer, R.Klein, and W.Braun, *J.Phys.Chem.*, 1991, **95**, 3218.

40. A.Fahr and A.H.Laufer, *J.Phys.Chem.*, 1990, **94**, 726.

41. A.Fahr, W.Braun, and A.H.Laufer, *J.Phys.Chem.*, 1993, **97**, 1502.

42. R.P.Duran, V.T.Amorebieta, and A.J.Colussi, *J.Phys.Chem.*, 1988, **92**, 636.

43. P.R.Westmoreland, A.M.Dean, J.B.Howard, and J.P.Longwell, *J.Phys.Chem.*, 1989, **93**, 8171.

44. R.P.Thorn, W.A.Payne, L.J.Stief, and D.C.Tardy, *J.Phys.Chem.*, 1996, **100**, 13594.

45. V.D.Knyazev, S.I.Stollarov, and I.R.Slagle, *Symp.Int.Combust.Proc.*, 1996, **26**, 513.

CHAPTER 6. MINOR PRODUCTS FORMED IN THE PYROLYSIS OF ACETYLENE

6-1. Introduction

As described in Chapter 1, the pyrolysis of acetylene has been studied for more than seventy years in static vessels and flow systems (T < 1000 K), and in shock tubes (T > 1000 K). The mechanism for the pyrolysis of acetylene at temperatures below 1500 K is still a subject argued by various workers in terms of free radical mechanisms[1-4] and molecular mechanisms.[5-7] Free radical mechanisms have been shown in previous chapters to dominate the process at temperatures above 850 K.[8] However, the details of the mechanism are still not very clear. The study of the formation of minor products should provide important, additional information.

The pyrolysis of acetylene has been studied with static and flow reactors at moderate temperatures (below 1200 K) by various workers.[9-23] The gaseous products were observed to be C_4H_4 (vinylacetylene), C_6H_6 (benzene), C_2H_4, C_4H_2, CH_4, and H_2.[13,16,18,20,22] The condensable products were PAHs and other unidentified polymers.[12,13,22] Some workers suggested C_2H_4, CH_4, H_2 and C_4H_2 were formed by heterogeneous processes.[12,13,20] Vinylacetylene was supposed to be the sole primary product,[12,20,22] but some workers argued that both vinylacetylene and benzene were primary products.[17,18]

There are several weaknesses in the previous work. First, most of previous experiments were carried out at high conversions, where the effects of secondary and tertiary reactions were very serious. Secondly, most experiments were carried out in the presence of significant deposits of pyrolytic carbon on the walls of the reactors. The deposition of carbon on the surface of the reactor was found in Chapter 3 to significantly inhibit the gas phase reaction by a surface termination process.[24] In addition, heavy products might have condensed in the transfer lines in some experiments, so they couldn't be observed.

The present chapter describes a study of the pyrolysis of acetylene at low conversions with special procedures to minimize carbon deposition, as described in section 2-2-4-1. A reactor and a high temperature injection valve were installed in a GC oven, maintained at 210 ^{0}C, to reduce possible condensation of products heavier than styrene. Gas chromatography-mass spectrometry (GC-MS) was used to identify products. The residence time, pressure of acetylene, and temperature were varied in wide ranges.

6-2. Results

6-2-1. Observation and identification of minor products

Experiments were performed to study the formation of minor products at temperatures between 854 and 971 K, pressures between 104 and 403 Torr, and residence times

between 25 and 3320 ms. Reactors with smaller inner diameters were used at high pressures or high temperatures to keep conversions low (0.39-14%).

Figures 6-1 and 6-2 show a typical GC chromatogram for a sample taken from acetylene which had been pyrolysed at 970 K, 200 Torr, and 700 ms. Several of the smaller peaks in Figure 6-2 couldn't be detected with the mass spectrometric detector. More than twenty-four products were observed at most conditions. Other small peaks couldn't be identified. Retention times and molecular formulas of various products are listed in Table 6-1.

The elution order of products in Figures 6-1 and 6-2 basically increased with an increase in the number of carbon atoms in the products. For species with the same number of carbon atoms, retention times increased with an increase in the number of π-bonds. There were two additional tiny peaks with the formula C_5H_6 between the vinylacetylene and benzene peaks. The styrene peak (85.25') in Figure 6-1 had a long tail on the column, because the interaction between it and the alumina stationary phase was very strong, and the amount of styrene was sufficient to overload the column.

Acetylene was pyrolysed to observe the formation of minor products heavier than styrene at 970 K and 200 Torr, and at residence times between 196 and 1890 ms, by installing the reactor and a high-temperature injection valve in the GC oven to minimize the condensation of heavy products. Conversions were kept below 17%.

Figure 6-3 shows a typical GC chromatogram of a gaseous sample collected after pyrolysis at 970 K, 200 Torr, and 1420 ms. Partial identities of the numbered peaks are also listed in Table 6-1. Various heavy products were observed including styrene,

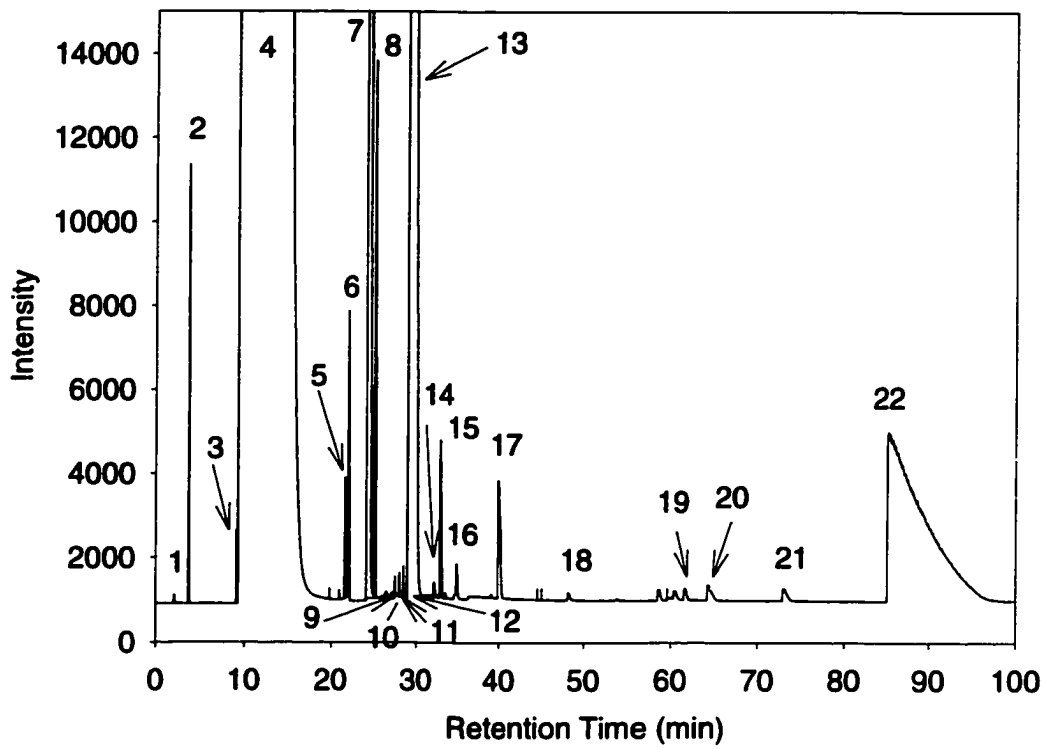

Figure 6-1. GC chromatogram of a gaseous sample collected at 298 K from a furnace external to the GC oven after pyrolysis at 970 K, 200 Torr, and 700 ms; column, alumina, 50 m × 0.32 mm × 8 μm; detector, FID. Identities of some of the numbered peaks are listed in Table 1.

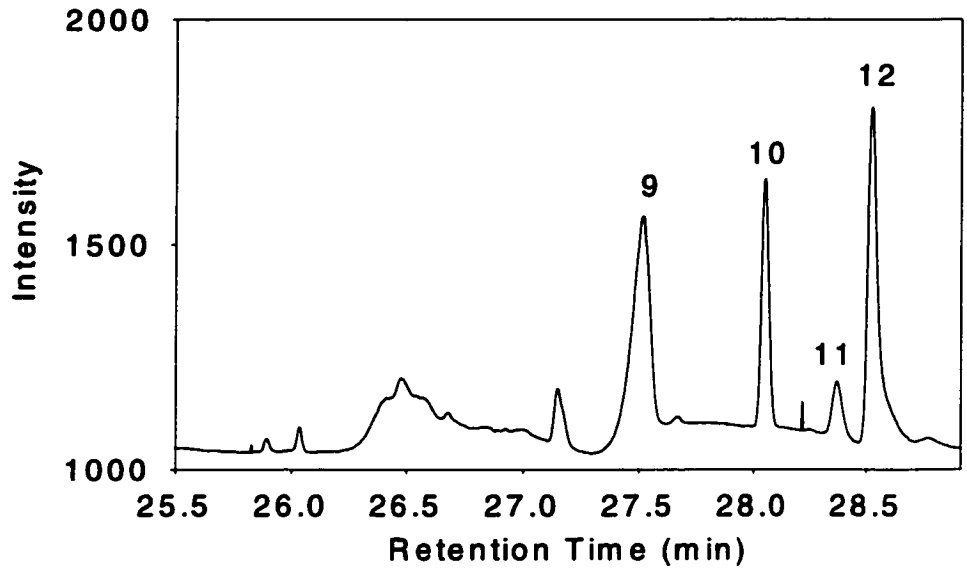

Figure 6-2. An expanded area from Figure 6-1.

Table 6-1. Identification of GC peaks illustrated in Figures 1 and 3 using an alumina column and a Porapak Q column.

Peak No.	Retention Time (min)	Identification	source
1	2.06	ethane	tertiary
2	3.65	ethylene	partially primary
3	9.17	propylene	secondary and tertiary
4	12	acetylene	reactant
5	21.64	1,3-butadiene	partially primary
6	21.98	propyne	tertiary
7	24.5	vinylacetylene	primary
8	25.09	cyclopentadiene	partially primary
9	27.52	C_5H_6	partially primary
10	28.06	1,3-cyclohexadiene	partially primary
11	28.37	C_5H_6	partially primary
12	28.52	1,4-cyclohexadiene	partially primary
13	29.8	benzene	primary
14	32.15	C_4H_2	partially primary
15	34.14	C_6H_6	partially primary
16	36.19	C_6H_6	partially primary
17	39.93	toluene	secondary
18	48.22	C_6H_6	partially primary
19	61.7	ethylbenzene and/or 6,6-dimethylfulvene	partially primary
20	64.31	m- and/or p-xylenes	partially primary
21	73.01	o-xylene	partially primary
22	85.25, 16.03*	styrene	partially primary
23	33.95*	C_{10}	secondary
24	62.62*	C_{10}	secondary
25	76.08*	naphthalene	secondary

* Retention times on a Porapak Q column, other retention times were obtained on an alumina column.

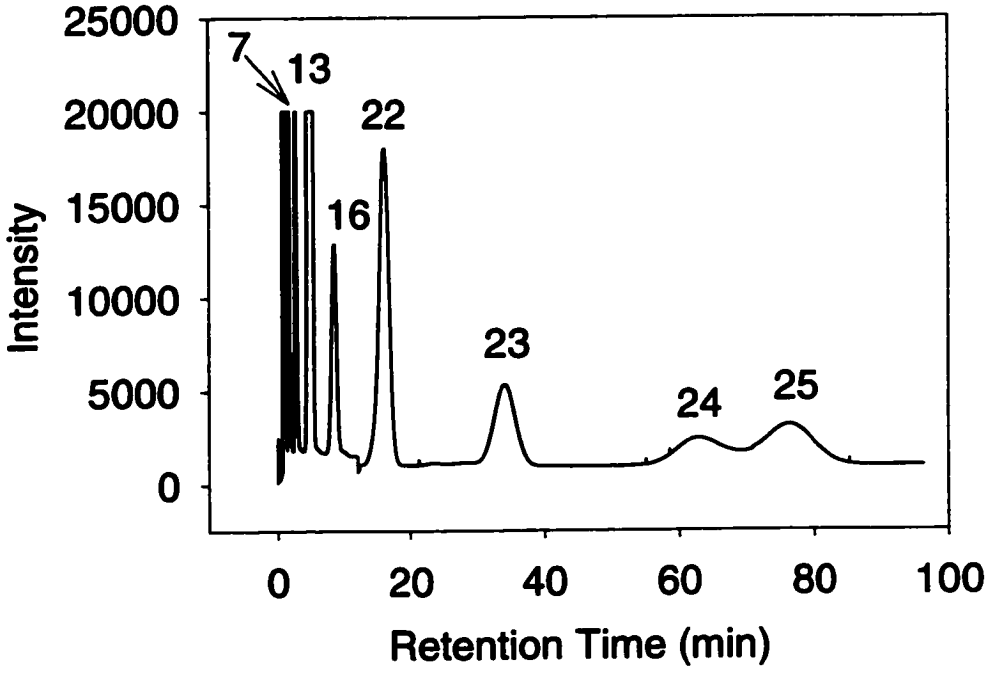

Figure 6-3. GC chromatogram of a gaseous sample collected at 483 K with the reactor furnace inside the GC oven, after pyrolysis at 970 K, 200 Torr, and 1420 ms; column, Porapak Q, 2 m; detector, FID. Identities of the numbered peaks are listed in Table 1. The signal was attenuated by a factor of two after twelve minutes.

naphthalene, and two peaks with peak areas similar to that of naphthalene and with retention times between styrene and naphthalene. These two peaks could be C_{10} species (not divinylbenzene due to different retention times) instead of C_9 species, because products with even number of carbon atoms were observed to be prominent, consistent with the hydrogen-abstraction-C_2H_2-addition mechanism.[25]

Each product not heavier than styrene was identified using the procedure described below. Gas samples were collected from the reactor at various conditions to run GC-MS. Masses of products were obtained from their molecular ions in the mass spectrum. The computer search of matched mass spectra in a database (MassLynx) provided several candidates for each product. The mass spectra for the candidates were so similar that it was not possible to identify any products directly. Therefore, standard samples were sought for each candidate. Each available standard sample was injected into the GC to compare retention times. An agreement of retention times was taken to give an identification of the product. Vinylacetylene was the only product identified using IR, because the yield of vinylacetylene was high enough for an IR identification,[26] and commercial vinylacetylene was not available. Commercial compounds available for identification were very limited because most candidates are not stable. Molecular formulas were provided in Table 6-1 when commercial compounds were not available. 2,4-hexadiyne was ruled out as a significant C_6H_6 product because of disagreement in retention times (54.98 minutes for 2,4-hexadiyne). For the same reason, 1,4-cyclohexadiene was not an observed C_6H_8 product, and 2-methyl-1-buten-3-yne was not an observed C_5H_6 product. A computer search for matched mass spectra indicated that the

possible compounds with the formula C_5H_6 were 1,3-cyclopentadiene, 3-penten-1-yne, 1-penten-3-yne, and 2-methyl-1-buten-3-yne. For C_6H_8 the possible isomers were 1,4-cyclohexadiene, 1,3-hexadiene, 1,3,5-hexatriene, 1,2-bis(methylene)-cyclobutane, 2-hexen-4-yne, and 1-hexen-4-yne. For C_6H_6, the suggested compounds were 1,5-hexadien-3-yne, 1,5-hexadiyne, 1,3-hexadien-5-yne, 2,4-hexadiyne, 3-methylene-1-penten-5-yne, and fulvene. Methane and allene were not observed. For C_8H_{10} products, the candidates were o-, m-, and p-xylenes, 6,6-dimethylfulvene, and ethylbenzene.

Retention times for unknown products heavier than styrene were compared with those of compounds that were said to have been observed in previous work.[23,27] Divinylbenzene was not one of the C_{10} products due to its unmatched retention time of 49.0 minutes. Naphthalene was identified to be a C_{10} product. The yields and the vapor pressures of products heavier than styrene were too low for GC-MS analysis.

The typical amounts for these unidentified products were in the range of 1-10 ng mL^{-1}. These amounts were too small for IR or NMR analysis.

Yields of various products were fitted by a polynomial equation (E6-1) to determine the contributions of primary and other reactions.

$$y = a + bt + ct^2 + dt^3 \qquad \text{(E6-1)}$$

Here, y is the yield of a product; t, the residence time; a, b, c and d represent contributions from an impurity, a primary reaction, a secondary reaction and a tertiary reaction. The procedure of fitting equation (E6-1) was as follows. The parameter, a, was included in equation (E6-1) only for products that were also impurities in acetylene. For products which were not impurities, parameters, b, c, and d, b and c, b and d, or c and d were

included in equation (E6-1), in sequence, to fit the data. Then, the fitting result giving the lowest sum of squares of the residuals, and lowest deviations for the parameters, was accepted.

Of all these products, seventeen were identified to be primary or partially primary products. Vinylacetylene and benzene have been considered in Chapter 4. Three C_8H_{10} (o-, m-, p-xylenes etc.) were not systematically analyzed, because their retention times in the Al_2O_3 column were too long. Eleven of these seventeen products will be considered in two groups. Five partially primary products, ethylene, 1,3-butadiene, cyclopentadiene, and the two C_6H_6 products at 34 and 36 min, respectively, will be discussed in the first group. Peak areas were converted to concentrations using standard compounds in GC calibration mixtures, as described in section 2-2-4-4. GC sensitivities for products without standard materials were calculated from compounds with similar numbers of carbon atoms. Figure 6-4 shows the yields of the five products as functions of the residence time at 970-971 K and 203 Torr. Contributions from primary reactions dominated at short residence times, and contributions from secondary processes gradually became significant at long residence times. For instance, the parameters for the yield of 1,3-butadiene measured at 203 Torr and 970 K were $(5.77\pm0.35) \times 10^{-8}$ mol L^{-1} s^{-1}, $(9.10\pm1.7) \times 10^{-8}$ mol L^{-1} s^{-2}, and $(1.98\pm0.18) \times 10^{-7}$ mol L^{-1} s^{-3}, for *b*, *c*, and *d*, respectively.

Figure 6-5 shows the yields of the second group of products, C_5H_6(27.52'), 1,3-cyclohexadiene, C_5H_6(28.37'), 1,4-cyclopentadiene, C_4H_2 and C_6H_6(48.22'), as functions of the residence time at 937 K and 202 Torr.

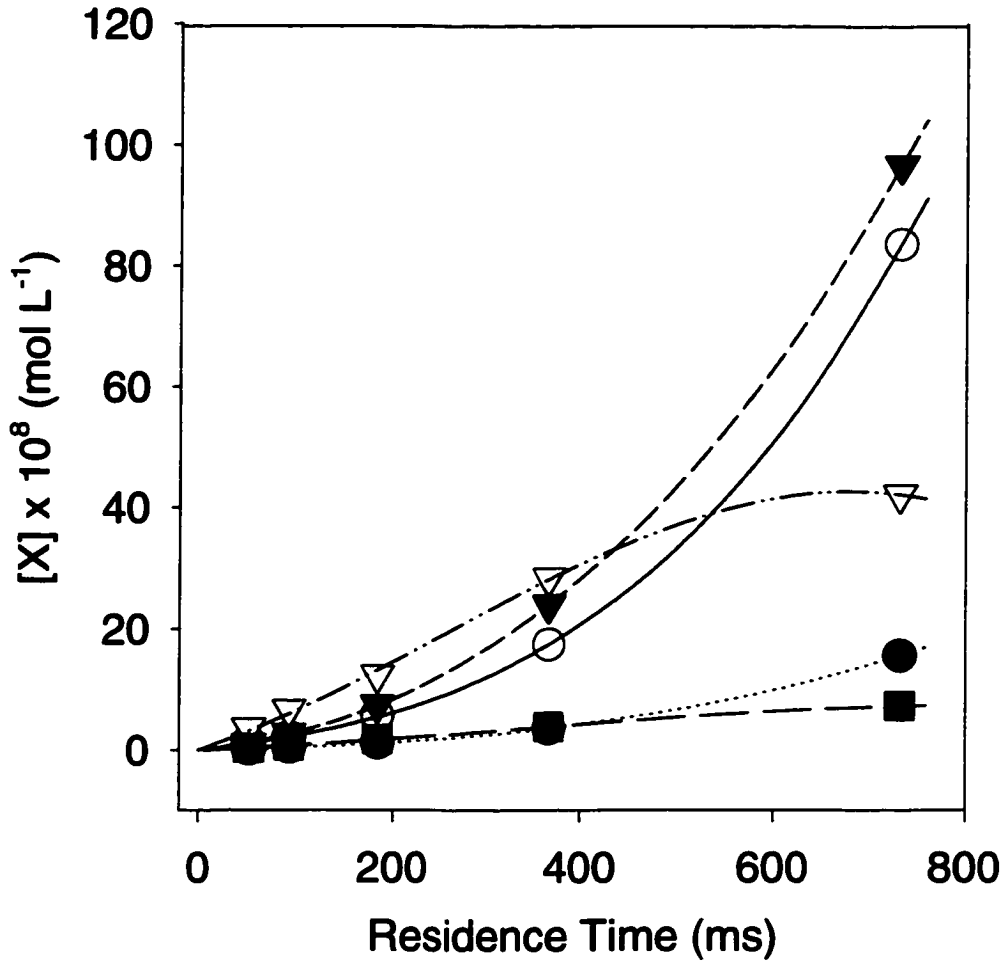

Figure 6-4. Dependence of concentrations of five light products, X, on the residence times at 970 K and 203 Torr; ○, ethylene; ●, 1,3-butadiene; ▼, cyclopentadiene; ▽, C_6H_6(34'); ■, C_6H_6(36'); lines are least-square fits of equation (E6-1) to the data.

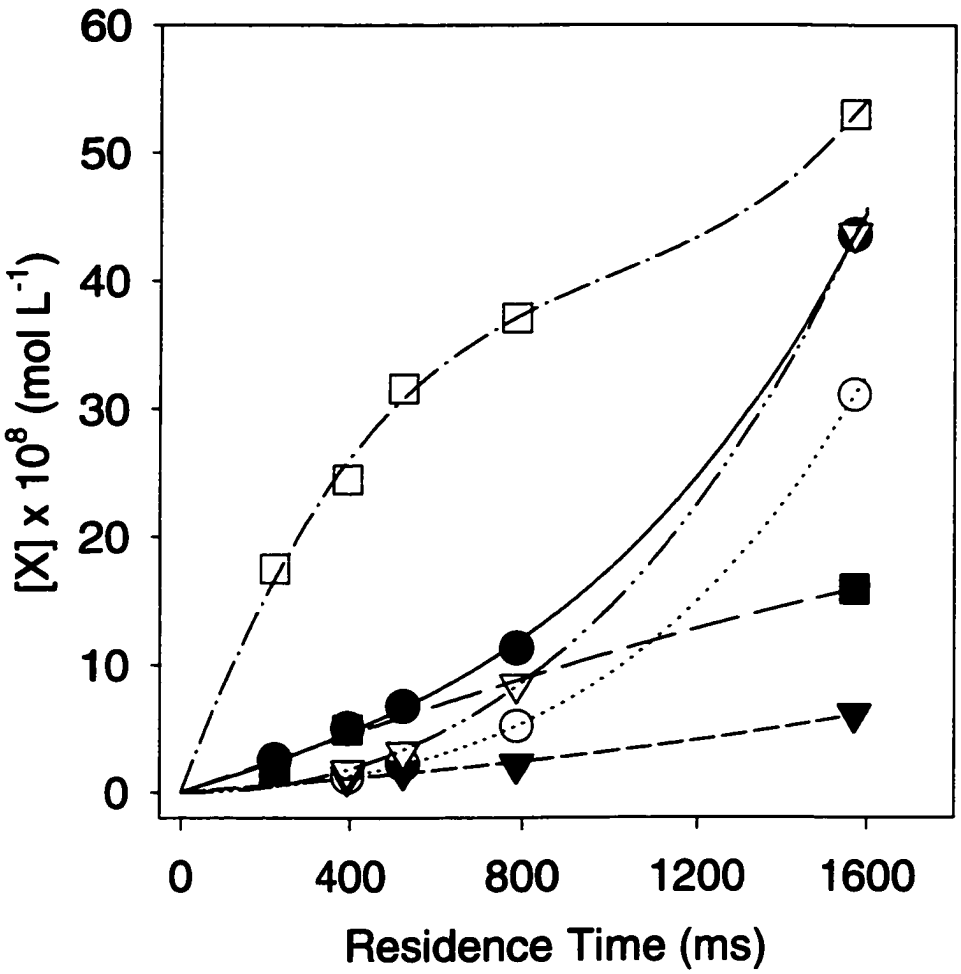

Figure 6-5. Dependence of concentrations of six light products, X, on the residence times at 937 K and 202 Torr; ●, C_5H_6(27.52'), ○, 1,3-cyclohexadiene; ▼, C_5H_6(28.37'); ▽, 1,4-cyclohexadiene; ■, C_4H_2; and □, C_6H_6(48.22'); lines are least-square fits of equation (E6-1) to the data.

Figure 6-6 shows the yields of heavy products as functions of the residence time. Styrene was found to be a partially primary product, but all other heavy products were observed to be secondary products.

6-2-2. Pressure and temperature dependences of the rates of formation of primary products

Table 6-2 lists the rates of formation from primary reactions of twelve products. The parameters were obtained by fitting equation (E6-1) to yield-residence time curves obtained at various conditions. Vinylacetylene and benzene were studied in Chapters 3 to 5.[8]

The pressure of acetylene was varied between 104 and 403 Torr, at 970-971 K to study the pressure dependence of products. Figures 6-7 and 6-8 show the order plots for the primary rates of formation of eleven minor products in two groups, respectively. The second column of Table 6-3 lists the orders for the primary reactions determined at 970-971 K.

The temperature was varied between 854 and 971 K. At 970-971K, rate constants of formation of various products were obtained from their order plots. Rate constants at

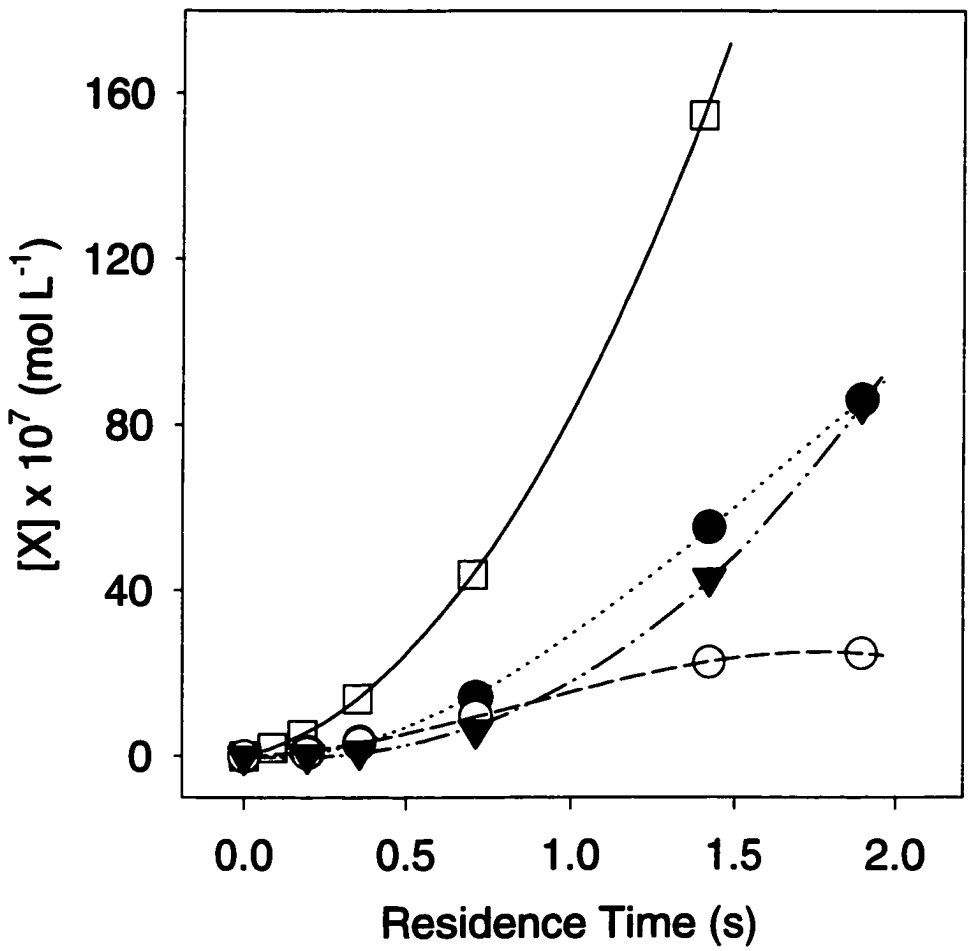

Figure 6-6. Dependence of concentrations of four heavy products, X, on the residence times at 970 K and 200 Torr; ❐, styrene; ●, C_{10}(34'); ○, C_{10}(63'); ▼, naphthalene; lines are least-square fits of equation (E6-1).

Table 6-2. The rates, $b \times 10^8$ mol L^{-1} s^{-1}, of formation of twelve products from primary reactions, obtained by fitting equation (E6-1) to the yields of various products.

T (K)	971	970	971	970	937	895	854
P (Torr)	104	203	302	403	202	302	402
i.d. (mm)	3.96	1.96	1.96	0.969	3.96	3.96	3.96
ethylene	7.03±0.21	24.7±0.8	77.6±2.3	169±7	11.0±0.4	11.9±0.8	9.70±0.86
1,3-butadiene	1.36±0.11	5.77±0.35	20.1±0.8	42.0±2.0	2.42±0.17	2.56±0.20	1.83±0.22
cyclopentadiene	4.91±0.44	19.2±1.7	58.4±0.6	142±13	21.7±0.2	6.66±0.79	7.64±0.92
C_5H_6 (27.52')	0.256±0.026	2.24±0.20	5.30±0.80	13.4±0.9	1.07±0.04	1.08±0.02	0.876±0.026
1,3-cyclohexadiene	0.167±0.020	1.40±0.25	2.58±0.44	5.87±0.41	0.215±0.009	0.319±0.029	0.291±0.038
C_5H_6 (28.37')	*	*	1.46±0.22	3.14±0.16	0.271±0.027	0.260±0.009	0.179±0.009
1,4-cyclohexadiene	0.82±0.10	*	2.26±0.57	6.91±0.83	0.401±0.072	0.284±0.068	0.195±0.021
C_4H_2	*	0.644±0.13	1.14±0.41	7.6±2.3	*	0.44±0.18	0.50±0.20
C_6H_6 (34')	15.4±0.4	61.8±5.3	135±8	209±12	25.8±1.3	17.9±0.7	8.50±0.26
C_6H_6 (36')	2.69±0.10	10.5±0.2	24.7±0.7	35.1±1.1	4.02±0.12	2.44±0.56	0.662±0.020
C_6H_6 (48.22')	1.05±0.20	13.8±2.3	23.2±4.9	*	4.00±0.52	5.71±0.91	5.80±0.87
styrene		178±2					

* There was insufficient data to reliably obtain the missing rates.

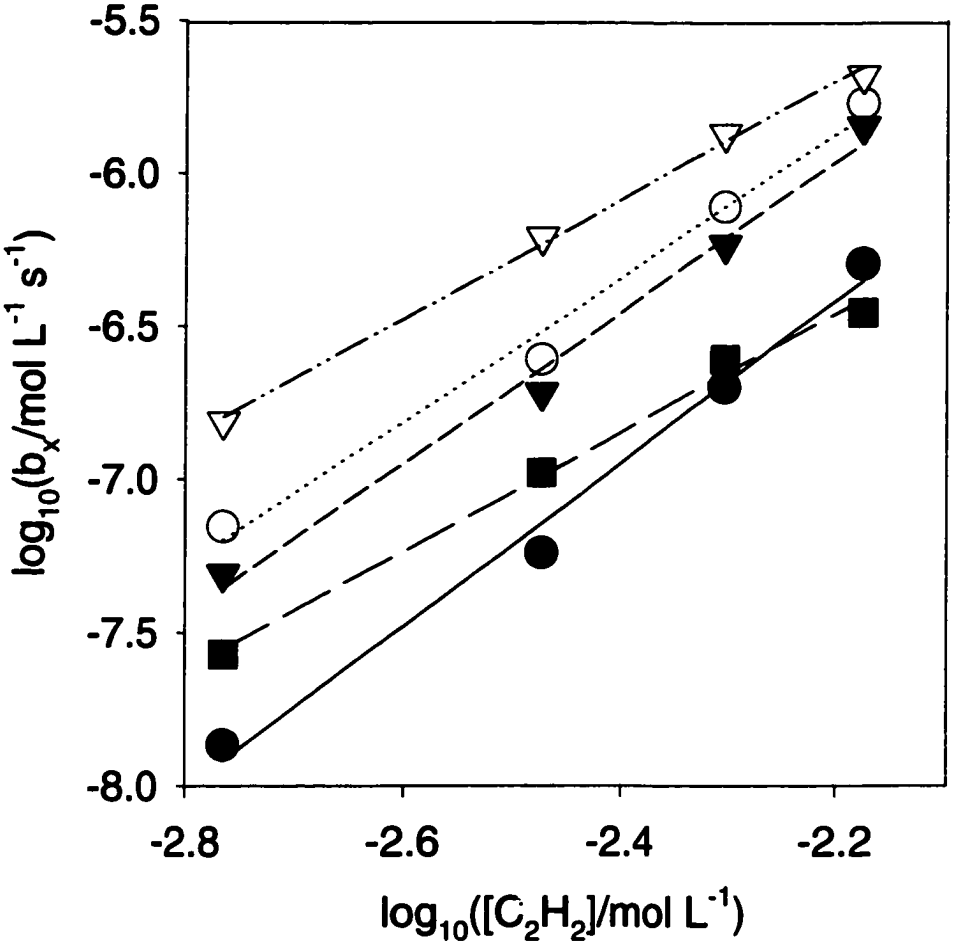

Figure 6-7. Order plots for the primary rates of formation of five light products at 970-971 K; ○, ethylene; ●, 1,3-butadiene; ▼, cyclopentadiene; ▽, C_6H_6 (34'); ■, C_6H_6 (36').

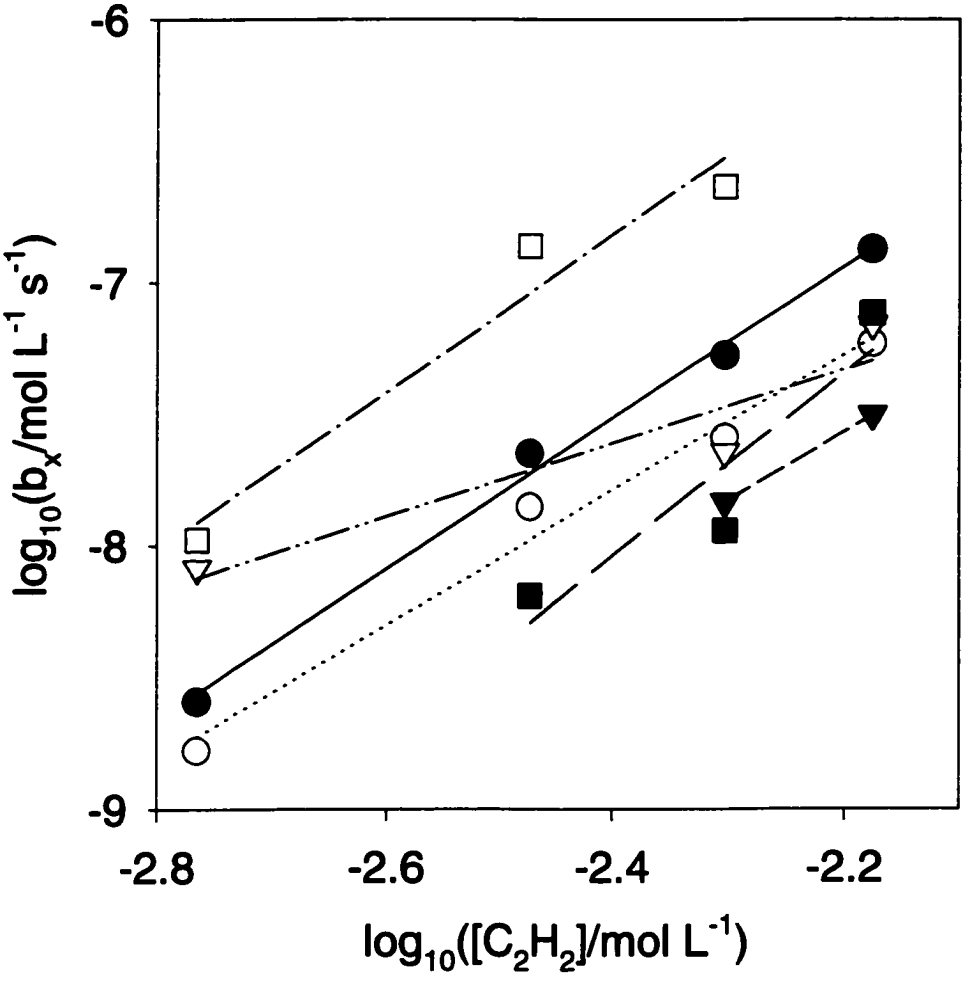

Figure 6-8. Order plots for the primary rates of formation of six light products at 970-971 K. ●, C_5H_6(27.52'); ○, 1,3-cyclohexadiene; ▼, C_5H_6(28.37'); ∇, 1,4-cyclohexadiene; ■, C_4H_2; and □, C_6H_6(48.22').

Table 6-3. Orders, Arrhenius parameters and acceleration factors, Q, (by 0.38% neopentane at 970 K and 104 Torr) for the formation of some products.

product	order	$\log_{10}A$[a]	E_A (kJ mol^{-1})	Q
ethylene	2.35±0.18	8.7±0.8	176±13	6.3
1,3-butadiene	2.66±0.20	10.7±0.5	210±9	7.4
vinylacetylene	1.8±0.1[b]	9.9±0.7[b]	165±11[b]	2.8
cyclopentadiene	2.46±0.17	10.6±2.5	205±44	16.3
C_5H_6 (27.52')	2.87±0.15	9.56±0.38	189±7	3.3
1,3-cyclohexadiene	2.57±0.23	8.38±2.03	189±35	2.9
C_5H_6 (28.37')	2.64	8.59±0.29	192±5	3.2
1,4-cyclohexadiene	1.40±0.51	6.16±1.99	196±35	6.2
benzene	2.4±0.1[b]	6.8±0.5[b]	100±9[b]	3.3
C_4H_2	3.5±1.4	9.40±0.21	169±3	c
C_6H_6 (34')	1.94±0.07	9.7±0.2	207±3	2.8
C_6H_6 (36')	1.94±0.11	11.4±0.8	252±14	3.0
C_6H_6 (48.22')	3.00±0.67	9.52±0.47	170±8	2.8

a. The units for A are liters, moles, and seconds.

b. Data obtained from Chapter 4.

c. Peaks were too small to measure reliably.

other temperatures were calculated using the orders measured at 970-971 K. Figures 6-9 and 6-10 show Arrhenius plots for the primary rates of formation of eleven minor products. The Arrhenius parameters for these eleven minor products were listed in the third and fourth columns of Table 6-3.

A small amount of neopentane has been shown to accelerate the formation of vinylacetylene and benzene by providing a new initiation step. Acceleration of the formation of ten minor products by 0.38% neopentane in acetylene was studied at 970 K and 104 Torr. The acceleration factors for the primary reaction rates are listed in Table 6-3.

6-3. Discussion

6-3-1. Possible sources of errors

As discussed in Chapter 2,[8] the flow rate of acetylene was controlled to be no faster than 2.16×10^{-5} mol s^{-1}, so the reduction of rate due to incomplete radial heat transfer was calculated to be less than 5%. The pressure drop along the reactor was controlled to be less than 6.5%. The maximum conversion of the reactant was calculated to be 17%, so axial diffusion and volume contraction should be negligible, as discussed in section 2-1-2.

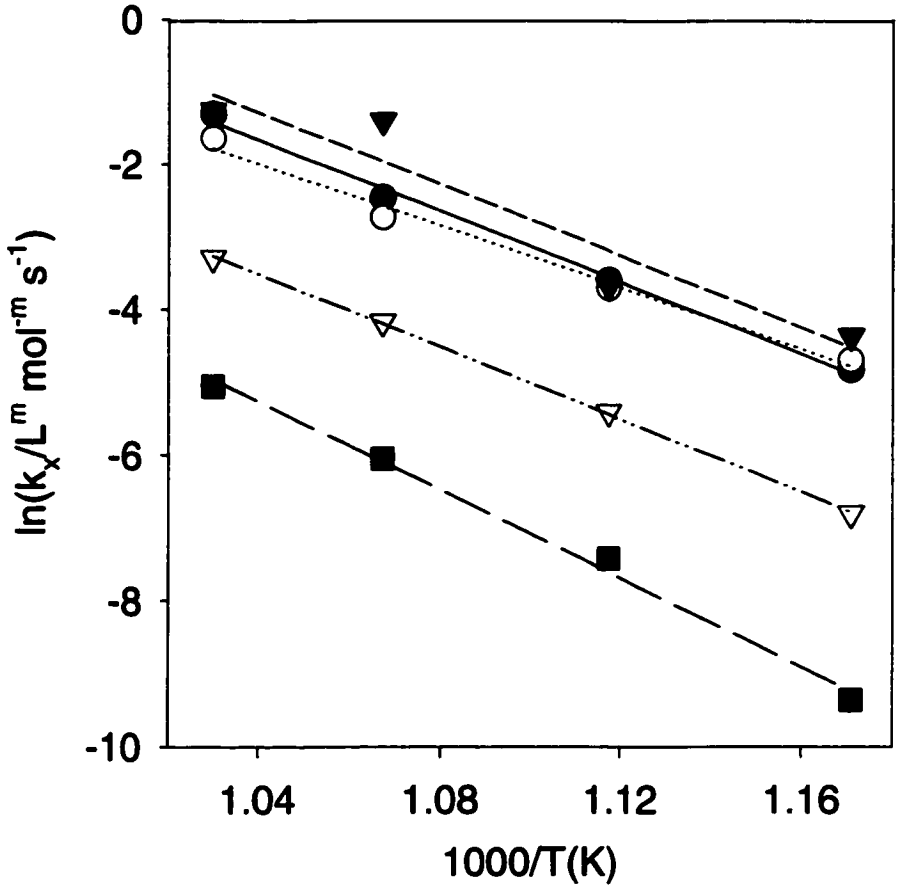

Figure 6-9. Arrhenius plots for the primary formation of five minor products; ○, ethylene, m = 1.35; ●, 1,3-butadiene, m = 1.66; ▼, cyclopentadiene, m = 1.46; ∇, C_6H_6 (34'), m = 0.94; ■, C_6H_6 (36'), m = 0.94.

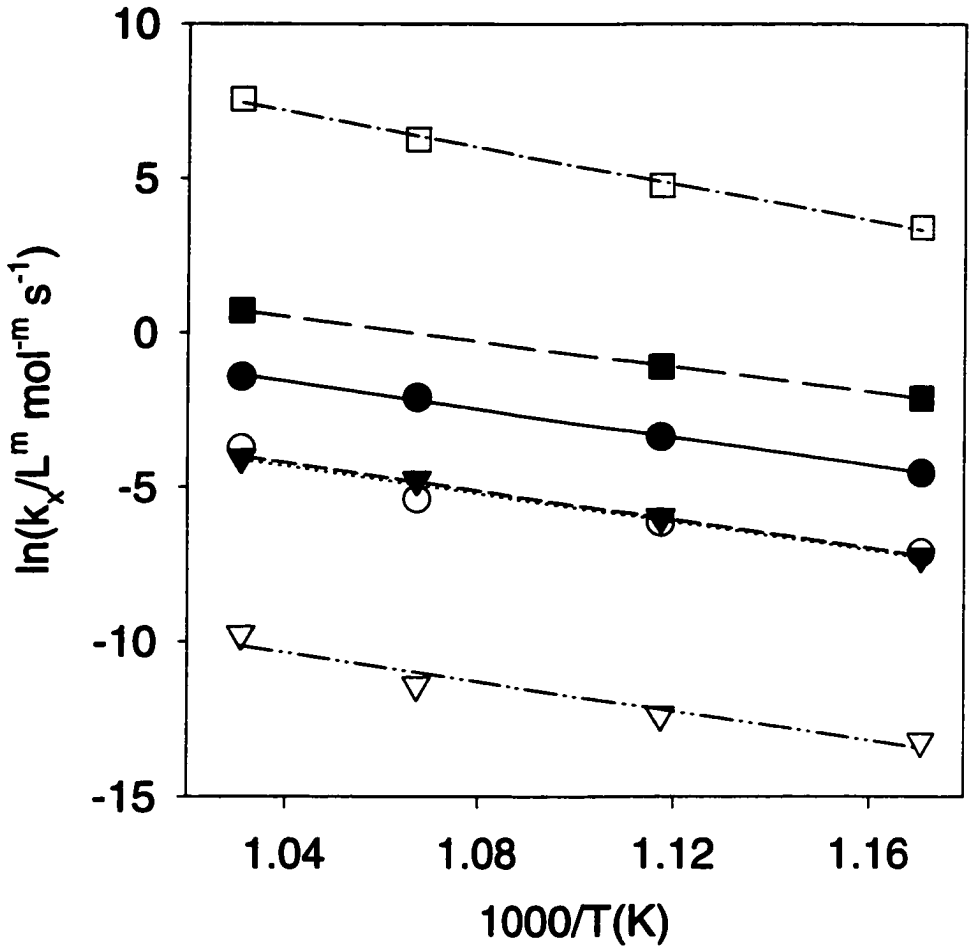

Figure 6-10. Arrhenius plots for the primary formation of six minor products; ●, C_5H_6(27.52'), m = 2.87; ○, 1,3-cyclohexadiene, m = 2.57; ▼, C_5H_6(28.37'), m = 2.64; ∇, 1,4-cyclohexadiene, m = 1.40; ■, C_4H_2, m = 3.48; and □, C_6H_6(48.22'), m = 4.11.

Surface reactions were shown to be insignificant in Chapter 3,[8] provided the reactor was washed with HF and provided carbon was burned off between analyses.

6-3-2. Initiation reaction

Now we can try to establish a mechanism for the pyrolysis of acetylene at low conversions based on our experimental results. In Chapter 4, a free radical mechanism was shown to dominate the pyrolysis of acetylene; and the order of the initiation reaction was determined to be two.[8] Therefore, a bimolecular initiation step could be written as,

$$C_2H_2 + C_2H_2 \rightarrow C_4H_3 + H \qquad [B1]$$

A hydrogen transfer initiation between two acetylene molecules, proposed by Back,[1] was too slow. An initiation by acetone, proposed by Colket et al.,[3] was unlikely in the purified acetylene, because the effect by acetone on the pyrolysis of acetylene was not detectable when the mole fraction of acetone in acetylene was less than 200 ppm.[26]

6-3-3. Termination reactions

The rate of formation for a product formed in a bimolecular termination step is directly proportional to the square of the concentration of a free radical, and the formation rate for a product formed from a propagation step is directly proportional to the concentration of the free radical. If a small amount of neopentane added to acetylene only introduced a

new initiation step and thus increased the radical concentration, the acceleration factor should be larger for a termination product than for a propagation product. Vinylacetylene and benzene have been shown to be products formed in propagation steps. Therefore, ethylene, 1,3-butadiene, cyclopentadiene and 1,4-cyclohexadiene, all of which had higher acceleration factors in Table 6-3 than vinylacetylene and benzene, could be formed in termination reactions. On the other hand, C_5H_6(27.52'), 1,3-cyclohexadiene, C_5H_6(28.37'), 1,4-cyclohexadiene, and three C_6H_6 products with similar acceleration factors to benzene were likely formed in propagation reactions. The unusually high acceleration factor for cyclopentadiene may indicate that methyl radicals formed in the new initiation reaction directly accelerated its formation.

The rate constant of the initiation reaction was determined in Chapter 5 by studying the acceleration by small amounts of neopentane. The rates of the initiation reaction in pure acetylene were calculated using equation (E5-7). The rates of formation of ethylene, 1,3-butadiene and 1,4-cyclohexadiene from primary reactions were taken from Table 6-2. These rates are listed in Table 6-4. The rate of formation of ethylene was much higher than that of the initiation reaction, indicating that ethylene might be formed from both a termination reaction and a propagation reaction. This will be further discussed in the next section. The sum of rates of formation of 1,3-butadiene and 1,4-cyclohexadiene was similar to that of the initiation reaction, supporting Benson's prediction[4] that 1,3-butadiene and 1,4-cyclohexadiene were products formed from termination reactions, and that 1,3-butadiene should be the main termination product.

Table 6-4. Rates of the initiation reaction, and of the formation of ethylene, 1,3-butadiene, 1,4-cyclohexadiene, and diacetylene from primary reactions.

T (K)	P (Torr)	R_i[a] $\times 10^8$ (mol L^{-1} s^{-1})	$b_{C2H4} \times 10^8$ (mol L^{-1} s^{-1})	$b_{C4H6} \times 10^8$ (mol L^{-1} s^{-1})	$b_{1,4\text{-cyclohexadiene}} \times 10^8$ (mol L^{-1} s^{-1})	$b_{C4H2} \times 10^8$ (mol L^{-1} s^{-1})
971	104	2.51	7.03±0.21	1.36±0.11	0.82±0.10	b
970	203	9.31	24.7±0.8	5.77±0.35	b	0.644±0.13
971	302	21.2	77.6±2.3	20.1±0.8	2.26±0.57	1.14±0.41
970	403	36.7	169±7	42.0±2.0	6.91±0.83	7.9±2.3
937	203	3.54	11.0±0.4	2.42±0.17	0.401±0.072	b
895	302	2.06	11.9±0.8	2.56±0.2	0.284±0.068	0.44±0.18
854	403	0.873	9.70±0.86	1.83±0.22	0.195±0.021	0.50±0.20

a. calculated from Arrhenius equation (E5-7)

b. There was insufficient data to reliably obtain the missing rates.

The order for the termination reaction was determined to be two in Chapter 5,[8] indicating a recombination of two free radicals. The chain termination reactions could include the following reactions, because of the observation of 1,3-butadiene and small amounts of C_8H_{10} and C_6H_8.

$C_2H_3 + C_2H_3 \rightarrow C_4H_6$(1,3-butadiene) [5-4]

$C_2H_3 + C_2H_3 \rightarrow C_2H_4 + C_2H_2$ [5-5]

$C_4H_5 + C_4H_5 \rightarrow C_8H_{10}$ [5-6]

$C_4H_5 + C_4H_5 \rightarrow C_4H_4 + C_4H_6$ [6-1]

$C_2H_3 + C_4H_5 \rightarrow C_6H_8$ [5-7]

$C_2H_3 + C_4H_5 \rightarrow C_2H_2 + C_4H_6$ [6-2]

$C_2H_3 + C_4H_5 \rightarrow C_2H_4 + C_4H_4$ [6-3]

Recombination of C_6H_7 and C_8H_9, and cross recombination between these free radicals may also be minor termination reactions. O-, m-, and p-xylenes, ethylbenzene, and 6,6-dimethylfulvene could be formed from recombination of C_4H_5 radicals involving hydrogen-shifts and a cyclization step.

Another possible source for the formation of 1,3-butadiene could be hydrogen-transfer reactions between C_4H_5 radicals and impurities in acetylene like ethane, propane, propylene, and acetone.

To compare concentrations of free radicals, the dependence of $ln(\Sigma b)$ on the number of carbon atoms in a product, n, is shown in Figure 6-11. The parameter, Σb, was defined as the sum of the primary formation rates, b, determined at 970 K and 203 Torr, of all the

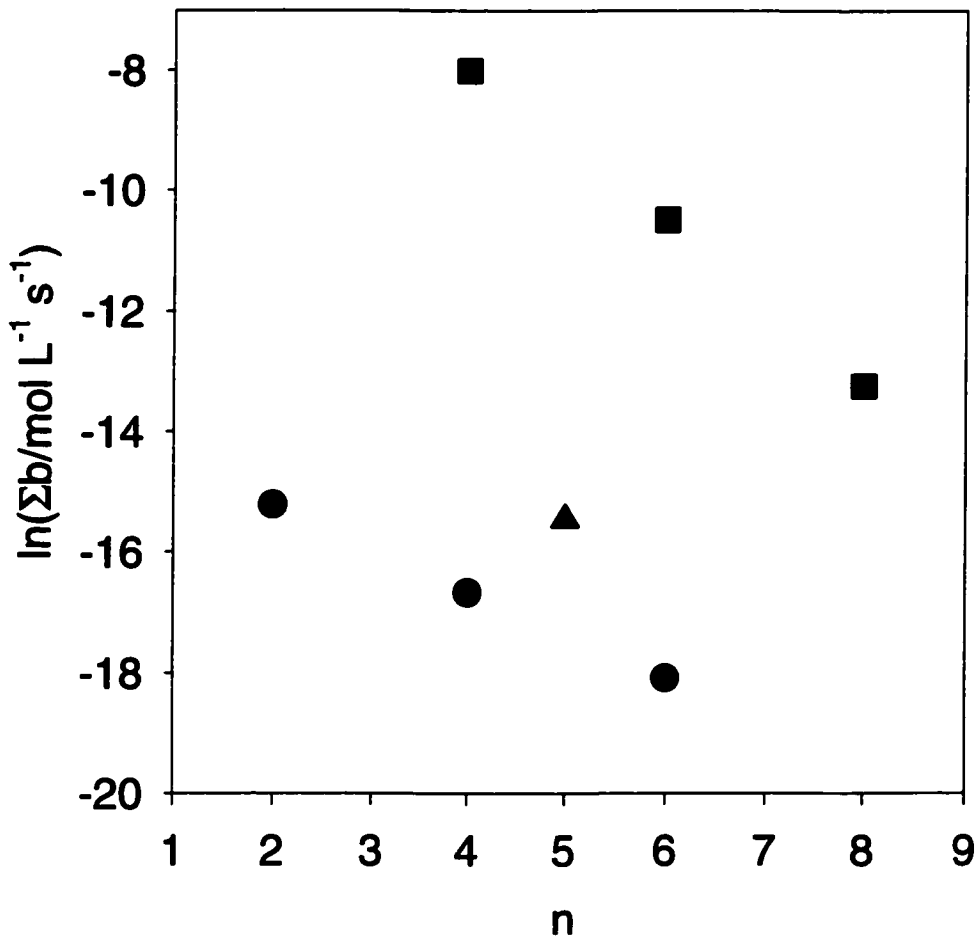

Figure 6-11. Dependence of $ln(\Sigma b)$ on the number, n, of carbon atoms in the products at 970 K and 203 Torr; ■, C_nH_n, vinylacetylene, benzene, and styrene, (Σb values for vinylacetylene and benzene were calculated using the Arrhenius parameters measured in Chapter 4); ●, C_nH_{n+2}, ethylene, 1,3-butadiene and C_6H_8; ▲, C_nH_{n+1}, C_5H_6.

products with the same molecular formula. The rates of formation of vinylacetylene, benzene, and styrene (C_nH_n series) gradually decreased with an increase of the number of carbon atoms. The rates of formation for ethylene, 1,3-butadiene, and C_6H_8 (C_nH_{n+2} series) gradually decreased with an increase of the number of carbon atoms, as well. The rates for the products in the C_nH_n series were at least 2000 times greater than the rates for products in the C_nH_{n+2} series with the same number of carbon atoms. This supports the idea that the former products were formed in propagation reactions, and that the products in the C_nH_{n+2} series were produced in termination reactions or reactions involving impurities. The products in the two series were likely to be formed from reactions involving C_2, C_4, and C_6 radicals. The rate constant for the formation of vinylacetylene from the reaction between C_2H_3 and acetylene at 970 K could be calculated to be 8.5×10^7 L mol^{-1} s^{-1} using the Arrhenius parameters measured by Knyazev et al.[28] Using the RRKM theory, Westmoreland et al.[29] calculated the rate constant for the formation of benzene from the reaction between C_4H_5 and acetylene at 970 K to be 1.1×10^8 L mol^{-1} s^{-1}, just a few percent faster than for the reaction above. Therefore, assuming that the rate constants for the formation of vinylacetylene, benzene, and styrene from different propagation reactions are almost the same, the ratio of the concentrations of C_2, C_4, and C_6 radicals could be estimated from the ratio of the *b* values of vinylacetylene, benzene, and styrene to be 187 : 15.8 : 1.

The rate for the formation of C_5H_6 didn't lie in either series, indicating that the C_5H_6 species were formed in different reactions. The ratio of ethylene, 1,3-butadiene, and C_6H_8 was calculated to be 17.7 : 4.10 : 1. These ratios are different from the previous ratios,

supporting the idea that products in the two series were formed from different types of reactions.

In addition, it has been discussed in section 4-4-4 that the similar induction periods observed for vinylacetylene and for benzene indicates that these compounds could be formed from reactions of two different radicals, vinylacetylene from C_2H_3 and benzene from C_4H_5. The ratio of yields between vinylacetylene and benzene was about two at low temperatures and high acetylene pressures, and about ten at high temperatures and low acetylene pressures. This also suggests that the concentration of C_2H_3 should be greater than that of C_4H_5 radicals.

The contributions of the termination reactions [5-4]-[6-3] will be considered in this paragraph. Taking the ratios of C_2, C_4 and C_6 radicals, 187 : 15.8 : 1, estimated at 970 K and 203 Torr, the ratios of rates of the termination reactions [5-4] + [5-5], [5-6] + [6-1], and [5-7] + [6-2] + [6-3] could be calculated to be 1.75×10^5 : 1.77×10^3 : 1, using rate constants of 8.49×10^{10} L mol^{-1} s^{-1} for terminations [5-4] + [5-5],[30] 1.21×10^{11} L mol^{-1} s^{-1} for terminations [5-6] + [6-1],[5] and of 1.70×10^{10} L mol^{-1} s^{-1} for terminations [5-7] + [6-2] + [6-3].[29] Using the ratios of C_2, C_4 and C_6 radicals, 17.7 : 4.10 : 1, the ratios of rates of the termination reactions [5-4] + [5-5], [5-6] + [6-1], and [5-7] + [6-2] + [6-3] could be calculated to be 1.56×10^3 : 1.19×10^2 : 1. Therefore, the main termination reactions should be [5-4] and [5-5].

The rate constants of the termination reactions [5-4]-[6-3] could be estimated as follows. Using an expression of a total rate constant for multiple termination reactions

proposed by Come et al.,[31] the total rate constant for the multiple termination reactions [5-4]-[5-7], k_t, could be written as,

$$k_t^{1/2} = k_{C2H3}^{1/2}[C_2H_3]/([C_2H_3]+[C_4H_5]) + k_{C4H5}^{1/2}[C_4H_5]/([C_2H_3]+[C_4H_5]) \quad \text{(E6-2)}$$

Here, k_{C2H3} and k_{C4H5} are the rate constants for the termination reactions by C_2H_3 and C_4H_5, respectively. Assuming that k_{C2H3} and k_{C4H5} are equal, k_{C2H3} and k_{C4H5} could be calculated to be 11×10^{10} L mol^{-1} s^{-1} using the rate constant for termination reactions determined in Chapter 5. These values are consistent with the reported rate constants, cited in the previous paragraph. The rate constants of termination reactions [5-4] and [5-5] could be calculated to be 8.4×10^{10} L mol^{-1} s^{-1} and 2.6×10^{10} L mol^{-1} s^{-1} using the total rate constant of termination reactions determined in Chapter 5, and using a ratio of 3.2 for $k_{6\text{-}1}/k_{6\text{-}2}$, reported by Fahr et al.[32] These rate constants are very close to values[33] of 7.23×10^{10} L mol^{-1} s^{-1} and 1.45×10^{10} L mol^{-1} s^{-1} reported for termination reactions [5-4] and [5-5], respectively. The rate constant for the termination reaction [5-7] + [6-2] + [6-3], $k_{C2H3+C4H5}$, could be expressed[31] as,

$$k_{C2H3+C4H5} = 2(k_{C2H3}k_{C4H5})^{1/2} \quad \text{(E6-3)}$$

Thus, a value of 22×10^{10} L mol^{-1} s^{-1} could be estimated for $k_{C2H3+C4H5}$. This value is greater than a value of 1.70×10^{10} L mol^{-1} s^{-1}, estimated by Westmoreland et al.[29] using thermochemistry. No rate constants were found in the literature for the termination reactions [6-1], [6-2], and [6-3], so it is difficult to estimate the rate constants for [5-6], [5-7], [6-1], [6-2], and [6-3]. The termination reactions [5-6] and [5-7] should be significantly faster than [6-1], and [6-2] + [6-3], respectively, by analogy with reactions [5-4] and [5-5].

The next question will be whether the rate constant of 8.4×10^{10} L mol^{-1} s^{-1} for reaction [5-4] is reasonable. This could be tested by comparing the collision diameter for C_2H_3 calculated using this rate constant with an interpolated value for C_2H_3. The collision diameter of C_2H_3 should be between the collision diameter of C_2H_2, 4.221×10^{-10} m, and that of C_2H_4, 4.232×10^{-10} m (measured from viscosity) or 4.523×10^{-10} m (measured from intermolecular forces.)[34] Assuming that the ratio of electronic degeneracies is ¼ for reaction [5-4], the rate constant of 8.4×10^{10} L mol^{-1} s^{-1} could be calculated using simple collision theory[35] to correspond to a collision diameter of 5.4×10^{-10} m. The collision diameters of C_2H_3 agree well. Thus, the rate constant of 8.4×10^{10} L mol^{-1} s^{-1} for reaction [5-4] is reasonable.

In summary, the contributions of termination reactions by C_2H_3, C_4H_5, and C_6H_7 significantly decreased with an increase in the number of carbon atoms in the radicals. The free radical, C_2H_3, was the main species involved in termination reactions.

6-3-4. Propagation reactions

Table 6-1 shows that species with even numbers of carbon atoms predominated, consistent with the free radical polymerization mechanism proposed by Benson,[4] and the hydrogen-abstraction-C_2H_2-addition mechanism proposed by Frenklach et al.[25] Vinylacetylene, benzene, styrene, and naphthalene were the most abundant. Other products with even numbers of carbon atoms might be formed in chain termination reactions or slow chain propagation reactions.

A series of products with odd numbers of carbon atoms were also observed, including propylene, propyne, several C_5H_6 species, and toluene. They could be formed in reactions involving methyl radicals[3] or propylene, an impurity in acetylene,

$CH_3 + C_2H_2 \rightarrow H_3C\text{-}CH{=}CH(\cdot)$ [CSP3]

$H_3C\text{-}CH{=}CH(\cdot) \rightarrow H_2C(\cdot)\text{-}CH{=}CH_2$ [CSP4]

$H_2C(\cdot)\text{-}CH{=}CH_2 + C_2H_2 \rightarrow HC(\cdot){=}CH\text{-}H_2C\text{-}CH{=}CH_2$ [CSP5]

$HC(\cdot){=}CH\text{-}H_2C\text{-}CH{=}CH_2 \rightarrow C_5H_6$ (cyclopentadiene etc.) + H [CSP6]

$HC(\cdot){=}CH\text{-}H_2C\text{-}CH{=}CH_2 + C_2H_2 \rightarrow HC(\cdot){=}CH\text{-}HC{=}CH\text{-}H_2C\text{-}CH{=}CH_2$ [6-4]

$HC(\cdot){=}CH\text{-}HC{=}CH\text{-}H_2C\text{-}CH{=}CH_2 \rightarrow C_7H_8$(toluene) +H [6-5]

Structures for unknown C_5H_6 species could be $HC{\equiv}C\text{-}HC{=}CH\text{-}CH_3$, and $H_2C{=}CH\text{-}C{\equiv}C\text{-}CH_3$. Propylene could be formed in hydrogen abstraction reactions of C_3H_5 with impurities in acetylene such as acetone, etc.

The order higher than two for 1,3-butadiene may indicate that it was formed by different pathways with different orders. Ethylene and cyclopentadiene may also have multiple sources.

In the present work, addition reactions would dominate in the propagation steps because a C-C π bond is 262 kJ mol^{-1} weaker than a C-H single bond in acetylene.[36] The strong C-H bonds make any hydrogen abstraction reactions difficult. A series of addition reactions (see section 1-5-7) can be proposed as,

$H + C_2H_2 \rightarrow C_2H_3$ [B3]

$C_2H_3 + C_2H_2 \rightarrow C_4H_5$ [B4a]

$C_4H_5 + C_2H_2 \rightarrow C_6H_7$ [B5a]

$C_6H_7 + C_2H_2 \rightarrow C_8H_9$ [B6a]

Benson[4] suggested that there was a series of equilibria between small radicals and large radicals. The equilibrium constant for reaction [B4a] should be similar to that for reaction [6-6], in which a terminal, vinylic C-H bond is added to both sides of equation [B4a],

$C_2H_4 + C_2H_2 \rightarrow C_4H_6$ [6-6]

The equilibrium constant for reaction [6-6] was calculated to be 363 atm^{-1} at 900 K using thermochemistry.[37] The ratio of the concentrations of ethylene and 1,3-butadiene, $[C_2H_4]/[C_4H_6]$, would be 0.00519 at 403 Torr of acetylene. This suggests that the concentrations of radicals would increase with an increase in the number of carbon atoms. Based on this proposal, the main products in the present work should be polymers instead of vinylacetylene. This is contrary to the observations in the present work. Therefore, equilibra did not exist between small and large radicals.

Vinylacetylene, benzene, and styrene might be formed by the decomposition of free radicals, as follows,

$$H_2C{=}CH{-}CH{=}\dot{C}H \longrightarrow H_2C{=}CH{-}C{\equiv}CH \text{ (VA)} + H \qquad \text{[B4b]}$$

$$H_2C{=}CH{-}CH{=}CH{-}CH{=}\dot{C}H \longrightarrow H_2C{=}CH{-}CH{=}CH{-}C{\equiv}CH \text{ (etc.)} + H \qquad \text{[B5b]}$$

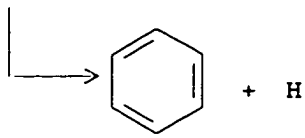

+ H [B5c]

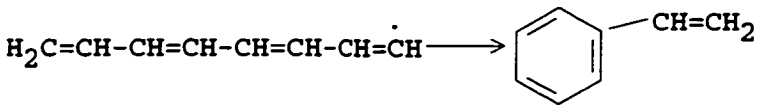

[B6b]

Reactions [B4b]-[B6b] must have been significantly faster than the reverses of reactions [B4a]-[B6a], respectively, so there were not equilibria in reactions [B4a]-[B6a]. Otherwise, the radical concentrations would increase from C_2H_3 to C_4H_5, and to C_6H_7, which would result in more styrene than benzene, and more benzene than vinylacetylene. This is contrary to the observations in the present work.

The reaction between C_2H_3 and C_2H_2 was studied theoretically by Miller et al.[38] using density functional theory (DFT) and RRKM theory. Their results showed that vinylacetylene could be formed mainly by the decomposition of an intermediate, n-C_4H_5. Also, it was found that n-C_4H_5 was about 160 kJ mol^{-1} lower in enthalpy than C_2H_3 + C_2H_2. This indicates that deactivated n-C_4H_5 species could be available to react with acetylene to form benzene at low temperatures, consistent with the observed lower activation energy for the formation of benzene than vinylacetylene.

Benson said[4] that benzene could be formed by the cyclisation of a cis-C_6H_7 radical, and that trans-C_6H_7 radicals could form linear C_6H_6 species or continue to add to acetylene to form larger radicals. However, the rate of formation of benzene was observed to be more than ten times greater than the sum of rates of formation of other C_6H_6 species and styrene in primary reactions at 970 K and 203 Torr. This indicates that most trans-C_6H_7 radicals were likely converted to cis-C_6H_7 to form benzene at high temperatures.

It is very interesting that four different C_6H_6 products were observed. They could be formed in different dissociation reactions of C_6 radicals or larger radicals. One of these reactions is the cyclization of C_6H_7 radicals to generate benzene according to Benson's mechanism (reaction [B5c]).[4]

Possible structures for three C_6H_6 species other than benzene could be fulvene, $H_2C{=}CH\text{-}C{\equiv}C\text{-}CH{=}CH_2$, and Z and E types of $HC{\equiv}C\text{-}HC{=}CH\text{-}CH{=}CH_2$. The structure, $H_2C{=}CH\text{-}C{\equiv}C\text{-}CH{=}CH_2$, could be formed by a 1,4-hydrogen shift in the radical, $H_2C{=}CH\text{-}CH{=}CH\text{-}CH{=}HC(\cdot)$, formed in step [B5a],

$$H_2C{=}CH\text{-}CH{=}CH\text{-}CH{=}CH(\cdot) \rightarrow H_2C{=}CH\text{-}(\cdot)C{=}CH\text{-}CH{=}CH_2$$

$$\rightarrow H_2C{=}CH\text{-}C{\equiv}C\text{-}CH{=}CH_2 + H \qquad [6\text{-}7]$$

Fulvene could be formed by a cyclization of the same radical, $H_2C{=}CH\text{-}CH{=}CH\text{-}CH{=}HC(\cdot)$,

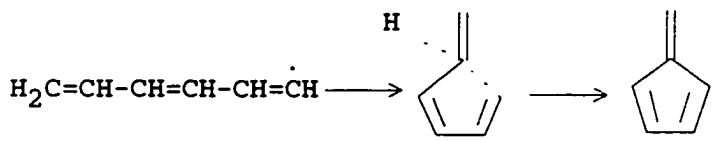

[6-8]

Z and E types of $HC{\equiv}C\text{-}HC{=}CH\text{-}CH{=}CH_2$ could be readily produced by the rupture of a secondary C-H bond in $H_2C{=}CH\text{-}CH{=}CH\text{-}CH{=}HC(\cdot)$, as shown by reaction [B5b].

The order of the initiation reaction was shown to be two in section 4-2-2. The discussion in section 6-3-3 suggested that the main termination reactions should be the recombination and disproportionation of two vinyl radicals. Therefore, the order for the concentration of C_2H_3 radicals would be unity according to equation (E6-4),

$$[C_2H_3] = (k_i/k_t)^{1/2}[C_2H_2] \qquad \text{(E6-4)}$$

An expression, (E6-6), for the concentration of C_4H_5 radicals could be derived by applying the steady-state assumption for C_4H_5 radicals, involved in reactions [B4a], [B4b], and [B5a],

$$k_{B4b}[C_4H_5] + k_{B5a}[C_2H_2]\,[C_4H_5] = k_{B4a}[C_2H_3][C_2H_2] \qquad \text{(E6-5)}$$

That is,

$$[C_4H_5] = k_{B4a}[C_2H_3][C_2H_2]/(k_{B4b} + k_{B5a}[C_2H_2]) \qquad \text{(E6-6)}$$

The order for the concentration of C_4H_5 would have a value between unity and two depending on the ratio of the two terms in the denominator of equation (E6-6). The order would be two if reaction [B4b] was significantly faster than reaction [B5a]. The ratio of k_{B4b} and $k_{B5a}[C_2H_2]$ could be calculated to be 1.6 at 970 K and 403 Torr, using rate constants in the literature.[3,29] The order for vinylacetylene, which was suggested to be formed from the decomposition of C_4H_5 (reaction [B4b]), would have a value between unity and two, consistent with the measured value, 1.8±0.1. Similarly, an expression for the concentration of C_6H_7 radicals could be derived by applying the steady-state assumption for C_6H_7 radicals,

$$[C_6H_7] = k_{B5a}[C_4H_5][C_2H_2]/(k_{B5b+B5c} + k_{B6a}[C_2H_2]) \qquad \text{(E6-7)}$$

Thus, the order for the concentration of C_6H_7 would have a value between 1.8 and 2.8 depending on the relative magnitudes of $k_{B5b+B5c}$ and $k_{B6a}[C_2H_2]$. The order for benzene, which was suggested to be formed from the decomposition of C_6H_7 (reaction [B5c]), would have a value between 1.8 and 2.8, agreeing with the measured order of 2.4±0.1. It could be shown in the same way that the order for C_8H_9 would have a value between 2.4 and 3.4. Therefore, the decomposition of a large free radical, such as C_8H_9, by rupture of

C-C bonds, to form vinylacetylene and a C_4H_5 radical or benzene and a C_2H_3 radical, should not be important, because this reaction would lead to an order between 2.4 and 3.4, contrary to the orders of formation of vinylacetylene and benzene.[8]

If the main termination reaction were assumed to be the recombination of two C_4H_5 radicals (reaction [6-12]), the concentration of C_4H_5 could be derived by applying the steady-state assumption,

$$[C_4H_5] = (k_i/k_t)^{1/2}[C_2H_2] \qquad \text{(E6-8)}$$

Thus, the order of C_4H_5 radicals would be unity. The order for the formation of vinylacetylene, formed from the decomposition of C_4H_5 (reaction [B4b]), would be unity as well. The order for the concentration of C_6H_7 would have a value between unity and two, depending on the relative magnitudes of k_{B5b} and $k_{B6a}[C_2H_2]$ in equation (E6-7). The order for benzene, which was suggested to be formed from the decomposition of C_6H_7 (reaction [B5b]), would have a value between unity and two, which is contrary to the observations in the present work. Therefore, the main termination reactions must be the recombination and disproportionation of two C_2H_3 radicals. C_4H_5 radicals might be involved in minor termination reactions.

According to the propagation reactions proposed in this section, reaction [B4a] is a prerequisite for the formation of C_4H_4, C_6H_6, and C_8H_8, etc. That is,

$$R_{B4a} = R_{C4H4} + R_{C6H6} + R_{C8H8} + \cdots\cdots \qquad \text{(E6-9)}$$

Here, R_{B4a} is the rate of reaction [B4a]; R_{C4H4}, R_{C6H6} and R_{C8H8} are the rates of formation of C_4H_4, C_6H_6, and C_8H_8, respectively. The rates of formation of vinylacetylene and benzene, two main products, were measured in Chapter 4 at 934-938 K and pressures

between 27 and 126 Torr. The order for $R_{C4H4} + R_{C6H6}$ was determined to be 1.89±0.06, which is very close to two. This indicates that the order for C_2H_3 radicals was unity. Therefore, C_2H_3 was the main termination species.

The rate constant for reaction [B4a] could be estimated using equation (E6-10),

$$k_{B4a} = (R_{C4H4} + R_{C6H6})/([C_2H_3][C_2H_2]) \quad \text{(E6-10)}$$

Using the values of R_{C4H4} and R_{C6H6}, listed in Table 4-1, and $[C_2H_3]$, calculated using the rate constants for the initiation reaction and for the termination reactions, determined in Chapter 5, k_{B4a} could be calculated using equation (E6-10). The results are listed in Table 6-5. Using the data in Table 6-5, an expression of k_{B4a} could be determined to be,

$$k_{B4a} = 10^{9.0\pm0.4} L\ mol^{-1}\ s^{-1} exp[(-27\pm7) kJ\ mol^{-1}/RT] \quad \text{(E6-11)}$$

which agrees very well with an expression, (E5-10), determined in section 5-3-5,

$$k_{VA}^{prop} = 10^{9.2\pm0.7} L\ mol^{-1}\ s^{-1} exp[(-32\pm12) kJ\ mol^{-1}/RT] \quad \text{(E5-10)}$$

This indicates that most C_4H_5 decomposed to form vinylacetylene, and that only a small portion added to acetylene to produce benzene. A value of 5.4×10^6 L mol^{-1} s^{-1} was reported at 910 K by DAC using a simulation.[39] Using equation (E6-11), a value of 2.8×10^7 L mol^{-1} s^{-1} could be calculated at 910 K.

The C_4H_3 radical formed in the initiation reaction [B1] could decompose as described by reaction [MB4].

$$C_4H_3 \rightarrow C_4H_2 \text{ (diacetylene)} + H \quad \text{[MB4]}$$

Table 6-5. The rate constants of reaction [B4a], k_{B4a}.

T (K)	P (Torr)	reactor id (mm)	$[C_2H_2] \times 10^4$ (mol L^{-1} s^{-1})	$[C_2H_3] \times 10^{11}$ (mol L^{-1} s^{-1})	$(R_{VA}+R_B) \times 10^6$ (mol L^{-1} s^{-1})	$k_{B4a} \times 10^{-7}$ (L mol^{-1} s^{-1})
970	52	1.96	8.60	23.57	7.57	3.74
970	35	0.969	5.79	15.87	3.41	3.71
938	126	0.969	21.55	35.78	26.00	3.37
936	69	1.96	11.83	19.01	7.53	3.35
934	52	3.96	8.93	13.90	4.76	3.83
934	34	3.96	5.84	9.09	2.31	4.36
935	27	3.96	4.63	7.33	1.32	3.88
895	60	3.96	10.76	8.61	2.96	3.20
854	120	3.96	22.55	8.40	4.49	2.37

Diacetylene was observed as product 14 in Table 6-1. As seen in Table 6-4, the rates of formation of C_4H_2 were lower than the rates of the initiation reaction, indicating that part of the C_4H_3 was involved in other reactions besides reaction [MB4]. A possible sink for C_4H_3 could be hydrogen abstraction from impurities to form vinylacetylene and a radical addition to acetylene,

$$C_4H_3 + C_2H_2 \rightarrow C_6H_5 \qquad [6\text{-}9]$$

Other products (except naphthalene) with fewer atoms of hydrogen than of carbon were not observed in the present work, indicating C_4H_3 was not a main chain transfer radical.

The C_{10} products (including naphthalene) were all secondary products, and could have been formed from the hydrogen-abstraction-C_2H_2-addition (HACA) processes proposed by Frenklach et al.[25]

The mechanism proposed here can be used to explain the observation of induction periods for vinylacetylene and for benzene, and the formation of all the primary or partially primary products except the C_5H_6 products.

6-3-5. Reactions involving impurities

The rate constant for termination step [5-5] is expected to be slower than that for step [5-4],[3,33,40] but the yield of ethylene was significantly higher than that of 1,3-butadiene. This indicates that there are other pathways for the formation of ethylene. It could be formed from hydrogen transfer reactions between a vinyl radical and an impurity like

acetone, propylene or propyne. The hydrogen transfer reaction between a vinyl radical and a neopentane molecule could be used to explain the high acceleration factor for ethylene. These will be estimated as follows.

The pyrolysis of purified acetylene at 971 K and 104 Torr will be discussed first. As mentioned in Chapter 2, the concentrations of impurities in purified acetylene were 120 ppm for acetone, 270 ppm for ethane, 250 ppm for propane, and 80 ppm for propylene. The concentration of vinyl radicals could be calculated to be 5.01×10^{-10} mol L^{-1} using the rate constants of the initiation reaction and the termination reaction, determined in Chapter 5. Then, the rates of formation of ethylene formed in reactions [6-10]-[6-14] could be estimated,

$CH_3COCH_3 + C_2H_3 \rightarrow CH_2COCH_3 + C_2H_4$ [6-10]

$C_2H_6 + C_2H_3 \rightarrow C_2H_5 + C_2H_4$ [6-11]

$C_3H_8 + C_2H_3 \rightarrow C_3H_7 + C_2H_4$ [6-12]

$CH_3CH{=}CH_2 + C_2H_3 \rightarrow CH_2CHCH_2 + C_2H_4$ [6-13]

$C_2H_2 + C_2H_3 \rightarrow C_2H + C_2H_4$ [6-14]

The rate of reaction [6-10] was estimated to be 5.8×10^{-9} mol L^{-1} s^{-1}, using the rate constant for reaction [6-15],[41]

$CH_3COCH_3 + CH_3 \rightarrow CH_2COCH_3 + CH_4$ [6-15]

and assuming that the activation energy for reaction [6-10] was 13.3 kJ mol^{-1} lower than that for reaction [6-15], because the change of enthalpy for reaction [6-10] is 26.6 kJ mol^{-1} more exothermic than that for reaction [6-15].[42] The rate of reaction [6-11] was

estimated to be 8.7×10^{-9} mol L^{-1} s^{-1} using the rate constant for reaction [6-16] reported by Pacey and Purnell,[43]

$$C_2H_6 + CH_3 \rightarrow C_2H_5 + CH_4 \qquad [6\text{-}16]$$

and assuming that the activation energy for reaction [6-11] was 13.3 kJ mol^{-1} lower than that for reaction [6-16], because the change of enthalpy for reaction [6-11] is 26.6 kJ mol^{-1} more exothermic than that for reaction [6-16]. The rate of reaction [6-12] was calculated to be 4.1×10^{-9} mol L^{-1} s^{-1} using the rate constant estimated by Tsang.[44] The rate of reaction [6-13] was calculated to be 3.8×10^{-10} mol L^{-1} s^{-1} using the rate constant reported by Tsang.[45] The rate of reaction [6-14] was calculated to be 8.1×10^{-9} mol L^{-1} s^{-1}, using the rate constant estimated for reaction [6-11] and assuming that the activation energy for reaction [6-14] was 66.9 kJ mol^{-1} higher than that for reaction [6-11], because the change of enthalpy for reaction [6-14] is 133.8 kJ mol^{-1} more endothermic than that for reaction [6-11]. The sum of the above rates could be calculated to be 2.7×10^{-8} mol L^{-1} s^{-1}, which is lower than the observed rate of formation for ethylene, 7.03×10^{-8} mol L^{-1} s^{-1}. The difference could be caused by the estimation of the rate constants for reactions [6-10]-[6-14].

The concentrations of C_4H_5 and C_6H_7 radicals could be estimated to be 4.2×10^{-11} mol L^{-1} s^{-1} and 2.7×10^{-12} mol L^{-1} s^{-1}, using the ratios of concentrations for C_2H_3, C_4H_5, and C_6H_7 radicals, 187:15.8:1, mentioned in section 6-3-3. No rate constants are available in the literature for reactions between C_4H_5 and impurities, and reactions between C_6H_7 and impurities. Assuming that these rate constants are similar to those in reactions [6-10]-[6-14], the total rate would be 1.6×10^{-9} mol L^{-1} s^{-1} for all the reactions between C_4H_5 and

impurities, and 1.5×10^{-10} mol L^{-1} s^{-1} for all the reactions between C_6H_7 and impurities. The former rate is an order of magnitude lower than the observed rate for the formation of 1,3-butadiene, 1.36×10^{-8} mol L^{-1} s^{-1}. The rate of 1.5×10^{-10} mol L^{-1} s^{-1} is two orders of magnitude lower than the observed rate for the formation of 1,4-cyclohexadiene, 82×10^{-10} mol L^{-1} s^{-1}. Therefore, the main sources for the formation of 1,3-butadiene and 1,4-cyclohexadiene were the termination reactions between two vinyl radicals, and terminations between a vinyl radical and a C_4H_5 radical, respectively, instead of the reactions between C_4H_5 or C_6H_7 radicals and impurities.

A similar calculation could be applied to the case of the pyrolysis of acetylene doped with 0.38% neopentane at 971 K and 104 Torr. The concentration of C_2H_3 radicals could be calculated to be 1.6×10^{-9} mol L^{-1} using the rate constants of the initiations by acetylene, determined in Chapter 5, and by neopentane,[46] and the rate constant of 11×10^{10} L mol^{-1} s^{-1}, determined in Chapter 5 for termination reactions. The rate of reaction [6-17],

$$C_5H_{12} + C_2H_3 \rightarrow C_5H_{11} + C_2H_4 \qquad [6\text{-}17]$$

could be estimated to be 7.8×10^{-8} mol L^{-1} s^{-1} using the rate constant[47] reported for reaction [6-18],

$$\text{iso-}C_4H_{10} + C_2H_3 \rightarrow \text{iso-}C_4H_9 + C_2H_4 \qquad [6\text{-}18]$$

The rates of reactions [6-10]-[6-14] were calculated to be 1.8×10^{-8} mol L^{-1} s^{-1}, 2.8×10^{-8} mol L^{-1} s^{-1}, 1.3×10^{-8} mol L^{-1} s^{-1}, 1.2×10^{-9} mol L^{-1} s^{-1}, and 2.6×10^{-8} mol L^{-1} s^{-1}, respectively, using the methods described above for the pyrolysis of purified acetylene. The total rate for the reactions between vinyl radicals and impurities could be calculated

to be 1.6×10^{-7} mol L^{-1} s^{-1}. Therefore, about 49% of the ethylene was formed from reaction [6-17]. The acceleration factor, Q, could be calculated to be 5.9 for ethylene, which is close to the observed value, 6.3.

On the other hand, assuming that the reactions between C_2H_3 and impurities were accelerated by neopentane by a factor the same as the average value of the acceleration factors for the formation of vinylacetylene and benzene, and that the extra C_2H_4 was formed from reaction [6-17], the rate constant for reaction [6-17] could be estimated to be 3.5×10^7 L mol^{-1} s^{-1} at 970 K and 104 Torr.

The high acceleration factor of 16.3 for the formation of cyclopentadiene, accelerated by 0.38% neopentane, indicates that almost the entire cyclopentadiene was formed from reactions involving neopentane, [CSP3]-[CSP6]. Thus, the rate of initiation by neopentane can be compared to the rate of the formation of cyclopentadiene. Using equation (E5-6), a value of 2.3×10^{-7} L mol^{-1} s^{-1}could be calculated for the rate of initiation by 0.38% neopentane in acetylene at 971 K and 104 Torr. This is somewhat slower than the rate of the formation of cyclopentadiene at this condition, $(8.0 \pm 0.7) \times 10^{-7}$ L mol^{-1} s^{-1}.

6-4. Conclusion

More than twenty-four minor products were observed. Of these products, fifteen species were found to be primary or partially primary products. Orders and Arrhenius

parameters of twelve partially primary products were measured. Equilibria between small radicals and large radicals, suggested by Benson,[4] were found not to exist in the present work. Concentrations of free radicals decreased with an increase of the number of carbon atoms in the radicals. 1,3-butadiene was found to be a product formed from a main chain termination reaction. Two C_6H_8 and three C_8H_{10} products were suggested to be minor products formed from minor termination reactions. A mechanism was proposed to interpret the formation of all the primary and partially primary products.

References for Chapter 6

1. M.H.Back, *Can.J.Chem.*, 1971, **49**, 2199.
2. T.Tanzawa and W.C.Gardiner Jr., *J.Phys.Chem.*, 1980, **84**, 236.
3. M.B.Colket III, D.J.Seery, and H.B.Palmer, *Combustion and Flame*, 1989, **75**, 343.
4. S.W.Benson, *Int.J.Chem.Kinet.*, 1992, **24**, 217.
5. R.P.Duran, V.T.Amorebieta, and A.J.Colussi, *J.Phys.Chem.*, 1988, **92**, 636.
6. J.H.Kiefer and W.A.Von Drasek, *Int.J.Chem.Kinet.*, 1990, **22**, 747.
7. J.H.Kiefer, *Int.J.Chem.Kinet.*, 1993, **25**, 215.
8. X.Xu and P.D.Pacey, *Phys.Chem.Chem.Phys.*, 2001, **3**, 2836.
9. R.N.Pease, *J.Am.Chem.Soc.*, 1929, **51**, 3470.
10. H.A.Taylor and A.von Hook, *J.Phys.Chem.*, 1935, **39**, 811.
11. H.D.Burnham and R.N.Pease, *J.Am.Chem.Soc.*, 1942, **64**, 1404.
12. D.A.Frank-Kamenetzky, *Acta Physicochim.U.R.S.S.*, 1943, **18**, 148.
13. C.G.Silcocks, *Proc.Roy.Soc.(London)*, 1957, **A242**, 411.
14. G.J.Minkoff, D.M.Newitt, and P.Rutledge, *J.Appl.Chem.*, 1957, **7**, 406.
15. G.J.Minkoff, *Can.J.Chem.*, 1958, **36**, 131.
16. C.F.Cullis, G.J.Minkoff, and M.A.Nettleton, *Trans.Faraday Soc.*, 1962, **58**, 1117.
17. F.G.Stehling, J.D.Frazee, and R.C.Anderson, *8th Symp.(Int.) on Combust., Williams and Wilkins, Baltimore*, 1962, p. 774.
18. M.S.B.Munson and R.C.Anderson, *J.Phys.Chem.*, 1963, **67**, 1582.
19. M.S.B.Munson and R.C.Anderson, *Carbon*, 1963, **1**, 51.
20. K.C.Hou and R.C.Anderson, *J.Phys.Chem.*, 1963, **67**, 1579.
21. H.B.Palmer and F.L.Dormish, *J.Phys.Chem.*, 1964, **68**, 1553.
22. C.F.Cullis and N.H.Franklin, *Roy.Soc.(London)*, 1964, **A280**, 139.

23. R.P.Duran, V.T.Amorebieta, and A.J.Colussi, *J.Am.Chem.Soc.*, 1987, **109**, 3154.

24. X.Xu and P.D.Pacey, *Carbon*, 2001, **39**, 1839.

25. M.Frenklach, D.W.Clary, W.C.Gardiner Jr., and S.E.Stein, *Twenty-First Symposium (International) on Combustion, The Combustion Institute*, 1986, 1067.

26. S.T.Dimitrijevic, S.Paterson, and P.D.Pacey, *J.Anal.& Appl.Pyrolysis*, 2000, **53**, 107.

27. A.Becker and K.J.Huttinger, *Carbon*, 1998, **36**, 177.

28. V.D.Knyazev, S.I.Stollarov, and I.R.Slagle, *Symp.Int.Combust.Proc.*, 1996, **26**, 513.

29. P.R.Westmoreland, A.M.Dean, J.B.Howard, and J.P.Longwell, *J.Phys.Chem.*, 1989, **93**, 8171.

30. R.P.Thorn, W.A.Payne, L.J.Stief, and D.C.Tardy, *J.Phys.Chem.*, 1996, **100**, 13594.

31. G.M.Come, J.F.Large, and J.A.Rondeau, *J.Chim.Phys.*, 1974, **71**, 1516.

32. A.Fahr, W.Braun, and A.H.Laufer, *J.Phys.Chem.*, 1993, **97**, 1502.

33. A.Fahr, A.Laufer, R.Klein, and W.Braun, *J.Phys.Chem.*, 1991, **95**, 3218.

34. J.O.Hirschfelder, C.F.Curtiss, and R.B.Bird, *Molecular Theory of Gases and Liquids, 2nd Edition, New York, John Wiley and Sons, Inc.*, 1964, p. 14, p. 1112.

35. P.D.Pacey, *J.Phys.Chem.*, 1998, **102**, 8541.

36. D.R.Lide, *Handbook of Chemistry and Physics, 81th Ed., CRC Press*, 2001, p. 5-1, p. 5-29, p. 5-32.

37. Thermodynamics Research Center and Texas A & M University, *API 44 Tables, Selected Values of Properties of Hydrocarbons and Related Compounds, American Petroleum Institute*, 1985, **6**, Tables 24x, 25x, 23-2-(5.2202)-x.

38. J.A.Miller, S.J.Klippenstein, and S.H.Robertson, *J.Phys.Chem.A*, 2000, **104**, 7525.

39. R.P.Duran, V.T.Amorebieta, and A.J.Colussi, *Int.J.Chem.Kinet.*, 1989, **21**, 947.

40. W.Tsang and R.F.Hampson, *J.Phys.Chem.Ref.Data*, 1986, **15**, 1087.

41. S.H.Mousavipour, *PhD Thesis, Dalhousie University*, 1996, 100.

42. K.J.Laidler, *Chemical Kinetics, 3rd Edition, New York, Harper & Row, Inc.*, 1987, p.70.

43. P.D.Pacey and J.H.Purnell, *J.Chem.Soc.Faraday Trans.I*, 1972, **68**, 1462.

44. W.Tsang, *J.Phys.Chem.Ref.Data*, 1988, **17**.

45. W.Tsang, *J.Phys.Chem.Ref.Data*, 1991, **20**, 221.

46. P.D.Pacey, *Can.J.Chem.*, 1973, **51**, 2415.

47. W.Tsang, *J.Phys.Chem.Ref.Data*, 1990, **19**, 1.

CHAPTER 7. SUMMARY AND FUTURE WORK

Acetylene is one of the smallest, simplest organic molecules. However, the pyrolysis of acetylene at high temperatures is so complicated that the mechanism was still not clear, although research had been carried out for more than seventy years by many workers using various techniques. The main reasons for the lack of clarity were (a) that early experiments were performed at high conversions, where secondary and tertiary reactions were involved, and (b) that techniques such as capillary GC and GC-MS were not efficiently employed in the research. Both free radical mechanisms and molecular mechanisms involving vinylidene were proposed by various workers, mainly based on limited experimental results and on theoretical calculations. More experiments needed to be carried out to distinguish between these mechanisms.

The present work was conducted at low conversions using a series of micro-reactors. The products were carefully analyzed using packed-column GC, capillary GC and GC-MS. The residence times of acetylene in the reactor, the pressures of acetylene and the temperatures were carefully varied to probe the reaction. Surface reactions were thoroughly studied, and were significantly minimized by treating surfaces of reactors with HF solution and by burning carbon formed in the reactor between the collection of samples. Small amounts of neopentane were added to acetylene to study the acceleration. New evidence has been obtained regarding the mechanism of the pyrolysis of acetylene and regarding the formation of carbon nanotubes. Our results will be summarized in this

chapter. Questions described in the first chapter will be addressed. Future work will be proposed.

7-1. Observed products

The main products were observed to be vinylacetylene and benzene, a finding which agrees with previous work. However, benzene was clearly shown to be a primary product instead of a secondary product, as erroneously reported by some workers. In addition, more than twenty minor products were observed using GC-MS. Of these products, fifteen were observed to be primary or partially primary products. A series of products, including 1,3-butadiene, C_6H_8 and C_8H_{10} species, were suggested to be formed mainly by termination reactions. Methane was not observed in the present work.

7-2. Evidence for radicals

The main evidence to support the involvement of free radicals in the reaction below 1500 K was previously reported to be the inhibition of the reaction by nitric oxide (NO). However, Kiefer et al.[1] argued that NO might inhibit the reaction through a molecular pathway. Our work[2,3] provided new evidence to support the involvement of free radicals. An induction period in the formation of vinylacetylene and benzene, resulting from the buildup of free radicals to their steady-state concentrations, was observed for the first time in the present work. This is crucial evidence supporting the involvement of a series

of free radicals in the pyrolysis of acetylene. Small amounts of neopentane were observed to accelerate significantly the formation of vinylacetylene and benzene, by similar acceleration factors, in wide ranges of temperature and acetylene pressure. This indicates that free radicals played a crucial role in the formation of the main products. The similar inhibition factors for vinylacetylene and benzene by surface reactions also suggested the free-radical nature of the reaction.

7-3. Dependence on the reaction time, pressure and temperature

An acceleration of the decomposition of acetylene was observed at high conversions by early workers. A true induction period was observed for the first time in the present work.

For the first time, the orders and Arrhenius parameters for the formation of vinylacetylene and benzene were measured without significant effects from surface reactions. The orders were measured to be 1.8±0.1 for the formation of vinylacetylene, and 2.4±0.1 for benzene. This suggests that C_2H_3 was the main radical involved in the termination reactions, as discussed in section 6-3-4.

7-4. Surface reactions

Upon increasing the surface-to-volume ratio, different effects, including inhibition, no effect, and even acceleration, had been reported in the literature. The present work showed that carbon could be formed on the surface of a reactor and could inhibit the

formation of vinylacetylene and benzene by introducing new termination reactions. Carbon could be readily formed at high temperatures, high acetylene pressures and at large surface-to-volume ratios.

In addition, the main form of carbon generated in our system was observed to be carbon nanotubes. The real-time monitoring of the yield of carbon nanotubes using a unique laser system allowed us to study the kinetic characteristics of the formation of carbon nanotubes. Acetylene and free radicals formed directly from acetylene were shown for the first time to be the main precursors of nanotubes. A new process, involving free radicals, for the formation of carbon nanotubes was discovered, and was interpreted using a mechanism similar to Frenklach's hydrogen-abstraction-acetylene-addition (HACA) mechanism.[4,5]

7-5. Mechanisms proposed by previous workers

Minkoff's molecular polymerization mechanism[6] involving diradicals was too simple to interpret the formation of various products. The lifetime of the diradicals was too short to result in the induction period observed in the present work, as discussed in Chapter 4.

Back's free radical chain mechanism,[7] initiated by a bimolecular disproportion reaction between two acetylene molecules, includes some reasonable propagation reactions, but the activation energy for this initiation reaction was too high compared to that observed in our work.

A mechanism dominated by C_4H_3 and H was proposed by Tanzawa and Gardiner.[8] This mechanism assumed that the free radical chain reaction was propagated by H, C_4H_3, C_2H, C_4H, C_6H and C_8H, etc.. This is contrary to our observations. Their mechanism may be applied to the reaction above 1500 K, but it should not be used to model the reaction below 1500 K.

Molecular mechanisms involving vinylidene, proposed by Duran et al. (DAC),[9] and Kiefer et al.,[10] were shown in Chapter 4 not to play important roles in the present work, because the lifetimes of vinylidene and diradicals were too short to account for the induction periods observed in our work.

Colket et al.[11] suggested that trace amounts of acetone in purified acetylene were sufficient to generate enough methyl radicals for the initiation reaction. Our calculations showed that acetone could not significantly accelerate the reaction when its concentration was less than 200 ppm, which should be true for the purified acetylene used in previous work.

Benson's radical polymerization mechanism,[12] based on thermochemistry, was supported by our work. The reaction was shown to be propagated by C_2H_3, C_4H_5, C_6H_7 etc., a series of radicals. Benson predicted that there were a series of equilibra between small radicals and larger radicals. However, these equilibra have been shown not to exist in the present work.

7-6. Mechanism proposed in the present work

For the first time, the orders for the initiation reaction and for the main termination reaction were shown to be two. The Arrhenius parameters for the initiation reaction and the rate constant for the main termination reaction were determined experimentally. The order and the rate constant for vinylacetylene formation were measured. For the first time, the order and the rate constant for benzene formation were measured without significant effects from surface reactions.

More than twenty-four minor products were observed. Of these products, fifteen species were found to be primary or partially primary products for the first time. 1,3-butadiene was found to be a product formed from a main chain termination reaction, and from hydrogen-transfer reactions between C_4H_5 radicals and impurities in acetylene. Two C_6H_8 and three C_8H_{10} products were suggested to be minor products formed from minor termination reactions. The orders and the rate constants for the formation of eleven partially primary products were measured for the first time. A complete mechanism will be summarized as follows.

7-6-1. Mechanism of the pyrolysis of pure acetylene

Initiation, propagation, and termination reactions in the pyrolysis of pure acetylene are summarized here.

Initiation reaction:

$C_2H_2 + C_2H_2 \rightarrow C_4H_3 + H$ [B1]

Propagation reactions:

$H + C_2H_2 \rightarrow C_2H_3$ [B3]

$C_2H_3 + C_2H_2 \rightarrow C_4H_5$ [B4a]

$C_2H_2 + C_2H_3 \rightarrow C_2H + C_2H_4$ [6-14]

$H_2C{=}CH{-}CH{=}\dot{C}H \longrightarrow H_2C{=}CH{-}C{\equiv}CH$ (VA) + H [B4b]

$C_4H_5 + C_2H_2 \rightarrow C_6H_7$ [B5a]

$H_2C{=}CH{-}CH{=}CH{-}CH{=}\dot{C}H \longrightarrow H_2C{=}CH{-}CH{=}CH{-}C{\equiv}CH$ (etc.) + H [B5b]

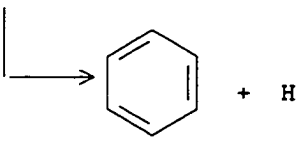

[B5c]

$H_2C{=}CH{-}CH{=}CH{-}CH{=}CH(\cdot) \rightarrow H_2C{=}CH{-}(\cdot)C{=}CH{-}CH{=}CH_2$

$\rightarrow H_2C{=}CH{-}C{\equiv}C{-}CH{=}CH_2 + H$ [6-7]

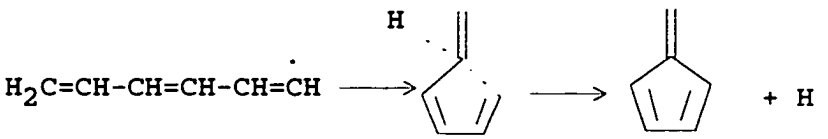

[6-8]

$C_6H_7 + C_2H_2 \rightarrow C_8H_9$ [B6a]

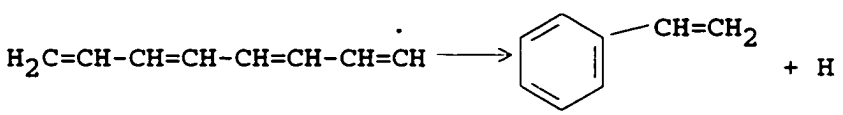

[B6b]

$C_4H_3 \rightarrow C_4H_2$ (diacetylene) + H [MB4]

$C_4H_3 + C_2H_2 \rightarrow C_6H_5$ [6-9]

Termination reactions:

$C_2H_3 + C_2H_3 \rightarrow C_4H_6$(1,3-butadiene) [5-4]

$C_2H_3 + C_2H_3 \rightarrow C_2H_4 + C_2H_2$ [5-5]

$C_4H_5 + C_4H_5 \rightarrow C_8H_{10}$ [5-6]

$C_4H_5 + C_4H_5 \rightarrow C_4H_4 + C_4H_6$ [6-1]

$C_2H_3 + C_4H_5 \rightarrow C_6H_8$ [5-7]

$C_2H_3 + C_4H_5 \rightarrow C_2H_2 + C_4H_6$ [6-2]

$C_2H_3 + C_4H_5 \rightarrow C_2H_4 + C_4H_4$ [6-3]

7-6-2. Reactions with impurities in acetylene

Reactions involving impurities in acetylene are summarized here.

$CH_3 + C_2H_2 \rightarrow H_3C\text{-}CH{=}CH(\cdot)$ [CSP3]

$H_3C\text{-}CH{=}CH(\cdot) \rightarrow H_2C(\cdot)\text{-}CH{=}CH_2$ [CSP4]

$H_2C(\cdot)\text{-}CH{=}CH_2 + C_2H_2 \rightarrow HC(\cdot){=}CH\text{-}H_2C\text{-}CH{=}CH_2$ [CSP5]

$HC(\cdot){=}CH\text{-}H_2C\text{-}CH{=}CH_2 \rightarrow C_5H_6$ (cyclopentadiene etc.) + H [CSP6]

$HC(\cdot){=}CH\text{-}H_2C\text{-}CH{=}CH_2 + C_2H_2 \rightarrow HC(\cdot){=}CH\text{-}HC{=}CH\text{-}H_2C\text{-}CH{=}CH_2$ [6-4]

$HC(\cdot){=}CH\text{-}HC{=}CH\text{-}H_2C\text{-}CH{=}CH_2 \rightarrow C_7H_8$(toluene) +H [6-5]

$CH_3COCH_3 + C_2H_3 \rightarrow CH_2COCH_3 + C_2H_4$ [6-10]

$C_2H_6 + C_2H_3 \rightarrow C_2H_5 + C_2H_4$ [6-11]

$C_3H_8 + C_2H_3 \rightarrow C_3H_7 + C_2H_4$ [6-12]

$CH_3CH{=}CH_2 + C_2H_3 \rightarrow CH_2CHCH_2 + C_2H_4$ [6-13]

7-6-3. Reactions with neopentane

An initiation reaction and a hydrogen-abstraction reaction were discussed in Chapters 5 and 6, respectively.

$C_5H_{12} \rightarrow CH_3 + C_4H_9$ [5-1]

$C_5H_{12} + C_2H_3 \rightarrow C_5H_{11} + C_2H_4$ [6-17]

C_4H_9 and C_5H_{11} could add to acetylene to form larger radicals,

$C_4H_9 + C_2H_2 \rightarrow C_6H_{11}$ [7-1]

$C_5H_{11} + C_2H_2 \rightarrow C_7H_{13}$ [7-2]

Heavy products could be formed in reactions involving the above radicals.

7-6-4. Rate constants determined in the present work

Thirty-three rate constants were measured in the present work. Of these rate constants, twenty-six rate constants were measured experimentally for the first time. Six rate constants were measured experimentally for the first time at temperatures between 854 and 971 K.

$$(k_i k_t)_{VA+B} = 10^{23.1\pm0.43}\, L^2\, mol^{-2}\, s^{-2} exp[\, -(261\pm7) kJ\, mol^{-1}/RT] \quad \text{(E4-5)}$$

$k_{VA} = 10^{9.86\pm0.65}\ L\ mol^{-1}\ s^{-1} exp[\ -(165\pm11) kJ\ mol^{-1}/RT]$ (E4-6)

$k_B = 10^{6.77\pm0.48}\ L^{1.4}\ mol^{-1.4}\ s^{-1}\ exp\ [-(100\pm9) kJ\ mol^{-1}/RT]$ (E4-7)

$c_{VA} = 10^{4.82\pm0.52}\ s^{-1}\ exp\ [-(95.4\pm9.3) kJ\ mol^{-1}/RT]$ (E4-8)

$c_B = -10^{3.56\pm0.78}\ s^{-1}\ exp\ [-(67.0\pm14.1) kJ\ mol^{-1}/RT]$ (E4-9)

$(b/[C_2H_2])_{VA} = 10^{-1.74\pm0.69}\ exp[-(31\pm12) kJ\ mol^{-1}/RT]$ (E4-13)

$(b/[C_2H_2]^{1.4})_B = 10^{-4.82\pm0.52}\ mol^{0.4}\ L^{0.4}\ exp\ [(34\pm10) kJ\ mol^{-1}/RT]$ (E4-14)

$k_{i,C5H12}/k_{i,C2H2} = 10^{7.02\pm0.35}\ mol\ L^{-1}\ exp\ [-(119\pm6)\ kJ\ mol^{-1}/RT]$ (E5-5)

$k_{i,C2H2} = 10^{10.68\pm0.46}\ L\ mol^{-1}\ s^{-1}\ exp(-237\pm9\ kJ\ mol^{-1}/RT)$ (E5-7)

$k_{B4a} = 10^{9.0\pm0.4} L\ mol^{-1}\ s^{-1} exp[(-27\pm7) kJ\ mol^{-1}/RT]$ (E6-11)

$k_{t,VA+B} = (11\pm6) \times 10^{10}\ L\ mol^{-1}\ s^{-1}$ (E7-1)

$k_{VA}^{prop} = 10^{9.2\pm0.7} L\ mol^{-1}\ s^{-1} exp[(-32\pm12) kJ\ mol^{-1}/RT]$ (E5-10)

$k_B^{prop} = (5.7\pm2.1)\times10^6\ L\ mol^{-1}\ s^{-1}$ (E7-2)

$k_{5\text{-}4} = 8.4 \times 10^{10}\ L\ mol^{-1}\ s^{-1}$ (E7-3)

$k_{5\text{-}5} = 2.6 \times 10^{10}\ L\ mol^{-1}\ s^{-1}$ (E7-4)

$k_{B4a} = (3.5\pm0.6) \times 10^7\ L\ mol^{-1}\ s^{-1}$ (E7-5)

$k_{6\text{-}18} = 3.5 \times 10^7\ L\ mol^{-1}\ s^{-1}$ at 970 K (E7-6)

Using $k_i k_t$ determined in Chapter 4, the rate constants of surface termination on various surfaces, k_s, and the probabilities of surface reactions on each collision, γ, could be updated and shown in Table 7-1.

Table 7-1. The estimated rate constants of surface termination on different surfaces at 1018 and 894 K

Treatments of surfaces	T (K)	P (Torr)	id (mm)	t_d (min)	k_s (s^{-1})	$\gamma \times 10^4$
HF	1018	58	1	5	9.1	0.10
Li_3PO_4/K_3PO_4	1018	58	1	5	78	0.88
HNO_3	1018	58	1	5	123	1.4
$LiOH/KOH/H_3BO_3$	1018	58	1	5	550	6.2
Carbon	1018	57	1	110	230	2.6
Carbon	894	31	2	*	19	0.44

The orders, Arrhenius parameters, and acceleration factors (by 0.38% neopentane in acetylene at 970 K and 104 Torr) of vinylacetylene, benzene, and eleven minor products are summarized in Table 7-2.

7-7. Significance of findings in the present work

The present work has successfully distinguished between free radical mechanisms and molecular mechanisms proposed for the pyrolysis of acetylene at temperatures below 1500 K. Many new insights into the mechanism have been achieved. Now we have a better understanding of the process of acetylene pyrolysis. Acetylene has been believed to be a precursor of PAHs and soot in the combustion of gasoline or diesel fuel in an engine, and a precursor to the formation of pyrolytic carbon (coke) in industrial pyrolysis. The findings in the present work will provide crucial information for simulating the formation of PAHs, soot, and coke. Most PAHs are carcinogens. Soot is one of the main pollutants in the atmosphere. Coke, formed on the surface of an industrial reactor, limits the transfer of heat through the wall, and even blocks the reactor. Therefore, the formation of PAHs, soot, and coke could be effectively controlled by choosing optimum reaction conditions or by adding certain chemicals.

7-8. Future work

Several projects should be performed in the future.

Table 7-2. Orders, Arrhenius parameters and acceleration factors, Q, (by 0.38% neopentane at 970 K and 104 Torr) for the formation of some products.

product	order	$\log_{10}A$[a]	E_A (kJ mol^{-1})	Q
ethylene	2.35±0.18	8.7±0.8	176±13	6.3
1,3-butadiene	2.66±0.20	10.7±0.5	210±9	7.4
C_5H_6 (25')	2.46±0.17	10.6±2.5	205±44	16.3
C_5H_6 (27.52')	2.87±0.15	9.56±0.38	189±7	3.3
C_6H_8 (28.06')	2.57±0.23	8.38±2.03	189±35	2.9
C_5H_6 (28.37')	2.64	8.59±0.29	192±5	3.2
C_6H_8 (28.52')	1.40±0.51	6.16±1.99	196±35	6.2
C_4H_2	3.5±1.4	9.40±0.21	169±3	b
C_6H_6 (34')	1.94±0.07	9.7±0.2	207±3	2.8
C_6H_6 (36')	1.94±0.11	11.4±0.8	252±14	3.0
C_6H_6 (48.22')	3.00±0.67	9.52±0.47	170±8	2.8

a. The units for A are liters, moles, and seconds.

b. Peaks were too small to measure reliably.

To minimize the reactions involving impurities, high purity, e.g. 99.6%, acetylene should be used. Acetylene should be purified by repeated distillation at liquid nitrogen temperature, discarding the first and last fractions.

The effects of a possible turbulent flow due to the presence of the semi-circular window, and the possible lack of uniformity within the quartz reactors should be studied.

More minor products should be identified by comparing their mass spectra and retention times with possible candidates. Therefore, more compounds need to be synthesized or purchased. The formation of styrene, C_6H_8 and C_8H_{10} species should be studied using a proper capillary GC column to shorten their retention times. The formation of various products should be simulated using the mechanism established in this work.

In addition, the formation of free radicals should be studied in situ. One possible way to achieve this purpose is to radiate laser light through the two windows of the reactor, and to directly detect free radicals formed in the reactor using resonance absorption spectroscopy. Another method would be to couple a mass spectrometer to the reactor, and to detect radicals using the molecular beam sampling technique.

Theoretical calculations, such as *ab initio* and *RRKM*, should be performed for the reactions [B5b], [B5c], [6-7], [6-9], [B6a], [B6b], [MB4], and [6-14] (*ab initio* only).

References for Chapter 7

1. J.H.Kiefer, *Int.J.Chem.Kinet.*, 1993, **25**, 215.

2. S.T.Dimitrijevic, S.Paterson, and P.D.Pacey, *J.Anal.& Appl.Pyrolysis*, 2000, **53**, 107.

3. X.Xu and P.D.Pacey, *Phys.Chem.Chem.Phys.*, 2001, **3**, 2836.

4. M.Frenklach, D.W.Clary, W.C.Gardiner Jr., and S.E.Stein, *Twentieth Symposium (International) on Combustion, The Combustion Institute, Pittsburgh, PA*, 1985, 887.

5. M.Frenklach, *Twenty-Second Symposium (International) on Combustion, The Combustion Institute, Pittsburgh, PA*, 1988, 1075.

6. G.J.Minkoff, *Can.J.Chem.*, 1958, **36**, 131.

7. M.H.Back, *Can.J.Chem.*, 1971, **49**, 2199.

8. T.Tanzawa and W.C.Gardiner Jr., *J.Phys.Chem.*, 1980, **84**, 236.

9. R.P.Duran, V.T.Amorebieta, and A.J.Colussi, *J.Phys.Chem.*, 1988, **92**, 636.

10. J.H.Kiefer and W.A.Von Drasek, *Int.J.Chem.Kinet.*, 1990, **22**, 747.

11. M.B.Colket III, D.J.Seery, and H.B.Palmer, *Combustion and Flame*, 1989, **75**, 343.

12. S.W.Benson, *Int.J.Chem.Kinet.*, 1992, **24**, 217.

Appendix

Table 8-1. Yields of vinylacetylene (VA) and benzene (B) measured at 895 K and 60 Torr in a 3.96 mm (i.d.) reactor by pyrolysing purified and unpurified acetylene.

acetylene	t (s)	$X_{acetone}$	[VA] × 10^8 (mol L^{-1} s^{-1})	[B] × 10^8 (mol L^{-1} s^{-1})
unpurified	0.063	2.90E-02	24.34	8.36
"	0.063	2.99E-02	26.53	8.81
"	0.063	3.02E-02	25.78	8.46
"	0.063	3.09E-02	28.88	9.05
"	0.115	3.07E-02	51.89	16.33
"	0.115	3.04E-02	52.92	17.40
"	0.228	2.97E-02	102.30	34.50
"	0.228	3.01E-02	102.98	35.14
"	0.458	2.97E-02	174.54	68.82
"	0.458	3.00E-02	169.57	68.93
"	0.916	2.96E-02	262.92	125.12
purified	0.063	8.21E-05	6.14	2.11
"	0.063	5.17E-05	6.61	2.17
"	0.063	4.54E-05	6.74	2.23
"	0.063	2.98E-05	6.40	2.13
"	0.115	6.34E-05	17.08	5.52
"	0.115	5.65E-05	16.19	5.46
"	0.228	8.97E-05	40.04	13.46
"	0.229	5.70E-05	39.95	13.30
"	0.457	1.18E-04	88.70	29.67
"	0.915	1.88E-04	161.02	63.80

Table 8-2. Yields of vinylacetylene (VA) and benzene (B) measured at 935 K and 27 Torr in a 3.96 mm (i.d.) reactor by pyrolysing purified and unpurified acetylene.

acetylene	t (s)	$X_{acetone}$	[VA] × 10^8 (mol L^{-1} s^{-1})	[B] × 10^8 (mol L^{-1} s^{-1})
unpurified	0.027	2.94E-02	5.00	0.85
"	0.027	2.96E-02	6.55	0.99
"	0.027	2.98E-02	6.77	1.01
"	0.027	2.89E-02	7.05	0.98
"	0.049	3.00E-02	15.45	2.17
"	0.049	2.99E-02	15.38	2.16
"	0.098	2.99E-02	30.71	4.83
"	0.098	2.96E-02	32.37	4.91
"	0.098	2.91E-02	31.70	4.87
"	0.195	2.87E-02	60.08	10.62
"	0.390	2.78E-02	93.78	21.79
purified	0.027	1.32E-04	0.74	0.11
"	0.027	7.79E-05	0.69	0.07
"	0.027	5.21E-05	0.59	0.07
"	0.049	1.00E-04	2.08	0.24
"	0.049	8.69E-05	2.07	0.25
"	0.098	1.15E-04	6.57	0.93
"	0.195	1.70E-04	17.83	2.60
"	0.390	2.76E-04	39.51	7.01

Table 8-3. Yields of vinylacetylene (VA) and benzene (B) measured at 935 K and 34 Torr in a 3.96 mm (i.d.) reactor by pyrolysing purified and unpurified acetylene.

acetylene	t (s)	$X_{acetone}$	[VA] × 10^8 (mol L^{-1} s^{-1})	[B] × 10^8 (mol L^{-1} s^{-1})
unpurified	0.036	2.95E-02	22.20	3.21
"	0.036	3.28E-02	20.82	3.21
"	0.036	3.38E-02	22.29	3.24
"	0.045	3.37E-02	32.25	4.73
"	0.065	3.36E-02	46.22	7.23
"	0.064	3.37E-02	45.65	6.91
"	0.129	3.35E-02	81.90	14.84
"	0.258	3.28E-02	131.10	32.19
"	0.514	3.20E-02	190.32	64.19
"	1.027	3.12E-02	252.54	123.61
purified	0.036	8.74E-05	2.86	0.48
"	0.045	8.28E-05	4.83	0.71
"	0.064	8.95E-05	8.35	1.23
"	0.129	1.17E-04	18.68	3.29
"	0.258	1.31E-04	43.90	7.85
"	0.514	1.73E-04	90.93	19.56
"	1.027	2.73E-04	151.56	46.93

Table 8-4. Yields of vinylacetylene (VA) and benzene (B) measured at 934 K and 52 Torr in a 3.96 mm (i.d.) reactor by pyrolysing purified and unpurified acetylene.

acetylene	t (s)	$X_{acetone}$	[VA] × 10^7 (mol L^{-1} s^{-1})	[B] × 10^8 (mol L^{-1} s^{-1})
unpurified	0.053	3.15E-02	7.44	12.88
"	0.053	3.10E-02	7.46	13.53
"	0.095	3.20E-02	12.61	26.81
"	0.095	3.17E-02	12.72	26.65
"	0.191	3.10E-02	20.01	52.32
"	0.191	3.08E-02	20.02	52.20
"	0.191	3.06E-02	20.20	53.51
"	0.380	2.97E-02	28.44	112.36
"	0.380	3.24E-02	31.38	110.66
"	0.762	3.14E-02	43.00	217.78
"	0.762	3.20E-02	42.68	210.26
purified	0.053	8.58E-05	1.34	2.40
"	0.053	9.68E-05	1.41	2.48
"	0.066	7.17E-05	1.86	3.21
"	0.095	8.68E-05	2.85	5.48
"	0.191	1.36E-04	6.67	12.97
"	0.381	1.61E-04	12.87	28.67
"	0.762	1.64E-04	22.34	66.61
"	1.520	3.27E-04	34.65	150.76

Table 8-5. Yields of vinylacetylene (VA) and benzene (B) measured at 935 K and in a 3.96 mm (i.d.) reactor by pyrolysing purified and unpurified acetylene.

acetylene	t (s)	P (Torr)	$X_{acetone}$	[VA] × 10^7 (mol L^{-1} s^{-1})	[B] × 10^8 (mol L^{-1} s^{-1})
unpurified	0.129	34.2	2.99E-02	6.65	12.31
"	0.129	34.2	2.96E-02	6.96	12.95
"	0.129	34.2	2.94E-02	6.98	13.02
"	0.129	34.2	3.04E-02	6.74	12.37
"	0.258	34.2	2.84E-02	11.46	26.18
"	0.258	34.2	2.85E-02	11.68	26.15
"	0.097	51.5	2.82E-02	10.31	23.98
"	0.195	51.6	2.77E-02	17.38	50.47
"	0.054	51.6	2.88E-02	6.09	12.69
"	0.114	109.1	2.86E-02	34.50	144.57
"	0.206	109.0	2.81E-02	50.18	265.59
purified	0.258	34.2	3.62E-04	3.98	6.76
"	0.258	34.2	4.28E-04	4.45	7.43
"	0.258	34.2	2.43E-04	4.15	7.07
"	0.258	34.2	1.21E-04	3.86	6.52
"	0.258	34.2	1.24E-04	3.89	6.56
"	0.516	34.2	3.02E-04	8.03	17.07
"	0.516	34.2	3.33E-04	8.01	17.18
"	0.390	51.6	1.70E-04	11.32	28.85
"	0.778	51.5	2.35E-04	19.77	65.12
"	0.206	109.0	9.99E-05	21.08	83.09
"	0.411	108.9	9.82E-05	37.22	173.72

Table 8-6. Yields of vinylacetylene (VA) and benzene (B) measured at 935 K and in a 3.96 mm (i.d.) reactor by pyrolysing purified and unpurified acetylene.

acetylene	t (s)	P (Torr)	$X_{acetone}$	[VA] × 10^7 (mol L^{-1} s^{-1})	[B] × 10^8 (mol L^{-1} s^{-1})
unpurified	0.205	109.0	3.35E-02	58.31	272.30
"	0.205	109.0	3.43E-02	57.74	256.58
"	0.387	51.6	3.09E-02	28.82	99.67
"	0.387	51.6	3.22E-02	28.40	96.73
"	0.256	34.2	3.24E-02	12.14	25.35
"	0.256	34.2	3.28E-02	12.10	25.31
"	0.407	27.1	8.17E-03	10.97	24.92
"	0.407	27.1	3.16E-02	10.05	22.20
purified	0.205	109.0	1.14E-04	22.10	71.05
"	0.205	109.0	9.36E-05	22.15	70.82
"	0.387	51.6	1.57E-04	11.50	24.12
"	0.387	51.6	1.68E-04	11.46	24.49
"	0.256	34.1	1.53E-04	3.96	5.67
"	0.256	34.1	1.49E-04	3.90	5.51
"	0.407	27.1	1.86E-04	3.84	5.68
"	0.407	27.1	1.90E-04	4.10	6.12

Table 8-7. Yields of vinylacetylene (VA) and benzene (B) measured at 935 K and in a 3.96 mm (i.d.) reactor by pyrolysing purified and unpurified acetylene.

t (s)	P (Torr)	$X_{acetone}$	[VA] × 10^7 (mol L^{-1} s^{-1})	[B] × 10^8 (mol L^{-1} s^{-1})
0.200	27.1	7.34E-05	2.37	3.81
0.199	27.0	7.34E-05	2.23	3.70
0.199	27.0	6.06E-03	6.24	11.01
0.199	27.0	2.40E-02	7.49	14.17
0.251	34.1	8.22E-05	4.69	8.16
0.251	34.0	9.57E-05	4.71	8.11
0.251	34.0	7.48E-03	10.84	23.13
0.251	34.0	7.50E-03	10.97	24.08
0.251	34.0	1.58E-02	12.09	27.48
0.251	34.0	1.63E-02	12.09	27.47
0.251	34.0	3.37E-02	12.81	30.95
0.251	34.0	4.50E-03	8.60	18.23
0.381	51.6	1.25E-04	12.78	33.64
0.380	51.5	1.04E-04	12.78	33.36
0.380	51.5	1.52E-02	27.46	101.63
0.380	51.5	3.22E-02	29.46	123.98
0.804	108.9	8.93E-05	69.10	426.40
0.804	109.0	9.76E-05	70.21	433.21
0.804	109.0	1.52E-02	111.63	868.81
0.804	109.0	2.92E-02	115.27	927.55
0.804	109.0	2.92E-02	122.58	1043.35

Table 8-8. Yields of vinylacetylene (VA) and benzene (B) measured at 937 K and 52 Torr, at a residence time of 0.377 s in a 3.96 mm (i.d.) reactor by pyrolysing purified acetylene and acetylene doped with CCl_4.

acetylene	X_{CCl4}	[VA] × 10^7 (mol L^{-1} s^{-1})	[B] × 10^8 (mol L^{-1} s^{-1})
purified	0	1.39	3.91
purified	0	1.51	4.14
doped	1.39E-03	1.31	3.52
doped	5.58E-03	1.27	3.58

Table 8-9. Yields of vinylacetylene (VA) and benzene (B) measured at 936 K and 52 Torr, at a residence time of 0.389 s in a 3.96 mm (i.d.) reactor by pyrolysing purified acetylene and acetylene doped with propylene.

acetylene	$X_{propylene}$	[VA] × 10^7 (mol L^{-1} s^{-1})	[B] × 10^8 (mol L^{-1} s^{-1})
purified	0	1.37	3.70
purified	0	1.45	3.94
doped	5.86E-03	2.06	6.34
doped	5.86E-03	2.04	6.42
doped	4.40E-03	1.98	6.01
doped	1.47E-03	1.82	5.36
doped	2.93E-03	2.02	6.27
doped	5.86E-03	2.13	6.61

Table 8-10. Yields of vinylacetylene (VA) and benzene (B) measured at 935 K in a 3.96 mm (i.d.) reactor by pyrolysing purified acetylene and acetylene doped with butene-1.

acetylene	t (s)	P (torr)	$X_{butene-1}$	[VA] × 10^7 (mol L^{-1} s^{-1})	[B] × 10^8 (mol L^{-1} s^{-1})
purified	0.390	51.6	0	1.43	3.72
purified	0.390	51.6	0	1.46	3.81
doped	0.390	51.6	5.48E-04	3.10	11.12
doped	0.390	51.6	1.03E-03	3.53	13.80
doped	0.390	51.6	1.91E-03	3.92	16.62
purified	0.823	108.9	0	8.93	57.92
doped	0.823	108.9	7.67E-04	13.72	115.30

Table 8-11. The rates, $c \times 10^8$ mol L^{-1} s^{-2}, of formation of twelve products from secondary reactions obtained by fitting yields of various products to equation (E6-1).

T (K)	971	970	971	970	937	895	854
P (Torr)	104	203	302	403	202	302	402
i.d. (mm)	3.96	1.96	1.96	0.969	3.96	3.96	3.96
ethylene	-	-	-	-	-	-	-
1,3-butadiene	-	-	-	87±50	-	-	-
cyclopentadiene	9.30±0.96	98.4±7.7	421±4	1174±39	-	24.8±0.4	7.44±0.32
C_5H_6 (27.52')	-	-	-	-	-	-	-
1,3-cyclohexadiene	-	-	-	-	-	-	-
C_5H_6 (28.37')	*	*	1.21±0.75	3.28±0.47	-	-	-
1,4-cyclohexadiene	-	*	-	-	-	-	-
C_4H_2	*	-	-	-	*	-	-
C_6H_6 (34')	-	-	-	-	-	-	-
C_6H_6 (36')	-	-	-	-	-	-	-
C_6H_6 (48.22')	-	-10.6±3.6	-	*	-	-	-
styrene		616±5					

* There was insufficient data to reliably obtain the missing rates.

Table 8-12. The rates, $d \times 10^8$ mol L^{-1} s^{-3}, of formation of twelve products from tertiary reactions obtained by fitting yields of various products to equation (E6-1).

T (K)	971	970	971	970	937	895	854
P (Torr)	104	203	302	403	202	302	402
i.d. (mm)	3.96	1.96	1.96	0.969	3.96	3.96	3.96
ethylene	12.5±0.1	165±2	708±9	2137±64	22.1±0.2	7.78±0.17	1.95±0.09
1,3-butadiene	1.63±0.05	28.7±0.6	136±3	256±99	3.82±0.08	1.48±0.04	0.44±0.02
cyclopentadiene	5.81±0.46	74.4±7.4	222±6	-	24.8±1.1	-	-
C_5H_6 (27.52')	-	-	34±13	-	0.69±0.02	0.155±0.004	-
1,3-cyclohexadiene	-	-	21.0±1.8	78.6±3.1	0.715±0.004	0.302±0.006	0.088±0.004
C_5H_6 (28.37')	*	*	-	-	0.047±0.013	0.012±0.002	-
1,4-cyclohexadiene	0.347±0.049	*	31.6±2.3	66.6±7	0.965±0.035	0.244±0.014	0.045±0.002
C_4H_2	*	-	-	63±0.6	*	-	-
C_6H_6 (34')	-	-	-	-	-	-	-
C_6H_6 (36')	-	-	-	-	-	0.050±0.1	-
C_6H_6 (48.22')	-	-	-	*	-	-	-
styrene		33.2±2.6					

* There was insufficient data to reliably obtain the missing rates.